UNIVERSIDAD DE EXTREMADURA

# TESIS DOCTORAL

## Desarrollo de metodologías analíticas basadas en la utilización de datos de tres y cuatro vías combinadas con calibración multivariante, para la evaluación de la calidad de alimentos de origen vegetal

Programa de Doctorado en
Modelización y Experimentación en Ciencia y Tecnología

**Manuel Cabrera Bañegil**

**2021**

UNIVERSIDAD DE EXTREMADURA

# TESIS DOCTORAL

## Desarrollo de metodologías analíticas basadas en la utilización de datos de tres y cuatro vías combinadas con calibración multivariante, para la evaluación de la calidad de alimentos de origen vegetal

Programa de Doctorado en
Modelización y Experimentación en Ciencia y Tecnología

**Manuel Cabrera Bañegil**
**2021**

Conformidad de los directores:

La conformidad de los directores de la tesis consta en el original en papel de esta Tesis Doctoral

Isabel Durán Martín-Merás  Arsenio Muñoz de la Peña Castrillo  Daniel Martín Vertedor

**AGRADECIMIENTOS**

Esta Tesis Doctoral ha sido realizada con la ayuda de un contrato predoctoral (REF. PD16015) para formación de doctores (Orden de 11 de mayo de 2016, DOE nº 97, de 23 de mayo) con la financiación de Junta de Extremadura (Consejería de Economía e Infraestructuras) y la cofinanciación del Fondo Social Europeo (FSE) (desde 16/06/2017 hasta 01/08/2018). (Resolución de 10 de mayo de 2017, DOE nº 95, de 19 de mayo)

Los resultados que se presentan en esta Tesis Doctoral también han sido financiados por los siguientes proyectos y ayudas:

- Ministerio de Economía y Competitividad. Proyecto de investigación (REF. CTQ2014-52309-P). Resolución de 1 de agosto de 2014, de la Secretaría de Estado de Investigación, Desarrollo e Innovación. (Resolución de 8 de agosto de 2014, BOE nº 192). Cofinanciado por el Fondo Europeo de Desarrollo Regional.
- Ministerio de Economía, Industria y Competitividad (REF. CTQ2017-82496-P). Resolución de la Secretaría de Estado de Investigación, Desarrollo e Innovación y de la Presidencia de la Agencia Estatal de Investigación. (Resolución de 13 de junio de 2017, BOE nº 140). Cofinanciado por el Fondo Europeo de Desarrollo Regional.
- Junta de Extremadura y Fondo Europeo de Desarrollo Regional. Proyecto de investigación (REF. IB16058). Consejería de Economía e Infraestructuras. Decreto 68/2016, de 31 de mayo de 2016. (Resolución de 24 de mayo de 2017, DOE nº 105).
- Junta de Extremadura y Fondo Europeo de Desarrollo Regional. Ayuda a Grupos de Investigación (REF. GR18041). Consejería de Economía, Competitividad e Innovación. Decreto 14/2018, de 6 de febrero de 2018. (Resolución de 12 de abril de 2019, DOE nº 78).



Fondo Social Europeo
Una manera de hacer Europa.

**ÍNDICE**

## ABREVIATURAS Y ACRÓNIMOS

- **ºBrix**. Grados brix
- **DOP**. Denominación de Origen Protegida
- **DAD**. Detector de serie de diodos (Diode array detector)
- **EEM**. Matriz de excitación-emisión (Excitation-emission matrix)
- **ETc**. Evapotranspiración del cultivo
- **ESI**. Ionización mediante electrospray (Electrospray ionization)
- **IGP**. Indicación Geográfica Protegida
- **IM**. Índice de madurez
- **FAO**. Food and Agriculture Organization. Organización de las Naciones Unidas para la Alimentación y la Agricultura
- **FT-IR.** Espectroscopia de infrarrojo con transformada de Fourier
- **FLD** Detector de fluorescencia rápida (Fluorescence detection)
- **GRAS**. Generalmente Reconocido como Seguro (Generally recognized as safe)
- **LC**. Cromatografía de líquidos (Liquid chromatography)
- **LDA**. Análisis lineal discriminante (Linear discriminant analysis)
- **MCR-ALS**. Resolución multivariante de curvas en combinación con mínimos cuadrados alternantes (Multivariate curve resolution and alternating least-squares).
- **MLR**. Regresión lineal multiple (Multiple linear regression)
- **MS**. Detector de masas (Mass detection)
- **MS/MS**. Detección masas/masas (Mass/Mass detection)

- **N-PLS**. Mínimos cuadrados parciales multivía (Multiway partial least-squares)

- **N-PLS-DA.** Mínimos cuadrados parciales multivía – análisis discriminante (Multiway partial least-squares discriminant analysis)

- **N-PLS/RBL**. Mínimos cuadrados parciales multivía en combinación con bilinealización residual (Multiway partial least-squares with residual bilinearization).

- **N-PLS/RTL**. Mínimos cuadrados parciales multivía en combinación con trilinealización residual (Multiway partial least-squares with residual trilinearization)

- **NIRS**. Espectroscopía de infrarrojo cercano. Near infrared spectroscopy

- **OIVE**. La Organización Interprofesional del Vino de España

- **PARAFAC**. Análisis paralelo de factores (Parallel factor analysis)

- **PARAFAC-LDA.** Análisis paralelo de factores – análisis lineal discriminante (Parallel factor analysis – linear discriminant analysis)

- **PCA**. Análisis por componentes principales (Principal component analysis)

- **PCA-LDA**. Análisis por componentes principales - análisis lineal discriminante (Principal component analysis - linear discriminant analysis)

- **PCR**. Regresión por componentes principales (Principal component regresssion)

- **PLS**. Mínimos cuadrados parciales (Partial least-squares)

- **PLS-CM**. Mínimos cuadrados parciales-modelado de clases (Principal least-squares class-modelling)

- **PLS-DA**. Mínimos cuadrados parciales-análisis discriminante (Principal least-squares discriminant analysis)

- **QDA**. Análisis cuadrático discriminante (Quadratic discriminant analysis)

- **RP**. Fase inversa (Reversed phase)

- **RBL**. Bilinealización residual (Residual bilinearization)
- **RDC**. Riego deficitario controlado
- **RTL**. Trilinealización residual
- **SFS**. Espectroscopía de fluorescencia sincrónica
- **SIMCA**. Modelado blando independiente de analogías de clases (Soft independent modelade class analogy)
- **SPA-LDA**. Algoritmo de sucesión progresivo – análisis lineal discriminante (Successive projection algorithm - linear discriminant analysis)
- **TSFS**. Espectroscopia de fluorescencia sincrónica total
- **UHPLC**. Cromatografía de líquidos de ultra alta resolución (Ultra high performance liquid chromatography)
- **U-PLS**. Mínimos cuadrados parciales desdoblados (Unfolded-partial least squares)
- **U-PLS-DA**. Mínimos cuadrados parciales desdoblados-análisis discriminante (Unfolded-partial least squares discriminant analysis)
- **U-PCA**. Análisis por componentes principales desdoblados (Unfolded-principal component analysis)
- **U-PLS/RBL**. Mínimos cuadrados parciales desdoblados con bilinearización residual (Unfolded-partial least-squares with residual bilinearization)
- **U-PLS/RT**. Mínimos cuadrados parciales desdoblados con trilinearización residual (Unfolded-partial least-squares with residual trilinearization)
- **UV-Vis**. Ultravioleta-visible (Ultraviolet-visible)

# RESUMEN

## 1. RESUMEN

La presente Tesis Doctoral aborda el desarrollo de nuevos métodos analíticos utilizando fluorescencia molecular en combinación con algoritmos quimiométricos de calibración multivariante para la determinación e identificación de compuestos polifenólicos de interés en el campo agroalimentario. Como matrices alimentarias, se seleccionaron cuatro tipos, representativos de la economía agroalimentaria de Extremadura, como son uvas, vinos, ciruelas y aceitunas.

Así, el presente documento se divide en las siguientes partes: resumen, objetivos, introducción, resultados y discusión, publicaciones y conclusiones obtenidas de este trabajo.

La introducción se centra en la descripción de las matrices alimentarias, así como de los compuestos fluorescentes objeto de análisis. También se incluye una breve descripción de las técnicas instrumentales analíticas para su determinación y de los algoritmos quimiométricos utilizados.

En la descripción de las matrices alimentarias se recogen las cifras a nivel autonómico, nacional y mundial de superficie de plantación y producción de cada uno de los cultivos. También se describe la influencia de la maduración en todas las matrices seleccionadas y del riego en el cultivo de los viñedos y del olivar. Se incluyen las técnicas mínimamente destructivas que se emplean actualmente para ofrecer información sobre el estado de maduración óptimo y del estado hídrico de cada una de las matrices objeto de estudio.

En referencia a la descripción de los compuestos polifenólicos fluorescentes objeto de estudio, se recogen las características más representativas de cada una de las familias a las que pertenecen, así como algunas de sus características más singulares.

En cuanto a las técnicas analíticas utilizadas, se recoge una visión general de las que se han empleado, clásicamente, en la determinación de familias de compuestos polifenólicos o compuestos individuales. También se ha realizado una revisión bibliográfica sobre la utilización de datos fluorimétricos en combinación con herramientas quimiométricas.

La sección de resultados y discusión presenta un resumen de la secuenciación de cómo se han obtenidos los resultados recogidos en esta Tesis, mostrando la novedad de las metodologías aplicadas, así como de la información generada.

La sección de conclusiones muestra los principales logros de estos estudios.

Finalmente, la sección de publicaciones incluye ocho artículos científicos publicados con los resultados de los estudios realizados en la presente Tesis Doctoral:

- *Front-face fluorescence spectroscopy combined with second-order multivariate algorithms for the quantification of polyphenols in red wine samples.* **Food Chemistry 220 (2017), 168-176.**

La primera publicación se basa en la determinación de varios compuestos polifenólicos en muestras de vinos sin pretratamiento, en la que se realiza una calibración y validación de los compuestos polifenólicos para obtener una matriz sintética similar al vino, que servirá de base para ser aplicada sobre muestras reales. Así, se procedió a la cuantificación de ácidos fenólicos, flavanoles y estilbenos en las muestras reales de vino mediante el registro de matrices de excitación y emisión en combinación con algoritmos de segundo orden (PARAFAC, U-PLS/RBL).

- *Front-face fluorescence excitation-emission matrices in combination with three-way chemometrics for the discrimination and prediction of phenolic response to vineyard agronomic practices.* **Food Chemistry 270 (2019), 162-172.**

La segunda publicación consiste en la caracterización de muestras de uvas de la variedad '*Tempranillo*' y su discriminación en función de su estado hídrico y la carga del cultivo, empleando algoritmos de clasificación de segundo orden (PARAFAC, PARAFAC-LDA y U-PLS-DA). Se detalla, además, la cuantificación de catequinas y resveratrol utilizando calibración de segundo orden mediante los algoritmos PARAFAC y U-PLS/RBL.

- *Combination of fluorescence excitation emission matrices in polar and non-polar solvents to obtain three- and four-way arrays for classification of Tempranillo grapes according to maturation stage and hydric status.* **Talanta 199 (2019), 652-661.**

La tercera publicación consiste en la discriminación de muestras de uva de la variedad '*Tempranillo*', en función de su fecha de muestreo, empleando algoritmos de clasificación de segundo orden (PARAFAC-LDA y U-PLS-DA). También se detalla la generación de datos de tercer orden, usando los resultados de la extracción en dos disolventes (agua y dietiléter) y su tratamiento quimiométrico, para diferenciar entre muestras de uva de secano y regadío.

- *Evolution of polyphenols content in plum fruits (Prunus salicina) with harvesting time by second-order excitation-emission fluorescence multivariate calibration.* **Microchemical Journal 158 (2020), 105299.**

La cuarta publicación se centra en la cuantificación de compuestos polifenólicos, pertenecientes a las familias de ácidos fenólicos y flavanoles, por U-PLS y PARAFAC, de muestras de ciruela de la variedad '*Angeleno*', en piel y pulpa, recogidas en dos fechas distintas de maduración del fruto.

- *First-order discrimination of methanolic extracts from plums according to harvesting date using fluorescence spectra. Quantification of polyphenols.* Enviado a **Microchemical Journal**.

La quinta publicación se refiere a la clasificación de muestras de ciruelas de la variedad '*Angeleno*', recogidas en dos fechas de muestreo (mayo y septiembre) y de diferentes partes del fruto (piel y pulpa), mediante la aplicación de PCA y PLS-DA sobre espectros de fluorescencia.

- *Control of olive cultivar irrigation by front-face fluorescence excitation-emission matrices in combination with PARAFAC.* **Journal of Food Composition and Analysis 69 (2018), 189-196.**

La sexta publicación se centra en la aplicación de diferentes estrategias de riego en el cultivo del olivo, consiguiendo discriminar las pastas de aceituna de la variedad '*Arbequina*' por medio de PARAFAC-PCA. Además, se procedió a predecir la concentración de varios polifenoles por medio de una correlación entre los "s*cores*" y las concentraciones cromatográficas.

- *Fluorescence Study of Four Olive Varieties Paste According to Sampling Dates and the Control in the Elaboration of Table Olives of "Ascolana tenera"*. **Food Analytical Methods 14 (2021), 307-318.**

En la séptima publicación, se estudió la influencia de la maduración de la aceituna en cuatro variedades: '*Piantone di Fallerone*', '*Piantone di Mogliano*', '*Arbequina*' y '*Maurino*'. Se consiguió diferenciar las variedades por medio de los métodos de clasificación, PARAFAC-LDA y U-PLS-DA, y en función de su estado de maduración por PARAFAC. Como aplicación industrial se llevó a cabo un seguimiento por medio de fluorescencia de la elaboración de las aceitunas de la variedad '*Ascolana tenera*' para el control de su calidad.

- *Avances en la utilización de datos de cuatro y cinco vías, basados en matrices de excitación-emisión de fluorescencia, para aplicaciones analíticas.* **Boletín de la Sociedad Española de Química Analítica. Actualidad Analítica 70 (2020), 9-12.**

Por último, se incluye una octava publicación que se centra en la revisión de los avances en la utilización de datos de cuatro y cinco vías basados en matrices de excitación-emisión de fluorescencia, para aplicaciones analíticas.

# OBJETIVOS

## 2. OBJETIVOS

El objetivo general de esta Tesis Doctoral, enmarcada en el campo agroalimentario, es el desarrollo de nuevas metodologías analíticas para la determinación e identificación de compuestos polifenólicos en muestras de origen vegetal. Para ello, y teniendo en consideración los inconvenientes de las metodologías convencionales, se han desarrollado métodos simples, rápidos y no destructivos, que reducen las etapas tediosas de pretratamiento de muestras y el uso de disolventes. Por lo que estas técnicas permiten analizar muestras vegetales sin alterar su composición inicial.

Se han utilizado metodologías analíticas basadas en la fluorescencia molecular y en la cromatografía de líquidos de alta eficacia con detectores de ultravioleta-visible y fluorescencia acoplados en serie. Estas herramientas nos han permitido obtener datos de segundo y tercer orden que, en combinación con métodos de calibración multi-vía y con técnicas de clasificación, nos han permitido extraer suficiente información para poder caracterizar y clasificar las muestras en función de algunos parámetros agronómicos como el estado de maduración del fruto y el estado hídrico del cultivo.

Los objetivos específicos de la presente Tesis son los siguientes:

**1.** Utilizar técnicas espectroscópicas (fluorescencia molecular en modo *front-face*), acopladas con algoritmos quimiométricos multivariantes, para monitorizar el proceso de maduración de uvas, ciruelas y aceitunas.

**2.** Estudiar la influencia del estrés hídrico en uvas y aceitunas, mediante la cuantificación de los compuestos fenólicos en estas matrices, con mínimo tratamiento de muestra para no modificar la distribución de la matriz y validar los resultados obtenidos mediante métodos cromatográficos.

**3.** Obtener datos de 4 vías y aplicación de algoritmos quimiométricos de tercer orden para la clasificación de uvas en función de fechas de muestreo.

# INTRODUCCIÓN

# 3. INTRODUCCIÓN

La introducción de la presente Tesis Doctoral incluye las cifras comerciales de los cultivos objeto de estudio (vid, ciruelos y olivar), así como una breve descripción de los procesos químicos y bioquímicos que transcurren durante la maduración de los frutos y la influencia de ciertas técnicas agronómicas sobre la calidad de los mismos, junto con la descripción de técnicas mínimamente invasivas para la determinación del estado de maduración e hídrico. Seguidamente, se describen las principales características de diferentes familias de compuestos polifenólicos, presentes en las matrices alimentarias objeto de estudio. También se incluye un repaso bibliográfico sobre los métodos de determinación con técnicas separativas de las familias polifenólicas analizadas en el presente documento. Tras ello, se describe el uso y modalidades de la fluorescencia molecular, como técnica mínimamente invasiva para el análisis de alimentos, los algoritmos quimimétricos usados en el presente documento y una revisión de las principales aplicaciones de la espectrofluorimetría en combinación con Quimiometría para el análisis de compuestos polifenólicos.

## 3.1 MATRICES ALIMENTARIAS

### 3.1.1 ***Uvas y vinos***

#### 3.1.1.1 El cultivo de la vid para la producción de vino

La Organización de las Naciones Unidas para la Alimentación (FAO) sitúa a España como el cuarto país productor de uva del mundo y segundo a nivel europeo. El principal productor a nivel mundial es China, seguido de Italia y Estados Unidos (FAOSTAT, 2018).

En lo que respecta al cultivo de la vid, el Anuario de Estadística de 2018 del Ministerio de Agricultura, Pesca y Alimentación recoge los datos más recientes de producción y superficie cultivada, siendo los últimos datos mostrados los del 2017 (MAPA, 2019a).

Tal y como se recoge en dicho anuario, el viñedo de uva para vinificación en España cuenta con una superficie total de plantación regular de 921.642 ha, de las que 678.368 están dedicadas a secano y 243.274 a regadío. El rendimiento en secano es de 4.250 kg/ha, mientras

que en regadío es de 11.418 kg/ha. La producción total ha sido de 5.119.117 t de uvas de vinificación. Por comunidades, Castilla-La Mancha ocupa el primer lugar en producción con un total de 2.965.358 t, seguida de Extremadura y Cataluña con 395.332 y 371.669 t, respectivamente (MAPA, 2019a).

En cuanto a la producción de vino tinto, por Comunidades, las principales productoras de vino son Castilla-La Mancha, Comunidad Valenciana y Extremadura con 8.078.925, 1.426.424 y 1.046.048 hectolitros, respectivamente. Respecto al vino blanco las principales productoras son Castilla La Mancha, Cataluña y Extremadura (MAPA, 2019a).

A continuación, y con los datos de dicho anuario, se muestra la evolución de la superficie total cultivada en España, **Gráfico 1**; la producción de uva, **Gráfico 2**; y la producción de vino blanco y tinto producido, en el periodo 2007-2018, **Gráfico 3**.

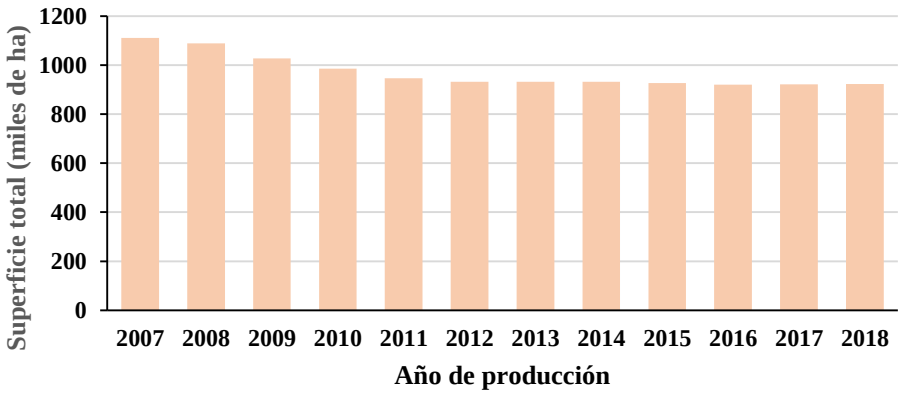


***Gráfico 1.*** *Evolución de la superficie de viñedo. Elaborado a partir de datos del Ministerio de Agricultura (MAPA, 2019a).*

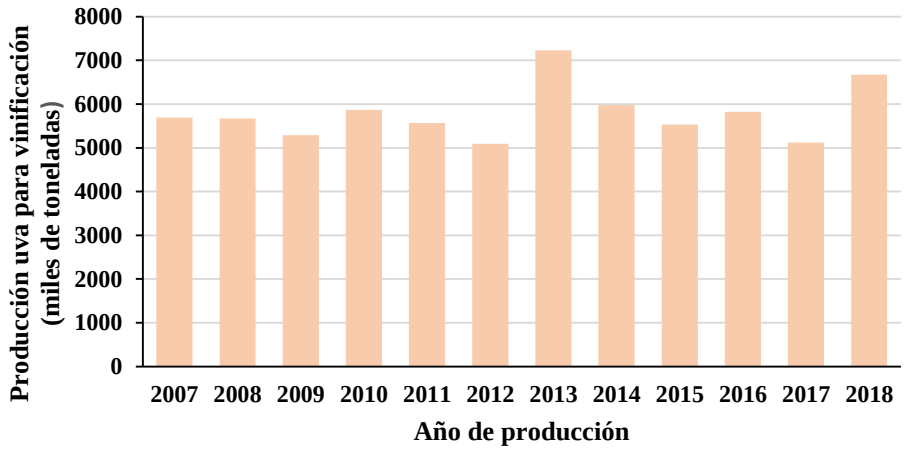


***Gráfico 2.*** *Evolución de la producción de uva para vinificación. Elaborado a partir de datos del Ministerio de Agricultura (MAPA, 2019a).*

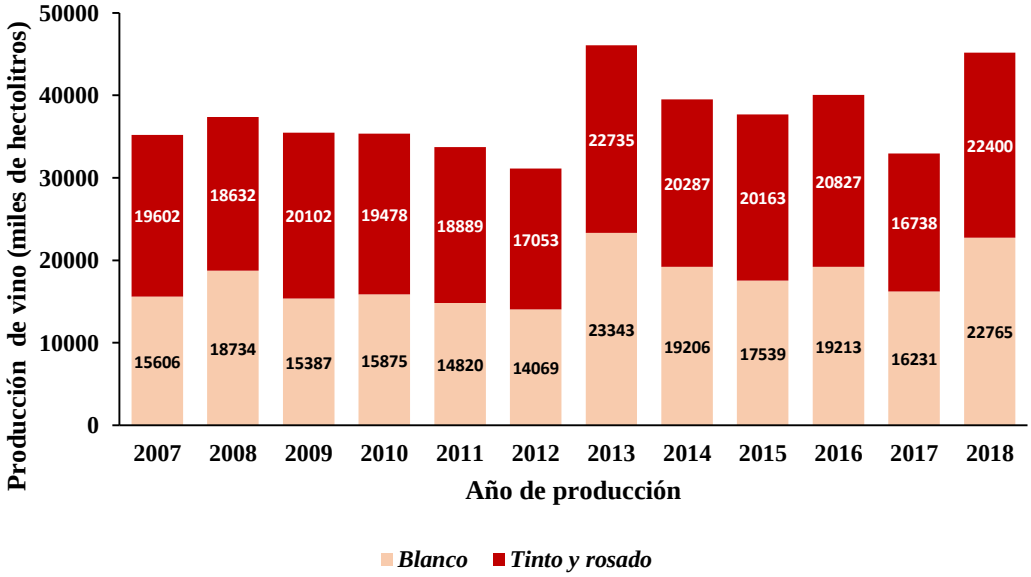


***Gráfico 3.*** *Evolución del volumen de vino blanco y tinto y rosado. Elaborado a partir de datos del Ministerio de Agricultura (MAPA, 2019a).*

Como se puede observar en el **Gráfico 1,** la evolución de la superficie de viñedo ha sido descendente desde 2007, estabilizándose a partir de 2012.

La producción de uva y, por consiguiente, de vino en España se caracteriza por su gran variabilidad de unas campañas a otras debido a la fuerte dependencia de este cultivo de las condiciones climatológicas (**Grafico 2 y 3**). Los años de mayor producción de este cultivo fueron 2013 y 2018 con diferencias de hasta 1 millón de toneladas de uvas y de hectolitros de vino con respecto al resto de campañas. Además, no se aprecian diferencias significativas en cuanto a la producción de vino blanco y tinto en cada campaña.

La Organización Interprofesional del Vino de España (OIVE) ha presentado al Ministerio una relación de posibles actuaciones para la estabilidad y calidad del sector vitivinícola español. Entre ellas se propone mejorar la calidad del sector estableciendo requisitos mínimos de calidad para las uvas de vinificación que se encuentran fuera de las Denominaciones de Origen Protegidas/Indicaciones Geográficas Protegidas (DOP/IGP), tales como la madurez de la uva para conseguir un grado alcohólico volumétrico natural mínimo de 9% Vol. y un rendimiento máximo por parcela de cultivo con el propósito de evitar que se produzcan vinos de baja calidad. Con estos requisitos se evitarían vinos de insuficiente grado alcohólico y de poco color debido a uvas poco maduras (MAPA, 2019b).

Con el objetivo de destacar y mantener la calidad de los vinos, la Unión Europea potencia herramientas para el reconocimiento de una calidad diferenciada en estos productos con la designación de zonas con Denominación de Origen Protegida (DOP) y zonas de Indicación Geográfica Protegida (IGP), que permiten a los viticultores elaborar sus vinos con unas variedades de uva u otras, distinguiendo entre variedades tintas y las de uva blanca. La labor de los Consejos Reguladores de las DOP es regular las condiciones bajo las cuales se elaboran los vinos, atendiendo principalmente a parámetros de calidad, procesos de producción o el que quizás sea el más evidente, la localización geográfica de la que procede y en la que se elabora este producto.

En la Comunidad Autónoma de Extremadura, la vitivinicultura es un sector de enorme importancia en la economía extremeña por su extensión y valor económico. Según datos del 2015, este sector garantiza la ocupación de aproximadamente 22.000 agricultores y la puesta en funcionamiento de alrededor de 250 bodegas (Díaz González, 2015). En el año 2018, la superficie extremeña de viñedo para vinificación fue de 81.561 ha, con una producción de 160.266 toneladas de uva y 2.738.289 hl de vino (Picón Toro et al., 2018).

Respecto a las variedades predominantes en Extremadura, destaca la variedad tinta '*Tempranillo*', ampliamente extendida por toda la región por su buena adaptación al clima extremeño. Otras variedades tintas de gran interés son '*Cabernet Sauvignon*', '*Merlot*' y '*Shiraz*'. En cuanto a las variedades blancas, predominan '*Cayetana*' y '*Macabeo*' (Díaz González, 2015).

En cuanto a la calidad de los vinos, en la Comunidad Autónoma de Extremadura se declaran oficialmente varias DOPs que permiten destacar la calidad de la producción de los vinos en esta región, como son: la IGP "Extremadura" (Vinos de la Tierra) y Vinos de DOP "Ribera del Guadiana".

La DOP "Ribera del Guadiana" comprende varias subzonas de producción, tal y como se muestra en la **Figura 1**: Cañamero y Montánchez, en la provincia de Cáceres, y Matanegra, Ribera Alta del Guadiana, Ribera Baja del Guadiana y Tierra de Barros, esta última la de mayor extensión, en la provincia de Badajoz. Esta denominación cuenta con 17 variedades de uva blanca y 13 variedades tintas entre las que se encuentra la variedad '*Tempranillo*' (DECRETO 74/2018) (Modificación Normal del Pliego de Condiciones «RIBERA DEL GUADIANA», 2020).


***Figura 1.*** *Subzonas de producción de la DOP Ribera del Guadiana. Modificación de (Díaz González 2015).*

### 3.1.1.2 Maduración de las uvas. Métodos de análisis

Durante el ciclo vegetativo del cultivo de la vid, el crecimiento de las bayas de uva presenta una doble función sigmoidal que se divide en tres fases (Coombe, 1960):

- **Estado I.** Fase en la que la baya aumenta en tamaño y en masa debido a la rápida división celular que hace que se produzca un rápido crecimiento exponencial del fruto.
- **Estado II.** Se caracteriza por un lento crecimiento del pericarpio y por la maduración de las semillas. La transición del Estado II al III se denomina envero y en él aparecen los pigmentos antociánicos, principales responsables del cambio de color en variedades tintas. A lo largo de esta fase se produce un descenso de la acidez total (especialmente, ácido málico).
- **Estado III.** Se caracteriza por la acumulación de fotoasimilados y por un engrosamiento celular (Hidalgo Togores, 2006).

La maduración de las uvas se puede definir como el periodo de tiempo que va desde el envero del fruto hasta la cosecha de la uva. A lo largo de este proceso, se producen un conjunto de cambios físico-químicos en el fruto, que en función de distintos factores agroambientales afectarán en mayor o menor medida a la calidad final del producto obtenido. Desde el punto de vista del análisis de rutina, los cambios químicos más interesantes que ocurren durante la maduración en la uva son el aumento de azúcares, el aumento del peso de la baya y la disminución de la acidez (Topalovic & Petkovsek, 2010).

La concentración de azúcares, medida con un refractómetro y expresada en sólidos solubles totales o grados Brix (ºBrix) (Daniels, Poblete-Echeverría, Opara, & Nieuwoudt, 2019) es una de las variables a controlar por los productores y cooperativas de vinos ya que su valor es determinante en la calidad del producto final. En algunos casos, también se realizan medidas de la densidad de los mostos (escala Baumé), dado que este parámetro está relacionado con el contenido de sólidos solubles y con el grado de alcohol probable o potencial (International Organisation of Vine and Wine, 2020).

La selección del momento óptimo para la recolección de la uva es uno de los procesos de mayor importancia y que más condiciona la calidad del vino (Bindon, Varela, Kennedy, Holt,

& Herderich, 2013). Las uvas para vinificación se cosechan cuando ciertos parámetros químicos de la uva logran los valores requeridos determinados por el tipo de vino que se pretende producir. De lo contrario, cuando se cosechan uvas en las que no se ha completado la maduración, se corre el riesgo de obtener vinos muy amargos y astringentes (Kontoudakis, Esteruelas, Fort, Canals, & Zamora, 2010). A día de hoy, es muy común todavía cosechar las uvas para vinificación tomando como referencia lo que se conoce como madurez tecnológica, es decir, a partir de los resultados de las medidas de los componentes mayoritarios como son azúcares y ácidos. De hecho, muchas veces, solamente se toma como referencia la concentración de azúcares para determinar el momento de cosecha, dado que esta determina el grado alcohólico potencial. Sin embargo, estos parámetros solamente proporcionan información sobre la maduración de la pulpa y se pasa por alto el grado de maduración real de la piel y las semillas (Meléndez, Ortiz, Sarabia, Íñiguez, & Puras, 2013).

Adicionalmente a estos análisis, la madurez fenólica o el momento en el que la síntesis de compuestos fenólicos de la uva es máxima, es uno de los parámetros más importantes para decidir el momento óptimo de cosecha. Para variedades tintas, el color de la piel es otro parámetro importante para evaluar la calidad y maduración de las bayas, ya que condiciona el color y la calidad del vino a producir (Pérez-Magariño & González-San José, 2006). La madurez fenólica óptima se logra cuando los taninos de las semillas presentan su concentración más baja y el contenido de los fenoles en la piel presenta máxima concentración (Zuñiga, Mora, Oyarce, & Fredes, 2014). Pero esta madurez fenólica, en la que es máximo el contenido de taninos en el hollejo y de antocianos, no siempre coincide con la maduración tecnológica o momento de máxima relación azúcar/acidez de la pulpa. Tradicionalmente, la medida de compuestos fenólicos totales se lleva a cabo con el método de Folin-Ciocalteu (García Martínez, Fernández Segovia, & Fuentes López, 2015; Singleton & Rossi, 1965).

Basándose en las características espectrales de las diferentes familias fenólicas, para la determinación total de algunas de ellas, se suelen utilizar técnicas espectroscópicas con mosto de uva o vino, generalmente este último diluido (Aleixandre-Tudo, Buica, Nieuwoudt, Aleixandre, & du Toit, 2017; Harbertson & Spayd, 2006). A partir de ellas, se definen índices de determinación de ciertas familias polifenólicas que sirven de referencia para mejorar el seguimiento de la maduración y de la vinificación. Uno de los índices de mayor extensión es

el índice de extractabilidad de los antocianos, basado en la extracción de antocianos y taninos a partir de muestras de uva entera que se trituran y maceran a dos pH diferentes (1 y 3,2) (Glories & Augustin, 1993). La extractabilidad se considera óptima cuando la diferencia entre estos dos valores de pH es pequeña y, por tanto, el valor del índice de extractabilidad es bajo.

Cualquiera de los métodos de rutina mencionados han resultado útiles para la caracterización bioquímica de la maduración de las uvas hasta el momento de la vendimia (Daniels et al., 2019), pero requieren mucho tiempo en el laboratorio, especialmente cuando el número de muestras a analizar es elevado, y muchos de ellos son métodos destructivos.

La gran influencia de los compuestos fenólicos de la uva en la calidad del vino elaborado es debida a la importancia de su color y a los atributos en boca (Laguna, Bartolomé, & Moreno-Arribas, 2017). Las antocianinas, responsables de la pigmentación roja, púrpura y azul en las variedades tintas, empiezan a acumularse durante el envero en las células de la piel y llegan a su máximo en las últimas fases de la maduración cuando la síntesis se detiene (Teixeira, Eiras-Dias, Castellarin, & Gerós, 2013). Su principal forma es la malvidina-3-*O*-glucósido (Fontes, Gerós, & Delrot, 2011; Revilla, García-Beneytez, Cabello, Martín-Ortega, & Ryan, 2001).

Con el fin de obtener datos sobre la composición de las uvas en función de la fecha de cosecha, Gao et al., (2019) analizaron muestras de uva de la variedad '*Cabernet Sauvignon*', procedentes de la provincia de Xinjiang (China). Estos investigadores recogieron uvas en tres fechas de maduración y determinaron la composición de antocianinas y 3-flavanoles en la piel durante las campañas del 2015 y 2016, observando que la concentración de antocianinas fue mayor en las uvas de cosecha más tardía. En cuanto al contenido de 3-flavanoles de la piel, este disminuyó a medida que se retrasó la fecha de cosecha.

Un estudio similar se realizó con uvas '*Merlot*' muestreadas en tres momentos diferentes del ciclo de maduración, caracterizadas en función del promedio de los ºBrix como inmaduras (20,7 ºBrix), maduras (24,0 ºBrix) y sobremaduras (27,4 ºBrix). Se observó que la concentración de antocianinas se incrementó al aumentar el grado de madurez de la uva. Así, los vinos obtenidos de las uvas inmaduras tuvieron, significativamente, menor concentración

de antocianinas que los de uvas sobremaduras (Sherman, Greenwood, Villas-Boâs, Heymann, & Harbertson, 2017).

También se ha estudiado la evolución de la maduración de uvas de las variedades '*Merlot*' y '*Shiraz*' durante dos campañas vitivinícolas (2015 y 2016), observando que glucosa y fructosa, así como los azúcares totales, se generan en su mayor parte entre el envero y un estado de madurez temprana, mientras que los fenoles totales aumentaron conforme avanzaba la maduración del fruto. El contenido de flavonoides fue bajo aumentando durante la maduración de la uva (Bashir, Kaur, & Arora, 2019). Del mismo modo, Jediyi et al., (2019) analizaron la concentración de compuestos fenólicos totales en uvas de las variedades '*Adari*' y '*Abbou*' en Marruecos, observando que los fenoles aumentaban durante la maduración.

Respecto a la influencia de la maduración en el perfil de compuestos fenólicos individuales, se estudió la evolución de varios de ellos en extractos de la piel de uvas de las variedades '*BRS Violeta*' e '*Isabel Precoce*' recogidas en Bahía (Brasil). La concentración de ácidos fenólicos tales como los ácidos siríngico, cafeico y gálico y el contenido en ácido clorogénico se vio influenciada por la maduración, siendo su nivel máximo en febrero y mínimo en mayo para todos ellos. Sin embargo, la concentración de los estilbenos *cis* y *trans*-resveratrol no mostró una tendencia clara, mientras que la mayor concentración de los flavanoles tales como catequina, epicatequina, y procianidinas B1 y B2 se observó en las uvas recolectadas en el mes de noviembre (etapa de crecimiento en el hemisferio sur) (Valéria da Silva Padilha, dos Santos Lima, Maia Toaldo, Elias Pereira, & Terezinha Bordignon-Luiz, 2019).

En Extremadura, en uvas de la variedad '*Tempranillo*', se ha estudiado la evolución de los ºBrix, y del contenido en fenoles y en flavonoides totales a lo largo del proceso de maduración. Los ºBrix aumentaron desde el Estado II al III de crecimiento del fruto, mientras que los fenoles totales y flavonoides mostraron sus mayores contenidos en fechas más tardías de la maduración del fruto (Garrido et al., 2016).

Por otra parte, desde hace más de una década, se han desarrollado tecnologías no destructivas para la determinación de parámetros químicos de calidad de la uva como la espectroscopia de infrarrojo cercano (NIR). Para su correcta validación se han ensayado estos

equipos con la medida directa de los racimos y/o baya (Daniels et al., 2019; Fernández-Novales et al., 2019), en el mosto de uva (Petrovic, Aleixandre-Tudo, & Buica, 2020; Véstia, Barroso, Ferreira, Gaspar, & Rato, 2019) y en los vinos elaborados (Genisheva et al., 2018; Hu, Yin, Ma, & Liu, 2018).

La aplicación espectroscopia del NIR, cubriendo el rango de longitudes de onda entre 780-2500 nm, y combinada con algoritmos quimiométricos, ha despertado un gran interés en la determinación del grado de madurez de las uvas y en la calidad del vino, sobre todo en variedades de uva tinta. Las uvas contienen moléculas orgánicas, tales como azúcares, ácidos orgánicos, compuestos volátiles, así como otros compuestos químicos, con grupos O-H, N-H, C-H y otros grupos enlazados con hidrógeno que emiten señales detectadas con esta técnica analítica no destructiva (Blanco & Villarroya, 2002; Boido, Fariña, Carrau, Dellacassa, & Cozzolino, 2013; Musingarabwi, Nieuwoudt, Young, Eyéghè-Bickong, & Vivier, 2016). Así, se ha empleado, entre otras, en la caracterización de la evolución de los cambios físicos y químicos que ocurren durante la maduración de los racimos, para servir de apoyo sobre la decisión del momento óptimo de cosecha (González-Caballero, Pérez-Marín, López, & Sánchez, 2011).

La espectroscopia de infrarrojo con transformada de Fourier (FT-IR) se ha aplicado en el estudio de evaluaciones cuantitativas en uvas de la variedad '*Sauvignon blanc*' de ácido tartárico, ácido málico, ácido succínico, glucosa y fructosa combinando la información de los espectros NIR con métodos de análisis multivariante tales como mínimos cuadrados parciales (PLS). Igualmente, se observó una buena predicción cuantitativa del contenido en azúcares y ácidos orgánicos. Se consiguió discriminar entre diferentes etapas de crecimiento de la baya por mínimos cuadrados parciales-análisis discriminante (PLS-DA) y por análisis por componentes principales (PCA) (Musingarabwi et al. 2016). También se ha aplicado esta técnica para estudiar la evolución de la maduración de muestras de uva de las variedades '*Pedro Ximénez*' y '*Cabernet Sauvignon*' en combinación con PLS-DA, cuyo modelo consiguió clasificar el 81% de las uvas blancas y el 86% de las uvas tintas (González-Caballero, Sánchez, Fernández-Novales, López, & Pérez-Marín, 2012). También se ha desarrollado un modelo predictivo de los atributos de calidad y maduración de uvas '*Syrah*' y '*Cabernet Sauvignon*' como sólidos solubles y contenido en antocianinas y en flavonoides.

Estos datos se han usado para diferenciar distintas etapas de desarrollo del fruto como el envero y la maduración. Para la regresión utilizaron regresión por componentes principales (PCR) y PLS. Se obtuvieron buenas regresiones y predicciones por ambos algoritmos. Posteriormente, la clasificación se realizó por PCA, PLS-DA y análisis por componentes principales-análisis lineal discriminante (PCA-LDA). El análisis por PCA de los datos no permitió diferenciar entre uvas recolectadas en envero y al final de la maduración del fruto debido a la poca diferencia entre el color de las uvas de cada uno de estos periodos. A través de PLS-DA y PCA-LDA se clasificaron correctamente las tres etapas de maduración con una exactitud del 93,2 y 92,9%, respectivamente (dos Santos Costa, Oliveros Mesa, Santos Freire, Pereira Ramos, & Teruel Mederos, 2019).

Con espectrofotómetros portátiles Vis/NIR, se han analizado uvas blancas de vinificación para la elaboración de vinos en la comarca italiana de Franciacorta con el objeto de correlacionar a través de PLS y regresión lineal múltiple (MLR) los espectros obtenidos con este equipo con los parámetros de maduración tales como los sólidos solubles y acidez valorable. Los resultados permitieron diferenciar entre uvas maduras de aquellas con un menor grado de maduración. Las técnicas de análisis quimiométricos PCA y MLR también permitieron diferenciar entre uvas cosechadas en diferentes fechas (Giovenzana, Civelli, Beghi, Oberti, & Guidetti, 2015). Recientemente, se ha evaluado la concentración de aminoácidos en uvas intactas de la variedad '*Grenache*' durante la maduración en combinación con PLS (Fernández-Novales et al., 2019).

Pese a la gran cantidad de publicaciones científicas que demuestran el gran potencial del NIR en el análisis de cara a una implementación industrial, el número de estudios a escala industrial de procesos *on-line/at line* es todavía escaso (Grassi & Alamprese, 2018).

### 3.1.1.3 Prácticas agronómicas en el cultivo de la vid. Métodos de análisis

Entre las prácticas agronómicas que influyen directamente en la composición de la uva y en el rendimiento de los viñedos se incluyen diferentes prácticas de riego y las técnicas de clareo de racimos.

La especie *Vitis sp. (grapevines)*, en general, manifiesta una alta tolerancia a la sequía gracias a su largo y profundo sistema radicular que explora un gran volumen de suelo en la búsqueda de agua y elementos nutritivos, así como debido al mecanismo fisiológico para el control estomático de la transpiración (Chaves et al., 2010; Rogiers et al., 2011).

Aun así, el agua se considera un factor crítico para la sostenibilidad de la viticultura, dado que la producción de uva y la viabilidad económica se pueden ver influenciadas por la disponibilidad de agua. El consumo de agua anual en los viñedos oscila entre 300 y 700 mm, siendo, por lo general, mayor que la precipitación media anual. La mejora del uso eficiente del agua es crucial para la sostenibilidad de la industria vitícola en las regiones semiáridas, especialmente en el periodo que coincida con la escasez de agua y las altas temperaturas (Medrano et al., 2015). De hecho, en Extremadura, la pluviometría anual se suele concentrar en el periodo de meses comprendido desde el otoño a la primavera. Dado que esta región presenta veranos secos y calurosos, se hace necesario emplear dosis de riego para mantener o aumentar la producción de la uva durante este periodo crítico (Campillo Torres, Moñino Espino, Pérez Rodríguez, & Picón Toro, 2009). La escasez de agua provoca en la planta un estrés hídrico, moderado o severo (Gutiérrez-Gamboa, Pérez-Donoso, Pou-Mir, Acevedo-Opazo, & Valdés-Gómez, 2019), que si sobrepasa unos niveles críticos tiene un impacto negativo en el crecimiento y rendimiento del viñedo y en la composición de la uva y del vino (Marciniak, Reynolds, & Brown, 2013; Romero et al., 2015).

Los métodos que se usan para controlar el riego involucran parámetros atmosféricos, edáficos y parámetros relacionados con la naturaleza de la planta (Basile et al., 2020; Jones, 2006). Las medidas del estado hídrico de la planta se realizan a través de métodos indirectos relacionados con el suelo y la atmósfera, y de métodos directos, basados en la planta. Los métodos indirectos relacionados con el suelo se basan en la determinación de la humedad del mismo a distintas profundidades. Los métodos atmosféricos se basan en determinar el

consumo de agua por medio de la evapotranspiración del viñedo (ETc). Por su parte, los métodos directos son la observación visual del estado del viñedo, medidas del potencial hídrico del tronco y del tallo, y medidas del flujo de savia, entre otros (Rienth & Scholasch, 2019). Sin embargo, la mayoría de estos indicadores son destructivos, requieren un manejo laborioso de los equipos y son tomados de manera manual en un punto local sin conocer el verdadero estado hídrico de todo el cultivo (Ribera-Fonseca et al., 2019; Romero-Trigueros, Bayona Gambín, Nortes Tortosa, Alarcón Cabañero, & Nicolás Nicolás, 2019).

Dada la influencia que tiene el estrés hídrico en la composición final de las uvas, diversos investigadores han ensayado el uso de diferentes estrategias de riego, siendo la más habitual el empleo del riego deficitario controlado (RDC). Esta técnica consiste en aplicar durante ciertos periodos de su ciclo vegetativo, una cantidad de agua menor que la necesaria para satisfacer plenamente la evapotranspiración del viñedo (Kriedemann & Goodwin, 2003; Ruiz-Sánchez, Domingo, & Castel, 2010). El uso de esta estrategia mejora la calidad de la uva y del vino, sin embargo reduce el tamaño de las bayas, resultando en una elevada proporción de la piel respecto a la pulpa, y produciendo un efecto de concentración de ciertos compuestos (Cáceres-Mella, Ribalta-Pizarro, Villalobos-González, Cuneo, & Pastenes, 2018; Kennedy, Matthews, & Waterhouse, 2002; Romero et al., 2013). Algunos estudios demuestran que este tipo de riego puede mejorar eficientemente varios índices de calidad de las cosechas con los consiguientes ahorros de agua (Yang et al., 2020). El déficit de agua estimula el metabolismo secundario en las bayas, concretamente durante el envero se induce una acumulación transitoria de azúcar y de ácido abscísico. Ambos procesos son señales de expresión de genes y síntesis de proteínas involucrados en la ruta de los fenilpropanoides de la piel de uvas, conduciendo a la acumulación de flavanoles, flavonoles, y antocianinas (Cáceres-Mella et al., 2018; Castellarin, Matthews, Di Gaspero, & Gambetta, 2007; Deluc et al., 2009; Villalobos-González, Peña-Neira, Ibáñez, & Pastenes, 2016). Respecto a las antocianinas totales, un riego moderado aumentó su concentración en la variedad '*Cabernet Sauvignon*' en las campañas de 2015 y 2016 (Ju et al., 2019).

En un estudio sobre la influencia del riego en la composición de la piel de la variedad '*Cabernet Sauvignon*' se observó que los compuestos fenólicos totales incrementaron su concentración de 14,02 a 21,09 mg de ácido gálico·$g^{-1}$ de piel durante la maduración, con

valores de fenoles totales significativamente mayores en los tratamientos con menor dosis de riego, desde los días 13 al 41 después del envero. Respecto a los compuestos 3-flavanoles monoméricos, se observaron pocas diferencias entre los distintos tratamientos de riego (Cáceres-Mella, Talaverano, Villalobos-González, Ribalta-Pizarro, & Pastenes, 2017). En otro estudio con esta misma variedad se observó que empleando un estrés hídrico más severo se obtenía mayor concentración de fenoles totales y antocianinas, y además, este estrés hídrico no afectó negativamente a la concentración de 3-flavanoles (Cáceres-Mella et al., 2018).

En un estudio llevado a cabo en Extremadura, una región semiárida, en el que aplicaron riego a un viñedo de la variedad '*Tempranillo*' de acuerdo a sus necesidades de ETc, se observó que el riego alargaba el ciclo de crecimiento y que no hubo diferencias significativas en la evolución de los fenoles y flavonoides totales en la maduración, en las muestras sometidas a riego y en las de secano (Garrido et al., 2016).

Respecto a las tecnologías no invasivas para controlar el estado hídrico de los viñedos, se ha utilizado la espectroscopia NIR para estudiar la influencia de tres regímenes hídricos en uvas de la variedad '*Tempranillo*'. Se registraron *in situ* los espectros de infrarrojo de las hojas de los viñedos y se tomaron medidas del potencial hídrico y de la conductancia de las hojas. Los modelos de calibración, validación y predicción se llevaron a cabo con PLS y, mediante PLS-DA, se consiguió clasificar los tres regímenes hídricos (Fernández-Novales, Tardaguila, Gutiérrez, Marañón, & Diago, 2018).

Es común en las plantaciones limitar el rendimiento para obtener, en su mayoría, uvas de mayor calidad (Wang et al., 2018). El nivel de carga de las uvas es un factor que está estrechamente ligado a la calidad del fruto e influye en el rendimiento y en la calidad de la cosecha de la siguiente campaña (Gil et al., 2013; Song, Wang, Xie, & Zhang, 2018). Los aclareos de racimos, es decir, la supresión total o de una parte del mismo, son una práctica agronómica ampliamente aceptada para regular el rendimiento. En las investigaciones recientes, no hay acuerdo en cómo afecta el aclareo de racimos a la maduración de la baya (Wang et al., 2018). En un estudio en el que se analizaron variedades de uva '*Cabernet Sauvignon*' durante dos campañas, la aplicación de aclareos de racimos tempranos promovió significativamente la concentración de antocianinas totales en el envero, sin encontrar diferencias con el control en cosecha en ambas campañas. En cosecha, los aclareos tempranos

y tardíos no afectaron significativamente a la concentración de flavonoles totales en ambas campañas. En la cosecha de la campaña 2013, los aclareos de racimos, tempranos y tardíos, no tuvieron efecto en la concentración de 3-flavanoles mientras que en la campaña 2014, la aplicación del aclareo temprano disminuyó el nivel de 3-flavanoles mientras que el aclareo tardío tuvo el efecto opuesto (Wang et al., 2018). En otro estudio con uvas '*Summer Black*', la aplicación de aclareos de racimos aumentó significativamente el contenido de antocianinas y el total de sólidos solubles (Xi, Zha, Jiang, & Tian, 2016). Los efectos del aclareo de racimos también se han estudiado en vinos de la variedad '*Syrah*', encontrando que los vinos procedentes de viñedos con aclareos de racimos presentaban mayor concentración de flavonoides totales, polifenoles totales y monómeros de antocianinas totales (Condurso et al., 2016). También se ha aplicado la técnica del aclareo en uvas de la variedad '*Pinot Noir*', encontrando que esta técnica no afectó los fenoles totales, taninos totales y fenoles no tánicos (Mawdsley, Dodson Peterson, & Casassa, 2018). En un estudio en vinos elaborados a partir de uvas de la variedad '*Istrian Malvasia*' se observó que la concentración de compuestos fenólicos tales como ácido cafeico, ácido *p*-cumárico, y ácido gálico aumentaban con un nivel bajo de carga durante dos campañas, aunque las diferencias fueron no significativas (Bubola, Rusjan, & Lukić, 2020).

La aplicación combinada del aclareo de racimos con otras técnicas agronómicas, como la eliminación de hojas, es recomendable en la producción de vinos tintos de alta calidad de las variedades '*Cabernet Sauvignon*' y '*Probus*' en Serbia (Ivanišević, Kalajdžić, Drenjančević, Puškaš, & Korać, 2020).

### 3.1.2 ***Ciruela***

#### 3.1.2.1 El cultivo del ciruelo y su producción en fresco

La Organización de las Naciones Unidas para la Alimentación sitúa a España como el decimosexto productor de ciruelas del mundo y séptimo a nivel europeo (FAOSTAT, 2018). El principal productor a nivel mundial es China seguido de Rumanía y Serbia.

En lo que respecta al cultivo de ciruelo en España, el Anuario de Estadística de 2018 del Ministerio de Agricultura, Pesca y Alimentación recoge los datos más recientes de producción y superficie cultivada, siendo los últimos datos mostrados los del 2017 (MAPA, 2019a).

Tal como se recoge en dicho anuario, el ciruelo en España cuenta con una superficie de plantación regular de 15.199 ha, de las que 1.888 ha están dedicadas a secano y 13.311 ha a regadío. Estas cifras colocan al ciruelo como el quinto frutal de hueso más cultivado en España. El rendimiento en secano ha sido de 3.321 kg/ha y en regadío 14.414 kg/ha. La producción total ascendió a 172.325 t de ciruelas. Por comunidades, Extremadura ocupa el primer lugar en producción con un total de 78.150 t, seguida de Andalucía y Murcia con 30.663 y 16.492 t, respectivamente (MAPA, 2019a).

A continuación, en los **Gráficos 4 y 5** elaborados con los datos de dicho anuario, se muestra la evolución de la superficie total cultivada y la producción de ciruela, en el periodo 2007-2018.

En el **Gráfico 4** se observa como desde el año 2007 se ha producido un descenso de la superficie destinada a las plantaciones de ciruelos, llegando hasta el mínimo de superficie plantada en 2018. En cuanto a la producción de ciruela, **Gráfico 5,** se puede observar que se han producido oscilaciones en la producción durante el periodo comprendido entre 2007-2013, pero a partir del año 2014 se muestra una clara disminución. Esta merma en la producción de ciruela de los últimos años viene dada, mayoritariamente, por heladas y mala floración, que ha propiciado la falta de cuajado de las flores, efectos que han sido muy significativos en las tres principales zonas productoras de España: Extremadura, Andalucía y Murcia.

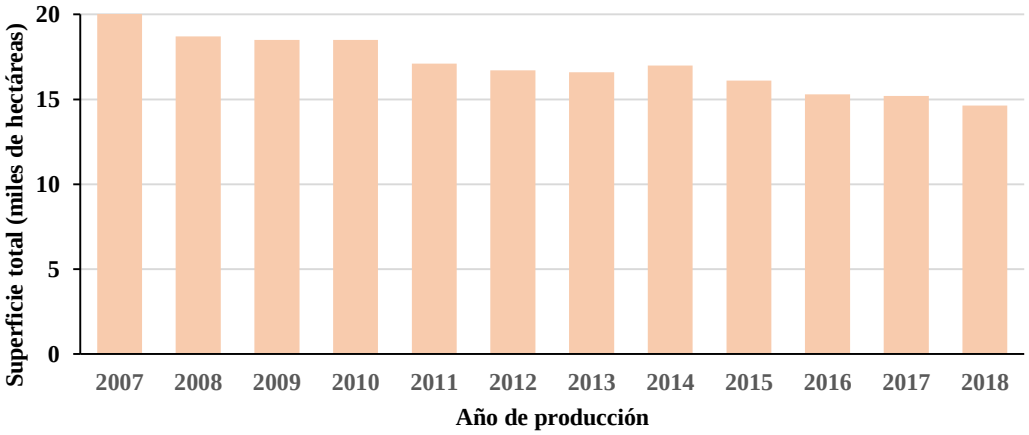


***Gráfico 4.*** *Evolución de la superficie de cultivo de ciruelo. Elaborado a partir de datos del Ministerio de Agricultura (MAPA, 2019a).*

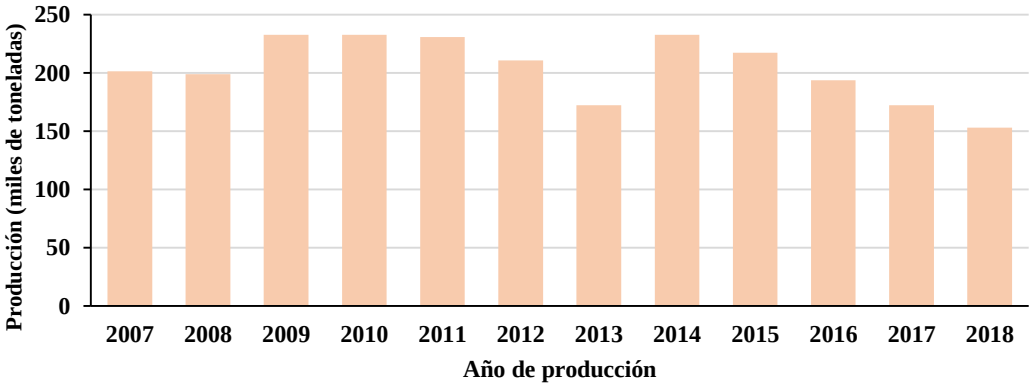


***Gráfico 5.*** *Evolución de la producción de ciruela. Elaborado a partir de datos del Ministerio de Agricultura (MAPA, 2019a).*

En cuanto a Extremadura, en el año 2018, cuenta con una superficie de ciruelo de 6.806 ha y una producción 74.150 t (Picón Toro et al., 2018).

El Plan de Medidas para la mejora del sector de fruta dulce del Ministerio de Agricultura, Pesca y Alimentación incluye el fomento de la calidad de las producciones, debido a que existen estudios estadísticos que evidencian que la comercialización de productos de mala calidad provoca experiencias negativas en los consumidores, que acaban dirigiendo sus preferencias de consumo hacia otras frutas sustitutivas. A menudo, la falta de calidad del

producto es atribuible a una recolección excesivamente temprana o a un almacenamiento prolongado antes de su comercialización (MAPAMA, 2018).

Para mejorar la calidad de estos productos, las principales organizaciones de productores, al comienzo de cada campaña, deben hacer llegar a sus socios cuáles son los requisitos mínimos de calidad: contenido mínimo en ºBrix, consistencia de la fruta, periodos de almacenamiento adecuados, así como cualquier otra información relevante que ayude a la mejora de la calidad de esta fruta (MAPAMA, 2018).

Otra medida para fomentar la calidad sería el desarrollo de parámetros de calidad diferenciada en el sector de la fruta para ser acogidos a DOP o a IGP, ya que constituyen una oportunidad para aumentar el valor de las producciones que estén amparadas en estos distintivos de calidad diferenciada, que proporcionan una garantía para que el consumidor asocie la fruta dulce con el concepto de calidad (MAPAMA, 2018). Sin embargo, para el cultivo del ciruelo no existen estos distintivos de calidad, como DOP o IGP, a nivel nacional, mientras que otros países como Italia y Francia sí que tienen reconocidas varias DOPs. Recientemente se ha creado en Extremadura la marca de calidad CiEx® (Ciruela de Extremadura), impulsada por el colectivo Afruex (Asociación de Fruticultores de Extremadura), con el fin de dar valor añadido a las ciruelas de esta región. La marca incluye las siguientes variedades de ciruela: '*Angeleno*', '*Black Splendor*', '*Crimson Globe*', '*Fortune*', '*Golden Globe*', '*Larry Ann*', '*Owen-T*' y '*Primetime*'(Guerrero, Rodrigo, & Guerra, 2018). Dentro de estas variedades de ciruelo, '*Angeleno*' es la más extendida en el mundo. El éxito de esta variedad se debe a su alto rendimiento, alto contenido en azúcares y buena apariencia, maduración tardía y amplia vida útil (Corelli Grappadelli, Morandi, Manfrini, & O'Connell, 2019).

### 3.1.2.2 Maduración en ciruelas. Métodos de análisis

Durante la maduración de los frutos, tienen lugar una serie de procesos fisiológicos y bioquímicos, que promueven, entre otros, cambios en el color, sabor, textura, aroma y contenido nutricional del mismo (Rodrigo, Alquézar, Alférez, & Zacarías, 2012). En ciertas variedades de ciruelas, con la maduración se incrementa tanto el peso de las mismas como el contenido en sólidos solubles, azúcares totales y antocianinas y se produce una disminución de la firmeza (Usenik, Kastelec, Veberič, & Štampar, 2008).

Las ciruelas son frutos altamente perecederos que experimentan un rápido deterioro durante el transporte, almacenamiento y puesta en los mercados en detrimento de la vida útil (Wang et al., 2018). El estado de maduración de las ciruelas en el momento de la cosecha guarda una estrecha relación con su vida útil durante el almacenamiento. Mientras la ciruela permanece en el árbol, las pérdidas producidas por la respiración y transpiración son restituidas por el flujo de la savia del árbol, sin embargo, una vez que se cosecha el fruto, los procesos fisiológicos comienzan a consumir las reservas del propio fruto. Las ciruelas, generalmente se cosechan en una etapa temprana de maduración, antes de los cambios de color que se producen naturalmente en el fruto durante la maduración, por lo que se conservan a baja temperatura para prologar su vida útil post-cosecha, antes de ser puesta en los mercados (Li et al., 2017; Pan, Wang, Wang, Xie, & Cao, 2018). Por todos estos motivos, es fundamental la determinación del momento óptimo de cosecha de la ciruela, puesto que tiene una gran influencia en el tiempo de almacenamiento durante las operaciones comerciales y en los parámetros finales de calidad.

Tradicionalmente, los agricultores y técnicos, en base a su experiencia, han evaluado *in situ* en los propios cultivos el estado de maduración de las ciruelas de manera visual, fijándose en cambios morfológicos tales como el color de la piel, la forma, el sabor y la textura (Ndou, Tinyani, Slabbert, Sultanbawa, & Sivakumar, 2019). Es cierto que el control del estado de maduración es bastante complejo dado que hay que monitorizarlos siguiendo múltiples parámetros de calidad internos y externos tales como concentración de sólidos solubles, acidez valorable, tamaño y firmeza, entre otros (El-Sharkawy, Sherif, Qubbaj, Sullivan, & Jayasankar, 2016). Estos parámetros de calidad se llevan a cabo con técnicas instrumentales

que son destructivas, laboriosas y en muchos casos no están estandarizadas (ElMasry & Nakauchi, 2016; Pathare, Opara, & Al-Said, 2013).

El color de la piel, otro de los parámetros de calidad en las frutas de hueso, está condicionado, entre otros factores, por la concentración y distribución de las antocianinas (Usenik, Štampar, & Veberič, 2009). Es uno de los parámetros más importantes en el seguimiento de la maduración de frutas de hueso. Sin embargo, no siempre resulta útil su monitorización dado que, en algunas variedades, el color definitivo del fruto se alcanza de forma temprana, cuando el fruto todavía es inmaduro y no tiene suficiente sabor ni flavor (Usenik et al., 2008).

En un estudio llevado a cabo durante el proceso de maduración de ciruelas de la variedad *Sanshua*, en el que los diferentes estados de desarrollo se establecieron en base al color: verde, aparición incipiente del color rojo, rojo parcial, rojo intenso y rojo violáceo, mostró que la acidez disminuyó durante la maduración, mientras que los azúcares solubles aumentaron. Respecto al contenido fenólico, tanto los fenoles totales como los flavonoides totales disminuyeron durante el desarrollo del fruto, mientras que las antocianinas aumentaron (Li, Chang, Wang, Stephen Brennan, & Guo, 2019).

En un estudio reciente, se han analizado los principales compuestos de la piel en muestras de ciruela de tres variedades, en seis periodos diferentes de cosecha. Los fenoles totales no mostraron una tendencia clara, excepto para una de las variedades en las que aumentó el contenido a medida que se cosechaba más tarde. El contenido de flavonoides totales disminuyó en las tres variedades, siendo su disminución estadísticamente significativa en dos de ellas. Considerando solo las tres últimas fechas de cosechas, las antocianinas aumentaron en las tres variedades (Vlaic et al., 2018). En ciruelas de la variedad '*Furongli*', el mayor contenido de antocianinas y el menor contenido de compuestos fenólicos y flavonoides se encontró en las frutas maduras (Jiang, Fang, Zhou, Pan, & Ye, 2019).

Existen datos sobre la evolución de los compuestos químicos más usuales en las variedades '*Mirabolano*', '*President*' y '*Shiro*' a partir de los 20 días después de la floración. Se observó que la firmeza del fruto disminuyó mientras que los ºBrix aumentaron durante la maduración. El contenido de fenoles totales, así como de los fenoles individuales por g de

materia seca, disminuyeron durante la maduración. Por último la concentración de los ácidos neclorogénico y clorogénico también disminuyó sustancialmente durante la maduración, en algunos casos más del 50% (Moscatello et al., 2019).

El uso de tecnologías no destructivas para evaluar la madurez y la calidad de las frutas permiten la determinación simultánea de múltiples parámetros de calidad (Louw & Theron, 2010). Entre las técnicas no destructivas que se han desarrollado para el control de la maduración destacan las imágenes multiespectrales e imágenes hiperespectrales (Li et al., 2018). Imágenes hiperespectrales, en la región del infrarrojo y visible, de ciruelas de la variedad '*Victoria*' y '*Marjorie´s Seedling*', en combinación con PLS han permitido la predicción de la cantidad de sólidos solubles y el color (B. Li et al., 2018). También se ha propuesto un método basado en el análisis de imágenes hiperespectrales de los frutos de ciruelo japonés mediante técnicas de aprendizaje profundo (DeepLearning), utilizando para ello redes neuronales convolucionales para lograr una correcta clasificación de los frutos por su variedad y su fecha de maduración (Rodríguez, García, Pardo, Chávez, & Luque-Baena, 2018). Imágenes de rayos láseres han sido utilizadas para analizar la evolución en el contenido de antocianinas a lo largo del proceso de maduración (Rezaei Kalaj, Mollazade, Herppich, Regen, & Geyer, 2016).

La autofluorescencia de las ciruelas intactas debida a la presencia de pigmentos clorofílicos también ha sido utilizada para evaluar la evolución de la maduración. En este sentido, Monago-Maraña et al. (2020) obtuvieron las matrices de excitación-emisión por medio de una fibra óptica en las cuatro caras de cada fruto que les permitió obtener la información fluorescente a lo largo de 8 semanas de maduración. Estas matrices fueron analizadas mediante análisis paralelo de factores (PARAFAC), mínimos cuadrados parciales multivía (N-PLS), mínimos cuadrados parciales desdoblados (U-PLS) y resolución multivariante de curvas en combinación con mínimos cuadrados alternantes (MCR-ALS). De los dos componentes obtenidos por PARAFAC, para los "*scores*" del primero se observó un aumento del mismo durante las primeras cinco semanas, disminuyendo en las últimas. En las últimas semanas se obtuvo un aumentó en el número de componentes de PARAFAC para explicar el modelo. Mediante MCR-ALS se observó una clara disminución de la intensidad de fluorescencia de los espectros de excitación de la clorofila *b* a lo largo de la maduración

de las ciruelas. En cuanto a la predicción de las concentraciones de las clorofilas, se obtuvo mejor resultado por U-PLS y N-PLS en la piel de las ciruelas (Monago-Maraña, Domínguez-Manzano, Muñoz de la Peña, & Durán-Merás, 2020).

### 3.1.3 ***Aceitunas***

#### 3.1.3.1 El cultivo del olivo y su producción para aceituna de mesa y aceite

La Organización de las Naciones Unidas para la Alimentación sitúa a España como primer productor de aceitunas a nivel mundial (FAOSTAT, 2018). El segundo y tercer productor de aceitunas son Italia y Marruecos, respectivamente.

En lo que respecta al cultivo del olivo, el Anuario de Estadística de 2018 del Ministerio de Agricultura, Pesca y Alimentación recoge los datos más recientes de producción y superficie cultivada, siendo los últimos datos mostrados los del 2017 (MAPA, 2019a). El cultivo del olivo en España cuenta con una superficie de plantación total de 2.554.829 ha, de las que 166.997 ha corresponden a olivar de aceitunas de mesa, mientras que 2.387.832 ha a olivar de aceituna con destino a almazara. Del total de la superficie de cultivo de aceituna de mesa, 131.665 ha corresponden a secano y 35.332 ha a regadío. De la superficie dedicada al cultivo de aceituna para almazara, 546.785 ha corresponden a regadío y 1.841.047 ha corresponden a secano (MAPA, 2019a).

El olivar de aceituna de mesa presenta un rendimiento en secano de 2.436 kg/ha y en regadío de 5.485 kg/ha y para almazara presenta un rendimiento en secano de 1.988 kg/ha y en regadío 4.976 kg/ha. La producción total ha sido de 505.046 t de aceitunas de mesa y 6.044.453 t de aceitunas para almazara. En la campaña 2017/2018 se han obtenido 570.153 t de aceituna aderezada, 1.238.629 t de aceite de oliva virgen y 61.477 t de aceite de orujo. Del total de aceite de oliva virgen, 730.297 t corresponden a virgen extra, 329.844 t a aceite virgen y 178.488 t a aceite lampante (MAPA, 2019a).

Destacar los nuevos sistemas de plantación, en los que se colocan los olivos en hileras conocidas como “setos” y separados por calles anchas que permiten el paso de maquinaria para realizar las labores y la recolección mecanizada. Estos son sistemas superintensivos en los que las producciones casi duplican a las obtenidas por sistemas tradicionales. Este tipo de cultivo está cada vez más extendido, sobre todo cuando la aceituna se destina a la elaboración de aceite en almazara. En general, resaltar que las aceitunas producidas de forma tradicional conllevan a una mayor calidad del producto final y suelen estar más valoradas en el mercado que las cultivadas en sistemas de producción intensivos o superintensivos.

A continuación, se muestran los gráficos elaborados con los datos presentes en dicho anuario, en los cuales se representa la evolución de la superficie total cultivada y la producción de aceitunas, en el periodo 2007-2018.

En el **Gráfico 6** se observa que a partir de 2009 se ha producido un aumento de la superficie de olivar destinada a aceituna de almazara, mientras que la superficie de olivar para aceituna de mesa se mantiene prácticamente constante desde 2007 hasta la fecha.

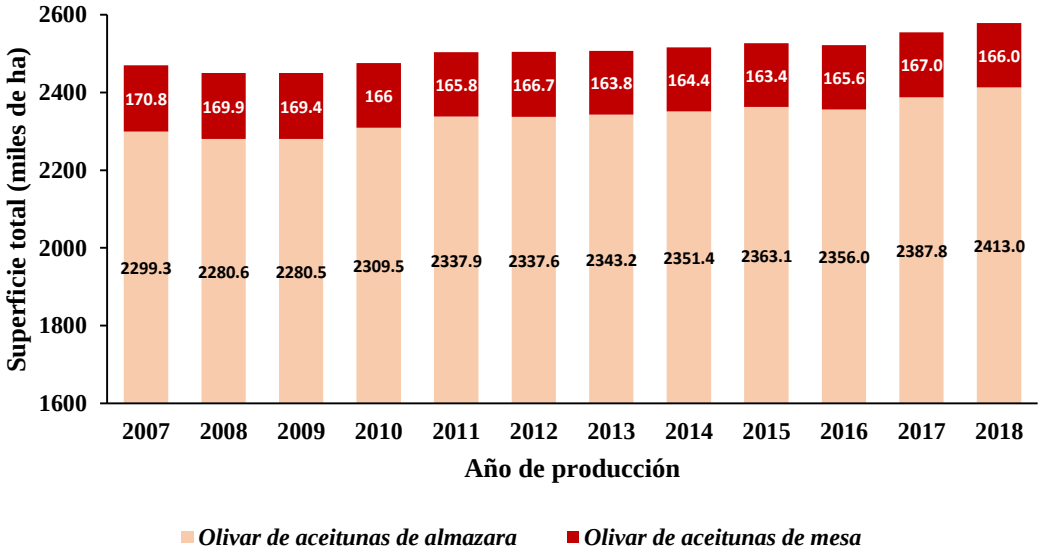


***Gráfico 6.*** *Evolución de la superficie de olivar. Elaborado a partir de datos del Ministerio de Agricultura (MAPA, 2019a).*

En el **Gráfico 7** se observan marcadas oscilaciones de la producción de aceituna para almazaras. En cuanto a la producción de aceituna de mesa, también se distinguen oscilaciones en torno a 500.000 t. Esto es debido a la propia vecería del olivo que hace que en un año se produzca abundante cosecha, mientras que en otro esta producción se ve mermada significativamente. Este fenómeno se da más en los olivares tradicionales. Además, las condiciones ambientales juegan un papel fundamental en la fructificación del olivo.

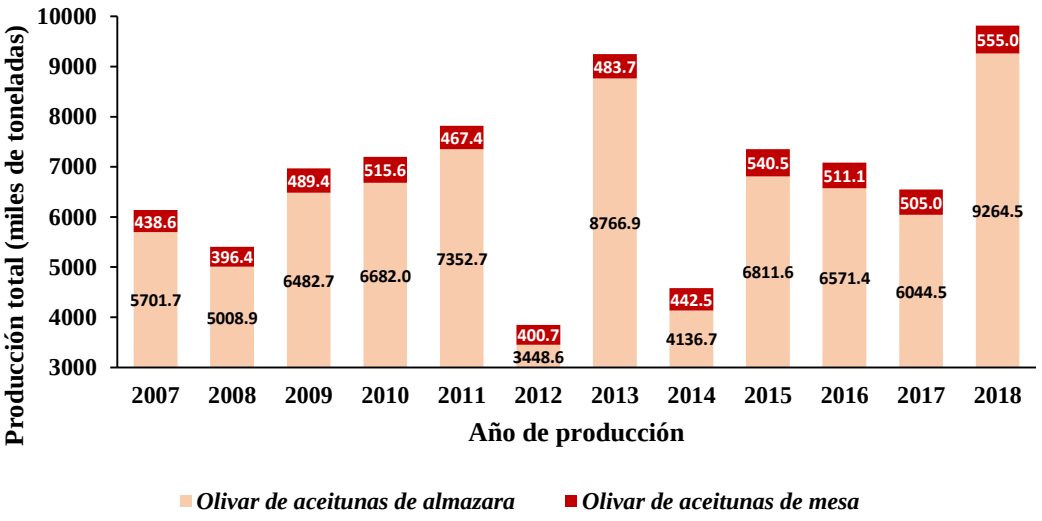


***Gráfico 7.*** *Evolución de la producción de aceitunas. Elaborado a partir de datos del Ministerio de Agricultura (MAPA, 2019a).*

Por comunidades, Andalucía ocupa el primer lugar en producción de aceitunas de mesa con un total de 348.176 t, seguida de Extremadura con un total de 149.266 t. Entre ambas superan el 98% de la producción nacional de aceituna de mesa. Respecto a la producción de aceituna para almazara, Andalucía ocupa el primer lugar con 4.671.729 t, seguida de Castilla La Mancha y de Extremadura con un total de 463.037 y 370.635 t, respetivamente (MAPA, 2019a).

En Extremadura, la superficie de aceituna de mesa en 2018 es de 68.357 ha. La producción de aceituna de mesa fue de 113.352 t en 2018, lo que supone una disminución del 3,69% respecto a la producida en 2017, en el que se recogieron 117.700 t. En 2018, la superficie de aceituna para almazara fue de 192.992 ha. La producción de aceituna para almazara aumentó un 4,48% respecto a 2017, alcanzando 205.979 t. La producción de aceite de oliva aumentó un 56,87% respecto a 2017 (Picón Toro et al., 2018).

En Extremadura, el olivar es uno de los cultivos de mayor importancia, estando presente en, prácticamente, todas las comarcas. Extremadura presenta 12 zonas de producción homogénea de aceite de oliva o comarcas oleícolas las cuales se muestran en la **Figura 2**. En

la provincia de Cáceres se encuentran las siguientes comarcas: Gata-Hurdes, La Vera-Ambroz-Jerte, Ibores, Logrosán-Guadalupe, Montánchez y el resto de la provincia. En Badajoz, se localizan las siguientes: Alburquerque, Vegas del Guadiana, Tierra de Barros, La Siberia, La Serena y Jerez-Llerena (Reglamento (CE) nº 2138/97).


***Figura 2.*** *Comarcas oleícolas extremeñas. Gata-Hurdes (GH), La Vera-Ambroz-Jerte (VAJ), Ibores (I), Logrosán Guadalupe (LG), Montánchez (M), el resto de Cáceres (RC), Alburquerque (A), las Vegas del Guadiana (VG), Tierra de Barros (TB), La Siberia (LSI), La Serena (LSE) y Jerez-Llerena (SL). Modificación de (Llerena Ruiz, 2005).*

En cuanto a la distribución de variedades de aceitunas en Extremadura, las principales variedades autóctonas son '*Cornicabra*', '*Manzanilla Cacereña*', '*Pico Limón*' y '*Verdial*. Otras variedades que con el paso de los años han ido ganando peso son '*Picual*', '*Hojiblanca*' y '*Arbequina*', esta última muy extendida en sistemas superintensivos (Llerena Ruiz, 2005).

Las industrias transformadoras, almazaras y entamadoras han permitido el desarrollo económico básico de muchas de estas comarcas extremeñas. Desde hace años, se están haciendo enormes esfuerzos por mejorar la calidad en la producción de productos oleícolas.

De hecho, la región cuenta con la DOP Gata Hurdes y la DOP Aceite de Monterrubio (Llerena Ruiz, 2005).

### 3.1.3.2 Maduración en las aceitunas. Métodos de análisis

La maduración de las aceitunas es una combinación de procesos bioquímicos y fisiológicos, marcados genéticamente por la variedad de aceituna, y que además están muy condicionados entre otros factores, por aspectos edafoclimáticos relativos al clima, el suelo y también a la edad del olivo y prácticas agronómicas (Connor & Fereres Castiel, 2005).

Durante la maduración, se producen cambios físico-químicos en el fruto que afectan a las características sensoriales y a la composición del aceite y de las aceitunas de mesa obtenidas (Alowaiesh, Singh, Fang, & Kailis, 2018; Cabrera-Bañegil, Pérez-Nevado, Montaño, Pleite, & Martín-Vertedor, 2018; Kiai, Raiti, El Abbassi, & Hafidi, 2020; Nsir et al., 2017). En un estudio con diferentes variedades de aceitunas tales como '*Frantoio*', '*Leccino*', '*Picholine*' y '*Coratina*', se concluyó que el contenido en polifenoles disminuye a lo largo de las últimas etapas de maduración (Kong et al., 2019). El mismo efecto se observó en el contenido de fenoles totales durante la maduración en las variedades '*Frantoio*' y '*Manzanilla*'. Además, se cuantificaron individualmente algunos fenoles, encontrándose que la concentración de hidroxitirosol y tirosol también disminuían a medida que avanzaba la maduración (Alowaiesh et al., 2018). Por el contrario, en otro estudio se ha encontrado que el contenido de hidroxitirosol, tirosol y ácido cafeico en '*Manzanilla*' aumentaba con la maduración, mientras que la concentración de oleuropeína disminuía (Crawford, Holstege, & Wang, 2018). Por su parte, en variedades portuguesas, la concentración de oleuropeína muestra una tendencia diferente con la maduración. Mientras que en la variedad '*Cobrançosa*' se ha descrito que la oleuropeína presenta una concentración máxima en el estado de maduración más tardío, en la variedad '*Galega Vulgar*', el máximo se alcanza en un estado de maduración intermedio (Ferro et al., 2020). En un estudio en el que se cosecharon aceitunas de la variedad '*Moroccan Picholine*' se encontraron mayores contenidos de azúcar, fenoles totales y flavonoides en envero que cuando las aceitunas se encontraban más maduras (Kiai et al., 2020). Por el

contrario, en aceitunas de la variedad '*Cellina di Nardo*', se ha observado un progresivo incremento del contenido de fenoles totales durante la maduración (Aprile et al., 2019).

Todos estos cambios en la composición química, así como el contenido de aceite, los atributos sensoriales y la fuerza de retención del fruto determinan el momento óptimo de cosecha (Guzmán, Baeten, Fernández Pierna, & García-Mesa, 2015). El método más común para evaluar la maduración de las aceitunas es el índice de madurez (IM), basado en la determinación visual del color de la piel y la pulpa de cien frutos maduros clasificados en una escala de valores de 0 a 7 (Uceda & Frías, 1975). Estos cambios del color de la aceituna se deben a la variación de los pigmentos con la maduración como las clorofilas y carotenoides, entre otros (Mínguez-Mosquera & Gallardo-Guerrero, 1995; Roca & Mínguez-Mosquera, 2000). La decisión del momento de cosecha depende del destino final de las aceitunas: elaboración de aceite o aceitunas de mesa. Para este último, además, el valor del índice de maduración es diferente en función del método de elaboración de las aceitunas (Rallo et al., 2018). En este sentido, para la elaboración de aceitunas verdes al estilo español, elaboración muy común en industrias de la región extremeña, se recolectan las "aceitunas de verdeo", las primeras de la campaña, es decir, cuando presentan un índice de maduración verde (IM = 1). No obstante, la determinación del índice de maduración en el laboratorio consume mucho tiempo y es una determinación bastante subjetiva, dado que depende de la experiencia del evaluador y de las condiciones ambientales del momento de la toma de muestra en el campo (Guzmán et al., 2015).

Para estimar la masa, tamaño y geometría de las aceitunas a partir de técnicas de análisis de imágenes, se fotografiaron aceitunas de la variedad '*Picual*' y '*Arbequina*' en el laboratorio. Se estableció una correlación entre la segmentación adquirida en la imagen y la masa y tamaño de las aceitunas (Ponce, Aquino, Millán, & Andújar, 2018). En otro estudio se fotografiaron nueve variedades, entre ellas, '*Arbequina*' y '*Picual*', y también se correlacionó la información de la imagen con la masa y el tamaño obteniendo errores en torno al 1% en la determinación del eje mayor y de la masa de las aceitunas (Ponce, Aquino, Millan, & Andújar, 2019). Sin embargo, las técnicas que evalúan la madurez de la cosecha, generalmente, están relacionadas exclusivamente con el color (Lazzez et al., 2011) y la fecha de cosecha depende de muchos otros parámetros como la firmeza, el contenido en grasa, la

composición química y las características sensoriales (González-Cabrera, Domínguez-Vidal, & Ayora-Cañada, 2018). La FT-IR complementa las técnicas basadas en la obtención de imágenes proporcionando información a nivel bioquímico (González-Cabrera et al., 2018). El NIRS permite la determinación, entre otros parámetros, de la grasa y humedad en aceitunas intactas (Lee, Polari, Kramer, & Wang, 2018). Así, se ha empleado en la monitorización de la maduración de aceitunas de la variedad '*Picual*' durante las campañas 2015/2016. En combinación con PLS-DA se ha conseguido agrupar a las aceitunas según su nivel de maduración (verde, color cambiante y negro) (González-Cabrera et al., 2018).

#### 3.1.3.3 Riego en el cultivo del olivo. Métodos de análisis

Aunque como se ha indicado previamente el olivo es un árbol de secano, el gran aumento de la producción que se consigue con un riego controlado ha conllevado que la superficie de olivar con riego haya aumentado considerablemente durante los últimos años, observándose que el riego es una práctica común en los olivares intensivos y superintensivos (Ahumada-Orellana, Ortega-Farías, & Searles, 2018; Casanova et al., 2019; López-Olivari, Ortega-Farías, & Poblete-Echeverría, 2016). La aplicación del riego se debe de hacer de forma controlada y, dependiendo de las características edafológicas, climatológicas y del sistema de plantación (García-Tejera, López-Bernal, Orgaz, Testi, & Villalobos, 2018), el tipo de riego a aplicar podrá ser RDC o riego de apoyo. El olivar en regadío implica la presencia continua de agua en el suelo, lo que conlleva un enorme consumo. El RDC trata de racionalizar el riego del olivo en función del efecto del aporte de agua, suministrando una mayor cantidad de agua durante la floración y primeras semanas de endurecimiento del hueso, recortando los aportes de agua durante la temporada estival y volviendo a aumentar la dosis de riego poco antes de la recogida de las aceitunas (Hueso, Trentacoste, Junquera, Gómez-Miguel, & Gómez-del-Campo, 2019). El riego de apoyo consiste en aportar los recursos hídricos en momentos puntuales del ciclo vegetativo del cultivo, con el objetivo de obtener una cosecha óptima durante las etapas más críticas como son la floración, el cuajado del fruto y el endurecimiento del hueso, ya que un déficit hídrico en estos periodos podría provocar la abscisión del fruto.

En los olivares españoles el riego más implantado es el riego deficitario, teniendo en cuenta que su efecto depende de la etapa fenológica de la planta en la que se instaura, dado

que algunas de ellas son más sensibles que otras a la falta de agua (Campillo Torres et al., 2009).

Entre los beneficios que produce la aplicación de RDC sobre la composición de la aceituna y los aceites, indicar que se han encontrado mejoras en el contenido de compuestos fenólicos y ácidos grasos en ambas matrices (Cano-Lamadrid et al., 2015; Sánchez-Rodríguez et al., 2019; Sánchez-Rodríguez, Corell et al., 2019).

Las estrategias de riego deficitario pueden ser más o menos moderadas en función del momento fenológico en el que se aplican y de la duración de los periodos de estrés hídrico. Así, en la aplicación de dos estrategias de riegos deficitarios diferentes sobre la variedad de aceituna '*Manzanilla*', se observó que el contenido de fenoles totales aumentaba con un estrés hídrico (Sánchez-Rodríguez et al., 2019).

En cuanto a la influencia del riego deficitario en ensayos con la variedad '*Arbequina*', una de las más utilizadas en olivares superintensivos, en general se observa que el contenido de compuestos fenólicos tendió a disminuir a medida que la dosis de riego era menor. Algunos compuestos fenólicos como hidroxitirosol y tirosol disminuyeron con los tratamientos de riego de menor aporte de agua (García, Hueso, & Gómez-del- Campo, 2020). Sin embargo, en otro estudio en el que se analizó la variedad '*Frantoio*', también en olivar superintensivo, se encontró que los mayores contenidos de compuestos fenólicos totales se dieron con un tratamiento de riego deficitario intermedio sin observar una tendencia clara para tirosol e hidroxitirosol (Gucci et al., 2019).

Por lo tanto, sería de utilidad en el sector un método de determinación rápido que permita realizar medidas "*in situ*" para tomar decisiones en función del estado hídrico del olivo. En este contexto, la espectroscopia NIR, por sus características no invasivas, rápidas y económicas, es una buena alternativa respecto a los métodos tradicionales (Torres, Sánchez, Benlloch-González, & Pérez-Marín, 2019). En un trabajo en el que se analizaron por NIRS hojas de olivos de variedades '*Picual*' y '*Arbequina*' a lo largo de un año de estudio, permitió obtener una medida cuantitativa del estado hídrico del cultivo del olivo (Torres et al., 2019). Sin embargo, no siempre los datos obtenidos en las hojas muestran la misma tendencia que en el fruto. En un estudio con la variedad '*Picual*' se encontró que, mientras con riego

aumentaba la concentración de oleuropeína en las hojas, en el fruto las mayores concentraciones se dieron aplicando un cierto estrés hídrico. Las concentraciones de tirosol fueron mayores en hojas y fruto con estrés hídrico, mientras que cuando el olivo presentaba un buen estado hídrico del cultivo, el contenido en hidroxitirosol fue mayor en hoja y fruto (Jiménez-Herrera, Pacheco-López, & Peragón, 2019).

## 3.2 CARACTERÍSTICAS DE LOS COMPUESTOS FENÓLICOS

Los analitos estudiados en esta Tesis Doctoral son principalmente compuestos fenólicos, por lo que a continuación se va a hacer una breve descripción de los compuestos fenólicos más abundantes en las diferentes matrices alimentarias estudiadas a lo largo de la parte experimental de la misma.

Los compuestos fenólicos son los antioxidantes más abundantes en la dieta humana y componentes comunes de frutas, vegetales y derivados (Ruiz-Ruiz, Esapadas Aldana, Corona Cruz, & Segura-Campos, 2020). Proceden del metabolismo secundario de las plantas jugando un papel esencial en su defensa y supervivencia (Tsimogiannis & Oreopoulou, 2019). Estos compuestos tienen una gran diversidad estructural cuya base común (o esqueleto) son los grupos hidroxilos en los anillos aromáticos (Vuolo, Lima, & Maróstica Junior, 2019). Las familias de polifenoles, en función del número de átomos de carbono que están presentes en su estructura química básica, se pueden clasificar como: fenoles simples, ácidos fenólicos, flavonoides, taninos, cumarinas, estilbenos y lignanos y alcoholes fenólicos, entre otros (Bravo, 1998; Ryan, Robards, Prenzler, & Antolovich, 1999). El conjunto de estas familias, su número de átomos de carbono y su esqueleto básico se encuentran resumidos en la **Tabla 1**.

Cada grupo tiene un mecanismo de acción diferente en base a su estructura química, que le confiere propiedades propias (Vuolo et al., 2019). En el campo agro-frutícola, existe un alto interés en estos compuestos por su influencia en diferentes atributos organolépticos como el color, sabor y el aroma de los frutos (Al-Farsi, Al-Amri, Al-Hadhrami, & Al-Belushi, 2018; Perez-Jiménez, Chaya, & Pozo-Bayón, 2019). También y debido a las propiedades antioxidantes y habilidades de interaccionar con las proteínas, presentan efectos beneficiosos en la salud humana (Fraga, Croft, Kennedy, & Tomás-Barberán, 2019; Manjón, Fernandes Brás, García-Estévez, & Escribano-Bailon, 2020; Sobhani, Farzaei, Kiani, & Khodarahmi, 2020).

Dentro del amplio abanico de estructuras solo nos centraremos en cuatro familias de compuestos fenólicos debido a que son los que tienen un mayor interés en la industria agroalimentaria, como son: ácidos fenólicos, alcoholes fenólicos, flavanoles y estibenos.

***Tabla 1.*** *Clasificación de los polifenoles de mayor interés. Tabla modificada (Bravo, 1998).*

| **Familia de compuestos fenólicos** | **Nº de átomos de carbono** | **Esqueleto** |
|---|---|---|
| Fenoles simples | 6 | $C_6$ |
| Ácidos hidroxibenzoicos | 7 | $C_6$-$C_1$ |
| Alcoholes fenólicos | 8 | $C_6$-$C_2$ |
| Ácidos hidroxicinámicos, fenilpropenos, cumarinas | 9 | $C_6$-$C_3$ |
| Estilbenos | 14 | $C_6$-$C_2$-$C_6$ |
| Flavonoides, isoflavonoides | 15 | $C_6$-$C_3$-$C_6$ |
| Lignanos | 18 | $(C_6$-$C_3)_2$ |
| Taninos condensados | $n^{15}$ | $(C_6$-$C_3$-$C_6)n$ |

### 3.2.1 ***Ácidos fenólicos***

Los ácidos fenólicos y sus derivados son metabolitos secundarios presentes ampliamente en cereales, legumbres, semillas vegetales, frutas y vegetales (Chandrasekara, 2019). Dentro de los ácidos fenólicos hay que distinguir entre los derivados del ácido benzoico (ácidos hidroxibenzoicos) y los derivados del ácido cinámico (ácidos hidroxicinámicos) (Manach, Scalbert, Morand, Rémésy, & Jiménez, 2004). Estos derivados difieren en el grado de hidroxilación y metilación del anillo aromático. Los derivados del ácido benzoico son los ácidos *p*-hidroxibenzoico, vaníllico, siríngico y gálico, mientras que los derivados del ácido cinámico incluyen a los ácidos *p*-cumárico, cafeico y ferúlico (Padmanabhan, Correa-Betanzo, & Paliyath, 2016; Vincente, Manganaris, Ortiz, Sozzi, & Crisosto, 2014). La distribución de los mismos cambia durante el desarrollo y maduración de las frutas (Herrmann & Nagel, 1989).

### 3.2.1.1 Ácidos hidroxibenzoicos

Derivan del ácido *p*-hidroxibenzoico y responden en general a la estructura $C_6$-$C_1$ mostrada en la **Figura 3**. Normalmente, estos compuestos se encuentran como formas conjugadas con azúcares o ácidos orgánicos (Rashmi & Negi, 2020). Una clasificación de los mismos atendiendo al tipo de sustituyentes se presenta en la **Tabla 2**.

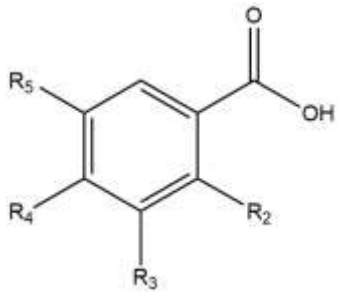


***Figura 3.*** *Esqueleto básico de los ácidos benzoicos. Modificación de (Fernández de Córdova & Medina, 2014).*

***Tabla 2.*** *Ácidos benzoicos más importantes. Modificación de (Fernández de Córdova & Medina, 2014).*

| **Ácido benzoico** | **$R_2$** | **$R_3$** | **$R_4$** | **$R_5$** |
|---|---|---|---|---|
| Ácido *p*-hidroxibenzoico | H | H | OH | H |
| Ácido vaníllico | H | $OCH_3$ | OH | H |
| Ácido siríngico | H | $OCH_3$ | OH | $OCH_3$ |
| Ácido gálico | H | OH | OH | OH |

El ácido gálico, ácido 3,4,5-trihidroxilbenzoico, es un compuesto presente en una amplia variedad de vegetales, frutas, tés, cafés y vinos (Perestrelo, Bordiga, Locatelli, Silva, & Câmara, 2020; Ramón-Gonçalves, Gómez-Mejía, Rosales-Conrado, León-González, & Madrid, 2019; Tan, Li, & Yang, 2020; Zaripour, Zare-Shahabadi, & Jahromi, 2019). Está

reconocido como un compuesto "Generalmente Reconocido como Seguro" (*Generally Recognized As Safe*", GRAS) para el consumo humano FDA, 2015 (Khan et al., 2018). Tiene efectos antimicrobianos y se considera beneficioso para disminuir las enfermedades cardiovasculares (Akbari, 2020; Wang, Leong, Elias, & Tikekar, 2019).

En cuanto al ácido vaníllico, ácido 4-hidroxi-3-metoxibenzoico, se encuentra en varias plantas y frutas (de Oliveira, Malunga, Perussello, Beta, & Ribani, 2020; Khanam, Oba, Yanase, & Murakami, 2012; Mojica, Meyer, Berhow, & de Mejía, 2015; Zaripour, Zare-Shahabadi, & Jahromi, 2019). Algunos estudios experimentales muestran que posee características farmacológicas interesantes como efectos beneficiosos contra enfermedades cardiovasculares (Stanely Mainzen Prince, Dhanasekar, & Rajakumar, 2015), óseas (Karatas et al., 2019) y diabetes (Vinothiya & Ashokkumar, 2017). También se asocia con características positivas del aroma del aceite de oliva virgen (Pedan, Popp, Rohn, Nyfeler, & Bongartz, 2019).

Un estudio reciente ha demostrado que tanto el ácido gálico como el ácido vaníllico tienen efectos antiinflamatorios, por lo que podrían usarse en tratamientos de enfermedades neurodegenerativas (Siddiqui, Kamal, Khan, Jamali, & Saify, 2019).

#### 3.2.1.2 Ácidos hidroxicinámicos

En la naturaleza, los ácidos hidroxicinámicos son más predominantes que los hidroxibenzoicos. Normalmente se presentan en formas conjugadas (Rashmi & Negi, 2020). En los alimentos, con frecuencia, los ácidos hidroxicinámicos se encuentran glicosilados o como ésteres con los ácidos quínico, siquímico o tartárico (Číž, Dvořáková, Skočková, & Kubala, 2020). Poseen una estructura $C_6$-$C_3$, **Figura 4** y, los de mayor importancia, se resumen en la **Tabla 3**:

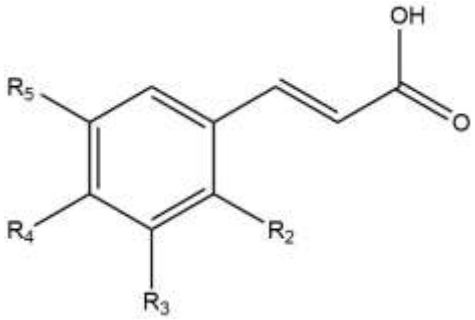


***Figura 4.*** *Esqueleto básico de los ácidos hidroxicinámicos. Modificación de (Fernández de Córdova & Medina, 2014).*

***Tabla 3.*** *Ácidos hidroxicinámicos más importantes. Modificación de (Fernández de Córdova & Medina, 2014).*

| **Ácido hidroxicinámico** | **$R_2$** | **$R_3$** | **$R_4$** | **$R_5$** |
|---|---|---|---|---|
| *p*-Cumárico | H | H | OH | H |
| Cafeico | H | OH | OH | H |
| Ferúlico | H | $OCH_3$ | OH | H |
| Sinápico | H | $OCH_3$ | OH | $OCH_3$ |

El ácido cafeico (ácido 3,4-dihidroxicinámico), es el ácido hidroxicinámico más abundante en frutas, especialmente en kiwis, ciruelas, manzanas y cerezas, entre otros (Číž et al., 2020). Es inhibidor del cáncer (Brautigan, Gielata, Heo, Kubicka, & Wilkins, 2018; Teng, Wang, Liao, Lan, & Hung, 2020), tiene efecto antioxidante (Spagnol et al., 2019; Tajner-Czopek et al., 2020) y actividad antimicrobiana (Kępa et al., 2018).

Dentro de este grupo, se encuentran los ácidos clorogénicos que se caracterizan por la presencia del ácido quínico unido a ácidos *trans*-cinámicos como los ácidos cafeico, ferúlico y *p*-cumárico mediante un enlace éster (Wei & Tanokura, 2015). Químicamente, los ácidos clorogénicos pueden clasificarse en base al tipo, número y posición de los grupos acilados

(Meinhart et al., 2019). Concretamente, la combinación del ácido cafeico y ácido quínico da lugar al ácido clorogénico (Tajik, Tajik, Mack, & Enck, 2017). En la **Figura 5** se muestran las estructuras del ácido clorogénico y ácido neoclorogénico.

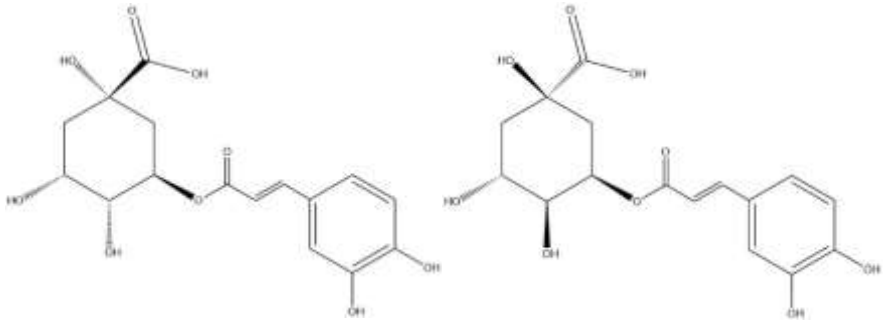

***Figura 5.*** *Estructura química del ácido clorogénico (izquierda) y del ácido neoclorogénico (derecha).*

Estos ácidos se encuentran presentes en el café, tés, frutas y vegetales, entre otros (Badmos, Fu, Granato, & Kuhnert, 2020; Crupi et al., 2018; Ertas & Yener, 2020; Meinhart et al., 2017). Varios estudios muestran que estos compuestos exhiben varios efectos beneficiosos para la salud, tales como actividad antioxidante (Tomac, Šeruga, & Labuda, 2020), propiedades antiinflamatorias (Yan, Zhou, Guo, Zhou, & Yang, 2020) y antidiabéticas, entre otras (Bagdas et al., 2015; Bao et al., 2018).

### 3.2.2 ***Alcoholes fenólicos***

El tirosol (4-hidrofeniletanol) y el hidroxitirosol (3,4-dihidroxifeniletanol) constituyen los principales representantes dentro del grupo de los alcoholes fenólicos, de estructura $C_6$-$C_2$, **Figura 6**, y se encuentran principalmente en las aceitunas y en el aceite de oliva virgen extra (Bonechi et al., 2019). Ambos son los más abundantes en el aceite de oliva, variando sus contenidos entre 0,25-14,97 mg/kg y entre 0,93-14,64 mg/kg, respectivamente (Wani et al., 2018). El contenido medio de hidroxitirosol en el aceite de oliva virgen extra es 7,7 mg/kg, en aceitunas verdes es 555,7 mg/kg y en aceitunas negras es 659,3 mg/kg (EFSA Panel on Dietetic Products, Nutrition and Allergies (NDA) et al., 2017). Además, el

hidroxitirosol está reconocido por la EFSA por sus altas propiedades antioxidantes y altos beneficios para la salud con una recomendación de consumo diario de 5 mg de hidroxitirosol y de sus derivados que contribuyen a la protección de la salud frente al daño oxidativo (EFSA Panel on Dietetic Products, Nutrition and Allergies (NDA), 2011).

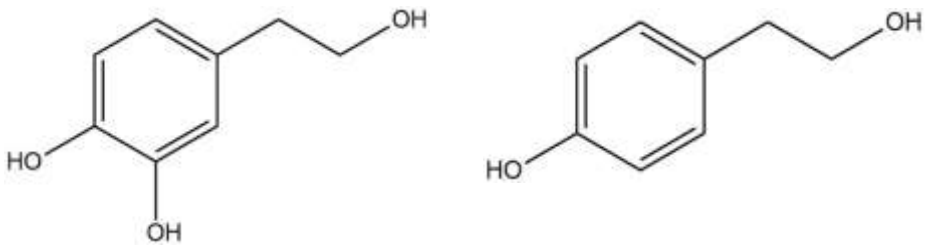


***Figura 6.*** *Estructura química de hidroxitirosol (izquierda) y tirosol (derecha).*

Un gran número de estudios han demostrado que muchos de los beneficios del aceite de oliva virgen extra están asociados al hidroxitirosol. Entre los beneficios que se le atribuyen destacan los efectos cardioprotectores, neuroprotectores, anticancerígenos y antimicrobianos, entre otros (Calahorra et al., 2019; Echeverría, Ortiz, Valenzuela, & Videla, 2017; Parkinson & Cicerale, 2016; Robles-Almazan et al., 2018; Rodríguez-Morató et al., 2015; Tomé-Carneiro et al., 2016; Wani et al., 2018). Se han llevado a cabo varios estudios dedicados a la biodisponibilidad y excreción del hidroxitirosol, demostrando que los precursores del hidroxitirosol son hidrolizados durante la digestión gastrointestinal, originándose este como metabolito (Domínguez-Perles, Auñón, Ferreres, & Gil-Izquierdo, 2017). Normalmente, el hidroxitirosol se absorbe en el intestino con una eficiencia que oscila entre el 75 hasta el 100% (Karković Marković, Torić, Barbarić, & Jakobušić Brala, 2019; Robles-Almazan et al., 2018). En lo que concierne al metabolismo del tirosol, sus precursores se someten a hidrólisis ácida llegando a triplicar su concentración en forma libre en un corto periodo de tiempo (Corona et al., 2006; Karković Marković et al., 2019).

El origen del hidroxitirosol, en las aceitunas es debido a la hidrólisis de la oleuropeína que ocurre durante la maduración del fruto, el almacenamiento y la elaboración de aceitunas de mesa (Charoenprasert & Mitchell, 2012). En el proceso de obtención del aceite, las aceitunas se trituran y se obtienen tres fases enriquecidas en polifenoles: aguas residuales de la almazara, orujo y aceite de oliva. Debido a su carácter anfipático, el hidroxitirosol se puede

encontrar en estas tres fases en forma libre, como acetato o como parte de compuestos más complejos como verbascósido y oleuropeína, entre otros (Boskou, 2008; Robles-Almazan et al., 2018). Este último es un compuesto perteneciente al grupo de los secoroides y se encuentra relacionado con el amargor del aceite de oliva virgen (Pedan et al., 2019), con sus propiedades neuroprotectoras (Kucukgul, Isgor, Duzguner, Atabay, & Kucukgul, 2018) y con sus propiedades antidegenerativas (Cordero, García-Escudero, Avila, Gargini, & García-Escudero, 2018).

También se ha encontrado que el hidroxitirosol está presente en los vinos tintos y blancos. Sin embargo, estas concentraciones siempre son menores que las que normalmente se encuentra en los aceites de oliva virgen extra (Álvarez-Fernández, Fernández-Cruz, Cantos-Villar, Troncoso, & García-Parrilla, 2018).

### 3.2.3 ***Flavonoides***

Los flavonoides constituyen un amplio grupo de compuestos fenólicos procedentes del metabolismo secundario de los vegetales con aproximadamente 10000 compuestos individuales identificados. Son los fenoles más comunes y de mayor distribución en las plantas, localizados, especialmente, en las células fotosintéticas (Akinmoladun, Farombi, & Farombi, 2019; Kumar & Pandey, 2013; Yechun Wang, Chen, & Yu, 2011). Su síntesis tiene lugar en las rutas shikimato/fenilpropanoides y acetato/malonato (Santos-Buelga & Feliciano, 2017). Los flavonoides protegen a las plantas de diferentes tipos de estrés biótico y abiótico y actúan como un filtro de luz ultravioleta (Panche, Diwan, & Chandra, 2016). Comprenden compuestos que poseen una estructura química común que es un difenilpropano ($C_6$-$C_3$-$C_6$), es decir, dos anillos aromáticos (anillo A y B) unidos entre sí por una cadena de 3 carbonos ciclada a través de un oxígeno que forman un heterociclo oxigenado de tipo pirano (anillo C) (Quiñones, Miguel, & Aleixandre, 2012; Santos-Buelga & Feliciano, 2017). El esqueleto básico de los compuestos flavonoides se muestra en la **Figura 7**. Los átomos de carbono se numeran del 2 al 10 en los anillos C y A y desde el 1´ al 6´ en el caso de los carbonos del anillo B (Valls, Millán, Martí, Borràs, & Arola, 2009).

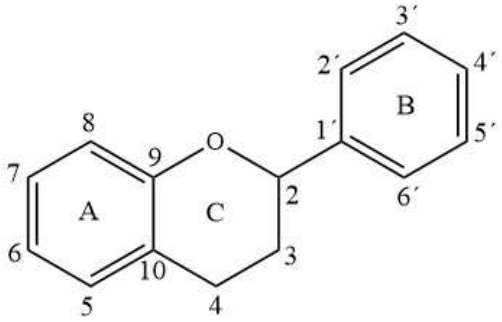


***Figura 7.*** *Esqueleto básico de los compuestos flavonoides (Balasundram, Sundram, & Samman, 2006).*

Las variaciones en el heterociclo (anillo C) definen las diferentes subclases de flavonoides: los grupos se establecen dependiendo del carbono del anillo C al cual se une el anillo B, del grado de instauración y oxidación del anillo heterociclo (anillo C) y de las hidroxilaciones y glicosilaciones de los tres anillos (Panche et al., 2016; Wang, Li, & Bi, 2018). Con frecuencia se encuentran como glucósido, aunque también pueden aparecer en forma libre. También se presentan como sulfatos, dímeros o polímeros (Quiñones et al., 2012).

Aquellos que presentan el anillo B en posición 2 están divididos en varios subgrupos definidos por la estructura característica del anillo C, entre los que se encuentran flavonas, flavanonas, flavononas, flavonoles o catequinas, flavanoles, antocianinas y calconas (Panche et al., 2016).

Las diferencias estructurales de los flavonoides determinan su comportamiento biológico y potencian o inhiben sus beneficios bioactivos (Wang et al., 2018) como efectos antivirales (Lalani & Poh, 2020), antibacterianos (Zhang et al., 2020), antiinflamatorios (Maleki, Crespo, & Cabanillas, 2019), cardioprotectores (Fusi et al., 2020), antidiabéticos (Ofosu et al., 2020), anticancerígenos (Kopustinskiene, Jakstas, Savickas, & Bernatoniene, 2020), por lo que hay un gran interés en ellos.

En la presente Tesis Doctoral, del grupo de los flavonoides, nos centraremos especialmente en el estudio de los flavanoles.

### 3.2.3.1 Flavanoles

Los flavanoles, también llamados dihidroflavanoles o catequinas, son derivados de las flavanonas, por hidroxilación en el carbono 3 del anillo C. Estos pueden aparecer como monómeros (catequinas), como dímeros condensados entre sí y como oligómeros (procianidinas), o bien como polímeros (proantocianidinas o taninos condensados) (Quiñones et al., 2012).

Los flavanoles son muy abundantes en bananas, manzanas, arándanos, peras, tés, chocolate, uvas y vinos, entre otros (Allgrove & Davison, 2018; Li, Zhang, & Sun, 2020; Lu, Liu, Lv, Ma, & Guan, 2020; Panche et al., 2016). La presencia de flavan-3-oles en alimentos afecta a la calidad, particularmente a la astringencia, amargor y estructura de los vinos. Los flavanoles se encuentran en las partes sólidas de las uvas (semilla, piel, etc.) y sufren cambios durante la maceración y fermentación (Stój, Kapusta, & Domagała, 2020).

En la presente Tesis se estudian, como analitos, las familias de las catequinas y las proantocianidinas. Las catequinas monoméricas poseen dos carbonos quirales en las posiciones 2 y 3 del anillo C. Pueden formar cuatro diastereomeros. Las configuraciones *trans* y *cis* se denominan (+)catequina y (-)epicatequina, respectivamente (Manna, Saha, & Ghoshal, 2014; Mena et al., 2014), **Figura 8**. Pueden contener ácido gálico unido mediante una unión éster al hidroxilo del anillo C, como en el caso de los catequingalatos. El grupo de las catequinas incluye catequina, epicatequina, catequingalato, epicatequingalato, galocatequingalato y epigalocatequingalato (Goto, Yoshida, Kiso, & Nagashima, 1996; Valls et al., 2009).

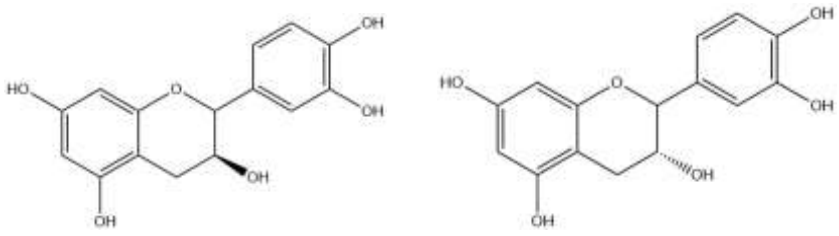


***Figura 8.*** *Estructura química de catequina (izquierda) y epicatequina (derecha).*

Las catequinas se encuentran en chocolate (Mudenuti et al., 2018), manzanas (Łysiak, Michalska-Ciechanowska, & Wojdyło, 2020), albaricoques (Wani, Masoodi, Haq, Ahmad, & Ganai, 2020), cervezas de frutas (Nardini & Garaguso, 2020), ciruelas (Radović et al., 2020), té verde (Donlao & Ogawa, 2019), fresas (Nowicka, Kucharska, Sokół-Łętowska, & Fecka, 2019) y uvas y vinos tintos (Perestrelo et al., 2020), entre otros. Estos compuestos son los que más contribuyen al amargor y astringencia de las infusiones de té verde (Narukawa, Kimata, Noga, & Watanabe, 2010; Xu et al., 2018) y al amargor del vino tinto (Conde et al., 2007). Varios de ellos se han explotado en el campo de alimentos nutracéuticos y se han usado como suplementos alimenticios (Valls et al., 2009).

Las proantiocianidinas son una mezcla de oligómeros y polímeros compuestos de unidades de flavan-3-oles unidas, generalmente, mediantes enlaces interflavano C4-C8 y C4-C6 (Ou & Gu, 2014; Valls et al., 2009). Cuando las proantocianidinas poseen un único enlace interflavano se conoce como tipo-B, mientras que cuando contienen dos enlaces interflavanos se les conoce como tipo-A (Gunawardena, Govindaraghavan, & Münch, 2014). De hecho, la procianidina B2, está formada por dos epicatequinas con unión C4-C8 (Foo, Lu, Howell, & Vorsa, 2000). La estructura química de la procianidina B1 y B2 se muestra en la **Figura 9**. Las catequinas y proantocianidinas son abundantes en las uvas, principalmente, en las semillas, seguidas de la piel y en pequeña cantidad en la pulpa (Sun, Ricardo-da-Silva, & Spranger, 2001).

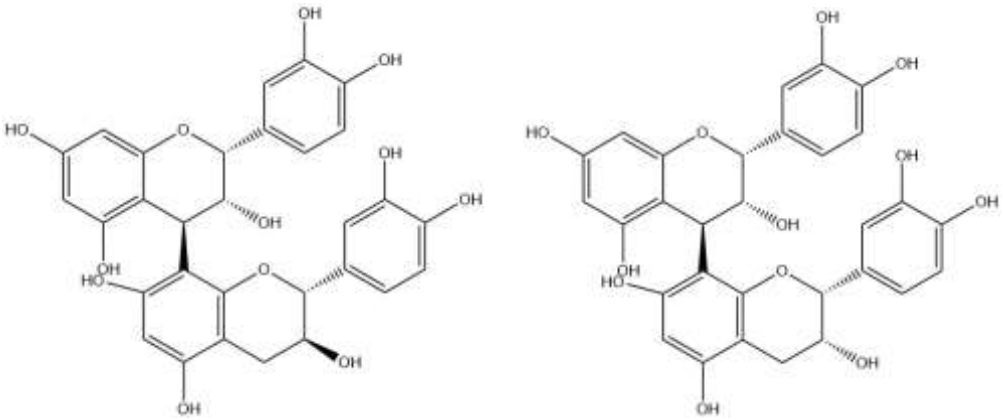


***Figura 9.*** *Estructura química de procianidina B1 (izquierda) y B2 (derecha).*

Las proantocianidinas se encuentran en una amplia variedad de alimentos como bayas, cereales, legumbres, chocolates, nueces y vinos (Gu et al., 2003). La estructura y la concentración de proantocianidinas son responsables, en parte, de la astringencia de los vinos tintos (Gonzalo-Diago, Dizy, & Fernández-Zurbano, 2013; Sun et al., 2013).

### 3.2.4 ***Estilbenos***

Los estilbenos son una familia de polifenoles no flavonoides que se encuentran en frutas, hortalizas y sus derivados, así como en los pistachos (Grippi et al., 2008), chocolate (Salvador et al., 2019), arándanos (Lyons et al., 2003), cervezas de frutas (Nardini & Garaguso, 2020) y en las uvas (Tzanova, Atanassova, Atanasov, & Grozeva, 2020) entre otros. Su estructura contiene dos anillos bencénicos unidos por un puente de etileno ($C_6$-$C_2$-$C_6$), siendo el resveratrol el más representativo de esta familia (Artero, Artero, Tarín, & Cano, 2015). El resveratrol presenta dos isómeros, *cis* y *trans*. La forma *trans*-resveratrol es más estable que la forma isomérica *cis* y es la forma predominante de resveratrol en las bayas de uva (Romero-Pérez, Ibern-Gómez, Lamuela-Raventós, & de la Torre-Boronat, 1999). La exposición a la luz ultravioleta facilita la isomerización de la forma *trans* a la forma *cis* (Zhao et al., 2015). Las estructuras de las formas *cis* y *trans* resveratrol se muestra en la **Figura 10**.

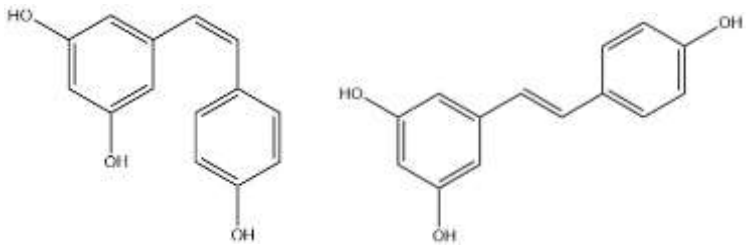


***Figura 10.*** *Estructura química de cis y trans resveratrol.*

El resveratrol (3,4´,5-trihidroxiestibeno) se sintetiza a partir de la fenilalanina a través de la ruta sikímica en la que intervienen tres enzimas: fenilalanina amonio liasa, coenzima ligasa A y la estilbeno sintasa, cuya síntesis puede ser inducida por estrés (Fabjanowicz,

Bystrzanowska, Namieśnik, Tobiszewski, & Płotka-Wasylka, 2018; Fernández-Mar, Mateos, García-Parrilla, Puertas, & Cantos-Villar, 2012; Fritzemeier & Kindl, 1981). Por tanto, el resveratrol es una fitoalexina que se sintetiza naturalmente en las plantas como mecanismo de autodefensa frente a condiciones de estrés o desfavorables, como daños o lesiones mecánicas (Billet et al., 2018), penetraciones bacterianas o fúngicas (Timperio, D'Alessandro, Fagioni, Magro, & Zolla, 2012) o exposición a la luz ultravioleta (Tang, Zhan, Yang, & Huang, 2010; Wang et al., 2010). Una de las infecciones fúngicas más comunes que afecta a las uvas durante su crecimiento es *Botrytis cinerea*. Se trata de un hongo filamentoso y fitopatógeno que puede infectar a más de 200 especies de plantas (Williamson, Tudzynski, Tudzynski, & Van Kan, 2007) excretando metabolitos como glicerol, ácido glucónico o β-glucanos y enzimas como pectinasas, proteasas, tirosinasas y lacasas, entre otros. La infección comienza en la baya de uva y continúa en el mosto, llegando a oxidar los polifenoles y alterando el color del mismo (Pourcel, Routaboul, Cheynier, Lepiniec, & Debeaujon, 2007; Vignault et al., 2020). También promueve la acumulación de metabolitos secundarios en el vino (Blanco-Ulate et al., 2015).

En uvas, la concentración de resveratrol depende de varios factores tales como la región geográfica (Rocha, Araújo, Almeida, de Pinho, & Fernandes, 2019), la variedad de uva (Tzanova et al., 2020) y la etapa de maduración (Barbará et al., 2019; Valéria da Silva Padilha et al., 2019), entre otros.

El resveratrol se encuentra principalmente en la piel de las uvas. Su concentración es mayor en los vinos tintos que los blancos, porque durante la vinificación del mosto, la piel de las uvas está en contacto con el mosto durante el proceso de fermentación (Fabjanowicz, Płotka-Wasylka, & Namieśnik, 2018). De hecho, durante la vinificación, uno de los factores tecnológicos que más condiciona la concentración de estilbenos en vinos es el tiempo de maceración (Barbará et al., 2019; Kostadinović et al., 2012). Se ha detectado que el proceso de vinificación provoca que cierta cantidad de *trans*-resveratrol se transforme en la forma *cis*. Sin embargo, si la forma *trans* se protege de la luz puede ser estable durante meses (Fabjanowicz, Płotka-Wasylka, et al., 2018; Trela & Waterhouse, 1996). Su presencia en las uvas y, como consecuencia, en el vino hace que este represente la mayor fuente de resveratrol en la dieta humana (Stój et al., 2020).

En cuanto a sus efectos saludables, el resveratrol se caracteriza por presentar gran cantidad de características positivas como efectos antioxidantes por su habilidad de capturar los radicales libres y metales, como el ion cobre, aluminio y cinc (Leonard et al., 2003). Estos efectos antioxidantes involucran una serie de mecanismos que han sido demostrados en estudios *in vitro* e *in vivo* (Venturini et al., 2010). Presenta, además, efectos antiinflamatorios (Lu et al., 2010) y neuroprotectores frente al Alzheimer (Menard, Bastianetto, & Quirion, 2013; Corpas, Griñán-Ferré, Rodríguez-Farré, Pallàs, & Sanfeliu, 2019) y al Parkinson (Xia, Sui, & Zhang, 2019), entre otros.

## 3.3 DESCRIPCIÓN Y ESTADO ACTUAL DE LAS TÉCNICAS DE DETERMINACIÓN DE COMPUESTOS FENÓLICOS

### 3.3.1 ***Técnicas separativas***

Para el análisis de compuestos fenólicos en matrices alimentarias, la técnica más utilizada es la cromatografía de líquidos de alta resolución, HPLC, acoplada con diferentes detectores: detector de serie de diodos (DAD), detector de masas (MS) o detector de fluorescencia rápida (FLD).

Excepto en el caso de muestras de vinos, que por su propia naturaleza se pueden analizar prácticamente sin pretramientos previos, en el resto de las matrices estudiadas es necesario realizar una extracción previa de los compuestos fenólicos antes de su análisis mediante HPLC. Para ello lo más usual es utilizar mezclas hidroalcohólicas tales como metanol:agua o etanol-agua en diferentes proporciones (Baltas, Pakyildiz, Can, Dincer, & Kolayli, 2017; Colombo et al., 2019; Colombo et al., 2020; Manzano Durán, Fernández Sánchez, Velardo-Micharet, & Rodríguez Gómez, 2019; Pérez-Navarro et al., 2019). También se han utilizado disolventes puros como metanol o etanol así como mezclas de ambos (Moreno-González, Juan, & Planas, 2019), dimetilsulfóxido (Crawford et al., 2018) o mezclas de agua-acetona-metanol (Sánchez-Rodríguez, Cano-Lamadrid, et al., 2019), entre otros.

La cuantificación de los compuestos fenólicos en muestras de vino mediante HPLC se realiza normalmente con muestras que han sido previamente diluidas y filtradas (Krstonošić, Hogervorst, Mikulić, & Gojković-Bukarica, 2019; Valentin, Barroso, Barbosa, de Paulo, & Castro, 2020).

Una revisión de los métodos propuestos para la determinación de compuestos fenólicos en vinos mediante HPLC durante la última década, se muestran en la **Tabla 4**. Las fases móviles empleadas usualmente consisten en mezclas de metanol o acetonitrilo con agua y electrolitos como ácido acético, ácido fórmico o acetato amónico. Generalmente, los métodos de HPLC usan columnas C18 en fase normal o en fase inversa (RP). Actualmente, también se usa la ultracromatografía líquida de alta resolución (UHPLC) en fase líquida, en la que se utilizan partículas más pequeñas 2 μm y fases móviles sometidas a gradientes rápidos que operan a presiones más altas (Fabjanowicz, Płotka-Wasylka, et al., 2018).

Típicamente, el resveratrol presente en vinos se encuentra en concentraciones muy bajas, por lo que se necesita con frecuencia, una etapa de preconcentración y técnicas muy sensibles para su cuantificación, siendo las más comunes la LC acoplada a DAD, FLD o MS (Fabjanowicz, Płotka-Wasylka, et al., 2018).

Para el análisis de compuestos fenólicos en uvas se han empleado diferentes técnicas como la espectrofotometría (Aleixandre-Tudo, Buica, Nieuwoudt, Luis Aleixandre, & du Toit, 2017), y las técnicas separativas de HPLC y UHPLC. Los métodos de determinación mediante LC en uvas se muestran en la **Tabla 5**. Tradicionalmente, la cromatografía líquida de alta resolución es la técnica que se usa con mayor frecuencia para tal fin. Generalmente, se emplea una columna en RP C18 y un gradiente con dos solventes (González de Peredo et al., 2021).

En lo que concierne a los métodos de determinación de polifenoles en ciruelas, estos se muestran en la **Tabla 6** y se constata que el número de publicaciones científicas es más escaso que para el resto de matrices alimentarias revisadas. En estos casos, se suelen emplear una columna en RP C18 y una detección por DAD.

Respecto a la pasta de aceitunas y aceitunas de mesa, los métodos de determinación mediante LC se muestran en la **Tabla 7**. Del conjunto de estrategias analíticas, las de cromatografía líquida acoplada a DAD son las de mayor extensión. Sin embargo, estos métodos a menudo emplean unos desarrollos cromatográficos largos y suelen tener unos límites de cuantificación altos, que no permiten la determinación de ciertos fenoles que se encuentran en baja concentración. Por este motivo, cada vez con más frecuencia se emplea la detección con MS, debido al incremento en la sensibilidad analítica (Moreno-González et al., 2019).

Aunque en todos los casos la cromatografía HPLC es la técnica más utilizada, en un número relativamente reducido de trabajos se propone la utilización de la cromatografía gaseosa acoplada con espectrometría de masas para la determinación de compuestos fenólicos en dichas matrices (Bajoub et al., 2016; Minuti & Pellegrino, 2008; Rodríguez-Cabo, Rodríguez, & Cela, 2012; Rodríguez-Cabo, Rodríguez, Ramil, Silva, & Cela, 2016).

***Tabla 4**. Métodos mediante HPLC para la determinación de compuestos fenólicos en vinos*

| Familia | Analitos | Modalidad Detector | Fase estacionaria | Tiempo de análisis | Referencia |
|---|---|---|---|---|---|
| **Ácidos fenólicos, flavanoles y estilbenos** | Ácido gálico, ácido vaníllico, ácido cafeico, ácido *p*-cumárico, ácido clorogénico, catequina, *t*-resveratrol | Gradiente, DAD | Poroshell 120 EC-C18 100 × 4,6 mm, 2,7µm | 30 min | Krstonošić et al., 2019 |
| **Ácidos fenólicos, flavanoles y estilbenos** | Ácido gálico, ácido vaníllico, ácido cafeico, ácido *p*-cumárico, epicatequina, catequina, resveratrol | Gradiente, DAD | Kinetex C18 100 × 4,6 mm, 2,6 µm | 40 min | Larrauri, Núñez, Hernández-Cassou, & Saurina, 2017 |
| **Ácidos fenólicos, flavanoles y estilbenos** | Ácido gálico, ácido vaníllico, ácido *p*-cumárico, ácido clorogénico, epicatequina, catequina, resveratrol | Gradiente, DAD | Zorbax Eclipse Plus C18 100 × 4,6 mm, 1,8 µm | 20 min | Somkuwar, Bhange, Oulkar, Sharma, & Ahammed Shabeer, 2018 |
| **Ácidos fenólicos, flavanoles y estilbenos** | Ácido gálico, ácido cafeico, ácido *p*-cumárico, ácido clorogénico, epicatequina, catequina, procianidina B2, *t*-resveratrol | Gradiente, DAD-FLD | Gemini-NX C18 150 × 4,6 mm, 3 µm | 55 min | Barbará et al., 2019 |
| **Ácidos fenólicos, flavanoles y estilbenos** | Ácido gálico, ácido cafeico, epicatequina, catequina, resveratrol | Gradiente, MS-MS | Rapid Resolution HT 50 × 2,1 mm, 1,8 µm | 12,75 min | Valentin et al., 2020 |

***Tabla 4***. *Continuación*

| Familia | Analitos | Modalidad/ Detector | Fase estacionaria | Tiempo de análisis | Referencia |
|---|---|---|---|---|---|
| **Ácidos fenólicos, flavanoles y estilbenos** | Ácido gálico, ácido cafeico, ácido *p*-cumárico, epicatequina, catequina, procianidina B1 y B2, *t*-resveratrol, *cis*-resveratrol | Gradiente, DAD-MS/MS | BEH C18 100 × 2,1 mm, 1,7 µm | 9,5 min | Stój et al., 2020 |
| **Ácidos fenólicos, flavanoles y estilbenos** | Ácido gálico, ácido vaníllico, ácido cafeico, ácido *p*-cumárico, ácido clorogénico, procianidina B1 y B2, epicatequina, catequina, resveratrol | Gradiente, MS | Syncronis C18 100 × 2,1 mm, 1,7 µm | 20 min | Šuković et al., 2020 |
| **Ácidos fenólicos, flavanoles y estilbenos** | Ácido gálico, ácido cafeico, ácido *p*-cumárico, epicatequina, catequina, procianidina B1 y B2, *t*-resveratrol | Gradiente, DAD-FLD | RP Kinetex C18 100 × 3,0 mm, 2,6 µm | 19 min | Ferreyra, Bottini, & Fontana, 2021 |
| **Ácidos fenólicos y flavanoles** | Ácido gálico, ácido vaníllico, ácido cafeico, ácido *p*-cumárico, ácido clorogénico, epicatequina, catequina | Gradiente, DAD | Synergi Hydro-RP C18 250 × 4,6 mm, 4 µm | 62 min | Yang et al., 2017 |
| **Ácidos fenólicos y flavanoles** | Ácido gálico, ácido vaníllico, ácido *p*-cumárico, epicatequina, catequina | Gradiente, DAD | Waters Symmetry C18 250 × 4,6 mm, 5 µm | 60 min | Suo et al., 2019 |
| **Ácidos fenólicos y flavanoles** | Ácido gálico, epicatequina | Gradiente, DAD | Agilent ZORBAX SB-C18 4,6 × 250 mm, 5 µm | 30 min | Li et al., 2020 |

***Tabla 4***. *Continuación*

| Familia | Analitos | Modalidad/ Detector | Fase estacionaria | Tiempo de análisis | Referencia |
|---|---|---|---|---|---|
| **Ácidos fenólicos y flavanoles** | Ácido gálico, ácido cafeico, ácido *p*-cumárico, epicatequina, catequina, procianidina B1 y B2 | Gradiente, DAD | RP Synergi™ Max-RP80Å 250 × 4,6 mm, 4 µm | 73 min | Perestrelo et al., 2020 |
| **Estilbenos** | *t*-resveratrol, *cis*-resveratrol | Gradiente, MS-MS | Acquity UPLC BEH C18 100 × 2,1 mm, 1,7 µm | 5,60 min | Guerrero, Valls-Fonayet, Richard, & Cantos-Villar, 2020 |
| **Estilbenos** | *t*-resveratrol, *cis*-resveratrol | Isocrático, DAD | Platisil ODS 250 × 4,6 mm, 5 µm | 20 min | Wei, Qiao, & Ma, 2019 |
| **Estilbenos** | *t*-resveratrol | Gradiente, DAD | Kinetex PFP 100A 100 × 4,6 mm, 5 µm | 10 min | Háková et al., 2020 |
| **Estilbenos** | *t*-resveratrol | Gradiente MS | Phenomenex Synergi TM Fusion, 50 × 2,0 mm, 4 µm | 20 min | Lu, LiaO, & Chen, 2018 |

***Tabla 5.*** *Métodos mediante HPLC para la determinación de compuestos fenólicos individuales en uvas*

| Familia | Analitos | Modalidad/ Detector | Fase estacionaria | Tiempo de análisis | Referencia |
|---|---|---|---|---|---|
| **Ácidos fenólicos y flavanoles** | Ácido gálico, epicatequina, catequina, procianidina B2 | Gradiente, DAD-ESI-MS | LiChrosorb RP18 250 × 4,6 mm, 5 µm | 117 min | Lucarini et al., 2019 |
| **Ácidos fenólicos, flavanoles y estilbenos** | Ácido gálico, ácido vaníllico, ácido cafeico, ácido *p*-cumárico, ácido clorogénico, epicatequina, catequina, *t*-resveratrol, *cis*-resveratrol | Gradiente, DAD | Chromolith Performance RP-18 100 × 4,6 mm, 5 µm | 74 min | Cotea et al., 2018 |
| **Ácidos fenólicos, flavanoles y estilbenos** | Ácido vaníllico, ácido cafeico, ácido *p*-cumárico, ácido clorogénico, epicatequina, catequina, procianidinas B1 y B2, resveratrol | Gradiente, MS-MS | Atlantis® T3 100 × 3,0 mm, 5 µm | 20 min | Savalekar et al., 2019 |
| **Ácidos fenólicos, flavanoles y estilbenos** | Ácido gálico, ácido vaníllico, ácido cafeico, ácido *p*-cumárico, ácido clorogénico, procianidina B1 y B2, epicatequina, catequina, resveratrol | Gradiente, MS | Syncronis C18 100 × 2,1 mm, 1,7 µm | 20 min | Šuković et al., 2020 |

***Tabla 5.*** *Continuación*

| Familia | Analitos | Modalidad/ Detector | Fase estacionaria | Tiempo de análisis | Referencia |
|---|---|---|---|---|---|
| **Ácidos fenólicos, flavanoles y estilbenos** | Ácido gálico, ácido vaníllico, ácido cafeico, ácido *p*-cumárico, ácido clorogénico, procianidinas B1 y B2, epicatequina, catequina, *t*-resveratrol | Gradiente, DAD-FLD | Acquity UPLC®BEH C18 50 × 2,1 mm, 1,7 µm | 13 min | González de Peredo et al., 2021 |
| **Flavanoles** | Epicatequina, catequina, procianidina B2 | Gradiente DAD-ESI-MS | Synergi 4u MAX-RP 80A 250 × 2,0 mm, 4 µm | - | Di Lorenzo, C. et al., 2019 |
| **Flavanoles** | Epicatequina, catequina, procianidinas B1 yB2 | Gradiente, DAD–ESI-MS-MS | RP Agilent Eclipse XDB-C18 150 × 2,1 mm, 3,5 µm | 80 min | Colombo et al., 2020 |
| **Flavanoles** | Epicatequina, catequina, procianidinas B1 yB2 | Gradiente, ESI-MS-MS | RP Agilent Eclipse XDB-C18 150 × 2,1 mm, 3,5 µm | 80 min | Pérez-Navarro et al., 2019 |
| **Flavanoles y estilbenos** | Epicatequina, catequina, procianidina B2, *t*-resveratrol, *cis*-resveratrol | Gradiente, DAD-ESI-MS | Synergi 4u MAX-RP 80A 250 × 2,0 mm, 4 µm | 48 min | Colombo et al., 2019 |
| **Estilbenos** | *t*-resveratrol | Isocrático, DAD | C18 Hypersil Gold 150 × 4,6 mm, 5 µm | 7 min | Tzanova & Peeva, 2018 |

***Tabla 6.*** *Métodos mediante HPLC para la determinación de compuestos fenólicos individuales en ciruelas*

| Familia | Analitos | Modalidad/ Detector | Fase estacionaria | Tiempo análisis | Referencia |
|---|---|---|---|---|---|
| **Ácidos fenólicos** | Ácido clorogénico, Ácido neoclorogénico | Gradiente, DAD | | | Manzano Durán et al., 2019 |
| **Ácidos fenólicos y flavanoles** | ácido vaníllico, ácido cafeico, ácido *p*-cumárico, catequina | Gradiente, DAD-MS-MS | Syncronis C18 100 × 2,1 mm, 1,7 µm | 20 min | Radović et al., 2020 |
| **Ácidos fenólicos y flavanoles** | Ácido gálico, ácido vaníllico. ácido cafeico ácido *p*-cumárico, epicatequina, catequina | Gradiente, DAD | RP C18 150 × 4,6 mm, 5 µm | 50 min | Baltas et al., 2017 |
| **Ácidos fenólicos y flavanoles** | Ácido clorogénico, ácido neoclorogénico, catequina, procianidina B1 y B2 | Isocrático, DAD | Gemini C18 150 × 4,6 mm, 3 µm | - | Drkenda, Music, Spaho, & Hudina, 2019 |
| **Ácidos fenólicos y flavanoles** | Ácido clorogénico, epicatequina, catequina, procianidina B2 | Gradiente, DAD-ESI-MS | Gemini RPC18 150 × 4,6 mm, 3 µm | 24 min | Mousavi, Zaiter, Modarressi, Baudelaire, & Dicko, 2019 |
| **Ácidos fenólicos y flavanoles** | Ácido gálico, ácido vaníllico, ácido cafeico, ácido *p*-cumárico, ácido clorogénico, catequina | Gradiente, ESI-MS | UPLC BEH C18 50 × 2,1 mm, 1,7 µm | 10 min | Ljekocevic et al., 2019 |

***Tabla 7.*** *Métodos mediante HPLC para la determinación de compuestos fenólicos en aceitunas*

| Familia | Analitos | Modalidad/ Detector | Fase estacionaria | Tiempo de análisis | Referencia |
|---|---|---|---|---|---|
| **Ácidos fenólicos, alcoholes fenólicos** | Ácido cafeico, hidroxitirosol, tirosol, oleuropeína | Gradiente, DAD | Agilent C18 Eclipse Plus 250 × 4,6 mm, 5 µm | 45 min | Crawford et al., 2018 |
| **Ácidos fenólicos, alcoholes fenólicos** | Ácido vaníllico. ácido cafeico, ácido *p*-cumárico, hidroxitirosol, tirosol, oleuropeína | Gradiente, ESI-MS-MS | C18 Zorbax Eclipse XDB 150 × 4,6 mm, 5 µm | 10 min | Moreno-González et al., 2019 |
| **Alcoholes fenólicos** | Hidroxitirosol, oleuropeína | Gradiente, MS | Acquity UPLC BEH C18 100 × 2,1 mm, 1,7 µm | 13,5 min | Sánchez-Rodríguez, Cano-Lamadrid, et al., 2019 |
| **Ácidos fenólicos, flavanoles, alcoholes fenólicos** | Ácido gálico, ácido cafeico, ácido *p*-cumárico, epicatequina, hidroxitirosol, tirosol, oleuropeína | Gradiente, ESI- MS/MS | Acclaim RSLC C18 100 × 2,1 mm, 2,2 µm | 20 min | Kalogiouri, Aalizadeh, Dasenaki, & Thomaidis, 2020 |
| **Ácidos fenólicos, alcoholes fenólicos** | Ácido cafeico, hidroxitirosol, tirosol, oleuropeína | Gradiente, DAD | Inertsil ODS3 250 × 4,6 mm, 5 µm | 55 min | Uslu & Özcan, 2020 |

***Tabla 7.*** *Continuación*

| Familia | Analitos | Modalidad/ Detector | Fase estacionaria | Tiempo de análisis | Referencia |
|---|---|---|---|---|---|
| **Ácidos fenólicos, alcoholes fenólicos** | Ácido gálico, ácido cafeico, ácido *p*-cumárico, hidroxitirosol, oleuropeína | Gradiente, DAD | Zorbax SB-C18 150 × 4,6 mm, 5µm | 60 min | Deng et al., 2017 |
| **Ácidos fenólicos, alcoholes fenólicos** | Ácido gálico, ácido cafeico, hidroxitirosol, tirosol, oleuropeína | Gradiente, MS | HSS T3 100 × 1,0 mm, 1,8 µm | 20 min | Fayek, Farag, & Saber, 2021 |

### 3.3.2 ***Fluorescencia molecular***

La demanda de alimentos de alta calidad y el interés en incluir información directa en el etiquetado ha propiciado, desde hace tiempo, el desarrollo de métodos analíticos rápidos y eficientes, utilizando técnicas mínimamente invasivas en muestras intactas o con un simple pretratamiento de las muestras, automatizando así parte de las tareas de control de calidad *on-line* y permitiendo el análisis de un gran número de muestras (Chen, Zhang, Zhao, & Ouyang, 2013; Karoui & Blecker, 2011; Karoui, Mazerolles, & Dufour, 2003). Dentro de esta filosofía de análisis, las técnicas espectroscópicas, como la fluorescencia molecular, acoplada con análisis quimiométrico, han demostrado ser muy útiles para la determinación de la calidad de un amplio rango de productos alimentarios (Sikorska, 2019). Frente a otras técnicas, las principales ventajas de la espectroscopia de fluorescencia molecular son su alta sensibilidad y selectividad, su fácil uso, su versatilidad instrumental, su rapidez de análisis, su carácter no destructivo y su capacidad de análisis multicomponente (Airado-Rodríguez, Durán-Merás, Galeano-Díaz, & Wold, 2011; Kumar, Tarai, & Mishra, 2017).

Sin embargo, aunque esta técnica presenta un gran potencial, hasta ahora ha sido poco utilizada para la caracterización de alimentos a pesar de que muchos presentan fluorescencia nativa (Christensen, Nørgaard, Bro, & Balling Engelsen, 2006). Esto ha sido debido a que la fluorescencia clásica no puede aplicarse a muestras turbias, opacas o disoluciones muy concentradas. Cuando la muestra en estudio presenta elevada absorción, la intensidad de la radiación emitida no es proporcional a la concentración de los fluoróforos presentes, los espectros de excitación y emisión disminuyen y además los espectros de excitación están distorsionados (Lakowicz, 2006; Sikorska, Khmelinskii, & Sikorski, 2019; Valeur, 2009). Para evitar este problema, lo más usual es diluir la muestra de tal forma que la absorbancia sea inferior a 0,1. Sin embargo, los resultados obtenidos para estas disoluciones diluidas no tienen por qué ser extrapolables a la matriz original de la muestra, ya que con la dilución se pierde la organización de la matriz original (Airado-Rodríguez et al., 2011; Karoui & Blecker, 2011; Karoui et al., 2003; Sikorska, 2019).

Este problema puede ser evitado utilizando la técnica de *front-face*, desarrollada por C.A. Parker en 1968 (Parker, 1968), cuya principal diferencia con respecto a la modalidad

tradicional, es la modificación del ángulo de incidencia de la radiación sobre la muestra, pasando de un ángulo de 90º en la técnica tradicional a un ángulo próximo a 30º en la técnica *de front-face*, con lo que prácticamente se mide la radiación emitida en la misma cara que la radiación incidente. Esta modalidad reduce los efectos de dispersión debido a la elevada concentración de las muestras no diluidas o a la presencia de turbidez. En un principio, su aplicación más relevante fueron los estudios de fluorescencia en matrices sólidas pero en las dos últimas décadas su aplicación en el análisis y caracterización de alimentos se ha incrementado considerablemente (Airado-Rodríguez et al., 2011; Karoui & Blecker, 2011; Karoui et al., 2003; Sikorska, 2019).

Entre sus posibilidades, esta se emplea a menudo para la determinación de la huella digital de los alimentos basada en la fluorescencia intrínseca que presentan, debido a la presencia de componentes fluorescentes naturales en los alimentos. Esta fluorescencia se puede emplear, por un lado, en el análisis cualitativo, dado que constituye una huella para cada tipo de muestra o en el análisis cuantitativo para la determinación de ciertos componentes, en ambos casos en combinación con herramientas quimiométricas (Sikorska, 2019).

Como hemos visto, las muestras alimentarias son complejas y contienen varios fluoróforos por lo que las medidas de los espectros de excitación y emisión convencionales no son suficientes para la caracterización completa de muestras complejas multicomponentes. En otras palabras, es difícil obtener la información analítica completa de todos los fluoróforos en una mezcla multicomponente compleja con un único espectro de emisión o excitación (Kumar et al., 2017). En este tipo de muestras, los espectros de excitación y emisión se superponen entre sí, y su fluorescencia se altera por el efecto matriz, incluyendo el efecto de filtro interno, efecto "*quenching"*, transferencia por energía de resonancia, viscosidad, interacción con compuestos no fluorescentes, entre otros (Sikorska et al., 2019). En estos casos, para obtener información sobre la composición de la muestra, se requieren técnicas más avanzadas que logren la selectividad y sensibilidad adecuada como: a) obtener matrices de fluorescencia de excitación-emisión (EEM) (Rho & Stuart, 1978; Warner, Callis, Davidson, Gouterman, & Christian, 1975),

b) utilizar la espectroscopía de fluorescencia sincrónica (SFS) (Lloyd, 1971), c) espectroscopia de fluorescencia sincrónica total (TSFS) (Patra & Mishra, 2002).

Las matrices de excitación-emisión (EEMs) se obtienen registrando de manera continuada espectros de emisión a diferentes longitudes de onda de excitación y permiten obtener más información sobre las especies fluorescentes presentes en la muestra (Rho & Stuart, 1978; Warner et al., 1975). La respuesta fluorescente de cualquiera de los fluoróforos presente en una EEM depende de la longitud de onda de excitación, longitud de onda de emisión y de su concentración (Kumar & Mishra, 2013). La EEM puede representarse en un sistema de coordenadas 3D, donde la intensidad fluorescente se representa como función de la longitud de onda de excitación y emisión o, alternativamente, como un mapa de contorno, en sistema de coordenadas 2 D, donde en los ejes se representan la longitudes de onda de excitación y emisión y, con una escala de colores, se proyectan los puntos con la misma intensidad de fluorescencia (Sikorska et al., 2019). A modo de ejemplo, en la **Figura 11**, se muestran un sistema de coordenadas 3D y mapa de contorno de un extracto de ciruela con metanol.

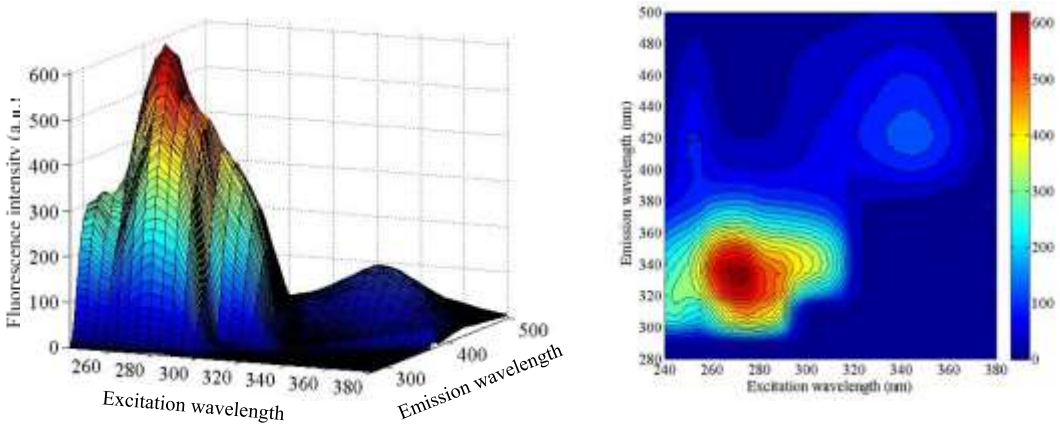


***Figura 11.*** *Ejemplo de sistema de coordenadas 3D (izquierda) y de un mapa de contorno o sistema de coordenadas 2D (derecha) de un extracto de ciruela con metanol*.

Por su parte, la SFS consiste en aplicar una velocidad de barrido constante para ambos monocromadores, variando las longitudes de onda de excitación y emisión de los monocromadores de forma sincronizada, de tal forma que $\Delta\lambda = \lambda_{em}-\lambda_{ex}$ se mantiene constante (Kumar et al., 2017). Al contrario de los espectros de excitación y emisión de la fluorescencia convencional, la SFS permite obtener bandas más estrechas, simplificar el espectro de emisión, minimizar distorsiones espectrales y mejorar la resolución.

Finalmente, en el modo TSFS se obtienen matrices de datos registrando espectros de fluorescencia sincrónica con diferentes valores de $\Delta\lambda$ (Sikorska et al., 2019). En comparación con las EEM, este modo evita las señales de dispersión.

A lo largo de este trabajo se han usado principalmente las EEMs de diversas matrices alimentarias que presentan autofluorescencia, para la caracterización y clasificación de las mismas. Además, si la información obtenida es combinada con técnicas quimiométricas, esto permite aumentar la selectividad, y posibilita que se pueda obtener información extra sobre parámetros que, de forma genérica, nos permiten agrupar y discriminar objetos, descritos mediante un vector de atributos, ya sea construyendo las clases o asignando los objetos a clases previamente definidas. Esta combinación permite obtener, en tiempos de análisis muy pequeños, información que puede ser usada como la "huella digital" de diversos alimentos.

A continuación se hará un breve repaso de las técnicas quimiométricas de análisis multivariante y de clasificación y discriminación más utilizadas para tratar datos de orden dos o superiores.

## 3.4 ALGORITMOS QUIMIOMÉTRICOS

El término análisis quimiométrico se refiere a la transformación de señales analíticas y datos más o menos complejos, en información cualitativa y/o cuantitativa. En el año 2001, esta rama de la ciencia fue definida por Siebert como: "Quimiometría es la aplicación de métodos matemáticos y estadísticos, así como de los principios de la buena ciencia de la medida, para extraer de forma eficiente información útil de datos químicos" (Siebert, 2001). Pero previamente a esta definición y reconocimiento de la quimiometría como rama de la ciencia, Massart et al., (1997) ya indicaban que dentro de la quimiometría se podían diferenciar tres áreas: 1) optimización de los procedimientos experimentales y mediciones químicas, 2) calibración, validación y significancia de las mediciones analíticas y 3) extracción de la máxima información química de los datos analíticos (Massart et al., 1997).

En el campo de la Química Analítica, una de las principales aplicaciones de la quimiometría es la calibración multivariante, término introducido por Haaland y Thomas para referirse a la cuantificación de uno o más componentes en muestras complejas, calibrando múltiples variables. Esto implica que para una única muestra se tendrán múltiples datos instrumentales que serán denominados datos multivariados (Haaland & Thomas, 1988a).

En las últimas décadas, el gran avance experimentado en la instrumentación analítica junto con el desarrollo de algoritmos matemáticos, ha supuesto que la calibración multivariante permita la resolución de un gran número de problemas analíticos complejos, aportando en todos los casos un acortamiento del tiempo de análisis, un menor uso de disolventes orgánicos y en muchos casos una reducción e incluso eliminación total de los procesos de pretratamiento de las muestras (Carabajal, Arancibia, & Escandar, 2017).

Los datos multivariados para una sola muestra, datos de primer orden o datos de dos vías, se pueden organizar en un arreglo matemático con al menos dos dimensiones diferentes. Sin embargo los datos obtenidos para un conjunto de muestras, se pueden organizar en al menos una matriz de tres vías, y se les denomina datos multi-vía. Dentro de estos, los más sencillos son los denominados datos de tres vías o de segundo orden, en

los que cada muestra genera una matriz de datos y el conjunto de datos para varias muestras se puede organizar de forma tridimensional o de tres vías (Olivieri, 2014). Un ejemplo de este tipo de datos, y que son los más utilizados en esta Tesis Doctoral, son las matrices de excitación-emisión de fluorescencia obtenidas registrando para cada muestra sucesivos espectros de emisión a diferentes longitudes de onda de excitación.

Datos de un orden superior, datos de tercer orden, son obtenidos añadiendo generalmente, una variable más a los de segundo orden, como por ejemplo registrando para cada muestra matrices de excitación-emisión en procesos cinéticos o fotosensibles. En estos casos para cada muestra se obtiene una hipermatriz de datos y el conjunto para varias muestras es un arreglo de cuatro vías. De manera similar se pueden obtener datos de orden superior (n-orden) de tal manera de los de cinco vías (cuarto orden) provendrían de arreglos tetradimensionales por cada muestra y así sucesivamente (Olivieri, Arancibia, Muñoz de la Peña, Durán-Merás, & Espinosa Mansilla, 2004).

### 3.4.1 ***Algoritmos multi-vía para datos de tres vías***

Son varios los algoritmos disponibles para el análisis de datos de tres vías, tal como se indica a continuación, donde están clasificados en función de la estructura interna del algoritmo (Olivieri, 2014):

- Basados en una solución de valor propio (eigenvectores) como son el método generalizado de reducción de rango (GRAM) (Sánchez & Kowalski, 1986) y el método de descomposición trilineal directo (DTLD) (Sanchez & Kowalski, 1990).
- Basados en mínimos cuadrados directos, como el algoritmo de mínimos cuadrados bilineales (BLLS) (Linder & Sundberg, 2002).
- Basados en mínimos cuadrados alternos trilineales tales como los algoritmos de análisis paralelo de factores (PARAFAC) (Bro, 1997), las variantes de descomposición trilineal alternada autoponderada (SWATLD) (Chen, Wu, Jiang, Li, & Yu, 2000) y la de descomposición trilineal alternada (APTLD) (Xia et al., 2005).

- Basados en mínimos cuadros alternos no-trilineales como es el método de resolución multivariada de curvas acoplado con mínimos cuadrados alternantes (MCR-ALS) (Tauler, 1995).
- Basados en variables latentes, como los algoritmos de mínimos cuadrados parciales concatenados o desdoblados (U-PLS) o multivariantes (N-PLS) (Bro, 1996; Wold, Geladi, Esbensen, & Öhman, 1987).

Todos ellos permiten en general, el cálculo de la concentración de un analito en una muestra desconocida, siguiendo procedimientos diferentes según el algoritmo seleccionado.

La elección de un algoritmo concreto debe hacerse en base a las propiedades de los datos y es importante comprobar si existen relaciones específicas entre los perfiles de los diferentes componentes de las muestras en cada una de las dimensiones de los datos. Una propiedad de los datos que tiene relevancia a la hora de seleccionar el algoritmo más adecuado es la denominada trilinealidad de los datos. Referida a un conjunto de datos de tres vías, los datos serían trilineales si el comportamiento de un constituyente dado se puede describir mediante una relación lineal con cada uno de sus perfiles en las dimensiones de los datos y, además, este perfil es único y común a todas las muestras (Azcarate, de Araújo Gomes, Muñoz de la Peña, & Goicoechea, 2018).

En el caso de los datos de segundo orden, se considera que son trilineales si se ajustan al siguiente modelo estructural:

$$x_{ijk} = \sum_{n=1}^{N} a_{in} b_{jn} c_{kn} + e_{ijk} \qquad (1)$$

Donde *N* representa el número total de componentes (constituyentes) que producen la respuesta, $a_{in}$ es la concentración relativa del componente $n$ en la muestra $i$ (también llamado "*score*"), $b_{jn}$ es la intensidad de la señal de excitación del componente $n$ a la longitud de onda $j$ y $c_{kn}$ es la intensidad de la señal de emisión del componente $n$ a la longitud de onda $k$. $b_{jn}$ y $c_{kn}$ reciben también el nombre de "*loadings*" y el término $e_{ijk}$ corresponde al error residual (o a la colección de errores de ajuste) (Escandar, Goicoechea, Muñoz de la Peña, & Olivieri, 2014).

De acuerdo con la ecuación (1) la condición de trilinealidad implica: 1) que la señal de cada constituyente sea directamente proporcional a su concentración y 2) que los perfiles sean únicos y comunes en todas las muestras. De acuerdo con la ecuación (1), los conjuntos de datos de tres vías que se ajustan a ella a menudo proporcionan una solución única. Esto significa que se pueden estimar las concentraciones de los componentes, independientemente de la presencia de otros constituyentes presentes en la muestra y esto es la base de la denominada ventaja de segundo orden (Azcarate et al., 2018; Booksh & Kowalski, 1994; Escandar et al., 2014).

Dentro de los algoritmos existentes para procesar datos instrumentales de tres-vías, en este trabajo se han utilizado principalmente algoritmos basados en variables latentes, como mínimos cuadrados parciales, tanto multivariantes (N-PLS) como concatenados o desdoblados (U-PLS) o en mínimos cuadrados alternantes trilineales como el análisis paralelo de factores (PARAFAC). Estos algoritmos están ampliamente descritos en la bibliografía por lo que a continuación solo se describirán las principales características de cada uno de ellos.

#### 3.4.1.1 Análisis paralelo de factores (PARAFAC)

Este modelo se puede utilizar tanto con fines cuantitativos como cualitativos. Fue desarrollado originariamente por Harshman, Carroll y Chang, de forma independiente (Carroll & Chang, 1970; Harshman, 1970). El modelo de PARAFAC asume que el conjunto de datos de segundo orden puede descomponerse como la suma triple del producto externo de vectores, denominados "*loadings*" que no son ortogonales. Cada componente consiste en un vector de "*scores*" y dos vectores de "*loadings*". Este algoritmo solo permite el estudio de datos que cumplan estrictamente la trilinealidad (Azcarate et al., 2018).

Si para una muestra dada se obtienen datos experimentales en forma de matrices de dimensiones $J \times K$, estamos en presencia de un arreglo de dos vías, en donde $J$ y $K$ denotan el número de datos en la primera y la segunda dimensión, respectivamente. Si las $I$ matrices de calibración y la matriz de la muestra incógnita se apilan, se genera un arreglo

de tres vías **X**, con dimensiones [(*I* + 1) × *J* × *K*]. De esta manera se agrega al sistema información sobre las posibles interferencias presentes en la muestra, aunque sin necesidad de identificarlas o conocer su concentración. Si **X** sigue un comportamiento trilineal, el modelo PARAFAC para un arreglo de tres vías está dado por la matriz de los "*scores*" **A** y las matrices de los "*loadings"* **B** y **C**, que contienen elementos $a_{in}$, $b_{jn}$ y $c_{kn}$ (Bro, 1997). El modelo trilineal busca minimizar la suma de los cuadrados de los residuos *SSE* en el modelo (Olivieri & Escandar, 2014):

$$\mathrm{SSE} = \sum_{i=1}^{I} \sum_{j=1}^{J} \sum_{k=1}^{K} e_{ijk}^2 \qquad (2)$$

PARAFAC comienza con una estimación inicial de $a_{in}$, $b_{jn}$ y $c_{kn}$ y entonces ajusta estos valores iniciales iterativamente hasta que el *SSE* es mínimo (Olivieri & Escandar, 2014). Esta aproximación proporciona la concentración relativa de cada fluoróforo y sus perfiles de excitación y emisión, permitiendo un análisis cuantitativo de una mezcla de analitos.

Una de las ventajas de PARAFAC es que para datos trilineales, la solución es única, es decir que cuando se lleva a cabo la descomposición por mínimos cuadrados alternantes, existe una única solución para todos los parámetros. Esto se traduce en que existe una única solución para los parámetros $a_{in}$, $b_{jn}$ y $c_{kn}$ cuando se descomponen los datos de segundo orden. Los elementos $b_{jn}$ y $c_{kn}$ corresponden a los perfiles de emisión (*J* × 1) y los perfiles de excitación (*K* × 1) para cada uno de los *N* componentes, respectivamente (Olivieri & Escandar, 2014).

Además, PARAFAC dispone de forma natural de la ventaja de segundo orden, ya que su modelo interno realiza la descomposición teniendo en cuenta la muestra problema, por lo que obtiene información de componentes sin calibrar en el set de calibración, es decir, es capaz de descomponer la contribución de los posibles interferentes, de la de los analitos de interés en la señal total.

### 3.4.1.2 Mínimos cuadrados parciales (PLS)

En el caso de que se observe una pérdida de la trilinealidad, debido a efectos de multicolinealidad en la estimación de los parámetros, los algoritmos basados en mínimos cuadrados parciales, tanto mínimos cuadrados parciales desdoblados o concatenados (U-PLS) como mínimos cuadrados parciales multidimensionales o multivía (N-PLS), al tener una estructura interna más flexible, ofrecen mejores resultados.

#### Mínimos cuadrados parciales desdoblados (U-PLS)

Cuando se emplean datos de tres vías con el método U-PLS, la matriz de datos de origen se reordena en vectores (datos de primer orden, espectros desdoblados) concatenando los diferentes espectros que forman la matriz inicial y se aplica una metodología de primer orden. La información de la concentración se emplea inicialmente en el paso de calibración, en el que no se incluye la muestra desconocida (Wold et al., 1987).

Las **I** matrices de datos de segundo orden de la calibración $\mathbf{X}_{i,cal}$ (de tamaño $J \times K$; donde $J$ y $K$ son el número de datos en cada una de las dos dimensiones) son primero vectorizados mediante el proceso de desdoblamiento (*unfolding*) en vectores de tamaño $JK \times 1$. El modelo U-PLS se calibra con estos datos y con el vector y ($I \times 1$, donde I es el número de muestras de calibración) de las concentraciones de calibración. Esto nos proporciona un conjunto de vectores directores o "*loadings*" P y vectores directores ponderados o "*weight loadings*" W ambos de tamaño $J \times K \times A$, donde $A$ es el número de factores necesarios para modelar la matriz de calibración, así como también los coeficientes de regresión b. El parámetro $A$ se selecciona por el criterio de Haaland y Thomas (Haaland & Thomas, 1988a, 1988b).

En el proceso anterior se genera $t_u$ que es el score de la muestra de validación, obtenido por proyección de los datos desdoblados de la muestra de validación vec ($X_{ii}$).

**Mínimos cuadrados parciales multivía (N-PLS)**

Consideramos un modelo en el que, para cada componente, se construye un modelo lineal X e Y, donde **X** es la matriz de datos e **Y** la matriz de concentraciones. Análogamente a PLS de dos vías, la matriz de datos **X** y la matriz de concentraciones **Y** se pueden descomponer de la forma:

$$\mathbf{X} = TW^{K} \otimes W^{J} + E_x \quad (3)$$

$$\mathbf{Y} = UQ^{M} \otimes Q^{L} + E_Y \quad (4)$$

donde **T** y **U** son las matrices de los "*scores*", **W** y **Q** las de los "*loadings*" y $E_x$ y $E_y$ son los errores para las variables independientes y dependientes respectivamente. El modelo de regresión se construye asumiendo la relación lineal interna de las matrices de los "*scores*" **T** y **U**.

$$\mathbf{U} = TB + Eu \quad (5)$$

siendo **B** una matriz diagonal.

Hay que tener en cuenta que estos métodos no disponen de la ventaja de segundo orden y, para que esta se alcance, es necesario someter a la muestra problema a un procedimiento adicional denominado bilinealización residual (RBL) (Öhman, Geladi, & Wold, 1990), que se lleva a cabo después de la calibración. Este proceso permite separar la señal que puede explicarse mediante la calibración, de aquella que se debe a la presencia de los posibles interferentes. En estos casos se habla de una metodología híbrida N-PLS/RBL y U-PLS/RBL (Olivieri, 2005).

La aplicación de RBL consiste en variar los "*scores*" de la muestra desconocida, con el objetivo de minimizar los valores de los residuales de U-PLS, usando el procedimiento de descomposición en valores singulares para modelar el efecto de los interferentes. Esta minimización se puede llevar a cabo por un procedimiento de Gauss-Newton. Los "*scores*" obtenidos se emplean, entonces, para predecir la concentración del analito en la muestra desconocida con el coeficiente de regresión obtenido en la etapa de calibración (Olivieri, 2005).

***Número óptimo de factores***

Independientemente del algoritmo seleccionado, todos tienen en común la necesidad de seleccionar el número óptimo de componentes.

En el caso de PARAFAC, uno de los procedimientos más utilizados es el que selecciona el número óptimo de componentes de acuerdo con el diagnóstico de la consistencia del modelo CORCONDIA (core consistency diagnostic). Se basa en conocer para qué componente se produce la mayor disminución del parámetro *core consistency*.

$$\text{Core consistency} = 100 \left[ \frac{1 - \sum_{d=1}^{F} \sum_{e=1}^{F} \sum_{f=1}^{F} (g_{def} - t_{def})^2}{\sum_{d=1}^{F} \sum_{e=1}^{F} \sum_{f=1}^{F} t_{def}^2} \right] \quad (6)$$

siendo *g* la denominada superdiagonalidad y *t* la denominada superidentidad.

Para un modelo de PARAFAC válido, *g* se aproxima a *t*. En caso contrario, *g* y *t* serán muy diferentes. En otras palabras, si a un conjunto de datos se le incrementa de forma progresiva el número de componentes, la superidentidad normalmente disminuye de forma progresiva. Después de aplicar el número de factores óptimo, al incluir uno más, la superidentidad disminuye de forma acusada. De esta forma, el número de componentes óptimo será el anterior al que genera el salto acusado en el valor del "*core*" (Bro & Kiers, 2003). Con este procedimiento, el número óptimo de factores coincide con un salto brusco en el valor del "*core*", es decir, cuando este valor cae bruscamente por debajo del 50%, se puede decir que se ha llegado al número óptimo de factores.

Otro criterio es el análisis de los residuales y para ello se define un parámetro $s_{fit}$ que deriva de aplicarle la raíz cuadrada resultante de dividir *SSE*, descrito en la ecuación (2), por el número total de elementos presentes en el conjunto de datos de segundo orden (Muñoz de la Peña, Espinosa Mansilla, González Gómez, Olivieri, & Goicoechea, 2003; Olivieri & Escandar, 2014):

$$s_{fit} = \sqrt{\frac{SSE}{I \times J \times K}} \quad (7)$$

Donde *I* es el número total de muestras del conjunto de datos de segundo orden (muestras de calibración +1), y *J* y *K* son el número de datos en cada modo instrumental en cada muestra (Olivieri & Escandar, 2014).

Este valor disminuye al aumentar el número de componentes de PARAFAC, hasta que se estabiliza en un cierto valor, que se considera óptimo (Olivieri & Escandar, 2014).

En el caso de los algoritmos U-PLS y N-PLS, la forma más usual de calcular el número de factores óptimos es mediante un proceso de validación cruzada aplicando los criterios de Haaland y Thomas. El parámetro estadístico PRESS (Prediction Residual Error Sum of Squares), para cada modelo generado, se puede expresar como:

$$\mathrm{PRESS} = \sum_{j=1}^{n} \sum_{i=1}^{m} \left(\hat{C} - C_i\right)^2 \qquad (8)$$

Siendo *n* el número total de muestras de calibración; m el número total de componentes en la mezcla; $\hat{C}$ la concentración calculada y $C_i$ la concentración de referencia.

Para un número de factores dado, el valor de PRESS nos da una medida de lo bien que una calibración está determinando la concentración. Con mayor número de factores, el error de predicción disminuye. El número de factores óptimo es aquel que proporciona el valor mínimo de PRESS.

Con número elevado de factores, se puede producir un sobreajuste. También en esta situación, se puede obtener un valor mínimo PRESS. El número de factores óptimo tiene que ser aquel que realmente introduce en el sistema un aumento de la capacidad predictiva estadísticamente mejor que cuando se emplea un número inferior. Para resolver este problema, hay que recurrir a un tratamiento estadístico. Generalmente, se emplea el criterio de Haaland y Thomas comparando los valores mínimos de PRESS con aquellos obtenidos con un número de factores menor que el que produce el mínimo PRESS haciendo uso del parámetro estadístico F (Haaland & Thomas, 1988a).

.

### 3.4.2 ***Algoritmos multi-vía para datos de cuatro vías***

Los datos de cuatro-vías se obtienen introduciendo una dimensión adicional a los datos de tres vías. En este tipo de datos, la multilinealidad se define de manera similar, así estos serán cuadri-lineales si el modelo cumple la siguiente ecuación:

$$x_{ijk} = \sum_{n=1}^{N} a_{in} b_{jn} c_{kn} d_{ln} + e_{ijk} \quad (9)$$

donde el significado de cada término es el descrito para la ecuación (1) y el término $d_{ln}$ describe el perfil del cuarto modo. Análogamente a la trilinealidad, la cuadrilinealidad significa que las señales para todos los constituyentes de la muestra pueden describirse mediante relaciones lineales con sus perfiles en cada modo de datos, y que estos últimos son únicos y comunes a todas las muestras (Alcaraz, Monago-Maraña, Goicoechea, & Muñoz de la Peña, 2019; Escandar et al., 2014).

Los algoritmos que suelen emplearse son similares a los citados anteriormente, ya que PARAFAC es un algoritmo multi-vía, por lo que teóricamente puede aplicarse a cualquier número de vías, siempre que los datos cumplan con la condición de cuadrilinealidad. Al aplicar CONCORDIA a datos fluorescentes de cuatro vías se identificarán los tres perfiles estimados, espectros de emisión, espectros de excitación y el perfil de la cuarta vía. La calibración, validación y predicción es igual que para los datos de segundo orden.

Si se da la pérdida de la cuadrilinealidad, se han desarrollado modelos basados en estructuras latentes que no tienen internamente la ventaja de segundo orden. Si se pretende lograr la ventaja de segundo orden, estos modelos deben acoplarse con un proceso de tri-linealización residual (RTL), que es la extensión natural de la RBL hacia una dimensión adicional, dando lugar a las regresiones en cuadrados mínimos desdoblados y multi-vía acopladas a RTL (U-PLS/RTL, N-PLS/RTL) (Arancibia et al., 2006).

### 3.4.3 ***Algoritmos quimiométricos con fines de clasificación***

Los métodos de clasificación multivariantes forman parte de una serie de técnicas diseñadas para encontrar modelos matemáticos capaces de asignar un objeto a su clase de procedencia a partir de un conjunto de observaciones o medidas.

Existe un gran número de métodos quimiométricos que pueden utilizarse con fines clasificatorios, pudiéndose clasificar entre métodos supervisados y no supervisados (Geladi, 2003). Estos últimos se definen con una sola matriz de datos **X**, en la que no se asume ningún modelo de clasificación previo, sino que es el propio método el que genera el modelo, determinando el número de posibles clases y caracterizando las variables que definen a cada una de ellas.

En los métodos supervisados se definen dos conjuntos de datos, objetos (X) y clases (Y). En estos métodos es necesario una etapa de entrenamiento para caracterizar las clases de las diferentes muestras para que posteriormente, en la etapa de validación, el modelo sea capaz de asignar las muestras nuevas a la pertenencia o no a una determinada clase.

En el caso de usar datos de segundo orden con fines clasificatorios, los algoritmos utilizados en esta memoria incluyen métodos no supervisados, como PARAFAC, y supervisados, como análisis lineal discriminante (LDA) y el acoplamiento de LDA con PARAFC y con U-PLS.

#### 3.4.3.1 Análisis lineal discriminante (LDA)

Es una técnica de análisis supervisado, que se basa en calcular una superficie que separa los grupos de muestras, estableciendo una función lineal discriminante que maximiza la relación de las varianzas dentro de una categoría y entre distintas categorías (Kemsley, 1998). Se supone que las categorías siguen una distribución multivariante normal y están separadas linealmente. Con la matriz variable **A** ($I \times JK$) y la matriz simulada **Y** ($I \times g$) de dígitos binarios representando la asignación de grupos donde g es el número de categorías, la mejor representación se obtiene si la relación entre de la varianza

de la matriz entre clases **Bc** y la varianza de la matriz **Wc** dentro de la misma clase se maximiza. La expresión de las matrices **Bc** y **Wc** son las siguientes (Azcarate et al., 2018):

$$\mathbf{Bc} = (\mathrm{g}-1)^{-1}\mathbf{A}^{\mathrm{T}}\mathbf{Y}(\mathbf{Y}^{\mathbf{T}}\mathbf{Y})^{-1}\mathbf{Y}^{\mathrm{T}}\mathbf{A} \quad (11)$$

$$\mathbf{Wc} = (\mathrm{I}-\mathrm{g})^{-1}[\mathbf{A}^{\mathrm{T}}\mathbf{A} - (\mathrm{g}-1)\mathbf{Bc}] \quad (12)$$

Los "*scores*" de la variable canónica (CV) contienen la relación maximizada de la varianza entre grupos y la varianza dentro de un mismo grupo. Estos se obtienen por análisis de componentes principales de la matriz ($\mathbf{Wc^{-1}Bc}$) y la proyección de los datos de la matriz **A** sobre el primero de los "*loadings*". Las muestras se proyectan en un espacio bidimensional o tridimensional definidos por los primeros "*scores*" de CV de cada muestra (Azcarate et al., 2018).

### 3.4.3.2 Análisis paralelo de factores - análisis lineal discriminante (PARAFAC-LDA)

Como ya se ha indicado PARAFAC se puede utilizar con fines diferentes a la cuantificación y se ha aplicado extensamente con fines de clasificación. Es un método no supervisado ya que no se asignan inicialmente clases diferentes, sino que se utilizan representaciones bi o tridimensionales de las valores de los "*scores*" correspondientes a los factores seleccionados para la optimización del modelo. Para dar un criterio de discriminación más seguro y restrictivo, y en el caso de que el número óptimo de factores obtenidos para el modelo sea de tres, se realiza una representación tridimensional de los tres "*scores*", utilizando la rutina de MatLab elipses-3D (Muñoz de la Peña et al., 2016), que rodea los puntos obtenidos en los "*clusters*" de datos con elipses, calculadas a partir de una distribución Chi-cuadrado con un intervalo de confianza del 95%, lo cual significa que el espacio que envuelve las elipses en los tres ejes, tiene una probabilidad del 95% de albergar los puntos de la categoría seleccionada (Azcarate et al., 2018; Slotani, 1964).

Con objeto de facilitar la visualización de los correspondientes "*clusters*" de las diferentes clases, cada figura incluye las proyecciones de las elipses de confianza al 95%, sobre los tres planos definidos por sus correspondientes ejes en los planos x, y, z (Muñoz de la Peña et al., 2016). El intervalo de predicción para una distribución multivariante

normal proporciona una elipse que consiste en vectores x que satisfacen la siguiente ecuación:

$$(\mathrm{x}-\mu)^{\mathrm{T}}\boldsymbol{\varphi}^{-1}(\mathrm{x}-\mu) \leq \mathrm{x}_{\mathrm{k}}^{2}(\mathrm{p}) \qquad (10)$$

donde $\mu$ es la media, $\boldsymbol{\varphi}$ es la matriz de covarianza y $x_k^2(p)$ es la función para la probabilidad *p* de la distribución Chi-cuadrado, con k grados de libertad, donde k es la dimensión de los datos. Los ejes se definen mediante los eigenvectores de la matriz de covarianzas y el radio de cada eje es igual a 2,796 veces la raíz cuadrada del correspondiente eigenvalor. El valor 2,796 se obtiene de la raíz cuadrada de la distribución Chi-cuadrado con tres grados de libertad y un intervalo de confianza del 95% (Azcarate et al., 2018; Slotani, 1964).

Además, la combinación de PARAFAC y LDA da lugar a un modelo supervisado de clasificación. Primeramente, utilizando PARAFAC, se obtienen los valores de los "*scores*" de las muestras de las diferentes clases y, posteriormente, se realiza un análisis supervisado por medio de LDA, con los valores de los "*scores*" como variables de partida.

Igual que en el caso de PARAFAC se pueden realizar representaciones bi- o tridimensionales que faciliten la asignación de las clases correspondientes (Muñoz de la Peña et al., 2016).

#### 3.4.3.3 Mínimos cuadrados parciales desdoblados – análisis discriminante (U-PLS-DA)

La teoría del algoritmo PLS ha sido explicada en epígrafes anteriores por lo que en este apartado nos centraremos en el algoritmo mínimos cuadrados parciales desdoblados-análisis discriminante (U-PLS-DA) que modela datos multidimensionales, cuya estructura se pierde al desdoblarse los datos. Es cierto que en este proceso se pierde la ventaja de segundo orden, tan importante para la cuantificación, pero en el caso de que la clasificación se lleve a cabo utilizando datos de tres vías, esto supone una ventaja, ya que pueden utilizarse los métodos de clasificación disponibles para datos de dos vías.

Con el uso de este algoritmo se requiere de una primera etapa de entrenamiento o aprendizaje en la que se estiman la relación entre las variables y los códigos o clases de las muestras, a partir de un grupo de muestras de entrenamiento. En la etapa de predicción se utilizan los parámetros de aprendizaje para asignar los códigos o clases a las muestras desconocidas (Azcarate et al., 2018).

La etapa de aprendizaje proporciona un "*loading*" **Q,** una matriz de peso de "*loading*" **W** (ambas de tamaño *JK x M*, donde *J* y *K* son las variables y *M* es el número de factores latentes) y el coeficiente de regresión **v** (tamaño *M x 1*). El modelo viene dado por la ecuación (3) (Azcarate et al., 2018):

$$p_{il} = \sum_{m=1}^{M} t_{im} q_{lm} + e_{il} \quad (13)$$

Donde $p_{il}$ es la señal medida de la muestra i y l se ejecuta desde 1 hasta *JK*, *M* es el número de variables latentes, $t_{im}$ es un elemento de la matriz de "*scores*" **T**, $q_{lm}$ es un elemento de la matriz de "*loading*" **Q**, y $e_{il}$ es un residuo que no se ajusta al modelo. La predicción del código de la clase para una muestra desconocida ($c_u$) puede hacerse de acuerdo a la siguiente ecuación (Azcarate et al., 2018):

$$c_u = \mathbf{t}_u^T \mathbf{v} \quad (14)$$

Donde $\mathbf{t}_u$ es el valor del score de la muestra desconocida, obtenido por la proyección de los datos vectorizados de la muestra test [vec (**X**u), donde vec (•) implica el operador de vectorización] sobre el espacio de los *M* factores latentes (Azcarate et al., 2018):

$$\mathbf{t}_u = (\mathbf{W}^T\mathbf{Q})^{-1}\mathbf{W}^T \mathrm{vec}(\mathbf{X}_u) \quad (15)$$

El gran número de monografías y trabajos utilizando los datos de fluorescencia acoplados con algoritmos de calibración multivariante pone de manifiesto el interés que este tema ha suscitado en las últimas décadas. En la siguiente sección se hace una revisión de las aplicaciones más relevantes en el análisis de compuestos fenólicos en alimentos.

### 3.4.4 ***Aplicaciones de la fluorescencia en combinación con algoritmos quimiométricos para el análisis de alimentos***

Generalmente, las EEMs de muestras pertenecientes a diferentes grupos se suelen analizar por más de un algoritmo, por lo que, a continuación, se hace una revisión de los trabajos publicados en los últimos años, que han utilizado datos de fluorescencia de segundo orden en combinación con algoritmos quimiométricos, para la identificación y cuantificación de determinados analitos en muestras alimentarias.

Una de las matrices más analizada ha sido la de los vinos, ya que al ser líquida y presentar fluorescencia nativa, no es necesario efectuar pretratamientos previos de la muestra. Las matrices de excitación-emisión, registradas en ángulo recto, se han empleado para distinguir vinos blancos de diferentes variedades: '*Chardonnay*', '*Pinot Gris*', '*Riesling*' y '*Sauvignon Blanc*', y procedentes de Francia y Rumanía. Los datos del conjunto de EEMs fueron analizados por PARAFAC, PCA y modelado blando independiente de analogías de clases (SIMCA). Las EEMs fueron tratadas con PARAFAC y tomaron como número óptimo de componentes: dos. Los perfiles de los "*loadings*" presentaron máximos a 280/350-360 nm atribuyendo esta señal al ácido gálico, entre otros compuestos. Las señales emitidas a las longitudes de onda 304-350/430-440 nm, lo atribuyeron al analito ácidos fenólicos, entre otros. Por PARAFAC se obtuvo información sobre los compuestos fluorescentes de la matriz analizada, permitiendo la diferenciación de las muestras de acuerdo a la variedad y al origen geográfico. Se tuvieron que emplear tres componentes de PCA para clasificar las muestras de acuerdo a su variedad y cuatros componentes para la discriminación geográfica. El modelo desarrollado de SIMCA probó una alta capacidad de predicción con un 98% para la clasificación simultánea de variedades y 96% para la discriminación geográfica. Por medio de la aplicación de SIMCA, de las 107 muestras de vino, se consiguió diferenciación de las muestras de acuerdo a su variedad, salvo 3 muestras que no se consiguieron clasificar correctamente. También se clasificaron las muestras de acuerdo a su origen geográfico, excepto 2 muestras que tampoco se clasificaron correctamente (Suciu, Zarbo, Guyon, & Magdas, 2019). Gracias a la fusión de datos de electroforesis capilar y de las matrices de excitación emisión del fluorescencia, se encontraron claros beneficios de cara a las clasificaciones.

por PLS-DA y mínimos cuadrados parciales multivía-análisis discriminante (N-PLS-DA), de vinos argentinos, de acuerdo a su origen y a su variedad cuando se comparan con datos de segundo orden, bien de CE-DAD o EEMs, respectivamente (Ríos-Reina, Azcarate, Camiña, & Goicoechea, 2020). Por otra parte, también se han clasificado muestras de vinos blancos argentinos en función de su variedad usando matrices de excitación-emisión, registradas en ángulo recto, y mediante análisis quimiométrico de las mismas. En un primer análisis usando PCA y PARAFAC no se consiguió una separación en grupos. Los datos se analizaron de nuevo usando el algoritmo de Kennard-Jones evaluando los datos con SIMCA, N-PLS-DA, U-PLS-DA y algoritmo de sucesión progresivo - análisis lineal discriminante (SPA-LDA), logrando los mejores resultados con U-PLS-DA y SPA-LDA al conseguir una correcta clasificación de los grupos (Azcarate et al., 2015).

También ha permitido hacer una comparación de los perfiles fluorescentes obtenidos como matrices de excitación-emisión, registradas en modo *front-face*, de vinos tintos comerciales de Nueva Zelanda. El tratamiento de los datos se llevó a cabo con PARAFAC, agrupándose las muestras de vinos en función del lugar del origen del viñedo, del tipo de elaboración y de las propiedades de la barrica. Los cuatro componentes del análisis de PARAFAC tuvieron sus máximos de excitación/emisión a 278/360 nm, 260/390 nm, 278/315 nm y 320/415 nm. Entre los compuestos a los que se asignaron los componentes, la catequina permitió diferenciar las muestras según el tipo de elaboración (Schueuermann, Silcock, & Bremer, 2018). La banda debida a las catequinas también ha sido observada en otras investigaciones (Hrobo\vnová & Sádecká, 2019).

También se han estudiado vinos botritizados (Tokaj) de diferentes categorías cuyas EEMs, registradas en ángulo recto, presentaron una banda intensa en el par de longitudes de onda 280/350 y otra más débil entre 320/430 nm, que asociaron con ácidos fenólicos y flavanoles. Sobre los datos, se aplicaron, PCA, LDA y PCA-LDA, siendo este último el mejor modelo para clasificar según las categorías comerciales (Sádecká, Jakubíková, & Májek, 2018). En la misma región eslovaca, Tokaj, se ha realizado otro estudio en el que se utilizó la fluorescencia sincrónica, en ángulo recto, para la caracterización de vinos de tres variedades: '*Muscat blanc*', '*Furmint*' y '*Lipovina*'. Se ha observado una banda intensa, con excitación a 280 nm, y un rango de emisión comprendido entre 340 y 350 nm,

y otra banda más débil, excitando a 300-320 nm, y una emisión entre 430-440 nm. Estas bandas han sido asignadas a compuestos pertenecientes a las familias de ácidos fenólicos y catequinas. La aplicación de PCA permitió la separación entre las tres variedades de vino. No obstante, para mejorarla, se empleó PCA-LDA. En todos los casos, las variedades '*Furmint*' y '*Muscat*' se separaron correctamente y para el mejor modelo se consiguió una clasificación con una separación del 100%, tanto en calibración como en validación cruzada y 93% en predicción (Sádecká & Jakubíková, 2020).

También los ácidos fenólicos contribuyen a las características de la fluorescencia intrínseca de los brandis. En un estudio dicha fluorescencia se analizó como espectro de emisión, matrices de excitación emisión y sincrónica, tanto en ángulo recto como en modo *front-face*. Los espectros de emisión y la fluorescencia sincrónica se analizaron por PCA, mientras que las matrices de excitación y emisión se analizaron por análisis de componentes principales desdoblados (U-PCA) y PARAFAC. Los "*scores*" obtenidos de este último también se analizaron por LDA. Se compararon los resultados obtenidos por PCA-LDA y por análisis paralelo de factores-análisis lineal discriminante (PARAFAC-LDA). Este último análisis permitió clasificar correctamente brandis en base al país de producción. Los componentes químicos responsables de tal fluorescencia fueron ácido gálico, ácido vaníllico, ácido cafeico y ácido *p*-cumárico, entre otros (Sádecká, Uríčková, Májek, & Jakubíková, 2019). En otro estudio, se analiza fluorescencia sincrónica de brandis de ciruela a través de PCA-LDA. Se hicieron diferentes sets de muestras en función de si los brandis eran coloreados o no, con el fin de clasificarlos en función de su país de origen. En los no coloreados, se consiguió una calibración y predicción del 100% de las muestras y, en los coloreados, del 94% en la calibración y del 100% en la predicción (Sádecká, Jakubíková, Májek, & Kleinová, 2016). Concretamente, en los brandis de ciruela, existen diferencias en la fluorescencia sincrónica de los mismos, registrada en ángulo recto, en función de la época en la que se hayan producido. Para brandis de ciruela del centro de Europa, se observó un descenso de la señal de fluorescencia en el espectro a medida que se producían los mismos con ciruela más madura. Se consiguió clasificarlas de acuerdo a su cosecha, temprana o tardía, a través de PCA-LDA, consiguiendo clasificaciones con porcentajes del 96% en la calibración y 100% en la predicción

(Jakubíková, Sádecká, & Kleinová, 2018). En otros estudios de fluorescencia sincrónica, se encontró, en muestras de brandis de ciruela diluidos, una alta señal fluorescente a longitudes de onda de emisión entre 320 y 340 nm y de excitación entre 260 y 280 nm, asociadas a compuestos polifenólicos. Otra banda se encuentra a excitación de 320 nm y emisión 420 nm. Por medio de PCA-LDA se consiguió diferenciar estos brandis de ciruelas de otros elaborados con otros tipos de frutas (Tomková, Sádecká, & Hrobo\vnová, 2015).

De bebidas de zumos, néctar y siropes, de grosella negra, aronia, fresas y frambuesa se han registrado sus matrices de excitación emisión y sus espectros sincrónicos, en ángulo recto. Por descomposición por PARAFAC, para el análisis exploratorio, se han necesitado cuatro componentes cuyos máximos, en orden, son 275/326, 319/410, 414/600 y 360/460 nm, respectivamente. En base a la literatura previa asociaron el primer componente, cuyos máximos son 275/326 nm, con ácidos hidroxibenzoicos y catequinas. El segundo componente, con máximos a 319/410 nm, se corresponde a ácidos hidroxicinámicos, como el ácido cafeico. El tercer componente lo relacionaron con antocianos y al cuarto con flavonoles. Como modelos de clasificación multivariante, se usó PLS-DA para discriminar las muestras en cuatro categorías. Sobre los "*scores*" de PARAFAC, el error medio de clasificación fue del 15,27%. El uso de PLS-DA sobre el conjunto de EEMs y TSFS permitió un error medio de clasificación de 4,86% para ambos (Sikorska, Włodarska, & Khmelinskii, 2020).

La fluorescencia *front-face* también se ha aplicado en el análisis de zumos de otras frutas como naranjas y manzanas. Así, se han analizado zumos de manzana comerciales, en cuyas matrices de excitación-emisión se han encontrado tres grupos de fluoróforos. Estas se analizaron por medio de PARAFAC, usando tres componentes, de los cuales dos de ellos fueron atribuidos a compuestos fenólicos. El primero de ellos, con un par de longitudes de onda de excitación y emisión máximas a 270/315 nm, señal que fue asignada a los compuestos flavanoles, como catequina y epicatequina. El segundo, con dos bandas de excitación centradas a 310 y 370 nm y de emisión a 455 nm fue atribuido al ácido clorogénico, ácido cafeico, ácido ferúlico y *p*-cumárico (Włodarska, Pawlak-Lemańska, Khmelinskii, & Sikorska, 2016). El estudio quimiométrico por N-PLS de los zumos de

manzana condujo a una buena calibración y validación cruzada para el análisis del contenido total de fenoles y de la capacidad antioxidante total (Włodarska et al., 2016). El análisis del espectro sincrónico, obtenido en modo *front-face*, de zumos de manzana procesados con MCR-ALS permitió la extracción de perfiles para cinco componentes, de los cuales el segundo se atribuyó a un posible flavonoide como catequina, epicatequina, procianidina B1 y procianidina B2, el tercero a un ácido fenólico y el quinto a un flavonoide como quercetina, entre otros. El análisis de estos zumos con MLR y PLS permitió la predicción del contenido de flavonoides totales (Włodarska, Pawlak-Lemańska, Khmelinskii, & Sikorska, 2017). El uso de la fluorescencia sincrónica, en modo *front-face*, permitió en combinación con PLS-DA, la discriminación entre zumos de manzana de diferentes categorías, como son aquellos producidos directamente, es decir, no concentrados, y aquellos que se reconstituyen una vez que han sido concentrados (Włodarska, Khmelinskii, & Sikorska, 2018).

Respecto al análisis de diferentes tipos de tés, se han analizado muestras de tés verdes sólidas de diferentes procedencias, China, Japón e India, en modalidad *front-face* y se han registrado las matrices de excitación emisión. Estos datos se han descompuesto por PCA obteniendo tres componentes principales. La representación de los "*scores*" del primer componente frente a los del tercero, permitió una buena diferenciación entre los tres tipos de muestras de acuerdo a su origen. Cuando se representaron los "*scores*" del primer componente frente a los del segundo, considerando ahora solo las muestras de China y Japón, se consiguieron separar las muestras. Al analizar los tés, ya como infusión, se analizaron las matrices de excitación emisión por PCA, necesitando dos componentes principales y, al representar los "*scores*" de uno frente al otro también se diferenciaron las muestras de acuerdo a su tipo. Para evaluar la sensibilidad y especificidad del modelo usaron SIMCA, logrando para todas las combinaciones una sensibilidad del 100% y una especificidad alta del modelo de los tés de China respecto a los de Japón (Hooshyari et al., 2019). En otro estudio, en el que se analizaron tés de seis tipos, se registró la fluorescencia sincrónica de los mismos con ángulo recto, encontrando máximos de emisión a 330 nm y a 460 nm en todos los tipos de tés, la cual se atribuyó a diferentes contenidos de compuestos polifenólicos, entre otros componentes. A continuación, se realizó un análisis

por PCA donde varios grupos de muestras se entremezclaban. En la fase de clasificación de los diferentes tipos de tés a partir de datos fluorescentes, los errores más bajos se obtuvieron con análisis cuadrático discriminante (QDA) mientras que los más altos por LDA (Dankowska & Kowalewski, 2019). En otro estudio, se ha demostrado que las EEMs, en ángulo recto, en combinación por mínimos cuadrados parciales-modelado de clases (PLS-CM) permite distinguir entre tés de China y de Japón y, a través de PARAFAC, se asocia uno de los componentes perteneciente a la familia de las catequinas (Casale et al., 2018).

La fluorescencia se ha usado para clasificar diferentes categorías comerciales de yerba mate argentinos cuya señal se asocia a altas concentraciones de compuestos fenólicos, como flavonoides y ácidos fenólicos, como ácido clorogénico y neoclorogénico. El estudio se llevó a cabo por PARAFAC y N-PLS. Por PARAFAC se necesitaron tres componentes, con máximos de emisión a 458, 490, y 520 nm y con máximos de excitación a 400, 420 y 458 nm para el primer, segundo y tercer componente, respectivamente. La categorización se llevó a cabo usando QDA sobre los datos de PARAFAC y N-PLS, obteniendo para ambos una sensibilidad del 100 y 83,3%, respectivamente, y especificidad del 100% para ambos modelos (Santos, Azcarate, Lima, & Goicoechea, 2020).

En relación a los vinagres, se han analizado muestras de vinagres pertenecientes a diferentes DOPs (Vinagre de Jerez, Vinagre de Montilla-Moriles y Vinagre de Condado de Huelva), registrando sus matrices de excitación y emisión con ángulo recto. Se eligió como factores de PARAFAC: 5 para los Vinagres de Jerez y Montilla-Moriles y 4 para Vinagre de Condado de Huelva. El perfil del tercer componente de los factores del Condado de Huelva y del cuarto componente de Montilla-Moriles y Vinagre de Jerez, con par de longitudes de onda de excitación/emisión a 300/425 nm, se asoció a compuestos fenólicos, especialmente ácidos fenólicos o aldehídos fenólicos. La aplicación de PLS-DA permitió diferenciar, de manera aceptable, entre las distintas categorías dentro de cada DOP (Ríos-Reina et al., 2017). Si los datos fluorescentes se fusionan con otros espectroscópicos las clasificaciones pueden mejorarse (Ríos-Reina, Callejón, Savorani, Amigo, & Cocchi, 2019).

En cuanto a matrices alimentarias de difícil tratamiento de muestra, las EEMs, en modo *front-face*, y en combinación con PCA y SIMCA han permitido clasificar, parcialmente, mieles etíopes en base a su origen floral. Entre los compuestos, parcialmente identificados en mieles, encontraron un máximo a 280/340 nm atribuido a un flavonoide y otro máximo con excitación sobre 250 nm y emisión a 450 nm, asignado a un compuesto fenólico no flavonoide (Mehretie, Al Riza, Yoshito, & Kondo, 2018). En otro estudio se clasificaron, también mieles, de acuerdo a su origen floral, por fluorescencia *front-face* a través de PLS-DA. Para su completa caracterización, se necesitaron, por PARAFAC, seis componentes, siendo el primero y el último, con longitudes de excitación de 330 nm y de emisión 430 nm y 396 nm, respectivamente, atribuidos a compuestos fenólicos (Lenhardt, Bro, Zeković, Dramićanin, & Dramićanin, 2015).

# BIBLIOGRAFÍA

## 4. BIBLIOGRAFÍA

Ahumada-Orellana, L. E., Ortega-Farías, S., & Searles, P. S. (2018). Olive oil quality response to irrigation cut-off strategies in a super-high density orchard. *Agricultural Water Management*, *202*, 81–88. https://doi.org/10.1016/j.agwat.2018.02.008

Airado-Rodríguez, D., Durán-Merás, I., Galeano-Díaz, T., & Wold, J. P. (2011). Front-face fluorescence spectroscopy: A new tool for control in the wine industry. *Journal of Food Composition and Analysis*, *24*(2), 257–264. https://doi.org/10.1016/j.jfca.2010.10.005

Akbari, G. (2020). Molecular mechanisms underlying gallic acid effects against cardiovascular diseases: An update review. *Avicenna Journal of Phytomedicine*, *10*(1), 11–23. Retrieved from https://pubmed.ncbi.nlm.nih.gov/31921604

Akinmoladun, A. C., Farombi, T. H., & Farombi, E. O. (2019). Food for Brain Health: Flavonoids. In *Encyclopedia of Food and Health* (pp. 370–386). https://doi.org/10.1016/B978-0-08-100596-5.21752-6

Al-Farsi, M., Al-Amri, A., Al-Hadhrami, A., & Al-Belushi, S. (2018). Color, flavonoids, phenolics and antioxidants of Omani honey. *Heliyon*, *4*, e00874. https://doi.org/10.1016/j.heliyon.2018.e00874

Alcaraz, M. R., Monago-Maraña, O., Goicoechea, H. C., & Muñoz de la Peña, A. (2019). Four- and five-way excitation-emission luminescence-based data acquisition and modeling for analytical applications. A review. *Analytica Chimica Acta*, *1083*, 41–57. https://doi.org/10.1016/j.aca.2019.06.059

Aleixandre-Tudo, J. L., Buica, A., Nieuwoudt, H., Aleixandre, J. L., & du Toit, W. (2017). Spectrophotometric Analysis of Phenolic Compounds in Grapes and Wines. *Journal of Agricultural and Food Chemistry*, *65*(20), 4009–4026. https://doi.org/10.1021/acs.jafc.7b01724

Allgrove, J. E., & Davison, G. (2018). Chapter 16 - Chocolate/Cocoa Polyphenols and Oxidative Stress. In *Polyphenols: Mechanisms of Action in Human Health and Disease (Second Edition)* (Second Edi, pp. 207–219). https://doi.org/10.1016/B978-0-12-813006-3.00016-7

Alowaiesh, B., Singh, Z., Fang, Z., & Kailis, S. G. (2018). Harvest time impacts the fatty acid

compositions, phenolic compounds and sensory attributes of Frantoio and Manzanilla olive oil. *Scientia Horticulturae*, *234*, 74–80. https://doi.org/10.1016/j.scienta.2018.02.017

Álvarez-Fernández, M. A., Fernández-Cruz, E., Cantos-Villar, E., Troncoso, A. M., & García-Parrilla, M. C. (2018). Determination of hydroxytyrosol produced by winemaking yeasts during alcoholic fermentation using a validated UHPLC–HRMS method. *Food Chemistry*, *242*, 345–351. https://doi.org/10.1016/j.foodchem.2017.09.072

Aprile, A., Negro, C., Sabella, E., Luvisi, A., Nicolì, F., Nutricati, E., … De Bellis, L. (2019). Antioxidant Activity and Anthocyanin Contents in Olives (cv Cellina di Nardò) during Ripening and after Fermentation. *Antioxidants*, *8*(5), 138. https://doi.org/10.3390/antiox8050138

Arancibia, J. A., Olivieri, A. C., Bohoyo-Gil, D., Espinosa-Mansilla, A., Durán-Merás, I., & Muñoz de la Peña, A. (2006). Trilinear least-squares and unfolded-PLS coupled to residual trilinearization: New chemometric tools for the analysis of four-way instrumental data. *Chemometrics and Intelligent Laboratory Systems*, *80*(1), 77–86. https://doi.org/10.1016/j.chemolab.2005.08.002

Artero, A., Artero, A., Tarín, J. J., & Cano, A. (2015). The impact of moderate wine consumption on health. *Maturitas*, *80*, 3–13. https://doi.org/10.1016/j.maturitas.2014.09.007

Azcarate, S. M., De Araújo Gomes, A., Alcaraz, M. R., Ugulino De Araújo, M. C., Camiña, J. M., & Goicoechea, H. C. (2015). Modeling excitation-emission fluorescence matrices with pattern recognition algorithms for classification of Argentine white wines according grape variety. *Food Chemistry*, *184*, 214–219. https://doi.org/10.1016/j.foodchem.2015.03.081

Azcarate, S. M., de Araújo Gomes, A., Muñoz de la Peña, A., & Goicoechea, H. C. (2018). Modeling second-order data for classification issues: Data characteristics, algorithms, processing procedures and applications. *TrAC Trends in Analytical Chemistry*, *107*, 151–168. https://doi.org/10.1016/j.trac.2018.07.022

Badmos, S., Fu, M., Granato, D., & Kuhnert, N. (2020). Classification of Brazilian roasted coffees from different geographical origins and farming practices based on chlorogenic

acid profiles. *Food Research International*, *134*, 109218. https://doi.org/10.1016/j.foodres.2020.109218

Bagdas, D., Etoz, B. C., Gul, Z., Ziyanok, S., Inan, S., Turacozen, O., … Gurun, M. S. (2015). In vivo systemic chlorogenic acid therapy under diabetic conditions: Wound healing effects and cytotoxicity/genotoxicity profile. *Food and Chemical Toxicology*, *81*, 54–61. https://doi.org/10.1016/j.fct.2015.04.001

Bajoub, A., Pacchiarotta, T., Hurtado-Fernández, E., Olmo-García, L., García-Villalba, R., Fernández-Gutiérrez, A., … Carrasco-Pancorbo, A. (2016). Comparing two metabolic profiling approaches (liquid chromatography and gas chromatography coupled to mass spectrometry) for extra-virgin olive oil phenolic compounds analysis: A botanical classification perspective. *Journal of Chromatography A*, *1428*, 267–279. https://doi.org/10.1016/j.chroma.2015.10.059

Balasundram, N., Sundram, K., & Samman, S. (2006). Phenolic compounds in plants and agri-industrial by-products: Antioxidant activity, occurrence, and potential uses. *Food Chemistry*, *99*(1), 191–203. https://doi.org/10.1016/j.foodchem.2005.07.042

Baltas, N., Pakyildiz, S., Can, Z., Dincer, B., & Kolayli, S. (2017). Biochemical properties of partially purified polyphenol oxidase and phenolic compounds of Prunus spinosa L. subsp. dasyphylla as measured by HPLC-UV. *International Journal of Food Properties*, *20*(sup2), 1377–1391. https://doi.org/10.1080/10942912.2017.1343349

Bao, L., Li, J., Zha, D., Zhang, L., Gao, P., Yao, T., & Wu, X. (2018). Chlorogenic acid prevents diabetic nephropathy by inhibiting oxidative stress and inflammation through modulation of the Nrf2/HO-1 and NF-κB pathways. *International Immunopharmacology*, *54*, 245–253. https://doi.org/10.1016/j.intimp.2017.11.021

Barbará, J., Silva, É., Biasoto, A., Gomes, A., Correa, L., Leão, P., … Zini, C. A. (2019). Maturation and Maceration Effects on Tropical Red Wines Assessed by Chromatography and Analysis of Variance - Principal Component Analysis. *Journal of the Brazilian Chemical Society*, *30*(7), 1357–1377. https://doi.org/10.21577/0103-5053.20190032

Bashir, S., Kaur, N., & Arora, N. K. (2019). Dynamics of partitioning of major sugars, total phenols and flavonoids in the juice of seven wine grape (Vitis spp.) cultivars during different stages of berry development. *Plant Physiology Reports*, *24*(1), 112–118.

https://doi.org/10.1007/s40502-018-0409-1

Basile, A., Albrizio, R., Autovino, D., Bonfante, A., De Mascellis, R., Terribile, F., & Giorio, P. (2020). A modelling approach to discriminate contributions of soil hydrological properties and slope gradient to water stress in Mediterranean vineyards. *Agricultural Water Management*, *241*, 106338. https://doi.org/10.1016/j.agwat.2020.106338

Billet, K., Houillé, B., Besseau, S., Mélin, C., Oudin, A., Papon, N., … Lanoue, A. (2018). Mechanical stress rapidly induces E-resveratrol and E-piceatannol biosynthesis in grape canes stored as a freshly-pruned byproduct. *Food Chemistry*, *240*, 1022–1027. https://doi.org/10.1016/j.foodchem.2017.07.105

Bindon, K., Varela, C., Kennedy, J., Holt, H., & Herderich, M. (2013). Relationships between harvest time and wine composition in Vitis vinifera L. cv. Cabernet Sauvignon 1. Grape and wine chemistry. *Food Chemistry*, *138*(2), 1696–1705. https://doi.org/10.1016/j.foodchem.2012.09.146

Blanco-Ulate, B., Amrine, K. C. H., Collins, T. S., Rivero, R. M., Vicente, A. R., Morales-Cruz, A., … Cantu, D. (2015). Developmental and Metabolic Plasticity of White-Skinned Grape Berries in Response to Botrytis cinerea during Noble Rot. *Plant Physiology*, *169*(4), 2422–2443. https://doi.org/10.1104/pp.15.00852

Blanco, M., & Villarroya, I. (2002). NIR spectroscopy: a rapid-response analytical tool. *TrAC Trends in Analytical Chemistry*, *21*(4), 240–250. https://doi.org/10.1016/S0165-9936(02)00404-1

Boido, E., Fariña, L., Carrau, F., Dellacassa, E., & Cozzolino, D. (2013). Characterization of Glycosylated Aroma Compounds in Tannat Grapes and Feasibility of the Near Infrared Spectroscopy Application for Their Prediction. *Food Analytical Methods*, *6*(1), 100–111. https://doi.org/10.1007/s12161-012-9423-5

Bonechi, C., Donati, A., Tamasi, G., Pardini, A., Rostom, H., Leone, G., … Rossi, C. (2019). Chemical characterization of liposomes containing nutraceutical compounds: Tyrosol, hydroxytyrosol and oleuropein. *Biophysical Chemistry*, *246*, 25–34. https://doi.org/10.1016/j.bpc.2019.01.002

Booksh, K. S., & Kowalski, B. R. (1994). Theory of Analytical Chemistry. *Analytical Chemistry*, *66*(15), 782–791. https://doi.org/10.1021/ac00087a001

Boskou, D. (2008). *Olive oil: Minor constituents and health* (C. Press., ed.).

Brautigan, D. L., Gielata, M., Heo, J., Kubicka, E., & Wilkins, L. R. (2018). Selective toxicity of caffeic acid in hepatocellular carcinoma cells. *Biochemical and Biophysical Research Communications*, *505*(2), 612–617. https://doi.org/10.1016/j.bbrc.2018.09.155

Bravo, L. (1998). Polyphenols: Chemistry, Dietary Sources, Metabolism, and Nutritional Significance. *Nutrition Reviews*, *56*(11), 317–333. https://doi.org/10.1111/j.1753-4887.1998.tb01670.x

Bro, R. (1996). Multiway calibration. Multilinear PLS. *Journal of Chemometrics*, *10*(1), 47–61. https://doi.org/10.1002/(SICI)1099-128X(199601)10:1<47::AID-CEM400>3.0.CO;2-C

Bro, R. (1997). PARAFAC. Tutorial and applications. *Chemometrics and Intelligent Laboratory Systems*, *38*(2), 149–171. https://doi.org/10.1016/S0169-7439(97)00032-4

Bro, R., & Kiers, H. A. L. (2003). A new efficient method for determining the number of components in PARAFAC models. *Journal of Chemometrics*, *17*(5), 274–286. https://doi.org/10.1002/cem.801

Bubola, M., Rusjan, D., & Lukić, I. (2020). Crop level vs. leaf removal: Effects on Istrian Malvasia wine aroma and phenolic acids composition. *Food Chemistry*, *312*, 126046. https://doi.org/10.1016/j.foodchem.2019.126046

Cabrera-Bañegil, M., Pérez-Nevado, F., Montaño, A., Pleite, R., & Martín-Vertedor, D. (2018). The effect of olive fruit maturation in Spanish style fermentation with a controlled temperature. *LWT - Food Science and Technology*, *91*, 40–47. https://doi.org/10.1016/j.lwt.2018.01.018

Cáceres-Mella, A., Ribalta-Pizarro, C., Villalobos-González, L., Cuneo, I. F., & Pastenes, C. (2018). Controlled water deficit modifies the phenolic composition and sensory properties in Cabernet Sauvignon wines. *Scientia Horticulturae*, *237*, 105–111. https://doi.org/10.1016/j.scienta.2018.04.008

Cáceres-Mella, A., Talaverano, M. I., Villalobos-González, L., Ribalta-Pizarro, C., & Pastenes, C. (2017). Controlled water deficit during ripening affects proanthocyanidin synthesis, concentration and composition in Cabernet Sauvignon grape skins. *Plant*

*Physiology and Biochemistry*, *117*, 34–41. https://doi.org/10.1016/j.plaphy.2017.05.015

Calahorra, J., Shenk, J., Wielenga, V. H., Verweij, V., Geenen, B., Dederen, P. J., … Kiliaan, A. J. (2019). Hydroxytyrosol, the Major Phenolic Compound of Olive Oil, as an Acute Therapeutic Strategy after Ischemic Stroke. *Nutrients*, *11*(10), 2430. https://doi.org/10.3390/nu11102430

Campillo Torres, C. M., Moñino Espino, M. J., Pérez Rodríguez, J. M., & Picón Toro, J. (2009). Capítulo 14. Necesidades hídricas y estrategias de riego en los principales cultivos de regadío. In *Agricultura y Ganadería Extremeñas* (pp. 223–238). Secretaría General de Agricultura, Desarrollo Rural, Población y Territorio.

Cano-Lamadrid, M., Girón, I. F., Pleite, R., Burló, F., Corell, M., Moriana, A., & Carbonell-Barrachina, A. A. (2015). Quality attributes of table olives as affected by regulated deficit irrigation. *LWT - Food Science and Technology*, *62*(1, Part 1), 19–26. https://doi.org/10.1016/j.lwt.2014.12.063

Carabajal, M. D., Arancibia, J. A., & Escandar, G. M. (2017). On-line generation of third-order liquid chromatography–excitation-emission fluorescence matrix data. Quantitation of heavy-polycyclic aromatic hydrocarbons. *Journal of Chromatography A*, *1527*, 61–69. https://doi.org/10.1016/j.chroma.2017.10.057

Carroll, J. D., & Chang, J.-J. (1970). Analysis of individual differences in multidimensional scaling via an n-way generalization of "Eckart-Young" decomposition. *Psychometrika*, *35*(3), 283–319. https://doi.org/10.1007/BF02310791

Casale, M., Pasquini, B., Hooshyari, M., Orlandini, S., Mustorgi, E., Malegori, C., … Furlanetto, S. (2018). Combining excitation-emission matrix fluorescence spectroscopy, parallel factor analysis, cyclodextrin-modified micellar electrokinetic chromatography and partial least squares class-modelling for green tea characterization. *Journal of Pharmaceutical and Biomedical Analysis*, *159*, 311–317. https://doi.org/10.1016/j.jpba.2018.07.001

Casanova, L., Corell, M., Suárez, M. P., Rallo, P., Martín-Palomo, M. J., Morales-Sillero, A., … Jiménez, M. R. (2019). Bruising response in 'Manzanilla de Sevilla' olives to RDI strategies based on water potential. *Agricultural Water Management*, *222*, 265–273. https://doi.org/10.1016/j.agwat.2019.06.007

Castellarin, S. D., Matthews, M. A., Di Gaspero, G., & Gambetta, G. A. (2007). Water deficits accelerate ripening and induce changes in gene expression regulating flavonoid biosynthesis in grape berries. *Planta*, *227*(1), 101–112. https://doi.org/10.1007/s00425-007-0598-8

Chandrasekara, A. (2019). Phenolic Acids. In *Encyclopedia of Food Chemistry* (Encycloped, pp. 535–545). https://doi.org/10.1016/B978-0-08-100596-5.22395-0

Charoenprasert, S., & Mitchell, A. (2012). Factors Influencing Phenolic Compounds in Table Olives (Olea europaea). *Journal of Agricultural and Food Chemistry*, *60*(29), 7081–7095. https://doi.org/10.1021/jf3017699

Chaves, M. M., Zarrouk, O., Francisco, R., Costa, J. M., Santos, T., Regalado, A. P., … Lopes, C. M. (2010). Grapevine under deficit irrigation: hints from physiological and molecular data. *Annals of Botany*, *105*(5), 661–676. https://doi.org/10.1093/aob/mcq030

Chen, Q., Zhang, C., Zhao, J., & Ouyang, Q. (2013). Recent advances in emerging imaging techniques for non-destructive detection of food quality and safety. *TrAC Trends in Analytical Chemistry*, *52*, 261–274. https://doi.org/10.1016/j.trac.2013.09.007

Chen, Z.-P., Wu, H.-L., Jiang, J.-H., Li, Y., & Yu, R.-Q. (2000). A novel trilinear decomposition algorithm for second-order linear calibration. *Chemometrics and Intelligent Laboratory Systems*, *52*(1), 75–86. https://doi.org/10.1016/S0169-7439(00)00081-2

Christensen, J., Nørgaard, L., Bro, R., & Balling Engelsen, S. (2006). Multivariate Autofluorescence of Intact Food Systems. *Chemical Reviews*, *106*(6), 1979–1994. https://doi.org/10.1021/cr050019q

Číž, M., Dvořáková, A., Skočková, V., & Kubala, L. (2020). The Role of Dietary Phenolic Compounds in Epigenetic Modulation Involved in Inflammatory Processes. *Antioxidants*, *9*(8), 691. https://doi.org/10.3390/antiox9080691

Colombo, F., Di Lorenzo, C., Regazzoni, L., Fumagalli, M., Sangiovanni, E., de Sousa, L., … Dell'Agli, M. (2019). Phenolic profiles and anti-inflammatory activities of sixteen table grape (Vitis vinifera L.) varieties. *Food Function*, *10*(4), 1797–1807. https://doi.org/10.1039/C8FO02175A

Colombo, R. C., Roberto, S. R., Nixdorf, S. L., Pérez-Navarro, J., Gómez-Alonso, S., Mena-Morales, A., … Hermosín-Gutiérrez, I. (2020). Analysis of the phenolic composition and yield of 'BRS Vitoria' seedless table grape under different bunch densities using HPLC–DAD–ESI-MS/MS. *Food Research International*, *130*, 108955. https://doi.org/10.1016/j.foodres.2019.108955

Conde, C., Silva, P., Fontes, N., Dias, A. C. P., Tavares, R. M., Sousa, M. J., … Gerós, H. (2007). Biochemical changes throughout grape berry development and fruit and wine quality. *Food*, *1*, 1–22.

Condurso, C., Cincotta, F., Tripodi, G., Sparacio, A., Giglio, D. M. L., Sparla, S., & Verzera, A. (2016). Effects of cluster thinning on wine quality of Syrah cultivar (Vitis vinifera L.). *European Food Research and Technology*, *242*(10), 1719–1726. https://doi.org/10.1007/s00217-016-2671-7

Connor, D. J., & Fereres Castiel, E. (2005). The physiology of adaptation and yield expression in olive. *Horticultural Reviews*, *31*, 155–229. Retrieved from http://hdl.handle.net/10261/11737

Coombe, B. G. (1960). Relationship of Growth and Development to Changes in Sugars, Auxins, and Gibberellins in Fruit of Seeded and Seedless Varieties of Vitis Vinifera. *Plant Physiology*, *35*(2), 241–250. https://doi.org/10.1104/pp.35.2.241

Cordero, J. G., García-Escudero, R., Avila, J., Gargini, R., & García-Escudero, V. (2018). Benefit of Oleuropein Aglycone for Alzheimer's Disease by Promoting Autophagy. *Oxidative Medicine and Cellular Longevity*, *2018*, 5010741. https://doi.org/10.1155/2018/5010741

Corelli Grappadelli, L., Morandi, B., Manfrini, L., & O'Connell, M. (2019). Apoplasmic and simplasmic phloem unloading mechanisms: Do they co-exist in Angeleno plums under demanding environmental conditions? *Journal of Plant Physiology*, *237*, 104–110. https://doi.org/10.1016/j.jplph.2019.04.005

Corona, G., Tzounis, X., DessÌ, M. A., Deiana, M., Debnam, E. S., Visioli, F., & Spencer, J. P. E. (2006). The fate of olive oil polyphenols in the gastrointestinal tract: Implications of gastric and colonic microflora-dependent biotransformation. *Free Radical Research*, *40*(6), 647–658. https://doi.org/10.1080/10715760500373000

Corpas, R., Griñán-Ferré, C., Rodríguez-Farré, E., Pallàs, M., & Sanfeliu, C. (2019). Resveratrol Induces Brain Resilience Against Alzheimer Neurodegeneration Through Proteostasis Enhancement. *Molecular Neurobiology*, *56*(2), 1502–1516. https://doi.org/10.1007/s12035-018-1157-y

Cotea, V., Luchian, C., Niculaua, M., Zamfir, C.-I., Moraru, I., Nechita, B. C., & Colibaba, C. (2018). Evaluation of phenolic compounds content in grape seeds. *Environmental Engineering and Management Journal*, *17*(4), 795–802. https://doi.org/10.30638/eemj.2018.080

Crawford, L. M., Holstege, D. M., & Wang, S. C. (2018). High-throughput extraction method for phenolic compounds in olive fruit (Olea europaea). *Journal of Food Composition and Analysis*, *66*, 136–144. https://doi.org/10.1016/j.jfca.2017.12.013

Crupi, P., Bleve, G., Tufariello, M., Corbo, F., Clodoveo, M. L., & Tarricone, L. (2018). Comprehensive identification and quantification of chlorogenic acids in sweet cherry by tandem mass spectrometry techniques. *Journal of Food Composition and Analysis*, *73*, 103–111. https://doi.org/10.1016/j.jfca.2018.06.013

Daniels, A. J., Poblete-Echeverría, C., Opara, U. L., & Nieuwoudt, H. H. (2019). Measuring Internal Maturity Parameters Contactless on Intact Table Grape Bunches Using NIR Spectroscopy. *Frontiers in Plant Science*, *10*, 1517. https://doi.org/10.3389/fpls.2019.01517

Dankowska, A., & Kowalewski, W. (2019). Tea types classification with data fusion of UV–Vis, synchronous fluorescence and NIR spectroscopies and chemometric analysis. *Spectrochimica Acta - Part A: Molecular and Biomolecular Spectroscopy*, *211*, 195–202. https://doi.org/10.1016/j.saa.2018.11.063

de Oliveira, A. M., Malunga, L. N., Perussello, C. A., Beta, T., & Ribani, R. H. (2020). Phenolic acids from fruits of Physalis angulata L. in two stages of maturation. *South African Journal of Botany*, *131*, 448–453. https://doi.org/10.1016/j.sajb.2020.02.029

DECRETO 74/2018. (2018). DECRETO 74/2018, de 5 de junio, por el que se aprueba el Reglamento de la Denominación de Origen "Ribera del Guadiana." In *Diario Oficial de Extremadura* (pp. 21987–22006).

Deluc, L. G., Quilici, D. R., Decendit, A., Grimplet, J., Wheatley, M. D., Schlauch, K. A., …

Cramer, G. R. (2009). Water deficit alters differentially metabolic pathways affecting important flavor and quality traits in grape berries of Cabernet Sauvignon and Chardonnay. *BMC Genomics*, *10*(1), 212. https://doi.org/10.1186/1471-2164-10-212

Deng, J., Xu, Z., Xiang, C., Liu, J., Zhou, L., Li, T., … Ding, C. (2017). Comparative evaluation of maceration and ultrasonic-assisted extraction of phenolic compounds from fresh olives. *Ultrasonics Sonochemistry*, *37*, 328–334. https://doi.org/10.1016/j.ultsonch.2017.01.023

Di Lorenzo, C., Colombo, F., Biella, S., Orgiu, F., Frigerio, G., Regazzoni, L., … Restani, P. (2019). Phenolic profile and antioxidant activity of different grape (Vitis vinifera L.) varieties. *BIO Web Conf.*, *12*, 4005. https://doi.org/10.1051/bioconf/20191204005

Díaz González, M. (2015). Capítulo 7. El sector vitivinícola. In *Agricultura y Ganadería Extremeñas* (pp. 139–154). Secretaría General de Agricultura, Desarrollo Rural, Población y Territorio.

Domínguez-Perles, R., Auñón, D., Ferreres, F., & Gil-Izquierdo, A. (2017). Gender differences in plasma and urine metabolites from Sprague–Dawley rats after oral administration of normal and high doses of hydroxytyrosol, hydroxytyrosol acetate, and DOPAC. *European Journal of Nutrition*, *56*(1), 215–224. https://doi.org/10.1007/s00394-015-1071-2

Donlao, N., & Ogawa, Y. (2019). The influence of processing conditions on catechin, caffeine and chlorophyll contents of green tea (Camelia sinensis) leaves and infusions. *LWT - Food Science and Technology*, *116*, 108567. https://doi.org/10.1016/j.lwt.2019.108567

dos Santos Costa, D., Oliveros Mesa, N. F., Santos Freire, M., Pereira Ramos, R., & Teruel Mederos, B. J. (2019). Development of predictive models for quality and maturation stage attributes of wine grapes using vis-nir reflectance spectroscopy. *Postharvest Biology and Technology*, *150*, 166–178. https://doi.org/10.1016/j.postharvbio.2018.12.010

Drkenda, P., Music, O., Spaho, N., & Hudina, M. (2019). Geographic and seasonal variation of biochemical parameters of the European native plum “Pozegaca” (Prunus domestica L.). *European Journal of Horticultural Science*, *84*(5), 282–293. https://doi.org/10.17660/eJHS.2019/84.5.4

Echeverría, F., Ortiz, M., Valenzuela, R., & Videla, L. A. (2017). Hydroxytyrosol and Cytoprotection: A Projection for Clinical Interventions. *International Journal of Molecular Sciences*, *18*(5), 930. https://doi.org/10.3390/ijms18050930

EFSA Panel on Dietetic Products, Nutrition and Allergies (NDA). (2011). Scientific Opinion on the substantiation of health claims related to polyphenols in olive and protection of LDL particles from oxidative damage (ID 1333, 1638, 1639, 1696, 2865), maintenance of normal blood HDL cholesterol concentrations (ID 1639), mainte. *EFSA Journal*, *9*(4), 2033. https://doi.org/10.2903/j.efsa.2011.2033

EFSA Panel on Dietetic Products, Nutrition and Allergies (NDA), Turck, D., Bresson, J.-L., Burlingame, B., Dean, T., Fairweather-Tait, S., … van Loveren, H. (2017). Safety of hydroxytyrosol as a novel food pursuant to Regulation (EC) No 258/97. *EFSA Journal*, *15*(3), e04728. https://doi.org/10.2903/j.efsa.2017.4728

El-Sharkawy, I., Sherif, S., Qubbaj, T., Sullivan, A. J., & Jayasankar, S. (2016). Stimulated auxin levels enhance plum fruit ripening, but limit shelf-life characteristics. *Postharvest Biology and Technology*, *112*, 215–223. https://doi.org/10.1016/j.postharvbio.2015.09.012

ElMasry, G. M., & Nakauchi, S. (2016). Image analysis operations applied to hyperspectral images for non-invasive sensing of food quality - A comprehensive review. *Biosystems Engineering*, *142*, 53–82. https://doi.org/10.1016/j.biosystemseng.2015.11.009

Ertas, A., & Yener, I. (2020). A comprehensive study on chemical and biological profiles of three herbal teas in Anatolia; rosmarinic and chlorogenic acids. *South African Journal of Botany*, *130*, 274–281. https://doi.org/10.1016/j.sajb.2020.01.008

Escandar, G. M., Goicoechea, H. C., Muñoz de la Peña, A., & Olivieri, A. C. (2014). Second- and higher-order data generation and calibration: A tutorial. *Analytica Chimica Acta*, *806*, 8–26. https://doi.org/10.1016/j.aca.2013.11.009

Fabjanowicz, M., Bystrzanowska, M., Namieśnik, J., Tobiszewski, M., & Płotka-Wasylka, J. (2018). An analytical hierarchy process for selection of the optimal procedure for resveratrol determination in wine samples. *Microchemical Journal*, *142*, 126–134. https://doi.org/10.1016/j.microc.2018.06.028

Fabjanowicz, M., Płotka-Wasylka, J., & Namieśnik, J. (2018). Detection, identification and

determination of resveratrol in wine. Problems and challenges. *TrAC - Trends in Analytical Chemistry*, *103*, 21–33. https://doi.org/10.1016/j.trac.2018.03.006

FAOSTAT. (2018). FAO Statistical Databases. Agriculture Data Collection. Organización de las Naciones Unidas para la Alimentación y la Agricultura. Retrieved from http://www.fao.org/faostat/es

Fayek, N. M., Farag, M. A., & Saber, F. R. (2021). Metabolome classification via GC/MS and UHPLC/MS of olive fruit varieties grown in Egypt reveal pickling process impact on their composition. *Food Chemistry*, *339*, 127861. https://doi.org/10.1016/j.foodchem.2020.127861

Fernández-Mar, M. I., Mateos, R., García-Parrilla, M. C., Puertas, B., & Cantos-Villar, E. (2012). Bioactive compounds in wine: Resveratrol, hydroxytyrosol and melatonin: A review. *Food Chemistry*, *130*(4), 797–813. https://doi.org/10.1016/j.foodchem.2011.08.023

Fernández-Novales, J., Garde-Cerdán, T., Tardáguila, J., Gutiérrez-Gamboa, G., Pérez-Álvarez, E. P., & Diago, M. P. (2019). Assessment of amino acids and total soluble solids in intact grape berries using contactless Vis and NIR spectroscopy during ripening. *Talanta*, *199*, 244–253. https://doi.org/10.1016/j.talanta.2019.02.037

Fernández-Novales, J., Tardaguila, J., Gutiérrez, S., Marañón, M., & Diago, M. P. (2018). In field quantification and discrimination of different vineyard water regimes by on-the-go NIR spectroscopy. *Biosystems Engineering*, *165*, 47–58. https://doi.org/10.1016/j.biosystemseng.2017.08.018

Fernández de Córdova, M. L., & Medina, A. R. (2014). Chapter 29 - Analytical Methods for Determination of Polyphenols in Beer. In *Processing and Impact on Antioxidants in Beverages* (pp. 289–299). https://doi.org/10.1016/B978-0-12-404738-9.00029-5

Ferreyra, S., Bottini, R., & Fontana, A. (2021). Tandem absorbance and fluorescence detection following liquid chromatography for the profiling of multiclass phenolic compounds in different winemaking products. *Food Chemistry*, *338*, 128030. https://doi.org/10.1016/j.foodchem.2020.128030

Ferro, M. D., Lopes, E., Afonso, M., Peixe, A., Rodrigues, F. M., & Duarte, M. F. (2020). Phenolic Profile Characterization of ‘Galega Vulgar’ and ‘Cobrançosa’ Portuguese Olive

Cultivars along the Ripening Stages. *Applied Sciences*, *10*(11), 3930. https://doi.org/10.3390/app10113930

Fontes, N., Gerós, H., & Delrot, S. (2011). Grape Berry Vacuole: A Complex and Heterogeneous Membrane System Specialized in the Accumulation of Solutes. *American Journal of Enology and Viticulture*, *62*(3), 270–278. https://doi.org/10.5344/ajev.2011.10125

Foo, L. Y., Lu, Y., Howell, A. B., & Vorsa, N. (2000). A-Type Proanthocyanidin Trimers from Cranberry that Inhibit Adherence of Uropathogenic P-Fimbriated Escherichia coli. *Journal of Natural Products*, *63*(9), 1225–1228. https://doi.org/10.1021/np000128u

Fraga, C. G., Croft, K. D., Kennedy, D. O., & Tomás-Barberán, F. A. (2019). The effects of polyphenols and other bioactives on human health. *Food Function*, *10*(2), 514–528. https://doi.org/10.1039/C8FO01997E

Fritzemeier, K.-H., & Kindl, H. (1981). Coordinate Induction by UV Light of Stilbene Synthase, Phenylalanine Ammonia-lyase and Cinnamate 4-Hydroxylase in Leaves of Vitaceae. *Planta*, *151*(1), 48–52. Retrieved from http://www.jstor.org/stable/23375009

Fusi, F., Trezza, A., Tramaglino, M., Sgaragli, G., Saponara, S., & Spiga, O. (2020). The beneficial health effects of flavonoids on the cardiovascular system: Focus on K+ channels. *Pharmacological Research*, *152*, 104625. https://doi.org/10.1016/j.phrs.2019.104625

Gao, X. T., Li, H. Q., Wang, Y., Peng, W. T., Chen, W., Cai, X. D., … Wang, J. (2019). Influence of the harvest date on berry compositions and wine profiles of Vitis vinifera L. cv. 'Cabernet Sauvignon' under a semiarid continental climate over two consecutive years. *Food Chemistry*, *292*, 237–245. https://doi.org/10.1016/j.foodchem.2019.04.070

García-Tejera, O., López-Bernal, Á., Orgaz, F., Testi, L., & Villalobos, F. J. (2018). Are olive root systems optimal for deficit irrigation? *European Journal of Agronomy*, *99*, 72–79. https://doi.org/10.1016/j.eja.2018.06.012

García, J. M., Hueso, A., & Gómez-del- Campo, M. (2020). Deficit irrigation during the oil synthesis period affects olive oil quality in high-density orchards (cv. Arbequina). *Agricultural Water Management*, *230*, 105858. https://doi.org/10.1016/j.agwat.2019.105858

García Martínez, E. M., Fernández Segovia, I., & Fuentes López, A. (2015). *Determinación de polifenoles totales por el método de Folin-Ciocalteu*. Retrieved from https://riunet.upv.es:443/handle/10251/52056

Garrido, I., Uriarte, D., Hernández, M., Llerena, J. L., Valdés, M. E., & Espinosa, F. (2016). The Evolution of Total Phenolic Compounds and Antioxidant Activities during Ripening of Grapes (Vitis vinifera L., cv. Tempranillo) Grown in Semiarid Region: Effects of Cluster Thinning and Water Deficit. *International Journal of Molecular Sciences*, *17*(11), 1923. https://doi.org/10.3390/ijms17111923

Geladi, P. (2003). Chemometrics in spectroscopy. Part 1. Classical chemometrics. *Spectrochimica Acta Part B: Atomic Spectroscopy*, *58*(5), 767–782. https://doi.org/10.1016/S0584-8547(03)00037-5

Genisheva, Z., Quintelas, C., Mesquita, D. P., Ferreira, E. C., Oliveira, J. M., & Amaral, A. L. (2018). New PLS analysis approach to wine volatile compounds characterization by near infrared spectroscopy (NIR). *Food Chemistry*, *246*, 172–178. https://doi.org/10.1016/j.foodchem.2017.11.015

Gil, M., Esteruelas, M., González, E., Kontoudakis, N., Jiménez, J., Fort, F., … Zamora, F. (2013). Effect of Two Different Treatments for Reducing Grape Yield in Vitis vinifera cv Syrah on Wine Composition and Quality: Berry Thinning versus Cluster Thinning. *Journal of Agricultural and Food Chemistry*, *61*(20), 4968–4978. https://doi.org/10.1021/jf400722z

Giovenzana, V., Civelli, R., Beghi, R., Oberti, R., & Guidetti, R. (2015). Testing of a simplified LED based vis/NIR system for rapid ripeness evaluation of white grape (Vitis vinifera L.) for Franciacorta wine. *Talanta*, *144*, 584–591. https://doi.org/10.1016/j.talanta.2015.06.055

Glories, Y., & Augustin, M. (1993). Maturité phénolique du raisin, consequences technologiques: application aux millésimes 1991 et 1992. *Compte Rendu Colloque Journée Technique CIVB.*, 56–61. Bordeaux, France.

González-Caballero, V., Pérez-Marín, D., López, M.-I., & Sánchez, M.-T. (2011). Optimization of NIR Spectral Data Management for Quality Control of Grape Bunches during On-Vine Ripening. *Sensors*, *11*(6), 6109–6124.

https://doi.org/10.3390/s110606109

González-Caballero, V., Sánchez, M.-T., Fernández-Novales, J., López, M.-I., & Pérez-Marín, D. (2012). On-Vine Monitoring of Grape Ripening Using Near-Infrared Spectroscopy. *Food Analytical Methods*, *5*(6), 1377–1385. https://doi.org/10.1007/s12161-012-9389-3

González-Cabrera, M., Domínguez-Vidal, A., & Ayora-Cañada, M. J. (2018). Hyperspectral FTIR imaging of olive fruit for understanding ripening processes. *Postharvest Biology and Technology*, *145*, 74–82. https://doi.org/10.1016/j.postharvbio.2018.06.008

González de Peredo, A. V., Vázquez-Espinosa, M., Piñeiro, Z., Espada-Bellido, E., Ferreiro-González, M., Barbero, G. F., & Palma, M. (2021). Development of a rapid and accurate UHPLC-PDA-FL method for the quantification of phenolic compounds in grapes. *Food Chemistry*, *334*, 127569. https://doi.org/10.1016/j.foodchem.2020.127569

Gonzalo-Diago, A., Dizy, M., & Fernández-Zurbano, P. (2013). Taste and Mouthfeel Properties of Red Wines Proanthocyanidins and Their Relation to the Chemical Composition. *Journal of Agricultural and Food Chemistry*, *61*(37), 8861–8870. https://doi.org/10.1021/jf401041q

Goto, T., Yoshida, Y., Kiso, M., & Nagashima, H. (1996). Simultaneous analysis of individual catechins and caffeine in green tea. *Journal of Chromatography A*, *749*(1), 295–299. https://doi.org/10.1016/0021-9673(96)00456-6

Grassi, S., & Alamprese, C. (2018). Advances in NIR spectroscopy applied to process analytical technology in food industries. *Current Opinion in Food Science*, *22*, 17–21. https://doi.org/10.1016/j.cofs.2017.12.008

Grippi, F., Crosta, L., Aiello, G., Tolomeo, M., Oliveri, F., Gebbia, N., & Curione, A. (2008). Determination of stilbenes in Sicilian pistachio by high-performance liquid chromatographic diode array (HPLC-DAD/FLD) and evaluation of eventually mycotoxin contamination. *Food Chemistry*, *107*(1), 483–488. https://doi.org/10.1016/j.foodchem.2007.07.079

Gu, L., Kelm, M. A., Hammerstone, J. F., Beecher, G., Holden, J., Haytowitz, D., & Prior, R. L. (2003). Screening of Foods Containing Proanthocyanidins and Their Structural Characterization Using LC-MS/MS and Thiolytic Degradation. *Journal of Agricultural and Food Chemistry*, *51*(25), 7513–7521. https://doi.org/10.1021/jf034815d

Gucci, R., Caruso, G., Gennai, C., Esposto, S., Urbani, S., & Servili, M. (2019). Fruit growth, yield and oil quality changes induced by deficit irrigation at different stages of olive fruit development. *Agricultural Water Management*, *212*, 88–98. https://doi.org/10.1016/j.agwat.2018.08.022

Guerrero, B., Rodrigo, J., & Guerra, M. E. (2018). Situación y perspectivas del cultivo del ciruelo japonés (híbridos de Prunus salicina Lindl.). La marca de calidad CiEx® en Extremadura. *Revista de Fruticultura*, *65*, 82–91.

Guerrero, R. F., Valls-Fonayet, J., Richard, T., & Cantos-Villar, E. (2020). A rapid quantification of stilbene content in wine by ultra-high pressure liquid chromatography – Mass spectrometry. *Food Control*, *108*, 106821. https://doi.org/10.1016/j.foodcont.2019.106821

Gunawardena, D., Govindaraghavan, S., & Münch, G. (2014). Chapter 30 - Anti-Inflammatory Properties of Cinnamon Polyphenols and their Monomeric Precursors. In *Polyphenols in Human Health and Disease* (pp. 409–425). https://doi.org/10.1016/B978-0-12-398456-2.00030-X

Gutiérrez-Gamboa, G., Pérez-Donoso, A. G., Pou-Mir, A., Acevedo-Opazo, C., & Valdés-Gómez, H. (2019). Hydric behaviour and gas exchange in different grapevine varieties (Vitis vinifera L.) from the Maule Valley (Chile). *South African Journal of Enology and Viticulture*, Vol. 40, pp. 181–191.

Guzmán, E., Baeten, V., Fernández Pierna, J. A., & García-Mesa, J. A. (2015). Determination of the olive maturity index of intact fruits using image analysis. *Journal of Food Science and Technology*, *52*(3), 1462–1470. https://doi.org/10.1007/s13197-013-1123-7

Haaland, D. M., & Thomas, E. V. (1988a). Partial least-squares methods for spectral analyses. 1. Relation to other quantitative calibration methods and the extraction of qualitative information. *Analytical Chemistry*, *60*(11), 1193–1202. https://doi.org/10.1021/ac00162a020

Haaland, D. M., & Thomas, E. V. (1988b). Partial least-squares methods for spectral analyses. 2. Application to simulated and glass spectral data. *Analytical Chemistry*, *60*(11), 1202–1208. https://doi.org/10.1021/ac00162a021

Háková, M., Havlíková, L. C., Švec, F., Solich, P., Erben, J., Chvojka, J., & Šatínský, D.

(2020). Novel nanofibrous sorbents for the extraction and determination of resveratrol in wine. *Talanta*, *206*, 120181. https://doi.org/10.1016/j.talanta.2019.120181

Harbertson, J. F., & Spayd, S. (2006). Measuring Phenolics in the Winery. *American Journal of Enology and Viticulture*, *57*(3), 280 LP – 288. Retrieved from http://www.ajevonline.org/content/57/3/280.abstract

Harshman, R. A. (1970). Foundations of the PARAFAC procedure: Models and conditions for an "explanatory" multimodal factor analysis, UCLA Work. Pap. *Phonetics*, *16*, 1–84.

Herrmann, K., & Nagel, C. W. (1989). Occurrence and content of hydroxycinnamic and hydroxybenzoic acid compounds in foods. *Critical Reviews in Food Science and Nutrition*, *28*(4), 315–347. https://doi.org/10.1080/10408398909527504

Hidalgo Togores, J. (2006). Capítulo 3. Etapas del desarrollo del racimo. In E. Mundi-Prensa. (Ed.), *La calidad del vino desde viñedo (Enología, Viticultura).* (pp. 109–116).

Hooshyari, M., Rubio, L., Casale, M., Furlanetto, S., Turrini, F., Sarabia, L. A., & Ortiz, M. C. (2019). D-Optimal Design and PARAFAC as Useful Tools for the Optimisation of Signals from Fluorescence Spectroscopy Prior to the Characterisation of Green Tea Samples. *Food Analytical Methods*, *12*(3), 761–772. https://doi.org/10.1007/s12161-018-01408-0

Hrobo\vnová, K., & Sádecká, J. (2019). Coumarins content in wine: application of HPLC, fluorescence spectrometry, and chemometric approach. *Journal of Food Science and Technology*, *57*(1), 200–209. https://doi.org/10.1007/s13197-019-04048-2

Hu, L., Yin, C., Ma, S., & Liu, Z. (2018). Rapid detection of three quality parameters and classification of wine based on Vis-NIR spectroscopy with wavelength selection by ACO and CARS algorithms. *Spectrochimica Acta Part A: Molecular and Biomolecular Spectroscopy*, *205*, 574–581. https://doi.org/10.1016/j.saa.2018.07.054

Hueso, A., Trentacoste, E. R., Junquera, P., Gómez-Miguel, V., & Gómez-del-Campo, M. (2019). Differences in stem water potential during oil synthesis determine fruit characteristics and production but not vegetative growth or return bloom in an olive hedgerow orchard (cv. Arbequina). *Agricultural Water Management*, *223*, 105589. https://doi.org/10.1016/j.agwat.2019.04.006

International Organisation of Vine andWine. (2020). *Compendium of International Methods of Wine and Must Analysis. 1*, 2020.

Ivanišević, D., Kalajdžić, M., Drenjančević, M., Puškaš, V., & Korać, N. (2020). The impact of cluster thinning and leaf removal timing on the grape quality and concentration of monomeric anthocyanins in Cabernet-Sauvignon and Probus (Vitis vinifera L.) wines. *OENO One*, *54*(1), 63–74. https://doi.org/10.20870/oeno-one.2020.54.1.2505

Jakubíková, M., Sádecká, J., & Kleinová, A. (2018). On the use of the fluorescence, ultraviolet–visible and near infrared spectroscopy with chemometrics for the discrimination between plum brandies of different varietal origins. *Food Chemistry*, *239*, 889–897. https://doi.org/10.1016/j.foodchem.2017.07.008

Jediyi, H., Naamani, K., Ait Elkoch, A., Dihazi, A., El Alaoui El Fels, A., & Arkize, W. (2019). First study on technological maturity and phenols composition during the ripeness of five Vitis vinifera L grape varieties in Morocco. *Scientia Horticulturae*, *246*, 390–397. https://doi.org/10.1016/j.scienta.2018.10.052

Jiang, C.-C., Fang, Z.-Z., Zhou, D.-R., Pan, S.-L., & Ye, X.-F. (2019). Changes in secondary metabolites, organic acids and soluble sugars during the development of plum fruit cv. 'Furongli' (Prunus salicina Lindl). *Journal of the Science of Food and Agriculture*, *99*(3), 1010–1019. https://doi.org/10.1002/jsfa.9265

Jiménez-Herrera, R., Pacheco-López, B., & Peragón, J. (2019). Water Stress, Irrigation and Concentrations of Pentacyclic Triterpenes and Phenols in Olea europaea L. cv. Picual Olive Trees. *Antioxidants*, *8*(8), 294. https://doi.org/10.3390/antiox8080294

Jones, H. G. (2006). Monitoring plant and soil water status: established and novel methods revisited and their relevance to studies of drought tolerance. *Journal of Experimental Botany*, *58*(2), 119–130. https://doi.org/10.1093/jxb/erl118

Ju, Y. lun, Yang, B. han, He, S., Tu, T. yao, Min, Z., Fang, Y. lin, & Sun, X. yu. (2019). Anthocyanin accumulation and biosynthesis are modulated by regulated deficit irrigation in Cabernet Sauvignon (Vitis Vinifera L.) grapes and wines. *Plant Physiology and Biochemistry*, *135*, 469–479. https://doi.org/10.1016/j.plaphy.2018.11.013

Kalogiouri, N. P., Aalizadeh, R., Dasenaki, M. E., & Thomaidis, N. S. (2020). Authentication of Greek PDO Kalamata Table Olives: A Novel Non-Target High Resolution Mass

Spectrometric Approach. *Molecules*, *25*(12), 2919. https://doi.org/10.3390/molecules25122919

Karatas, O., Balci Yuce, H., Taskan, M. M., Gevrek, F., Ucan Yarkac, F., Keskin, A., … Toker, H. (2019). The effect of vanillic acid on ligature-induced periodontal disease in Wistar rats. *Archives of Oral Biology*, *103*, 1–7. https://doi.org/10.1016/j.archoralbio.2019.05.010

Karković Marković, A., Torić, J., Barbarić, M., & Jakobušić Brala, C. (2019). Hydroxytyrosol, Tyrosol and Derivatives and Their Potential Effects on Human Health. *Molecules*, *24*(10), 2001. https://doi.org/10.3390/molecules24102001

Karoui, R., & Blecker, C. (2011). Fluorescence Spectroscopy Measurement for Quality Assessment of Food Systems—a Review. *Food and Bioprocess Technology*, *4*(3), 364–386. https://doi.org/10.1007/s11947-010-0370-0

Karoui, R., Mazerolles, G., & Dufour, É. (2003). Spectroscopic techniques coupled with chemometric tools for structure and texture determinations in dairy products. *International Dairy Journal*, *13*(8), 607–620. https://doi.org/10.1016/S0958-6946(03)00076-1

Kemsley, E. K. (1998). A genetic algorithm (GA) approach to the calculation of canonical variates (CVs). *TrAC - Trends in Analytical Chemistry*, *17*(1), 24–34. https://doi.org/10.1016/S0165-9936(97)00085-X

Kennedy, J. A., Matthews, M. A., & Waterhouse, A. L. (2002). Effect of maturity and vine water status on grape skin and wine flavonoids. *American Journal of Enology and Viticulture*, *53*(4), 268–274.

Kępa, M., Miklasińska-Majdanik, M., Wojtyczka, R. D., Idzik, D., Korzeniowski, K., Smoleń-Dzirba, J., & Wąsik, T. J. (2018). Antimicrobial Potential of Caffeic Acid against *Staphylococcus aureus* Clinical Strains. *BioMed Research International*, *2018*, 7413504. https://doi.org/10.1155/2018/7413504

Khan, B. A., Mahmood, T., Menaa, F., Shahzad, Y., Yousaf, A. M., Talib, H., & Ray, S. D. (2018). New Perspectives on the Efficacy of Gallic Acid in Cosmetics & Nanocosmeceuticals. *Current Pharmaceutical Design*, *24*(43), 5181–5187. https://doi.org/10.2174/1381612825666190118150614

Khanam, U. K. S., Oba, S., Yanase, E., & Murakami, Y. (2012). Phenolic acids, flavonoids and total antioxidant capacity of selected leafy vegetables. *Journal of Functional Foods*, *4*(4), 979–987. https://doi.org/10.1016/j.jff.2012.07.006

Kiai, H., Raiti, J., El Abbassi, A., & Hafidi, A. (2020). Chemical Profiles of Moroccan Picholine Olives and Its Brines during Spontaneous Fermentation. *International Journal of Fruit Science*, *20*, S1297–S1312. https://doi.org/10.1080/15538362.2020.1785986

Kong, W., Han, R., Liu, N., Bai, W., Ma, J., Bai, X., … Zhang, J. (2019). Dynamic assessment of the fruit quality of olives cultivated in Longnan (China) during ripening. *Scientia Horticulturae*, *253*, 8–16. https://doi.org/10.1016/j.scienta.2019.04.037

Kontoudakis, N., Esteruelas, M., Fort, F., Canals, J. M., & Zamora, F. (2010). Comparison of methods for estimating phenolic maturity in grapes: Correlation between predicted and obtained parameters. *Analytica Chimica Acta*, *660*(1), 127–133. https://doi.org/10.1016/j.aca.2009.10.067

Kopustinskiene, D. M., Jakstas, V., Savickas, A., & Bernatoniene, J. (2020). Flavonoids as Anticancer Agents. *Nutrients*, *12*(2), 457. https://doi.org/10.3390/nu12020457

Kostadinović, S., Wilkens, A., Stefova, M., Ivanova, V., Vojnoski, B., Mirhosseini, H., & Winterhalter, P. (2012). Stilbene levels and antioxidant activity of Vranec and Merlot wines from Macedonia: Effect of variety and enological practices. *Food Chemistry*, *135*(4), 3003–3009. https://doi.org/10.1016/j.foodchem.2012.06.118

Kriedemann, P. E., & Goodwin, I. (2003). Regulated deficit irrigation and partial rootzone drying. In *Irrigation Insights. Number 4.* Land & Water Australia.

Krstonošić, M. A., Hogervorst, J. C., Mikulić, M., & Gojković-Bukarica, L. (2019). Development of HPLC method for determination of phenolic compounds on a core shell column by direct injection of wine samples. *Acta Chromatographica*, *32*(2), 134–138. https://doi.org/10.1556/1326.2019.00611

Kucukgul, A., Isgor, M. M., Duzguner, V., Atabay, M. N., & Kucukgul, A. (n.d.). Antioxidant Effects of Oleuropein on Hydrogen Peroxide-Induced Neuronal Stress- An In Vitro Study. *Anti-Inflammatory & Anti-Allergy Agents in Medicinal Chemistry (Formerly Current Medicinal Chemistry - Anti-Inflammatory and Anti-Allergy Agents)*, Vol. 19, pp. 74–84. Retrieved from

https://www.ingentaconnect.com/content/ben/aiaamc/2020/00000019/00000001/art00007

Kumar, K., & Mishra, A. K. (2013). Analysis of dilute aqueous multifluorophoric mixtures using excitation–emission matrix fluorescence (EEMF) and total synchronous fluorescence (TSF) spectroscopy: A comparative evaluation. *Talanta*, *117*, 209–220. https://doi.org/10.1016/j.talanta.2013.09.002

Kumar, K., Tarai, M., & Mishra, A. K. (2017). Unconventional steady-state fluorescence spectroscopy as an analytical technique for analyses of complex-multifluorophoric mixtures. *TrAC Trends in Analytical Chemistry*, *97*, 216–243. https://doi.org/10.1016/j.trac.2017.09.004

Kumar, S., & Pandey, A. K. (2013). Chemistry and Biological Activities of Flavonoids: An Overview. *The Scientific World Journal*, *2013*, 162750. https://doi.org/10.1155/2013/162750

Laguna, L., Bartolomé, B., & Moreno-Arribas, M. V. (2017). Mouthfeel perception of wine: Oral physiology, components and instrumental characterization. *Trends in Food Science & Technology*, *59*, 49–59. https://doi.org/10.1016/j.tifs.2016.10.011

Lakowicz, J. R. (2006). Chapter 2. Instrumentation for Fluorescence Spectroscopy. In *Principles of Fluorescence Spectroscopy.* (Third Edit).

Lalani, S., & Poh, C. L. (2020). Flavonoids as Antiviral Agents for Enterovirus A71 (EV-A71). *Viruses*, *12*(2), 184. https://doi.org/10.3390/v12020184

Larrauri, A., Núñez, O., Hernández-Cassou, S., & Saurina, J. (2017). Determination of Polyphenols in White Wines by Liquid Chromatography: Application to the Characterization of Alella (Catalonia, Spain) Wines Using Chemometric Methods. *Journal of AOAC International*, *100*(2), 323–329. https://doi.org/10.5740/jaoacint.16-0407

Lazzez, A., Vichi, S., Kammoun, N. G., Arous, M. N., Khlif, M., Romero, A., & Cossentini, M. (2011). A four year study to determine the optimal harvesting period for Tunisian Chemlali olives. *European Journal of Lipid Science and Technology*, *113*(6), 796–807. https://doi.org/10.1002/ejlt.201000474

Lee, C., Polari, J. J., Kramer, K. E., & Wang, S. C. (2018). Near-Infrared (NIR) Spectrometry as a Fast and Reliable Tool for Fat and Moisture Analyses in Olives. *ACS Omega*, *3*(11), 16081–16088. https://doi.org/10.1021/acsomega.8b02491

Lenhardt, L., Bro, R., Zeković, I., Dramićanin, T., & Dramićanin, M. D. (2015). Fluorescence spectroscopy coupled with PARAFAC and PLS DA for characterization and classification of honey. *Food Chemistry*, *175*, 284–291. https://doi.org/10.1016/j.foodchem.2014.11.162

Leonard, S. S., Xia, C., Jiang, B.-H., Stinefelt, B., Klandorf, H., Harris, G. K., & Shi, X. (2003). Resveratrol scavenges reactive oxygen species and effects radical-induced cellular responses. *Biochemical and Biophysical Research Communications*, *309*(4), 1017–1026. https://doi.org/10.1016/j.bbrc.2003.08.105

Li, B., Cobo-Medina, M., Lecourt, J., Harrison, N. B., Harrison, R. J., & Cross, J. V. (2018). Application of hyperspectral imaging for nondestructive measurement of plum quality attributes. *Postharvest Biology and Technology*, *141*, 8–15. https://doi.org/10.1016/j.postharvbio.2018.03.008

Li, M., Lv, W., Zhao, R., Guo, H., Liu, J., & Han, D. (2017). Non-destructive assessment of quality parameters in 'Friar' plums during low temperature storage using visible/near infrared spectroscopy. *Food Control*, *73*, 1334–1341. https://doi.org/10.1016/j.foodcont.2016.10.054

Li, Q., Chang, X.-X., Wang, H., Stephen Brennan, C., & Guo, X.-B. (2019). Phytochemicals Accumulation in Sanhua Plum (Prunus salicina L.) during Fruit Development and Their Potential Use as Antioxidants. *Journal of Agricultural and Food Chemistry*, *67*(9), 2459–2466. https://doi.org/10.1021/acs.jafc.8b05087

Li, Y., Zhang, S., & Sun, Y. (2020). Measurement of catechin and gallic acid in tea wine with HPLC. *Saudi Journal of Biological Sciences*, *27*(1), 214–221. https://doi.org/10.1016/j.sjbs.2019.08.011

Linder, M., & Sundberg, R. (2002). Precision of prediction in second-order calibration, with focus on bilinear regression methods. *Journal of Chemometrics*, *16*(1), 12–27. https://doi.org/10.1002/cem.661

Ljekocevic, M., Jadranin, M., Stankovic, J., Popovic, B., Nikicevic, N., Petrovic, A., &

Tesevic, V. (2019). Phenolic composition and anti-DPPH radical scavenging activity of plum wine produced from three plum cultivars. *Journal of the Serbian Chemical Society*, *84*(2), 141–151. https://doi.org/10.2298/JSC180710096L

Llerena Ruiz, J. L. (2005). Capítulo 13. Olivar y aceite de oliva. In *Agricultura y Ganadería Extremeñas* (pp. 259–269). Secretaría General de Agricultura, Desarrollo Rural, Población y Territorio.

Lloyd, J. B. F. (1971). Synchronized Excitation of Fluorescence Emission Spectra. *Nature Physical Science*, *231*(20), 64–65. https://doi.org/10.1038/physci231064a0

López-Olivari, R., Ortega-Farías, S., & Poblete-Echeverría, C. (2016). Partitioning of net radiation and evapotranspiration over a superintensive drip-irrigated olive orchard. *Irrigation Science*, *34*(1), 17–31. https://doi.org/10.1007/s00271-015-0484-2

Louw, E. D., & Theron, K. I. (2010). Robust prediction models for quality parameters in Japanese plums (Prunus salicina L.) using NIR spectroscopy. *Postharvest Biology and Technology*, *58*(3), 176–184. https://doi.org/10.1016/j.postharvbio.2010.07.001

Lu, S.-C., LiaO, W.-R., & Chen, S.-F. (2018). Quantification of Trans-resveratrol in Red Wines Using QuEChERS Extraction Combined with Liquid Chromatography–Tandem Mass Spectrometry. *Analytical Sciences*, *34*(4), 439–444. https://doi.org/10.2116/analsci.17P528

Lu, X., Ma, L., Ruan, L., Kong, Y., Mou, H., Zhang, Z., … Le, Y. (2010). Resveratrol differentially modulates inflammatory responses of microglia and astrocytes. *Journal of Neuroinflammation*, *7*(1), 46. https://doi.org/10.1186/1742-2094-7-46

Lu, Y., Liu, Y., Lv, J., Ma, Y., & Guan, X. (2020). Changes in the physicochemical components, polyphenol profile, and flavor of persimmon wine during spontaneous and inoculated fermentation. *Food Science & Nutrition*, *8*(6), 2728–2738. https://doi.org/10.1002/fsn3.1560

Lucarini, M., Durazzo, A., Kiefer, J., Santini, A., Lombardi-Boccia, G., Souto, E. B., … Cecchini, F. (2019). Grape Seeds: Chromatographic Profile of Fatty Acids and Phenolic Compounds and Qualitative Analysis by FTIR-ATR Spectroscopy. *Foods*, *9*(1), 10. https://doi.org/10.3390/foods9010010

Luis Aleixandre-Tudo, J., Buica, A., Nieuwoudt, H., Luis Aleixandre, J., & du Toit, W. (2017). Spectrophotometric Analysis of Phenolic Compounds in Grapes and Wines. *Journal of Agricultural and Food Chemistry*, *65*(20), 4009–4026. https://doi.org/10.1021/acs.jafc.7b01724

Lyons, M. M., Yu, C., Toma, R. B., Cho, S. Y., Reiboldt, W., Lee, J., & van Breemen, R. B. (2003). Resveratrol in Raw and Baked Blueberries and Bilberries. *Journal of Agricultural and Food Chemistry*, *51*(20), 5867–5870. https://doi.org/10.1021/jf034150f

Łysiak, G. P., Michalska-Ciechanowska, A., & Wojdyło, A. (2020). Postharvest changes in phenolic compounds and antioxidant capacity of apples cv. Jonagold growing in different locations in Europe. *Food Chemistry*, *310*, 125912. https://doi.org/10.1016/j.foodchem.2019.125912

Maleki, S. J., Crespo, J. F., & Cabanillas, B. (2019). Anti-inflammatory effects of flavonoids. *Food Chemistry*, *299*, 125124. https://doi.org/10.1016/j.foodchem.2019.125124

Manach, C., Scalbert, A., Morand, C., Rémésy, C., & Jiménez, L. (2004). Polyphenols: food sources and bioavailability. *The American Journal of Clinical Nutrition*, *79*(5), 727–747. https://doi.org/10.1093/ajcn/79.5.727

Manjón, E., Fernandes Brás, N., García-Estévez, I., & Escribano-Bailon, M. (2020). Cell wall mannoproteins from yeast affect salivary protein–flavanol interactions through different molecular mechanisms. *Journal of Agricultural and Food Chemistry*, *68*(47), 13459–13468. https://doi.org/10.1021/acs.jafc.9b08083

Manna, M. S., Saha, P., & Ghoshal, A. K. (2014). Iron complexation of pharmaceutical catechins through selective separation. *RSC Advances*, *4*(50), 26247–26250. https://doi.org/10.1039/C4RA03683B

Manzano Durán, R., Fernández Sánchez, J. E., Velardo-Micharet, B., & Rodríguez Gómez, M. J. (2019). Multivariate optimization of ultrasound-assisted extraction for the determination of phenolic compounds in plums (Prunus salicina Lindl.) by high-performance liquid chromatography (HPLC). *Instrumentation Science & Technology*, *48*(2), 113–127. https://doi.org/10.1080/10739149.2019.1662438

MAPA. (2019a). *Anuario de Estadística del Ministerio de Agricultura, Pesca y Alimentación 2018*. Subsecretaría de Agricultura, Pesca y Alimentación.

MAPA. (2019b). *Sector del Vino. Medidas para la estabilidad y la calidad. Hoja de Ruta del Ministerio de Agricultura, Pesca y Alimentación.* Secretaría General de Agricultura y Alimentación.

MAPAMA. (2018). *Plan de medidas para la mejora del sector de fruta dulce del Ministerio de Agricultura y Pesca, Alimentación y Medio Ambiente*.

Marciniak, M., Reynolds, A. G., & Brown, R. (2013). Influence of water status on sensory profiles of Ontario Riesling wines. *Food Research International*, *54*(1), 881–891. https://doi.org/10.1016/j.foodres.2013.08.030

Massart, D. L., Vandeginste, B. G. M., Buydens, L. M. C., De Jong, S., Lewi, P. J., & Smeyers-Verbeke, J. (1997). *Handbook of Chemometrics and Qualimetrics* (Elsevier). Amsterdam.

Mawdsley, P., Dodson Peterson, J., & Casassa, L. (2018). Agronomical and Chemical Effects of the Timing of Cluster Thinning on Pinot Noir (Clone 115) Grapes and Wines. *Fermentation*, *4*(3), 60. https://doi.org/10.3390/fermentation4030060

Medrano, H., Tomás, M., Martorell, S., Escalona, J.-M., Pou, A., Fuentes, S., … Bota, J. (2015). Improving water use efficiency of vineyards in semi-arid regions. A review. *Agronomy for Sustainable Development*, *35*(2), 499–517. https://doi.org/10.1007/s13593-014-0280-z

Mehretie, S., Al Riza, D. F., Yoshito, S., & Kondo, N. (2018). Classification of raw Ethiopian honeys using front face fluorescence spectra with multivariate analysis. *Food Control*, *84*, 83–88. https://doi.org/10.1016/j.foodcont.2017.07.024

Meinhart, A. D., Damin, F. M., Caldeirão, L., da Silveira, T. F. F., Filho, J. T., & Godoy, H. T. (2017). Chlorogenic acid isomer contents in 100 plants commercialized in Brazil. *Food Research International*, *99*, 522–530. https://doi.org/10.1016/j.foodres.2017.06.017

Meinhart, A. D., Damin, F. M., Caldeirão, L., de Jesus Filho, M., da Silva, L. C., da Silva Constant, L., … Godoy, H. T. (2019). Chlorogenic and caffeic acids in 64 fruits consumed in Brazil. *Food Chemistry*, *286*, 51–63. https://doi.org/10.1016/j.foodchem.2019.02.004

Meléndez, E., Ortiz, M. C., Sarabia, L. A., Íñiguez, M., & Puras, P. (2013). Modelling phenolic and technological maturities of grapes by means of the multivariate relation between organoleptic and physicochemical properties. *Analytica Chimica Acta*, *761*, 53–61. https://doi.org/10.1016/j.aca.2012.11.021

Mena, P., Domínguez-Perles, R., Gironés-Vilaplana, A., Baenas, N., García-Viguera, C., & Villaño, D. (2014). Flavan-3-ols, anthocyanins, and inflammation. *IUBMB Life*, *66*(11), 745–758. https://doi.org/10.1002/iub.1332

Menard, C., Bastianetto, S., & Quirion, R. (2013). Neuroprotective effects of resveratrol and epigallocatechin gallate polyphenols are mediated by the activation of protein kinase C gamma. *Frontiers in Cellular Neuroscience*, *7*, 281. https://doi.org/10.3389/fncel.2013.00281

Mínguez-Mosquera, M. I., & Gallardo-Guerrero, L. (1995). Disappearance of chlorophylls and carotenoids during the ripening of the olive. *Journal of the Science of Food and Agriculture*, *69*(1), 1–6. https://doi.org/10.1002/jsfa.2740690102

Minuti, L., & Pellegrino, R. (2008). Determination of phenolic compounds in wines by novel matrix solid-phase dispersion extraction and gas chromatography/mass spectrometry. *Journal of Chromatography A*, *1185*(1), 23–30. https://doi.org/10.1016/j.chroma.2008.01.039

Modificación Normal del Pliego de Condiciones, & «RIBERA DEL GUADIANA». (2020). Publicación de una comunicación de aprobación de una modificación normal del Pliego de Condiciones de una denominación del sector vitivinícola, tal como se menciona en el artículo 17, apartados 2 y 3, del Reglamento Delegado (UE) 2019/33 de la Comisión. *Diario Oficial de La Union Europea*, *437*, 34–41.

Mojica, L., Meyer, A., Berhow, M. A., & de Mejía, E. G. (2015). Bean cultivars (Phaseolus vulgaris L.) have similar high antioxidant capacity, in vitro inhibition of α-amylase and α-glucosidase while diverse phenolic composition and concentration. *Food Research International*, *69*, 38–48. https://doi.org/10.1016/j.foodres.2014.12.007

Monago-Maraña, O., Domínguez-Manzano, J., Muñoz de la Peña, A., & Durán-Merás, I. (2020). Second-order calibration in combination with fluorescence fibre-optic data modelling as a novel approach for monitoring the maturation stage of plums.

*Chemometrics and Intelligent Laboratory Systems*, *199*, 103980. https://doi.org/10.1016/j.chemolab.2020.103980

Moreno-González, R., Juan, M. E., & Planas, J. M. (2019). Table olive polyphenols: A simultaneous determination by liquid chromatography–mass spectrometry. *Journal of Chromatography A*, *1609*, 460434. https://doi.org/10.1016/j.chroma.2019.460434

Moscatello, S., Frioni, T., Blasi, F., Proietti, S., Pollini, L., Verducci, G., … Famiani, F. (2019). Changes in Absolute Contents of Compounds Affecting the Taste and Nutritional Properties of the Flesh of Three Plum Species Throughout Development. *Foods (Basel, Switzerland)*, *8*(10), 486. https://doi.org/10.3390/foods8100486

Mousavi, M., Zaiter, A., Modarressi, A., Baudelaire, E., & Dicko, A. (2019). The positive impact of a new parting process on antioxidant activity, malic acid and phenolic content of Prunus avium L., Prunus persica L. and Prunus domestica subsp. Insititia L. powders. *Microchemical Journal*, *149*, 103962. https://doi.org/10.1016/j.microc.2019.103962

Mudenuti, N. V. de R., de Camargo, A. C., Shahidi, F., Madeira, T. B., Hirooka, E. Y., & Grossmann, M. V. E. (2018). Soluble and insoluble-bound fractions of phenolics and alkaloids and their antioxidant activities in raw and traditional chocolate: A comparative study. *Journal of Functional Foods*, *50*, 164–171. https://doi.org/10.1016/j.jff.2018.10.003

Muñoz de la Peña, A., Espinosa Mansilla, A., González Gómez, D., Olivieri, A. C., & Goicoechea, H. C. (2003). Interference-free analysis using three-way fluorescence data and the parallel factor model. Determination of fluoroquinolone antibiotics in human serum. *Analytical Chemistry*, *75*(11), 2640–2646. https://doi.org/10.1021/ac026360h

Muñoz de la Peña, A., Mujumdar, N., Heider, E. C., Goicoechea, H. C., Muñoz de la Peña, D., & Campiglia, A. D. (2016). Nondestructive Total Excitation–Emission Fluorescence Microscopy Combined with Multi-Way Chemometric Analysis for Visually Indistinguishable Single Fiber Discrimination. *Analytical Chemistry*, *88*(5), 2967–2975. https://doi.org/10.1021/acs.analchem.6b00264

Musingarabwi, D. M., Nieuwoudt, H. H., Young, P. R., Eyéghè-Bickong, H. A., & Vivier, M. A. (2016). A rapid qualitative and quantitative evaluation of grape berries at various stages of development using Fourier-transform infrared spectroscopy and multivariate

data analysis. *Food Chemistry*, *190*, 253–262. https://doi.org/10.1016/j.foodchem.2015.05.080

Nardini, M., & Garaguso, I. (2020). Characterization of bioactive compounds and antioxidant activity of fruit beers. *Food Chemistry*, *305*, 125437. https://doi.org/10.1016/j.foodchem.2019.125437

Narukawa, M., Kimata, H., Noga, C., & Watanabe, T. (2010). Taste characterisation of green tea catechins. *International Journal of Food Science & Technology*, *45*(8), 1579–1585. https://doi.org/10.1111/j.1365-2621.2010.02304.x

Ndou, A., Tinyani, P. P., Slabbert, R. M., Sultanbawa, Y., & Sivakumar, D. (2019). An integrated approach for harvesting Natal plum (Carissa macrocarpa) for quality and functional compounds related to maturity stages. *Food Chemistry*, *293*, 499–510. https://doi.org/10.1016/j.foodchem.2019.04.102

Nowicka, A., Kucharska, A. Z., Sokół-Łętowska, A., & Fecka, I. (2019). Comparison of polyphenol content and antioxidant capacity of strawberry fruit from 90 cultivars of Fragaria × ananassa Duch. *Food Chemistry*, *270*, 32–46. https://doi.org/10.1016/j.foodchem.2018.07.015

Nsir, H., Taamalli, A., Valli, E., Bendini, A., Gallina Toschi, T., & Zarrouk, M. (2017). Chemical Composition and Sensory Quality of Tunisian 'Sayali' Virgin Olive Oils as Affected by Fruit Ripening: Toward an Appropriate Harvesting Time. *Journal of the American Oil Chemists' Society*, *94*(7), 913–922. https://doi.org/10.1007/s11746-017-3000-4

Ofosu, F. K., Elahi, F., Daliri, E. B.-M., Yeon, S.-J., Ham, H. J., Kim, J.-H., … Oh, D.-H. (2020). Flavonoids in Decorticated Sorghum Grains Exert Antioxidant, Antidiabetic and Antiobesity Activities. *Molecules*, *25*(12), 2854. https://doi.org/10.3390/molecules25122854

Öhman, J., Geladi, P., & Wold, S. (1990). Residual bilinearization. Part 1: Theory and algorithms. *Journal of Chemometrics*, *4*(1), 79–90. https://doi.org/10.1002/cem.1180040109

Olivieri, A. C. (2005). On a versatile second-order multivariate calibration method based on partial least-squares and residual bilinearization: Second-order advantage and precision

properties. *Journal of Chemometrics*, *19*(4), 253–265. https://doi.org/10.1002/cem.927

Olivieri, A. C. (2014). Recientes desarrollos en calibración analítica empleando datos instrumentales multi-vía. In *Anales Academia Nacional de Ciencias Exactas, Físicas y Naturales* (Vol. 66, pp. 5–21).

Olivieri, A. C., Arancibia, J. A., Muñoz de la Peña, A., Durán-Merás, I., & Espinosa Mansilla, A. (2004). Second-Order Advantage Achieved with Four-Way Fluorescence Excitation−Emission−Kinetic Data Processed by Parallel Factor Analysis and Trilinear Least-Squares. Determination of Methotrexate and Leucovorin in Human Urine. *Analytical Chemistry*, *76*(19), 5657–5666. https://doi.org/10.1021/ac0493065

Olivieri, A. C., & Escandar, G. M. (2014). Chapter 5 - Parallel Factor Analysis: Trilinear Data. In *Practical Three-Way Calibration* (pp. 65–92). https://doi.org/10.1016/B978-0-12-410408-2.00005-3

Ou, K., & Gu, L. (2014). Absorption and metabolism of proanthocyanidins. *Journal of Functional Foods*, *7*, 43–53. https://doi.org/10.1016/j.jff.2013.08.004

Padmanabhan, P., Correa-Betanzo, J., & Paliyath, G. (2016). Berries and Related Fruits. In *Encyclopedia of Food and Health* (pp. 364–371). https://doi.org/10.1016/B978-0-12-384947-2.00060-X

Pan, H., Wang, L., Wang, R., Xie, F., & Cao, J. (2018). Modifications of cell wall pectin in chilling-injured 'Friar' plum fruit subjected to intermediate storage temperatures. *Food Chemistry*, *242*, 538–547. https://doi.org/10.1016/j.foodchem.2017.09.090

Panche, A. N., Diwan, A. D., & Chandra, S. R. (2016). Flavonoids: an overview. *Journal of Nutritional Science*, *5*, e47. https://doi.org/10.1017/jns.2016.41

Parker, C. A. (1968). Photoluminescence of solutions with applications to photochemistry and analytical chemistry. In *Parker C.A (ed.): Apparatus and Experimental Methods. Elsevier Publishing Company, Amsterdam* (pp. 128–302).

Parkinson, L., & Cicerale, S. (2016). The Health Benefiting Mechanisms of Virgin Olive Oil Phenolic Compounds. *Molecules*, *21*(12), 1734. https://doi.org/10.3390/molecules21121734

Pathare, P. B., Opara, U. L., & Al-Said, F. A. J. (2013). Colour measurement and analysis in

fresh and processed foods: a review. *Food Bioprocess Technol.*, *6*, 36–60. https://doi.org/10.1007/s11947-012-0867-9

Patra, D., & Mishra, A. (2002). Total synchronous fluorescence scan spectra of petroleum products. *Analytical and Bioanalytical Chemistry*, *373*(4), 304–309. https://doi.org/10.1007/s00216-002-1330-y

Pedan, V., Popp, M., Rohn, S., Nyfeler, M., & Bongartz, A. (2019). Characterization of Phenolic Compounds and Their Contribution to Sensory Properties of Olive Oil. *Molecules*, *24*(11), 2041. https://doi.org/10.3390/molecules24112041

Perestrelo, R., Bordiga, M., Locatelli, M., Silva, C., & Câmara, J. S. (2020). Polyphenols, biogenic amines and amino acids patterns in Verdelho wines according to vintage. *Microchemical Journal*, *153*, 104383. https://doi.org/10.1016/j.microc.2019.104383

Perez-Jiménez, M., Chaya, C., & Pozo-Bayón, M. Á. (2019). Individual differences and effect of phenolic compounds in the immediate and prolonged in-mouth aroma release and retronasal aroma intensity during wine tasting. *Food Chemistry*, *285*, 147–155. https://doi.org/10.1016/j.foodchem.2019.01.152

Pérez-Magariño, S., & González-San José, M. L. (2006). Polyphenols and colour variability of red wines made from grapes harvested at different ripeness grade. *Food Chemistry*, *96*(2), 197–208. https://doi.org/10.1016/j.foodchem.2005.02.021

Pérez-Navarro, J., Izquierdo-Cañas, P. M., Mena-Morales, A., Martínez-Gascueña, J., Chacón-Vozmediano, J. L., García-Romero, E., … Gómez-Alonso, S. (2019). Phenolic compounds profile of different berry parts from novel Vitis vinifera L. red grape genotypes and Tempranillo using HPLC-DAD-ESI-MS/MS: A varietal differentiation tool. *Food Chemistry*, *295*, 350–360. https://doi.org/10.1016/j.foodchem.2019.05.137

Petrovic, G., Aleixandre-Tudo, J.-L., & Buica, A. (2020). Viability of IR spectroscopy for the accurate measurement of yeast assimilable nitrogen content of grape juice. *Talanta*, *206*, 120241. https://doi.org/10.1016/j.talanta.2019.120241

Picón Toro, J., Montero Guerra, M. L., Simón Garzón, C., Sánchez Cordero, M. del C., Simón Lucas, P., & Cepeda Sánchez, N. (2018). Capítulo 2. Macromagnitudes Agrarias. In *Agricultura y Ganadería Extremeñas* (pp. 45–67). Secretaría General de Agricultura, Desarrollo Rural, Población y Territorio.

Ponce, J. M., Aquino, A., Millan, B., & Andújar, J. M. (2019). Automatic Counting and Individual Size and Mass Estimation of Olive-Fruits Through Computer Vision Techniques. *IEEE Access*, *7*, 59451–59465. https://doi.org/10.1109/ACCESS.2019.2915169

Ponce, J. M., Aquino, A., Millán, B., & Andújar, J. M. (2018). Olive-Fruit Mass and Size Estimation Using Image Analysis and Feature Modeling. *Sensors*, *18*(9), 2930. https://doi.org/10.3390/s18092930

Pourcel, L., Routaboul, J.-M., Cheynier, V., Lepiniec, L., & Debeaujon, I. (2007). Flavonoid oxidation in plants: from biochemical properties to physiological functions. *Trends in Plant Science*, *12*(1), 29–36. https://doi.org/10.1016/j.tplants.2006.11.006

Quiñones, M., Miguel, M., & Aleixandre, A. (2012). Los polifenoles, compuestos de origen natural con efectos saludables sobre el sistema cardiovascular . *Nutrición Hospitalaria* , Vol. 27, pp. 76–89. scieloes .

Radović, M., Milatović, D., Tešić, Ž., Tosti, T., Gašić, U., Dojčinović, B., & Dabić Zagorac, D. (2020). Influence of rootstocks on the chemical composition of the fruits of plum cultivars. *Journal of Food Composition and Analysis*, *92*, 103480. https://doi.org/10.1016/j.jfca.2020.103480

Rallo, L., Díez, C. M., Morales-Sillero, A., Miho, H., Priego-Capote, F., & Rallo, P. (2018). Quality of olives: A focus on agricultural preharvest factors. *Scientia Horticulturae*, *233*, 491–509. https://doi.org/10.1016/j.scienta.2017.12.034

Ramón-Gonçalves, M., Gómez-Mejía, E., Rosales-Conrado, N., León-González, M. E., & Madrid, Y. (2019). Extraction, identification and quantification of polyphenols from spent coffee grounds by chromatographic methods and chemometric analyses. *Waste Management*, *96*, 15–24. https://doi.org/10.1016/j.wasman.2019.07.009

Rashmi, H. B., & Negi, P. S. (2020). Phenolic acids from vegetables: A review on processing stability and health benefits. *Food Research International*, *136*, 109298. https://doi.org/10.1016/j.foodres.2020.109298

Reglamento (CE) nº 2138/97. (n.d.). *Reglamento (CE) nº 2138/97 de la Comisión de 30 de octubre de 1997 por el que se delimitan las zonas de producción homogéneas de aceite de oliva.*

Revilla, E., García-Beneytez, E., Cabello, F., Martín-Ortega, G., & Ryan, J.-M. (2001). Value of high-performance liquid chromatographic analysis of anthocyanins in the differentiation of red grape cultivars and red wines made from them. *Journal of Chromatography A*, *915*(1), 53–60. https://doi.org/10.1016/S0021-9673(01)00635-5

Rezaei Kalaj, Y., Mollazade, K., Herppich, W., Regen, C., & Geyer, M. (2016). Changes of backscattering imaging parameter during plum fruit development on the tree and during storage. *Scientia Horticulturae*, *202*, 63–69. https://doi.org/10.1016/j.scienta.2016.02.029

Rho, J. H., & Stuart, J. L. (1978). Automated three-dimensional plotter for fluorescence measurements. *Analytical Chemistry*, *50*(4), 620–625. https://doi.org/10.1021/ac50026a020

Ribera-Fonseca, A., Jorquera-Fontena, E., Castro, M., Acevedo, P., Parra, J. C., & Reyes-Diaz, M. (2019). Exploring VIS/NIR reflectance indices for the estimation of water status in highbush blueberry plants grown under full and deficit irrigation. *Scientia Horticulturae*, *256*, 108557. https://doi.org/10.1016/j.scienta.2019.108557

Rienth, M., & Scholasch, T. (2019). State-of-the-art of tools and methods to assess vine water status. *OENO One*, *53*(4), 619–637. https://doi.org/10.20870/oeno-one.2019.53.4.2403

Ríos-Reina, R., Azcarate, S. M., Camiña, J. M., & Goicoechea, H. C. (2020). Multi-level Data Fusion Strategies for Modeling Three-way Electrophoresis Capillary and Fluorescence Arrays Enhancing Geographical and Grape variety Classification of Wines. *Analytica Chimica Acta*, *1126*, 52–62. https://doi.org/10.1016/j.aca.2020.06.014

Ríos-Reina, R., Callejón, R. M., Savorani, F., Amigo, J. M., & Cocchi, M. (2019). Data fusion approaches in spectroscopic characterization and classification of PDO wine vinegars. *Talanta*, *198*, 560–572. https://doi.org/10.1016/j.talanta.2019.01.100

Ríos-Reina, R., Elcoroaristizabal, S., Ocaña-González, J. A., García-González, D. L., Amigo, J. M., & Callejón, R. M. (2017). Characterization and authentication of Spanish PDO wine vinegars using multidimensional fluorescence and chemometrics. *Food Chemistry*, *230*, 108–116. https://doi.org/10.1016/j.foodchem.2017.02.118

Robles-Almazan, M., Pulido-Moran, M., Moreno-Fernandez, J., Ramirez-Tortosa, C., Rodriguez-Garcia, C., Quiles, J. L., & Ramirez-Tortosa, Mc. (2018). Hydroxytyrosol:

Bioavailability, toxicity, and clinical applications. *Food Research International*, *105*, 654–667. https://doi.org/10.1016/j.foodres.2017.11.053

Roca, M., & Mínguez-Mosquera, M. I. (2000). Changes in Chloroplast Pigments of Olive Varieties during Fruit Ripening. *Journal of Agricultural and Food Chemistry*, *49*(2), 832–839. https://doi.org/10.1021/jf001000l

Rocha, S., Araújo, A. M., Almeida, A., de Pinho, P. G., & Fernandes, E. (2019). Development and Validation of a GC-MS/MS Method for cis- and trans-Resveratrol Determination: Application to Portuguese Wines. *Food Analytical Methods*, *12*(7), 1536–1544. https://doi.org/10.1007/s12161-019-01482-y

Rodrigo, M. J., Alquézar, B., Alférez, F., & Zacarías, L. (2012). Part 1.2. Biochemistry of Fruits and Fruit Products. In *Handbook of Fruits and Fruit Processing.* (Second Edi).

Rodríguez-Cabo, T., Rodríguez, I., & Cela, R. (2012). Determination of hydroxylated stilbenes in wine by dispersive liquid-liquid microextraction followed by gas chromatography mass spectrometry. *Journal of Chromatography A*, *1258*, 21–29. https://doi.org/10.1016/j.chroma.2012.08.037

Rodríguez-Cabo, T., Rodríguez, I., Ramil, M., Silva, A., & Cela, R. (2016). Multiclass semi-volatile compounds determination in wine by gas chromatography accurate time-of-flight mass spectrometry. *Journal of Chromatography A*, *1442*, 107–117. https://doi.org/10.1016/j.chroma.2016.03.005

Rodríguez-Morató, J., Xicota, L., Fitó, M., Farré, M., Dierssen, M., & de la Torre, R. (2015). Potential Role of Olive Oil Phenolic Compounds in the Prevention of Neurodegenerative Diseases. *Molecules*, *20*(3), 4655–4680. https://doi.org/10.3390/molecules20034655

Rodríguez, F. J., García, A., Pardo, P. J., Chávez, F., & Luque-Baena, R. M. (2018). Study and classification of plum varieties using image analysis and deep learning techniques. *Progress in Artificial Intelligence*, *7*(2), 119–127. https://doi.org/10.1007/s13748-017-0137-1

Rogiers, S. Y., Greer, D. H., Hatfield, J. M., Hutton, R. J., Clarke, S. J., Hutchinson, P. A., & Somers, A. (2011). Stomatal response of an anisohydric grapevine cultivar to evaporative demand, available soil moisture and abscisic acid. *Tree Physiology*, *32*(3), 249–261. https://doi.org/10.1093/treephys/tpr131

Romero-Pérez, A. I., Ibern-Gómez, M., Lamuela-Raventós, R. M., & de la Torre-Boronat, M. C. (1999). Piceid, the Major Resveratrol Derivative in Grape Juices. *Journal of Agricultural and Food Chemistry*, *47*(4), 1533–1536. https://doi.org/10.1021/jf981024g

Romero-Trigueros, C., Bayona Gambín, J. M., Nortes Tortosa, P. A., Alarcón Cabañero, J. J., & Nicolás Nicolás, E. (2019). Determination of Crop Water Stress Index by Infrared Thermometry in Grapefruit Trees Irrigated with Saline Reclaimed Water Combined with Deficit Irrigation. *Remote Sensing*, *11*(7), 757. https://doi.org/10.3390/rs11070757

Romero, P., Gil-Muñoz, R., del Amor, F. M., Valdés, E., Fernández, J. I., & Martinez-Cutillas, A. (2013). Regulated Deficit Irrigation based upon optimum water status improves phenolic composition in Monastrell grapes and wines. *Agricultural Water Management*, *121*, 85–101. https://doi.org/10.1016/j.agwat.2013.01.007

Romero, P., Gil-Muñoz, R., Fernández-Fernández, J. I., del Amor, F. M., Martínez-Cutillas, A., & García-García, J. (2015). Improvement of yield and grape and wine composition in field-grown Monastrell grapevines by partial root zone irrigation, in comparison with regulated deficit irrigation. *Agricultural Water Management*, *149*, 55–73. https://doi.org/10.1016/j.agwat.2014.10.018

Ruiz-Ruiz, J. C., Esapadas Aldana, G. del C., Corona Cruz, A. I., & Segura-Campos, M. R. (2020). 9 - Antioxidant Activity of Polyphenols Extracted From Hop Used in Craft Beer. In *Biotehcnological Progress and Beverage Consumption* (pp. 283–310). https://doi.org/10.1016/B978-0-12-816678-9.00009-6

Ruiz-Sánchez, M. C., Domingo, R., & Castel, J. R. (2010). Review. Deficit irrigation in fruit trees and vines in Spain. *Spanish Journal of Agricultural Research*, *8*, S5–S20.

Ryan, D., Robards, K., Prenzler, P., & Antolovich, M. (1999). Applications of mass spectrometry to plant phenols. *TrAC Trends in Analytical Chemistry*, *18*(5), 362–372. https://doi.org/10.1016/S0165-9936(98)00118-6

Sádecká, J., & Jakubíková, M. (2020). Varietal classification of white wines by fluorescence spectroscopy. *Journal of Food Science and Technology*, *57*(7), 2545–2553. https://doi.org/10.1007/s13197-020-04291-y

Sádecká, J., Jakubíková, M., & Májek, P. (2018). Fluorescence spectroscopy for discrimination of botrytized wines. *Food Control*, *88*, 75–84.

https://doi.org/10.1016/j.foodcont.2017.12.033

Sádecká, J., Jakubíková, M., Májek, P., & Kleinová, A. (2016). Classification of plum spirit drinks by synchronous fluorescence spectroscopy. *Food Chemistry*, *196*, 783–790. https://doi.org/10.1016/j.foodchem.2015.10.001

Sádecká, J., Uríčková, V., Májek, P., & Jakubíková, M. (2019). Comparison of different fluorescence techniques in brandy classification by region of production. *Spectrochimica Acta - Part A: Molecular and Biomolecular Spectroscopy*, *216*, 125–135. https://doi.org/10.1016/j.saa.2019.03.018

Salvador, I., Massarioli, A. P., Silva, A. P. S., Malaguetta, H., Melo, P. S., & Alencar, S. M. (2019). Can we conserve trans-resveratrol content and antioxidant activity during industrial production of chocolate? *Journal of the Science of Food and Agriculture*, *99*(1), 83–89. https://doi.org/10.1002/jsfa.9146

Sánchez-Rodríguez, L., Cano-Lamadrid, M., Carbonell-Barrachina, Á. A., Wojdyło, A., Sendra, E., & Hernández, F. (2019). Polyphenol Profile in Manzanilla Table Olives As Affected by Water Deficit during Specific Phenological Stages and Spanish-Style Processing. *Journal of Agricultural and Food Chemistry*, *67*(2), 661–670. https://doi.org/10.1021/acs.jafc.8b06392

Sánchez-Rodríguez, L., Corell, M., Hernández, F., Sendra, E., Moriana, A., & Carbonell-Barrachina, Á. A. (2019). Effect of Spanish-style processing on the quality attributes of HydroSOStainable green olives. *Journal of the Science of Food and Agriculture*, *99*(4), 1804–1811. https://doi.org/10.1002/jsfa.9373

Sánchez-Rodríguez, L., Lipan, L., Andreu, L., Martín-Palomo, M. J., Carbonell-Barrachina, A., Hernández, F., & Sendra, E. (2019). Effect of regulated deficit irrigation on the quality of raw and table olives. *Agricultural Water Management*, *221*, 415–421. https://doi.org/10.1016/j.agwat.2019.05.014

Sanchez, E., & Kowalski, B. R. (1990). Tensorial resolution: A direct trilinear decomposition. *Journal of Chemometrics*, *4*(1), 29–45. https://doi.org/10.1002/cem.1180040105

Sánchez, E., & Kowalski, B. R. (1986). Generalized Rank Annihilation Factor Analysis. *Analytical Chemistry*, *58*(2), 496–499. https://doi.org/10.1021/ac00293a054

Santos-Buelga, C., & Feliciano, A. S. (2017). Flavonoids: From Structure to Health Issues. *Molecules*, *22*(3), 477. https://doi.org/10.3390/molecules22030477

Santos, M. C. D., Azcarate, S. M., Lima, K. M. G., & Goicoechea, H. C. (2020). Fluorescence spectroscopy application for Argentinean yerba mate (Ilex paraguariensis) classification assessing first- and second-order data structure properties. *Microchemical Journal*, *155*, 104783. https://doi.org/10.1016/j.microc.2020.104783

Savalekar, K., Ahammed Shabeer, T. P., Khan, Z., Oulkar, D., Jain, P., Patil, C., & Banerjee, K. (2019). Targeted phenolic profiling of Sauvignon blanc and Shiraz grapes grown in two regions of India by liquid chromatography-tandem mass spectrometry. *Journal of Food Science and Technology*, *56*(7), 3300–3312. https://doi.org/10.1007/s13197-019-03802-w

Schueuermann, C., Silcock, P., & Bremer, P. (2018). Front-face fluorescence spectroscopy in combination with parallel factor analysis for profiling of clonal and vineyard site differences in commercially produced Pinot Noir grape juices and wines. *Journal of Food Composition and Analysis*, *66*, 30–38. https://doi.org/10.1016/j.jfca.2017.11.005

Sherman, E., Greenwood, D. R., Villas-Boâs, S. G., Heymann, H., & Harbertson, J. F. (2017). Impact of Grape Maturity and Ethanol Concentration on Sensory Properties of Washington State Merlot Wines. *American Journal of Enology and Viticulture*, *68*(3), 344–356. https://doi.org/10.5344/ajev.2017.16076

Siddiqui, S., Kamal, A., Khan, F., Jamali, K. S., & Saify, Z. S. (2019). Gallic and vanillic acid suppress inflammation and promote myelination in an in vitro mouse model of neurodegeneration. *Molecular Biology Reports*, *46*(1), 997–1011. https://doi.org/10.1007/s11033-018-4557-1

Siebert, K. J. (2001). Chemometrics in Brewing—A Review. *Journal of the American Society of Brewing Chemists*, *59*(4), 147–156. https://doi.org/10.1094/ASBCJ-59-0147

Sikorska, E. (2019). 5 - Fluorescence Spectroscopy and Chemometrics in Analysis of Beverages. *Quality Control in the Beverage Industry*, *17*, 161–203. https://doi.org/10.1016/B978-0-12-816681-9.00005-9

Sikorska, E., Khmelinskii, I., & Sikorski, M. (2019). 19 - Fluorescence spectroscopy and imaging instruments for food quality evaluation. In *Evaluation Technologies for Food*

*Quality* (pp. 491–533). https://doi.org/10.1016/B978-0-12-814217-2.00019-6

Sikorska, E., Włodarska, K., & Khmelinskii, I. (2020). Application of multidimensional and conventional fluorescence techniques for classification of beverages originating from various berry fruit. *Methods and Applications in Fluorescence*, *8*(1), 015006. https://doi.org/10.1088/2050-6120/ab6367

Singleton, V. L., & Rossi, J. A. (1965). Colorimetry of total phenolics with phosphomolybdic-phosphotungstic acid reagents. *American Journal of Enology and Viticulture*, *16*(3), 144–158.

Slotani, M. (1964). Tolerance regions for a multivariate normal population. *Annals of the Institute of Statistical Mathematics*, *16*(1), 135–153. https://doi.org/10.1007/BF02868568

Sobhani, M., Farzaei, M. H., Kiani, S., & Khodarahmi, R. (2020). Immunomodulatory; Anti-inflammatory/antioxidant Effects of Polyphenols: A Comparative Review on the Parental Compounds and Their Metabolites. *Food Reviews International*, 1–53. https://doi.org/10.1080/87559129.2020.1717523

Somkuwar, R. G., Bhange, M. A., Oulkar, D. P., Sharma, A. K., & Ahammed Shabeer, T. P. (2018). Estimation of polyphenols by using HPLC--DAD in red and white wine grape varieties grown under tropical conditions of India. *Journal of Food Science and Technology*, *55*(12), 4994–5002. https://doi.org/10.1007/s13197-018-3438-x

Song, C. Z., Wang, C., Xie, S., & Zhang, Z. W. (2018). Effects of leaf removal and cluster thinning on berry quality of Vitis vinifera cultivars in the region of Weibei Dryland in China. *Journal of Integrative Agriculture*, *17*(7), 1620–1630. https://doi.org/10.1016/S2095-3119(18)61990-2

Spagnol, C. M., Assis, R. P., Brunetti, I. L., Isaac, V. L. B., Salgado, H. R. N., & Corrêa, M. A. (2019). In vitro methods to determine the antioxidant activity of caffeic acid. *Spectrochimica Acta - Part A: Molecular and Biomolecular Spectroscopy*, *219*, 358–366. https://doi.org/10.1016/j.saa.2019.04.025

Stanely Mainzen Prince, P., Dhanasekar, K., & Rajakumar, S. (2015). Vanillic acid prevents altered ion pumps, ions, inhibits Fas-receptor and caspase mediated apoptosis-signaling pathway and cardiomyocyte death in myocardial infarcted rats. *Chemico-Biological*

*Interactions*, *232*, 68–76. https://doi.org/10.1016/j.cbi.2015.03.009

Stój, A., Kapusta, I., & Domagała, D. (2020). Classification of Red Wines Produced from Zweigelt and Rondo Grape Varieties Based on the Analysis of Phenolic Compounds by UPLC-PDA-MS/MS. *Molecules*, *25*(6), 1342. https://doi.org/10.3390/molecules25061342

Suciu, R.-C., Zarbo, L., Guyon, F., & Magdas, D. A. (2019). Application of fluorescence spectroscopy using classical right angle technique in white wines classification. *Scientific Reports*, *9*(1), 18250. https://doi.org/10.1038/s41598-019-54697-8

Šuković, D., Knežević, B., Gašić, U., Sredojević, M., Ćirić, I., Todić, S., … Tešić, Ž. (2020). Phenolic Profiles of Leaves, Grapes and Wine of Grapevine Variety Vranac (Vitis vinifera L.) from Montenegro. *Foods*, *9*(2), 138. https://doi.org/10.3390/foods9020138

Sun, B., Ricardo-da-Silva, J. M., & Spranger, M. I. (2001). Quantification of Catechins and Proanthocyanidins in Several Portuguese Grapevine Varieties and Red Wines. *Ciência e Técnica Vitivinícola*, *16*, 23–34. Retrieved from http://www.scielo.mec.pt/scielo.php?script=sci_arttext&pid=S0254-02232001000100002&nrm=iso

Sun, B., Sá, M. de, Leandro, C., Caldeira, I., Duarte, F. L., & Spranger, I. (2013). Reactivity of Polymeric Proanthocyanidins toward Salivary Proteins and Their Contribution to Young Red Wine Astringency. *Journal of Agricultural and Food Chemistry*, *61*(4), 939–946. https://doi.org/10.1021/jf303704u

Suo, H., Tian, R., Li, J., Zhang, S., Cui, Y., Li, L., & Sun, B. (2019). Compositional characterization study on high -molecular -mass polymeric polyphenols in red wines by chemical degradation. *Food Research International*, *123*, 440–449. https://doi.org/10.1016/j.foodres.2019.04.056

Tajik, N., Tajik, M., Mack, I., & Enck, P. (2017). The potential effects of chlorogenic acid, the main phenolic components in coffee, on health: a comprehensive review of the literature. *European Journal of Nutrition*, *56*(7), 2215–2244. https://doi.org/10.1007/s00394-017-1379-1

Tajner-Czopek, A., Gertchen, M., Rytel, E., Kita, A., Kucharska, A. Z., & Sokół-Łętowska, A. (2020). Study of Antioxidant Activity of Some Medicinal Plants Having High Content

of Caffeic Acid Derivatives. *Antioxidants*, *9*(5), 412. https://doi.org/10.3390/antiox9050412

Tan, X., Li, Q., & Yang, J. (2020). CdTe QDs based fluorescent sensor for the determination of gallic acid in tea. *Spectrochimica Acta Part A: Molecular and Biomolecular Spectroscopy*, *224*, 117356. https://doi.org/10.1016/j.saa.2019.117356

Tang, K., Zhan, J.-C., Yang, H.-R., & Huang, W.-D. (2010). Changes of resveratrol and antioxidant enzymes during UV-induced plant defense response in peanut seedlings. *Journal of Plant Physiology*, *167*(2), 95–102. https://doi.org/10.1016/j.jplph.2009.07.011

Tauler, R. (1995). Multivariate curve resolution applied to second order data. *Chemometrics and Intelligent Laboratory Systems*, *30*(1), 133–146. https://doi.org/10.1016/0169-7439(95)00047-X

Teixeira, A., Eiras-Dias, J., Castellarin, S., & Gerós, H. (2013). Berry Phenolics of Grapevine under Challenging Environments. *International Journal of Molecular Sciences*, *14*(9), 18711–18739. https://doi.org/10.3390/ijms140918711

Teng, Y.-N., Wang, C. C. N., Liao, W.-C., Lan, Y.-H., & Hung, C.-C. (2020). Caffeic Acid Attenuates Multi-Drug Resistance in Cancer Cells by Inhibiting Efflux Function of Human P-Glycoprotein. *Molecules*, *25*(2), 247. https://doi.org/10.3390/molecules25020247

Timperio, A. M., D'Alessandro, A., Fagioni, M., Magro, P., & Zolla, L. (2012). Production of the phytoalexins trans-resveratrol and delta-viniferin in two economy-relevant grape cultivars upon infection with Botrytis cinerea in field conditions. *Plant Physiology and Biochemistry*, *50*, 65–71. https://doi.org/10.1016/j.plaphy.2011.07.008

Tomac, I., Šeruga, M., & Labuda, J. (2020). Evaluation of antioxidant activity of chlorogenic acids and coffee extracts by an electrochemical DNA-based biosensor. *Food Chemistry*, *325*, 126787. https://doi.org/10.1016/j.foodchem.2020.126787

Tomé-Carneiro, J., Crespo, M. C., Iglesias-Gutierrez, E., Martín, R., Gil-Zamorano, J., Tomas-Zapico, C., … Dávalos, A. (2016). Hydroxytyrosol supplementation modulates the expression of miRNAs in rodents and in humans. *Journal of Nutritional Biochemistry*, *34*, 146–155. https://doi.org/10.1016/j.jnutbio.2016.05.009

Tomková, M., Sádecká, J., & Hrobo\vnová, K. (2015). Synchronous Fluorescence Spectroscopy for Rapid Classification of Fruit Spirits. *Food Analytical Methods*, *8*(5), 1258–1267. https://doi.org/10.1007/s12161-014-0010-9

Topalovic, A., & Petkovsek, M. M. (2010). Changes in sugars, organic acids and phenolics of grape berries of cultivar Cardinal during ripening. *Journal of Food, Agriculture and Environment*, *8*(3&4), 223–227. Retrieved from https://www.wflpublisher.com/Abstract/3017

Torres, I., Sánchez, M. T., Benlloch-González, M., & Pérez-Marín, D. (2019). Irrigation decision support based on leaf relative water content determination in olive grove using near infrared spectroscopy. *Biosystems Engineering*, *180*, 50–58. https://doi.org/10.1016/j.biosystemseng.2019.01.016

Trela, B. C., & Waterhouse, A. L. (1996). Resveratrol: Isomeric Molar Absorptivities and Stability. *Journal of Agricultural and Food Chemistry*, *44*(5), 1253–1257. https://doi.org/10.1021/jf9504576

Tsimogiannis, D., & Oreopoulou, V. (2019). Chapter 16 - Classification of Phenolic Compounds in Plants. In *Polyphenols in Plants* (pp. 263–284). https://doi.org/10.1016/B978-0-12-813768-0.00026-8

Tzanova, M., Atanassova, S., Atanasov, V., & Grozeva, N. (2020). Content of Polyphenolic Compounds and Antioxidant Potential of Some Bulgarian Red Grape Varieties and Red Wines, Determined by HPLC, UV, and NIR Spectroscopy. *Agriculture*, *10*(6), 193. https://doi.org/10.3390/agriculture10060193

Tzanova, M., & Peeva, P. (2018). Rapid HPLC Method for Simultaneous Quantification of trans-Resveratrol and Quercetin in the Skin of Red Grapes. *Food Analytical Methods*, *11*(2), 514–521. https://doi.org/10.1007/s12161-017-1022-z

Uceda, M., & Frías, L. (1975). Harvest dates: evolution of the fruit oil content, oil composition and oil quality. *In: Proceedings II Seminario Oleícola Internacional. International Olive Council.*, 125–128. Córdoba.

Usenik, V., Kastelec, D., Veberič, R., & Štampar, F. (2008). Quality changes during ripening of plums (Prunus domestica L.). *Food Chemistry*, *111*, 830–836. https://doi.org/10.1016/j.foodchem.2008.04.057

Usenik, V., Štampar, F., & Veberič, R. (2009). Anthocyanins and fruit colour in plums (Prunus domestica L.) during ripening. *Food Chemistry*, *114*, 529–534. https://doi.org/10.1016/j.foodchem.2008.09.083

Uslu, N., & Özcan, M. M. (2020). The effect of irrigation and harvest time on bioactive properties of olive fruits issued from some olive varieties grown in Mediterranean region. *European Food Research and Technology*, *246*, 2587–2599. https://doi.org/10.1007/s00217-020-03599-5

Valentin, L., Barroso, L. P., Barbosa, R. M., de Paulo, G. A., & Castro, I. A. (2020). Chemical typicality of South American red wines classified according to their volatile and phenolic compounds using multivariate analysis. *Food Chemistry*, *302*, 125340. https://doi.org/10.1016/j.foodchem.2019.125340

Valéria da Silva Padilha, C., dos Santos Lima, M., Maia Toaldo, I., Elias Pereira, G., & Terezinha Bordignon-Luiz, M. (2019). Effects of successive harvesting in the same year on quality and bioactive compounds of grapes and juices in semi-arid tropical viticulture. *Food Chemistry*, *301*, 125170. https://doi.org/10.1016/j.foodchem.2019.125170

Valeur, B. (2009). Molecular Fluorescence. In *digital Encyclopedia of Applied Physics* (pp. 477–531). https://doi.org/10.1002/3527600434.eap684

Valls, J., Millán, S., Martí, M. P., Borràs, E., & Arola, L. (2009). Advanced separation methods of food anthocyanins, isoflavones and flavanols. *Journal of Chromatography A*, *1216*(43), 7143–7172. https://doi.org/10.1016/j.chroma.2009.07.030

Venturini, C. D., Merlo, S., Souto, A. A., Fernandes, M. da C., Gomez, R., & Rhoden, C. R. (2010). Resveratrol and Red Wine Function as Antioxidants in the Nervous System without Cellular Proliferative Effects during Experimental Diabetes. *Oxidative Medicine and Cellular Longevity*, *3*, 568184. https://doi.org/10.4161/oxim.3.6.14741

Véstia, J., Barroso, J. M., Ferreira, H., Gaspar, L., & Rato, A. E. (2019). Predicting calcium in grape must and base wine by FT-NIR spectroscopy. *Food Chemistry*, *276*, 71–76. https://doi.org/10.1016/j.foodchem.2018.09.116

Vignault, A., Gombau, J., Jourdes, M., Moine, V., Canals, J. M., Fermaud, M., … Teissedre, P.-L. (2020). Oenological tannins to prevent Botrytis cinerea damage in grapes and musts: Kinetics and electrophoresis characterization of laccase. *Food Chemistry*, *316*,

126334. https://doi.org/10.1016/j.foodchem.2020.126334

Villalobos-González, L., Peña-Neira, A., Ibáñez, F., & Pastenes, C. (2016). Long-term effects of abscisic acid (ABA) on the grape berry phenylpropanoid pathway: Gene expression and metabolite content. *Plant Physiology and Biochemistry*, *105*, 213–223. https://doi.org/10.1016/j.plaphy.2016.04.012

Vincente, A. R., Manganaris, G. A., Ortiz, C. M., Sozzi, G. O., & Crisosto, C. H. (2014). Chapter 5 - Nutritional Quality of Fruits and Vegetables. In *Postharvest Handling (Third Edition)* (pp. 69–122). https://doi.org/10.1016/B978-0-12-408137-6.00005-3

Vinothiya, K., & Ashokkumar, N. (2017). Modulatory effect of vanillic acid on antioxidant status in high fat diet-induced changes in diabetic hypertensive rats. *Biomedicine and Pharmacotherapy*, *87*, 640–652. https://doi.org/10.1016/j.biopha.2016.12.134

Vlaic, R. A., Muresan, V., Muresan, A. E., Muresan, C. C., Paucean, A., Mitre, V., … Muste, S. (2018). The Changes of Polyphenols, Flavonoids, Anthocyanins and Chlorophyll Content in Plum Peels during Growth Phases: from Fructification to Ripening. *Notulae Botanicae Horti Agrobotanici Cluj-Napoca*, *46*(1), 148–155. https://doi.org/10.15835/nbha46111017

Vuolo, M. M., Lima, V. S., & Maróstica Junior, M. R. (2019). Chapter 2 - Phenolic Compounds: Structure, Classification, and Antioxidant Power. In *Bioactive Compounds* (pp. 33–50). https://doi.org/10.1016/B978-0-12-814774-0.00002-5

Wang, Q., Leong, W. F., Elias, R. J., & Tikekar, R. V. (2019). UV-C irradiated gallic acid exhibits enhanced antimicrobial activity via generation of reactive oxidative species and quinone. *Food Chemistry*, *287*, 303–312. https://doi.org/10.1016/j.foodchem.2019.02.041

Wang, R., Wang, L., Yuan, S., Li, Q., Pan, H., Cao, J., & Jiang, W. (2018). Compositional modifications of bioactive compounds and changes in the edible quality and antioxidant activity of 'Friar' plum fruit during flesh reddening at intermediate temperatures. *Food Chemistry*, *254*, 26–35. https://doi.org/10.1016/j.foodchem.2018.01.169

Wang, T. yang, Li, Q., & Bi, K. shun. (2018). Bioactive flavonoids in medicinal plants: Structure, activity and biological fate. *Asian Journal of Pharmaceutical Sciences*, *13*(1), 12–23. https://doi.org/10.1016/j.ajps.2017.08.004

Wang, W., Tang, K., Yang, H.-R., Wen, P.-F., Zhang, P., Wang, H.-L., & Huang, W.-D. (2010). Distribution of resveratrol and stilbene synthase in young grape plants (Vitis vinifera L. cv. Cabernet Sauvignon) and the effect of UV-C on its accumulation. *Plant Physiology and Biochemistry*, *48*(2), 142–152. https://doi.org/10.1016/j.plaphy.2009.12.002

Wang, Yechun, Chen, S., & Yu, O. (2011). Metabolic engineering of flavonoids in plants and microorganisms. *Applied Microbiology and Biotechnology*, *91*(4), 949–956. https://doi.org/10.1007/s00253-011-3449-2

Wang, Yu, He, Y. N., Chen, W. K., He, F., Chen, W., Cai, X. D., … Wang, J. (2018). Effects of cluster thinning on vine photosynthesis, berry ripeness and flavonoid composition of Cabernet Sauvignon. *Food Chemistry*, *248*, 101–110. https://doi.org/10.1016/j.foodchem.2017.12.021

Wani, S. M., Masoodi, F. A., Haq, E., Ahmad, M., & Ganai, S. A. (2020). Influence of processing methods and storage on phenolic compounds and carotenoids of apricots. *LWT - Food Science and Technology*, *132*, 109846. https://doi.org/10.1016/j.lwt.2020.109846

Wani, T. A., Masoodi, F. A., Gani, A., Baba, W. N., Rahmanian, N., Akhter, R., … Ahmad, M. (2018). Olive oil and its principal bioactive compound: Hydroxytyrosol – A review of the recent literature. *Trends in Food Science and Technology*, *77*, 77–90. https://doi.org/10.1016/j.tifs.2018.05.001

Warner, I. M., Callis, J. B., Davidson, E. R., Gouterman, M., & Christian, G. D. (1975). Fluorescence Analysis: A New Approach. *Analytical Letters*, *8*(9), 665–681. https://doi.org/10.1080/00032717508059038

Wei, C., Qiao, J., & Ma, Z. (2019). Rapid Determination of Resveratrol and Piceid in Wine by High-Performance Liquid Chromatography. *IOP Conference Series: Earth and Environmental Science*, *332*(3), 032012. https://doi.org/10.1088/1755-1315/332/3/032012

Wei, F., & Tanokura, M. (2015). Chapter 17 - Organic Compounds in Green Coffee Beans. In *Coffee in Health and Disease Prevention* (pp. 149–162). https://doi.org/10.1016/B978-0-12-409517-5.00017-6

Williamson, B., Tudzynski, B., Tudzynski, P., & Van Kan, J. A. L. (2007). Botrytis cinerea: the cause of grey mould disease. *Molecular Plant Pathology*, *8*(5), 561–580. https://doi.org/10.1111/j.1364-3703.2007.00417.x

Włodarska, K., Khmelinskii, I., & Sikorska, E. (2018). Authentication of apple juice categories based on multivariate analysis of the synchronous fluorescence spectra. *Food Control*, *86*, 42–49. https://doi.org/10.1016/j.foodcont.2017.11.004

Włodarska, K., Pawlak-Lemańska, K., Khmelinskii, I., & Sikorska, E. (2016). Explorative study of apple juice fluorescence in relation to antioxidant properties. *Food Chemistry*, *210*, 593–599. https://doi.org/10.1016/j.foodchem.2016.05.007

Włodarska, K., Pawlak-Lemańska, K., Khmelinskii, I., & Sikorska, E. (2017). Multivariate curve resolution – Alternating least squares analysis of the total synchronous fluorescence spectra: An attempt to identify polyphenols contribution to the emission of apple juices. *Chemometrics and Intelligent Laboratory Systems*, *164*, 94–102. https://doi.org/10.1016/j.chemolab.2017.02.011

Wold, S., Geladi, P., Esbensen, K., & Öhman, J. (1987). Multi-way principal components-and PLS-analysis. *Journal of Chemometrics*, *1*(1), 41–56. https://doi.org/10.1002/cem.1180010107

Xi, X., Zha, Q., Jiang, A., & Tian, Y. (2016). Impact of cluster thinning on transcriptional regulation of anthocyanin biosynthesis-related genes in "Summer Black" grapes. *Plant Physiology and Biochemistry*, *104*, 180–187. https://doi.org/10.1016/j.plaphy.2016.03.015

Xia, A. L., Wu, H. L., Fang, D. M., Ding, Y. J., Hu, L. Q., & Yu, R. Q. (2005). Alternating penalty trilinear decomposition algorithm for second-order calibration with application to interference-free analysis of excitation-emission matrix fluorescence data. *Journal of Chemometrics*, *19*(2), 65–76. https://doi.org/10.1002/cem.911

Xia, D., Sui, R., & Zhang, Z. (2019). Administration of resveratrol improved Parkinson's disease-like phenotype by suppressing apoptosis of neurons via modulating the MALAT1/miR-129/SNCA signaling pathway. *Journal of Cellular Biochemistry*, *120*(4), 4942–4951. https://doi.org/10.1002/jcb.27769

Xu, Y. Q., Zhang, Y. N., Chen, J. X., Wang, F., Du, Q. Z., & Yin, J. F. (2018). Quantitative

analyses of the bitterness and astringency of catechins from green tea. *Food Chemistry*, *258*, 16–24. https://doi.org/10.1016/j.foodchem.2018.03.042

Yan, Y., Zhou, X., Guo, K., Zhou, F., & Yang, H. (2020). Chlorogenic Acid Protects Against Indomethacin-Induced Inflammation and Mucosa Damage by Decreasing Bacteroides-Derived LPS. *Frontiers in Immunology*, *11*, 1125. https://doi.org/10.3389/fimmu.2020.01125

Yang, B., Yao, H., Zhang, J., Li, Y., Ju, Y., Zhao, X., … Fang, Y. (2020). Effect of regulated deficit irrigation on the content of soluble sugars, organic acids and endogenous hormones in Cabernet Sauvignon in the Ningxia region of China. *Food Chemistry*, *312*, 126020. https://doi.org/10.1016/j.foodchem.2019.126020

Yang, P., Li, H., Wang, H., Han, F., Jing, S., Yuan, C., … Xu, Z. (2017). Dispersive Liquid-Liquid Microextraction Method for HPLC Determination of Phenolic Compounds in Wine. *Food Analytical Methods*, *10*(7), 2383–2397. https://doi.org/10.1007/s12161-016-0781-2

Zaripour, M., Zare-Shahabadi, V., & Jahromi, H. J. (2019). Application of ultrasonic-assisted inclusion complex formation with α–cyclodextrin for simultaneous spectrophotometric determination of gallic acid and vanillic acids in fruit samples. *Spectrochimica Acta - Part A: Molecular and Biomolecular Spectroscopy*, *222*, 117197. https://doi.org/10.1016/j.saa.2019.117197

Zhang, W., Wu, Z., Wang, X., Li, X., Ma, D., Wang, F., … Pang, M. (2020). Antibacterial effect of flavonoids in *castanea mollissima blume* on common spoilage bacteria in low-temperature meat products. *IOP Conference Series: Earth and Environmental Science*, *508*, 012152. https://doi.org/10.1088/1755-1315/508/1/012152

Zhao, Y., Shi, M., Ye, J. H., Zheng, X. Q., Lu, J. L., & Liang, Y. R. (2015). Photo-induced chemical reaction of trans-resveratrol. *Food Chemistry*, *171*, 137–143. https://doi.org/10.1016/j.foodchem.2014.08.130

Zuñiga, A., Mora, M., Oyarce, M., & Fredes, C. (2014). Grape maturity estimation based on seed images and neural networks. *Engineering Applications of Artificial Intelligence*, *35*, 95–104. https://doi.org/10.1016/j.engappai.2014.06.007

# DISCUSIÓN GENERAL

## 5. DISCUSIÓN GENERAL

En la presente Tesis Doctoral se han desarrollado diferentes metodologías analíticas para la determinación de componentes fenólicos en diferentes matrices alimentarias: uvas, vinos, ciruelas y aceitunas de mesa. Para cada tipo, se ha llevado a cabo una caracterización de las mismas que ha permitido diferenciar estas muestras por grupos.

Tras una revisión bibliográfica, se comprobó que solamente se habían realizado estudios de caracterización fluorescente en el vino y en algunas bebidas alcohólicas derivadas de ciruelas. Del resto de matrices alimentarias, uvas y aceitunas de mesa, así como de las ciruelas frescas no existían estudios de fluorescencia previos. Para los tres tipos de muestras, existen múltiples trabajos en los que se cuantifican los componentes polifenólicos por técnicas separativas.

A continuación se van a resumir los resultados más relevantes en los estudios efectuados. Dichos resultados se presentan en las 7 publicaciones científicas así como en un trabajo de revisión que se adjuntan a continuación.

**Artículo 1.** *Front-face fluorescence spectroscopy combined with second-order multivariate algorithms for the quantification of polyphenols in red wine samples.* **Food Chemistry 220 (2017), 168-176.**

El primer estudio llevado a cabo como parte de esta Tesis se ha centrado en la cuantificación directa de compuestos polifenólicos en 11 muestras de vinos de dos regiones españolas, DOP "Rioja" y DOP "Ribera del Guadiana", sin pretratamiento de la muestra. Los compuestos polifenólicos de cada una de las muestras se cuantificaron por cromatografía líquida encontrando que todas tenían ácido gálico, ácido vaníllico, ácido cafeico, ácido *p*-cumárico, epicatequina y *t*-resveratrol mientras que solo cinco de ellos tenían catequina y quercetina.

En base a esta información, se realizaron dos calibraciones, con un diseño central compuesto de tres niveles. En la primera calibración, se separaron los grupos de analitos en base a sus características espectrales con muestras de calibración y validación que contenían ácido gálico, ácido vaníllico, ácido cafeico y epicatequina y muestras

calibración con ácido *p*-cumárico, quercetina y *t*-resveratrol. En la segunda calibración, las muestras de calibración y validación estaban compuestas, conjuntamente, de ácido gálico, ácido vaníllico, ácido cafeico, epicatequina, catequina y *t*-resveratrol más ácido *p*-cumárico y quercetina en concentración fija. Todos los patrones se prepararon simulando una matriz sintética de vino. Para ello, se prepararon las muestras de calibración con un 30% en volumen, con un tampón de ácido tartárico-tartrato sódico de 3 g/L (pH 3,7) y un 15% de etanol absoluto.

De cada una de las muestras de calibración y validación, así como de las muestras de vinos se obtuvo su señal de fluorescencia total (matriz de excitación-emisión, EEM), en modo *front-face*, en dos rangos de longitudes de onda, registrando los espectros de emisión entre 290 y 450 nm, cada 0,5 nm, variando la longitud de onda de excitación entre 240 y 290 nm, cada 5 nm; para el primer rango, y los espectros de emisión entre 330 y 400 nm, cada 0,5 nm, variando la longitud de onda de excitación entre 300 y 360 nm, cada 5 nm, para el segundo.

A continuación, se optimizaron los modelos de cuantificación, PARAFAC y U-PLS. Mediante PARAFAC, las mejores predicciones se obtuvieron para el ácido vaníllico, epicatequina más catequina y resveratrol. El algoritmo U-PLS, además de los analitos anteriores, también permitió predecir las concentraciones de ácido gálico y ácido cafeico.

Es necesario resaltar que, en la primera calibración, en la que se incluyó la epicatequina como único flavanol, los resultados de validación no fueron del todo satisfactorios por PARAFAC. Cuando epicatequina y catequina estuvieron presentes en las muestras de calibración, es decir, en la segunda calibración, las predicciones de la suma de ambos en las muestras de validación por PARAFAC tampoco fueron satisfactorias. Sin embargo, las predicciones por U-PLS, en la primera calibración, para epicatequina fueron satisfactorias y, en la segunda calibración, para la suma de epicatequina y catequina también fueron satisfactorias. El hecho de que PARAFAC no fuera capaz de predecir ambos analitos puede ser debido a la ausencia de selectividad debido a sus idénticas EEMs.

En las muestras de vinos, tomando como referencia las concentraciones obtenidas por cromatografía, se procedió a la cuantificación de los analitos, por U-PLS, para lo cual, se

hizo necesario el uso del acoplamiento con RBL y así obtener la ventaja de segundo orden. Se obtuvieron buenas predicciones en las concentraciones de ácido vaníllico, ácido cafeico, epicatequina y resveratrol. PARAFAC permitió la predicción de ácido vaníllico en muestras de vino.

Con estos resultados obtenidos se pudo concluir, que estos analitos, analizados por fluorescencia en combinación con quimiometría, podían ser cuantificados en muestras de vino sin pretratamiento y ofrecían un campo muy interesante de investigación, pudiéndose también emplear en otras matrices alimentarias que contuvieran estos analitos, así como otros con características similares.

**Artículo 2**. *Front-face fluorescence excitation-emission matrices in combination with three-way chemometrics for the discrimination and prediction of phenolic response to vineyard agronomic practices.* **Food Chemistry 270 (2019), 162-172.**

Una vez que se dispuso de información de los analitos fluorescentes que contenía el vino, se continuó con el análisis de muestras de uvas de la variedad '*Tempranillo*' de secano y regadío, cada una de las cuales sometidas a alta y baja carga. Se procedió a la caracterización de las muestras de uva de secano y regadío. Los grupos de muestras consistieron en un total de 48 muestras de uvas, 24 de ellas sometidas a regadío y 24 sometidas a secano.

Para llevar a cabo este estudio se obtuvo previamente un extracto acuoso de las uvas con una disolución de ácido oxálico en agua 0,3 M (pH 1,00) y, posteriormente, de este se obtuvo un segundo extracto con dietiléter (1:1) que se analizó por fluorescencia *front-face*.

Una vez fijadas las condiciones experimentales, se obtuvieron las EEMs registrando los espectros de emisión entre 284 y 399, cada 2,5 nm, y variando la longitud de onda de excitación entre 250 y 350 nm, cada 5 nm.

Cualitativamente, las EEMs presentaron dos regiones espectrales diferenciadas: una de ellas con emisión entre 335-365 nm y excitación entre 265-285 nm y otra con emisión entre 365-400 nm y excitación entre 320-340 nm. Además, en las muestras de uva de regadío, esta señal fluorescente fue de mayor intensidad.

De cara a obtener información del estado hídrico de las muestras se obtuvieron los "*scores*", por descomposición por PARAFAC del conjunto de datos, que se usaron para llevar a cabo un análisis exploratorio de las muestras y se observaron dos grupos definidos, en función de la aplicación de riego o no.

Posteriormente, se aplicó a los "*scores*" de PARAFAC la técnica de clasificación de LDA, obteniéndose una mejor clasificación. Con el propósito de usar una técnica de clasificación con un tratamiento de descomposición de datos diferente, se usó U-PLS-DA, que se empleó en el mismo sentido que para cuantificación, sustituyendo los valores de concentración por valores numéricos en función de los grupos a los que pertenezcan. También se consiguió con esta tercera técnica resultados satisfactorios de clasificación.

A continuación, se separaron dos sets de muestras independientes, de secano y regadío, para distinguir, dentro de cada set, entre las muestras de uvas procedentes de plantaciones de alta y baja carga. Solamente, dentro del set de muestras de riego, se consiguió diferenciar, satisfactoriamente, entre grupos en función de la carga del cultivo.

Para llevar a cabo la cuantificación individual de los analitos de las uvas, se realizó un diseño central con muestras de calibración con epicatequina, catequina y resveratrol en dietiléter. Los datos obtenidos se analizaron por PARAFAC y U-PLS.

Aplicando PARAFAC, en la primera región espectral, los perfiles fluorescentes del componente 3 del set de calibración eran prácticamente idénticos a los espectros de excitación/emisión de fluorescencia de epicatequina y catequina, y bastante coincidentes con el componente 3 del conjunto de las muestras de uva. También se apoya en las buenas correlaciones que tuvieron los "*scores*" de este componente con las concentraciones de epicatequina más catequina. Por su parte, en la segunda región espectral, por PARAFAC, los perfiles del componente 1 del conjunto de muestras de uva se parecían a los del componente 1 del set de calibración y a los espectros de excitación y emisión de resveratrol.

Respecto a la validación, ninguno de los algoritmos fue capaz de determinar la concentración individual de epicatequina o catequina. Sin embargo, las predicciones en

las muestras de validación fueron satisfactorias por ambos algoritmos para la suma de epicatequina y catequina, mientras que para resveratrol fueron mejores por U-PLS.

En cuanto a la cuantificación en muestras reales de uva, las predicciones por U-PLS de suma de epicatequina y catequina no fueron satisfactorias, mientras que por PARAFAC se obtuvieron concentraciones de suma de epicatequina y catequina similares a las obtenidas por cromatografía líquida. La suma de concentraciones de epicatequina y catequina osciló entre 19,98 a 24,84 $\mu g\ mL^{-1}$ en las muestras de secano y, entre 31,22 y 42,05 $\mu g\ mL^{-1}$, en las muestras de regadío. Para la cuantificación de resveratrol, las mejores predicciones se obtuvieron por U-PLS y su concentración osciló entre 2,43 y 3,03 $\mu g\ mL^{-1}$ en las muestras de secano y 3,46 y 4,67 $\mu g\ mL^{-1}$ en las muestras de regadío. Como posible explicación, se propuso que este aumento en la concentración de resveratrol podría deberse a la respuesta de la planta al aumento de la humedad ambiental.

Con este método analítico, se consiguió determinar tres compuestos fenólicos de las uvas, con un tiempo de análisis mucho más corto que los métodos de cromatografía líquida, que normalmente se utilizan, y con menos gasto de reactivos y disolventes.

**Artículo 3.** *Combination of fluorescence excitation emission matrices in polar and non-polar solvents to obtain three- and four-way arrays for classification of Tempranillo grapes according to maturation stage and hydric status.* **Talanta 199 (2019), 652-661.**

Siguiendo una metodología semejante al artículo anterior, se procedió a la caracterización de uvas de la variedad '*Tempranillo*' de dos estados de maduración. También se procedió a distinguir entre muestras de secano y regadío, aprovechando toda la información ofrecida a partir de la extracción de los compuestos fluorescentes en diferentes disolventes.

Se llevó a cabo la extracción con ácido oxálico en agua 0,3 M (pH 1,00) de 96 muestras de uva de dos estados de maduración diferentes (48 de cada estado). Estos extractos acuosos se analizaron por cromatografía líquida y por fluorescencia *front-face*.

Para los extractos acuosos de uva, la descomposición del conjunto de datos de tres vías: excitación-emisión-muestras, con la siguiente dimensión (21 × 47 × 96), se llevó a

cabo por PARAFAC y se necesitaron tres componentes: componente 1 (longitud de onda de excitación/emisión 280/315 nm), componente 2 (longitud de onda de excitación/emisión 280/360 nm) y componente 3 (longitud de onda de emisión a 360 nm). Los "*scores*" del primer componente se correlacionaron con las concentraciones de epicatequina y catequina.

A los "*scores*" de PARAFAC obtenidos, se les aplicó la técnica de clasificación LDA, permitiendo distinguir satisfactoriamente entre los dos estados de maduración. Con el mismo propósito, se usó U-PLS-DA, consiguiendo unos resultados satisfactorios.

Por otro lado, la información proporcionada en los extractos acuosos fue insuficiente para discriminar entre uvas de secano y regadío y, por este motivo, los extractos se sometieron a una segunda extracción con dietiléter.

Con la incorporación del disolvente, se pudo incorporar otra vía adicional al conjunto de datos. Las EEMs de los extractos acuosos y de dietiléter, conjuntamente organizadas, constituyeron datos de cuatro vías: excitación-emisión-muestras-disolvente con la siguiente dimensión ($21 \times 47 \times 48 \times 2$).

La descomposición de los datos de cuatro vías por PARAFAC necesitó de tres componentes: componente 1 (longitud de onda de excitación/emisión 330/380 nm), componente 2 (longitud de onda de excitación/emisión 280/315 nm) y componente 3 (longitud de onda de excitación/emisión a 270/346 nm). Los "*scores*" del segundo componente tuvieron buena correlación con la suma de epicatequina más catequina.

Con la incorporación de los datos de dietiléter, se produjo una modificación de los perfiles de PARAFAC respecto a los de tres vías. La principal modificación fue la aparición de uno o más analitos nuevos, cuya señal fluorescente en dietiléter fue la más alta, y relegó al resto de compuestos al segundo y tercer componente. En relación al perfil del disolvente, este aumentó para los tres componentes.

Posteriormente, se aplicó LDA a los "*scores*" de PARAFAC de cuatro vías obteniéndose clasificaciones satisfactorias de las muestras de uvas en función de su estado

hídrico. Es de destacar que, en la bibliografía, esta es la primera publicación en la que se emplean datos de cuatro vías con fines de clasificación.

**Artículo 4.** *Evolution of polyphenols content in plum fruits (Prunus salicina) with harvesting time by second-order excitation-emission fluorescence multivariate calibration.* **Microchemical Journal 158 (2020), 105299.**

Continuando con la caracterización de matrices de origen vegetal, se abordó el estudio encaminado a la cuantificación de compuestos polifenólicos en ciruelas de la variedad '*Angeleno*' en dos estados de maduración, mayo y septiembre.

En las ciruelas están presentes varios compuestos fenólicos que ya se han identificado en las uvas y vinos, como ácidos fenólicos y flavanoles, además de otros en mayor concentración, como los ácidos clorogénico y neoclorogénico y la procianidina B2. Se dispuso de 8 muestras de ciruelas recogidas en mayo y 8 muestras recogidas en septiembre, que fueron liofilizadas. A partir del liofilizado se obtuvieron extractos con metanol y agua. Estos extractos se analizaron por cromatografía líquida y por fluorescencia.

En los mapas de contorno de las muestras se encontró una primera región espectral con una elevada señal fluorescente en un rango de emisión entre 300-340 nm excitando entre 260-290 nm. Una segunda zona fluorescente, con una menor intensidad, se encontró en el rango de emisión entre 410-450 nm, excitando entre 310-350 nm. A lo largo de la maduración, la señal fluorescente disminuyó, desapareciendo prácticamente en las muestras cosechadas en septiembre. Aplicando PARAFAC sobre la primera región espectral, se obtuvieron cuatro componentes con longitudes de excitación/emisión: 280/315, 280/318, 275/336 y 250/340 nm. Con el uso de las concentraciones cromatográficas y los perfiles de los espectros de fluorescencia, se procedió a su identificación asignando al primer componente con catequina y epicatequina y al segundo con procianidina B2. En la segunda región espectral, se necesitaron cinco componentes asignando el tercero a los ácidos clorogénicos cuyas longitudes de excitación/emisión fueron 325/457 nm.

Como casos anteriores, en primer lugar, y utilizando un diseño central compuesto, se utilizó un conjunto de muestras de calibración en el que se incluyeron ácido gálico, ácido

cafeico, ácido clorogénico, ácido neoclorogénico, epicatequina, catequina y procianidina B2. Se llevó a cabo un estudio independiente en la piel y en la pulpa de las muestras de ciruela.

Los datos se analizaron por PARAFAC y por U-PLS. Una vez validado el sistema, las mayores correspondencias con las concentraciones cromatográficas de catequina más epicatequina y ácido clorogénico más ácido neoclorogénico se obtuvieron por U-PLS/RBL. Considerando estas, en piel, las concentraciones de catequina más epicatequina en mayo y septiembre fueron 1,91 y 0,75 μg $mL^{-1}$, respectivamente, y de ácido clorogénico más neoclorogénico fueron 1,09 y 0,08 μg $mL^{-1}$, respectivamente.

**Artículo 5.** *First-order discrimination of methanolic extracts from plums according to harvesting date using fluorescence spectra*. *Quantification of polyphenols*. *Enviado* **Microchemical Journal**

En este artículo se abordó la clasificación de las ciruelas de la variedad '*Angeleno*' considerando como variable la fecha de recogida. Se registraron los espectros de emisión de extractos metanólicos tanto de la piel como de la pulpa, a dos longitudes de onda de excitación 280 nm y 330 nm y se analizaron independientemente. El objetivo fue diferenciar entre muestras pertenecientes a cuatro grupos diferentes: piel mayo, pulpa mayo, piel septiembre y pulpa septiembre.

El conjunto de los espectros de emisión de las muestras de ciruelas, tanto de piel como de pulpa, registrados excitando a 280 nm, se descompuso con dos componentes por PCA. El "*loading"* del PC1 presentó un máximo a 318 nm y se asoció con procianidina B1 y epicatequina. Esta componente permitió diferenciar entre las muestras de mayo y septiembre. Por su parte, el componente PC2 se asoció a catequina, y permitió separar las muestras de pulpa y piel.

La aplicación de PCA sobre los espectros de emisión fijando la excitación a 330 nm de nuevo necesitó dos componentes y PC1 se asoció a los ácidos clorogénicos. Este análisis solamente permitió diferenciar las muestras de mayo y septiembre.

A continuación, se aplicó PLS-DA sobre ambos sets de espectros de emisión. Se ensayaron diferentes estrategias reduciendo el número de muestras del set de validación. En la primera estrategia, el total de muestra se usó en la validación. En esta primera estrategia, los errores fueron bajos y se mejoraron los resultados de PCA. En la segunda estrategia, el 50% de las muestras se usó en la validación y en la predicción. Todas las muestras se atribuyeron correctamente en sus grupos. En la tercera estrategia, el 30% de las muestras se usó en la validación y el 70% en la predicción. En esta tercera estrategia aumentaron los errores medios para ambos sets de espectros de emisión.

Finalmente, por PLS se correlacionaron los espectros con las concentraciones obtenidas por LC encontrando buenas correlaciones para catequina y epicatequina (R = 0,86), catequina y procianidina B2 (R = 0,85) y epicatequina y procianidina B2 (R = 0,90). Para los ácidos clorogénicos la correlación fue menor (R = 0,58). En general, al comparar los "*loadings*" y los espectros de los componentes puros, los errores de predicción para la mayoría de los analitos fueron aceptables.

**Artículo 6.** *Control of olive cultivar irrigation by front-face fluorescence excitation-emission matrices in combination with PARAFAC.* **Journal of Food Composition and Analysis 69 (2018), 189-196.**

Finalmente, la última matriz de origen vegetal analizada fue aceitunas, de las que han derivado en dos publicaciones. En la primera de ellas, se estudió la influencia del riego sobre aceitunas de la variedad '*Arbequina*'. Para ello, se analizaron muestras de pasta de aceitunas, de dicha variedad, sometidas a diferentes dosis de riego. Las EEMs se registraron en el rango de emisión entre 290-450 nm y de excitación 240-290 nm. Tras la descomposición por PARAFAC, se correlacionaron los "*scores*" obtenidos con las concentraciones de varios analitos analizadas por LC. Las mejores correlaciones para el primer componente se obtuvieron con catequina más epicatequina (R = 0,873), para el segundo componente con oleuropeína (solo cuando la concentración de epicatequina era baja), y para el tercer componente, con ácido vaníllico (R = 0,877). Cuando se aplicó PCA, usando el primer componente frente al segundo, se consiguió la diferenciación entre las muestras sometidas a diferentes dosis de riego.

El modelo de calibración se validó y permitió la predicción en muestras desconocidas de la concentración de suma catequina más epicatequina, oleuropeína y ácido vaníllico.

**Artículo 7.** *Fluorescence Study of Four Olive Varieties Paste According to Sampling Dates and the Control in the Elaboration of Table Olives of "Ascolana tenera".* **Food Analytical Methods 14 (2021), 307-318.**

El segundo trabajo de análisis de aceitunas se centra en el efecto del estado de maduración sobre cuatro variedades: '*Piantone di Fallerone'*, '*Piantone di Mogliano*', '*Arbequina*' y '*Maurino*' cosechadas, en Italia, en cuatro fechas de muestreo y así en el proceso de elaboración de la variedad italiana '*Ascolana tenera*'.

Se procedió a la descomposición de las muestras de cada variedad por PARAFAC y, por PCA, consiguiéndose diferenciar entre las cuatro fechas de muestreo. Por su parte, se construyeron sets de EEMs de dos variedades y, por medio de PARAFAC-LDA y U-PLS-DA, se logró diferenciar entre ellas, independientemente del estado de maduración.

También se realizó un estudio fluorescente de la elaboración de '*Ascolana tenera*' y, por medio, de PARAFAC-LDA y U-PLS-DA, se consiguió diferenciar entre diferentes etapas del proceso de elaboración de esta aceituna al estilo Español.

**Artículo 8.** *Avances en la utilización de datos de cuatro y cinco vías, basados en matrices de excitación-emisión de fluorescencia, para aplicaciones analíticas.* **Boletín de la Sociedad Española de Química Analítica. Actualidad Analítica 70 (2020), 9-12.**

Es muy escasa la bibliografía con datos de cuatro vías e incluso de cinco vías. A pesar de estar plenamente establecida la ventaja de segundo orden, cuando se calibra con datos de tres vías o superiores, no existe un acuerdo sobre la posible ventaja de tercer orden para datos de cuatro vías. A día de hoy se discute sobre la existencia de dicha ventaja así como sobre las limitaciones del uso de la calibración de tercer orden o de orden superior.

En esta revisión se proponen diferentes estrategias para la construcción de datos de cuatro vías mediante la inclusión de una vía adicional sobre las EEMs:

- EEMs-tiempo de reacción (cinética).

- EEMs-tiempo de retención (cromatografía de líquidos, LC).
- EEMs-otros tratamientos químicos.

Finalmente, se hace referencia al primer método de utilización de datos de 5 vías.

Pese a que se requiere una mayor complejidad experimental para obtener datos de cuatro y cinco vías, los avances teóricos han permitido el desarrollo de métodos analíticos de determinación de compuestos de alto interés de los campos medioambiental, biológico y de análisis de alimentos, entre otros, en muestras complejas. Por este motivo, se hace necesario profundizar en el desarrollo teórico de los mismos para comprender mejor las ventajas y potencialidades asociadas.

# CONCLUSIONES

## 6. CONCLUSIONES

Las conclusiones más importantes de los resultados obtenidos en la realización de esta Tesis Doctoral son las siguientes:

- El método propuesto mediante fluorescencia *front-face* para el análisis de polifenoles ha permitido la cuantificación de los mismos en muestras de vino. La simplicidad del análisis, especialmente respecto a las técnicas cromatográficas, pone de manifiesto que este método, basado en la calibración multivariante de segundo orden, es una buena alternativa para la cuantificación de los compuestos polifenólicos individuales en muestras de vino, sin necesidad de pretratamientos previos de la muestra.
- Ha sido posible la diferenciación de muestras de uvas de la variedad '*Tempranillo*' de acuerdo a su estado hídrico (secano y regadío), utilizando técnicas de clasificación no supervisadas (PARAFAC) y supervisadas (PARAFAC-LDA y U-PLS-DA). Además, el método desarrollado, basado en la combinación de las matrices de excitación-emisión con U-PLS/RBL, ha permitido la cuantificación de resveratrol y de la suma de catequina y epicatequina en ambos tipos de muestras.
- El análisis fluorescente de extractos acuosos de uva, obtenidos a valores de pH bajos, en combinación con PARAFAC-LDA y U-PLS-DA, ha conseguido diferenciar entre muestras de uva de la variedad '*Tempranillo*' cosechadas en dos fechas distintas.
- La construcción de datos de tercer orden por combinación de las EEMs de extractos de uvas de la variedad '*Tempranillo*', obtenidos con disolución acuosa y los obtenidos con dietileter en combinación con LDA, ha sido eficaz para diferenciar entre muestras de uva de secano y regadío.
- El registro de matrices de fluorescencia excitación-emisión, en combinación con PARAFAC y U-PLS, ha permitido la cuantificación de la suma de catequina y epicatequina, y la concentración total de los ácidos clorogénico y neoclorogénico, así como de procianidina B2 en piel y en pulpa de muestras de ciruela de la variedad '*Angeleno*'.
- Los espectros de fluorescencia de extractos de piel y de pulpa de ciruelas de la variedad '*Angeleno*' en combinación con PLS-DA y PCA, logra diferenciar entre muestras cosechadas en mayo y septiembre.

- La descomposición de las matrices de excitación y emisión de muestras de pasta de aceitunas de la variedad '*Arbequina*', sometidas a diferentes tratamientos de riego en combinación con PARAFAC, ha permitido, por PCA, diferenciar entre los diferentes grupos de muestras. La correlación entre los "*scores*" obtenidos y las concentraciones cromatográficas consiguen la predicción de la concentración de ácido vaníllico, suma de catequina y epicatequina e hidroxitirosol.
- Se ha optimizado un método de fluorescencia para diferenciar aceitunas de distintas variedades en diferentes estados de maduración tras la aplicación de PARAFAC y, con los "*scores*" obtenidos, se ha aplicado PCA para diferenciar entre cuatro fechas de muestreo. También se ha diferenciado para el conjunto de datos entre variedades cuando se comparan por pares aplicando PARAFAC-LDA y U-PLS-DA. Igualmente se han aplicado PARAFAC-LDA y U-PLS-DA para estudiar el seguimiento de elaboración de aceitunas de mesa de la variedad '*Ascolana tenera*'.

# PUBLICACIONES

# ARTÍCULO 1

## Front-face fluorescence spectroscopy combined with second-order multivariate algorithms for the quantification of polyphenols in red wine samples

Manuel Cabrera-Bañegil, María del Carmen Hurtado-Sánchez, Teresa Galeano-Díaz, Isabel Durán-Merás

*Food Chemistry,* ***2017****, 220, 168-176*
*DOI: http://dx.doi.org/10.1016/j.foodchem.2016.09.152*

Food Chemistry 220 (2017) 168–176

Contents lists available at ScienceDirect

Food Chemistry

journal homepage: www.elsevier.com/locate/foodchem

# Front-face fluorescence spectroscopy combined with second-order multivariate algorithms for the quantification of polyphenols in red wine samples

Manuel Cabrera-Bañegil [a], María del Carmen Hurtado-Sánchez [b], Teresa Galeano-Díaz [c], Isabel Durán-Merás [c,*]

[a] Technological Institute of Food and Agriculture (CICYTEX-INTAEX), Junta de Extremadura, Avda. Adolfo Suárez S/N, 06007 Badajoz, Spain
[b] Department of Analytical Chemistry, Faculty of Sciences, University of Extremadura, 06006 Badajoz, Spain
[c] Department of Analytical Chemistry and Research Institute on Water, Climate Change and Sustainability (IACYS), University of Extremadura, 06006 Badajoz, Spain

ARTICLE INFO

*Article history:*
Received 18 May 2016
Received in revised form 19 September 2016
Accepted 24 September 2016
Available online 26 September 2016

*Chemical compounds studied in this article:*
Caffeic acid (PubChem CID: 689043)
(+)-Catechin (PubChem CID: 9064)
Epicatechin (PubChem CID: 72276)
Gallic acid (PubChem CID: 370)
3,4′,5-Trihydroxystilbene (Resveratrol) (PubChem CID: 445154)
Vanillic acid (PubChem CID: 8468)

*Keywords:*
Wine
Polyphenols
Front-face fluorescence
Excitation-emission matrices
Parallel factor analysis
Unfolded partial least squares

ABSTRACT

The potential of front-face fluorescence spectroscopy combined with second-order chemometric methods was investigated for the quantification of the main polyphenols present in wine samples. Parallel factor analysis (PARAFAC) and unfolded-partial least squares coupled to residual bilinearization (U-PLS/RBL) were assessed for the quantification of catechin, epicatechin, quercetin, resveratrol, caffeic acid, gallic acid, *p*-coumaric acid, and vanillic acid in red wines.

Excitation-emission matrices of different red wine samples, without pretreatment, were obtained in front-face mode, recording emission between 290 and 450 nm, exciting between 240 and 290 nm, for the analysis of epicatechin, catechin, caffeic acid, gallic acid, and vanillic acid; and excitation and emission between 300–360 and 330–400 nm, respectively, for the analysis of resveratrol. U-PLS/RBL algorithm provided the best results and this methodology was validated by an optimized liquid chromatographic coupled to diode array and fluorimetric detectors procedure, obtaining a very good correlation for vanillic acid, caffeic acid, epicatechin and resveratrol.



## 1. Introduction

The European Union (EU-28) is the world's leader in wine production, with almost half of the global vine-growing area and approximately 65 percent of production by volume (Wine Annual, 2015). Wine is widely consumed around the world, especially in Europe, where consumption is on increase in several countries. The global demand of high quality wines requires rapid and economic procedures able to give quantitative responses about their chemical composition. These data are relevant because contribute to obtain more information about wine quality, and allow the industry responding for new demands of the market. In this sense, it is very important to develop fast and non-destructive analytical methods, without sample pretreatment for wine analysis.

Red wine is a complex matrix with a chemical composition that includes 80–86% of water, 10–15% of alcohol, and 1–2% of other minority compounds. Inside the last group, polyphenol compounds, such as flavonoids, anthocyanins, phenolic acids, stilbenes and polymeric tannins are included. It is well known that these compounds shown many biological activities, such as antioxidant, cardioprotective, anticancer, anti-inflammation, antiaging and antimicrobial properties (Vallverdú-Queralt et al., 2015). Moreover, sensorial and nutritional characteristics, such as color, astringency

* Corresponding author.
*E-mail address:* iduran@unex.es (I. Durán-Merás).

http://dx.doi.org/10.1016/j.foodchem.2016.09.152
0308-8146/

and bitterness depend on polyphenol contents (Granato, Katayama, & de Castro, 2011). They are the main components responsible for the chemical differences between red and white wines, especially the color, taste, and the mouth-feel sensations of red wines (Ivanova-Petropulos et al., 2015). The phenolic composition of the wine depends on the grape variety and of vinification process followed, which affects physical phenomena (diffusion from the solid parts, extraction of wood compounds, etc.), and chemical and biochemical phenomena (oxidation, degradation, condensation, etc.) (Mulero et al., 2015).

Many methods to characterize and quantify phenolic compounds in wine samples have been developed by employing a wide variety of analytical techniques. HPLC coupled to fluorimetric, diode array or mass detectors is the most employed technique (Albani, 2012; Fontana & Bottini, 2014; Gonçalves, Mendes, Silva, & Câmara, 2012). However, these methodologies are very time consuming, requiring sample pretreatment, and are not particularly advantageous for the quantification of a large number of samples.

During the last decade, applications of fluorescence spectroscopy in the food analysis field have significantly increased (García-Cañas, Simó, Herrero, Ibañez, & Cifuentes, 2012). In this context, it has been shown that problems, as the inner-filter effect, scattering light, and reflected light, that are presents under certain conditions, e.g. high concentrations of the fluorescent species, or turbid samples, are avoided using front-face fluorescence. The main advantages of this technique are rapid sample data acquisition, the potential to determine several parameters simultaneously, and the capacity to replace expensive and time consuming reference techniques. In this regard, front-face fluorescence has been combined with various multivariate analysis algorithms and, in this way, the analytical information contained in the fluorescence spectra can be correlated with several analytical variables (Sádecká & Tóthová, 2007). The most employed chemometric algorithms for fluorescence excitation emission matrices (EEMs) of food products decomposition have been PARAFAC (Bro, 1997), unfolded partial least squares (U-PLS) and N-way partial least squares (N-PLS) (Wold, Geladi, Esbensen, & Öhman, 1987). Several investigations, reporting the use of fluorescence matrices and chemometric techniques for characterization and quantification of fluorescence compound in food, have been recently published. Hougaard, Lawaetz, and Ipsen (2013) studied milk samples submitted to different pasteurization temperatures and the fluorescence EEMs of each milk sample were compared and analyzed by PARAFAC, allowing distinguishing between pasteurization treatments. Callejón et al. (2012) used PARAFAC to classify sherry vinegar EEMs according to barrel aging. Lenhardt, Bro, Zekovic, Dramicanin, and Dramicanin (2015) also achieved to classify different kinds of honey samples according to their botanical origin using PLS. Rubio, Sarabia, and Ortiz (2015) studied carbamates in lettuces. EEMs of lettuce sample were decomposed by PARAFAC and carbaril, naftol and carbendazim were quantified by standard addition calibration.

It is known that intact wine samples are very complex systems in which the presence of several fluorophores and other phenomena (physicochemical environment of the food matrix such as temperature and pH) may produce a remarkable influence in the corresponding fluorescence signals. The possibility of obtaining all the information without pretreatment of the samples has the advantage of avoiding physicochemical changes induced by the dilution. In the analysis of wines by front-face fluorescence, Dufour, Letort, Laguet, Lebecque, and Serra (2006) employed rapid fluorescence measurements applied directly on wines for monitoring the variety, the typicality and the vintage of a collection of French and German wines. This study showed that front-face fluorescence spectroscopy, combined with chemometrics, offers a promising approach for the authentication of wines. Airado-Rodríguez, Galeano-Díaz, Durán-Merás, and Wold (2009) identify the main fluorescent compounds in wines correlating the PARAFAC scores and chromatographic peak areas of red wine samples. On the other hand, Airado-Rodríguez, Durán Merás, Galeano Díaz, and Wold (2011) also showed the potential of the autofluorescence of wines, through the measurements of EEMs of untreated wine samples by front-face fluorescence, combined with three-way PARAFAC, for the purpose of wine discrimination, according to the appellation of origin. Finally, Argentine white wines were classified according to grape variety using PARAFAC, Principal Components Analysis (PCA) and the Kennard Stone algorithm (Azcarate et al., 2015).

Bearing in mind this information, front-face fluorescence spectroscopy combined with second-order multivariate methods seems to be a very attractive and alternative methodology for the determination of phenolic compounds in wines. In this work, both PARAFAC and U-PLS/RBL second-order algorithms have been assessed for the quantification of catechin, epicatechin, quercetin, resveratrol, caffeic acid, gallic acid, *p*-coumaric acid, and vanillic acid in red wines following this methodology. Finally, the results obtained in the quantification of the target compounds using the propose method were compared with the obtained by a liquid chromatographic method.

## 2. Material and methods

### 2.1. Chemicals, standards and samples

Catechin, epicatechin, gallic acid, *p*-coumaric acid, quercetin, and trans-resveratrol were obtained from Sigma-Aldrich (Madrid, Spain). Caffeic and vanillic acids were obtained from Fluka. Stock solutions of standards, containing 100 mg $L^{-1}$ of each compound, were prepared in ethanol and stored at 4 °C. Diluted solutions were prepared in a synthetic wine matrix, containing 3 g $L^{-1}$ of tartrate buffer at pH 3.7, and 15% (v/v) of ethanol. Tartrate buffer was prepared by dissolving disodium tartrate dehydrate (Panreac, Spain) in ultrapure water and fixing the pH at 3.7 with hydrochloric acid (Panreac, Barcelona, Spain). Methanol HPLC grade was purchased from Panreac, and formic acid from Sigma-Aldrich. Ultrapure water was obtained from a Milli-Q water system (Millipore S.A.S., Molsheim, France).

### 2.2. Apparatus

Fluorescence measurements were made using a Fluorescence Spectrophotometer Varian Model Cary Eclipse, equipped with two Czerny-Turner monochromators (excitation and emission), a xenon light source and two photomultiplier tubes as detector, and connected to a PC microcomputer via an IEEE 488 (GPIB) serial interface. The Cary Elipse 1.0 software was used for data acquisitions. Measurements were made with a variable-angle front-face accessory, to ensure that reflected light, scattered radiation, and depolarization phenomena were minimized. Angle of incidence, defined as the angle between the excitation beam and the perpendicular to the cell surface, was set at 34°. Fluorescence measurements were recorded in a 10-mm quartz cell at room temperature. The slits of excitation and emission monochromators were set at 2.5 and 5 nm, respectively. The EEMs were registered as a set of emission spectra with 0.5 nm of resolution. The photomultiplier tube sensitivity was 700 V, and scan rate was of 300 nm $min^{-1}$.

Chromatographic studies were performed using an Agilent Model 1260 LC instrument (Agilent Technologies, Palo Alto, CA, USA) equipped with a quaternary pump, degasser (G1311B), diode array detector (DAD) (G1315D), fluorescence detector (FLD) (G1321B), and the ChemStation software package to control the

instrument, data acquisition, and data analysis. The analytical column employed was a rapid resolution Zorbax Eclipse XDB-C18 column (50 × 4.6 mm, 1.8 μm) (Agilent Technologies). The components of the mobile phase were 2% (v/v) formic acid solution containing 10% MeOH (eluent A), and 2% (v/v) formic acid solution containing 90% MeOH (eluent B), and were filtered through a 0.22 μm membrane nylon filter (Teknokroma, Barcelona, Spain) and degassed by ultrasonication before using. The following gradient mode was used: between 0 and 15 min the percentage of eluent B increases from 0 up to 15%, between 15 and 25 min 30% B, and between 30 and 34 min 70% B. These conditions were maintained until 40 min and finally, the eluent B content was decreased to the initial conditions (0% B) and the column was re-equilibrated for 5 min. The flow rate was set constant at 0.5 mL $min^{-1}$ and the injection volume was 10 μL. The eluate was photometrically monitored at 270, 290, 340 and 370 nm, and fluorimetrically, in multiemission mode at 313, 360, 433 and 460 nm (exciting at 270 nm).

### 2.3. Calibration and test sets

In order to assess the ability of the different second-order multivariate analysis tools, in the determination of a mixture of the main fluorescent polyphenols in red wine samples, a 40-standards set was built for calibration with the PARAFAC and U-PLS/RBL models. Two calibration sets were constructed using a central composite design in the concentration ranges between 0.77 and 68.08 μg $mL^{-1}$. In both, samples were prepared in 10.0 mL calibrated flasks, containing 3 mL of tartrate buffer (3 g $L^{-1}$, pH 3.7), adding the corresponding volumes of the standard solutions of each analyte and diluting to volume with 15% (v/v) of ethanol. Moreover, a set of six test samples was prepared in the same way as the sample for calibration, but using a random design, i.e. selecting the target concentrations at random from the calibration range for each analyte. EEMs were measured in two different spectral regions: in the first spectral region, excitation range from 240 to 290 nm (each 5 nm), and emission from 290 to 450 nm (each 0.5 nm); and in the second spectral region the ranges were 300–350 nm (each 5 nm, excitation), and 350–400 nm (each 0.5 nm, emission). For the analysis of catechin, epicatechin, vanillic acid, caffeic acid and gallic acid, the excitation-emission matrix of each calibration solution was obtained in front-face mode, by recording emission spectra in the first wavelength region. The analysis of resveratrol was done with the front-face EEMs recorded in the second spectral region.

### 2.4. Wine samples

#### 2.4.1. LC analysis

The analysis of polyphenols was carried out by the standard addition method. Aliquots of 2 mL of each wine sample were added into a 10 mL volumetric flask, and increasing volumes of standard mixture of the polyphenols and ultrapure water were added to the mark. Aliquots of 10 μL were injected into the chromatographic system previous filtration through a 0.22 μm membrane nylon filter.

#### 2.4.2. Fluorescence measurements

The wines analyzed belong to the origin denomination (OD) "Ribera del Guadiana" and OD "Rioja" and all of them were purchased from local markets and stored at 4 °C in darkness. A total amount of 11 red wines were analyzed. Each sample was equilibrated at room temperature and its EEMs were registered immediately after each bottle was opened.

## 3. Results and discussion

Typically, the quantification of polyphenols in wine requires complex and time-consuming sample pre-treatment procedures, and are not suitable for on-site analysis. An alternative approach, which is the one covered by this paper, is to measure the intrinsic fluorescence (autofluorescence) of the red wine without pretreatment of the sample, and use this total signal for the quantification of the principal phenolic compounds present in wine samples. Two dimensional fluorescence spectra were obtained, and chemometrics in the form of multivariate and multiway data analysis was applied to handle this complex fluorescence signal. With this purpose, multivariate data analysis was performed using PARAFAC and U-PLS/RBL algorithms. For validation, the obtained results were compared with those obtained applying a LC methodology.

### 3.1. Chemometric methods

Taking into account the differences between the excitation and emission wavelengths of the polyphenols, and with the object of avoiding the signal corresponding to the Rayleigh scatter, the EEMs were registered in two spectral regions. A scheme of the spectral regions and of the standard solutions used in each one is shown in Fig. 1. In the first spectral region, the excitation-emission matrices were recorded in the excitation range comprised between 240 and 290 nm, with resolution of 5 nm, and an emission range comprised between 290 and 450 nm with resolution of 0.5 nm. In this region, phenolic acids such as vanillic acid, gallic acid, and caffeic acid, and the flavanols epicatechin and catechin were analyzed. All of them with excitation wavelengths comprised between 240 and 285 nm, and emission wavelengths between 302 and 405 nm (Airado-Rodríguez et al., 2009).

The second spectral region ranged from 300 to 360 nm for excitation and from 310 to 460 nm for emission, with resolutions of 5 nm and 0.5 nm, respectively and, in this region, resveratrol, quercetin and *p*-coumaric acid were investigated.

Two different calibration sets were assayed. In the first calibration set, two series of calibration standards were prepared with those analytes that present fluorescence in each spectral region, that is, standards containing vanillic acid, gallic acid, caffeic acid, and epicatechin for evaluating the first spectral region, and standards containing resveratrol, quercetin and *p*-coumaric acid for evaluating the second region. Fig. 2 shows the measured EEMs as contour maps for a standard of each polyphenol.

In the second calibration set assayed, only one series of standards containing all the above analytes, plus catechin in variable concentrations and quercetin (2.13 μg $mL^{-1}$) and *p*-coumaric acid (1.90 μg $mL^{-1}$) in fixed concentrations, were prepared. These last two analytes present a weak fluorescence in acidic medium, mainly quercetin (Monago-Maraña, Durán-Merás, Galeano-Díaz, & Muñoz de la Peña, 2016) but, as they are present in all wines, and with the purpose of simulating a genuine situation, were added to all calibration samples.

In both cases, the calibration sets were built with a central composite design in concentration ranges between 2.2 and 16.5; 1.7 and 9.7; 0.9 and 4.8; 1.9 and 9.6, 11.3 and 64.1, and 0.2 and 5.8 μg $mL^{-1}$, for catechin, epicatechin, vanillic acid, caffeic acid, gallic acid and resveratrol, respectively. The corresponding volumes of the standard solutions of each analyte were transferred into 10.0 mL volumetric flasks, containing 3 mL of tartrate buffer, pH 3.7, 1.5 mL of ethanol, and ultrapure water was added to the mark.

A set of 6 validation samples was prepared and processed in a similar way, having analyte concentrations different from the calibration ones and selected at random from the corresponding

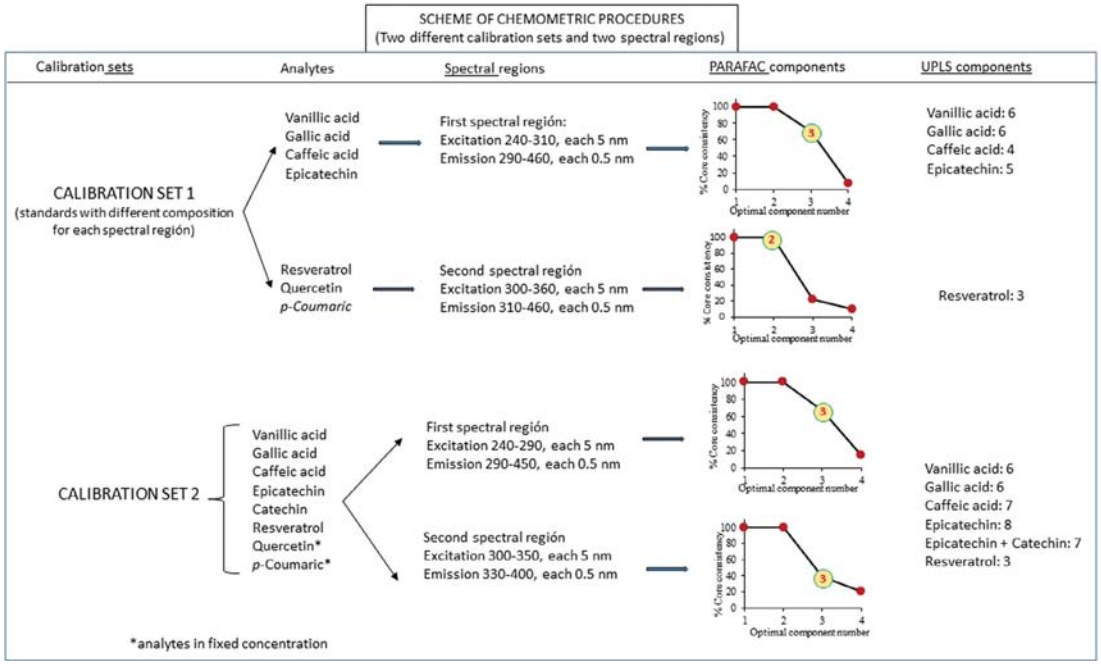


**Fig. 1.** Scheme of the calibration procedures and the number of components for each calibration in both spectral regions.

calibration ranges. All calculations were done using MatLab R2008a, using the MVC2 routine, an integrated MatLab toolbox for second-order calibration developed by Olivieri, Wu, and Yu (2009).

*3.1.1. PARAFAC results*

Each set of calibration samples was investigated with PARAFAC algorithm and, for calibration and prediction purposes, optimal regions were selected in order to remove Rayleigh scattering. Excitation wavelength from 240 to 285 nm and emission wavelength from 302 to 405 nm, for the first spectral region, and excitation wavelength between 300 and 335 nm and emission wavelength between 350 and 400 nm, for the second spectral region, were finally chosen. Also, PARAFAC was applied under constraints such as unimodality and non-negativity. In first place, the appropriate number of components was selected. Initialization was performed using the default PARAFAC option (which employs SVD vectors), and an unconstrained least-squares fit was then carried out. The selection of the number of spectral components has been independently checked by the method known as core consistency diagnostic (CORCONDIA) (Andersen & Bro, 2003). It is based on examining the model based on the data and the estimated parameters of gradually augmented models. The model is called appropriate if adding other combinations of the same components does not improve the fit considerably. When the core consistency drops from a high value, above ≈60%, to a low value, this indicates that an appropriately number of components has been attained. With both calibration sets, the core consistency dropped to a very low value when using four spectral components to model the data in all cases, suggesting that the optimum number of components was three in the first spectral region, independently of the calibration set used. When this study was made with the second spectral region, the optimum number of components were two at the first calibration set, and three at the second calibration set (with all analytes) (Fig. 1). This number of components in validation samples can be justified by the presence, in the first spectral region, of three fluorescence analytes: vanillic acid, caffeic acid and epicathechin. The number of components for the second spectral region, two for the first calibration and three for the second calibration, can be explained by the presence of resveratrol in both calibration sets and the presence of vanillic acid in the second calibration set. This analyte presents fluorescence in the wavelength ranges used in the second spectral region and this signal can be contributing to the third component.

In order to correlate the components with the polyphenols, the loading profiles of both spectral regions were compared with excitation and emission spectra of the standards. Also, PARAFAC scores were correlated with the concentration of the phenolic compounds in the calibration samples, Fig. 3. In the first spectral region, component 1 shows excitation and emission maxima at 280 and 315 nm respectively, and, as can be observed in Fig 3, the physiognomy of the profiles and the wavelengths are coincident with the spectrum of epicatechin and catechin. The third component has two excitation maxima at 255 and 265 nm and an emission maximum at 360 nm. The physiognomy of the emission profile is coincident with vanillic acid spectrum, whose excitation and emission maxima are 255 and 354 nm, respectively. On the other hand, in the first spectral region, the first component presented a very good correlation between the score values and epicatechin concentration ($r = 0.944$), when this analyte is alone, and between the addition of epicatechin and catechin concentrations ($r = 0.920$) when, in the second calibration, both compounds are present. The third component presents a good correlation between the score values and vanillic acid concentration ($r = 0.967$) at the first calibration set and some lower correlation ($r = 0.880$) at the second calibration set. However, no obvious correlation was found between the score values of the second component with a single analyte.

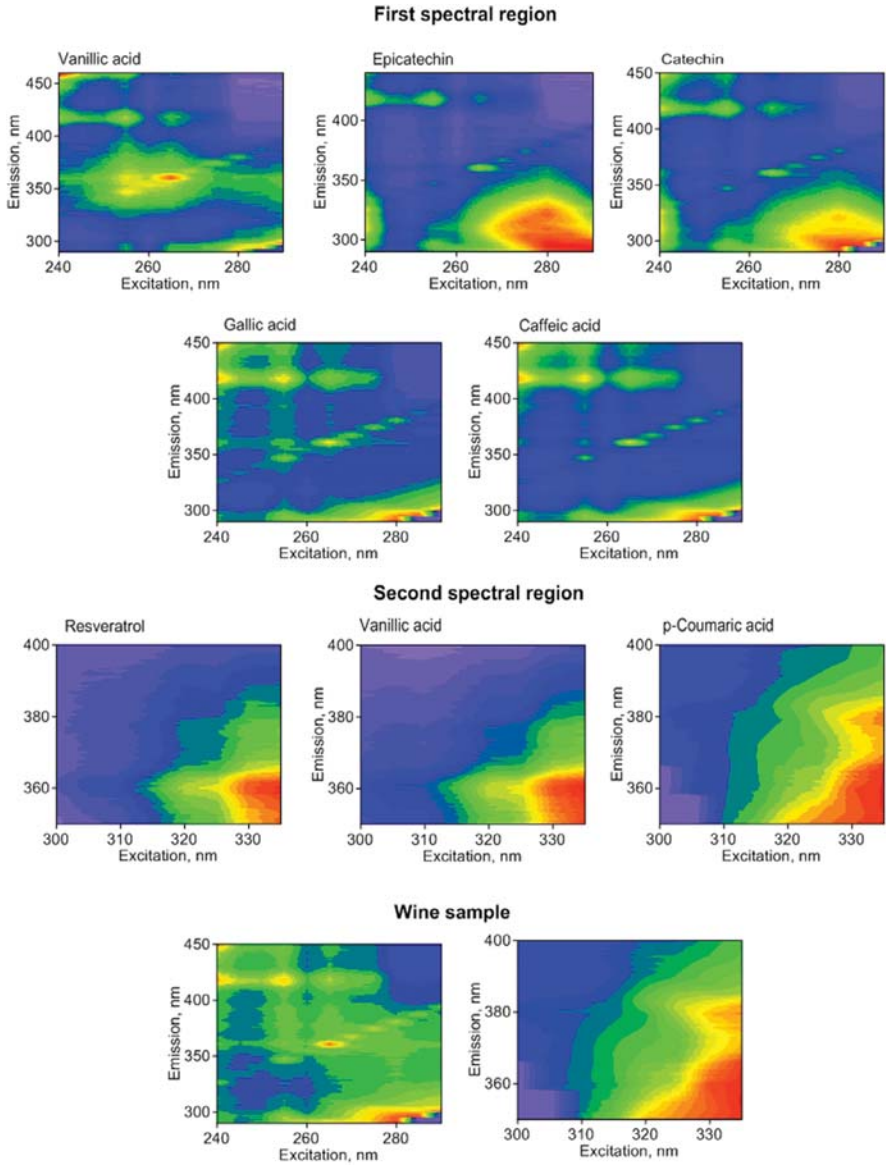


**Fig. 2.** Contour plots of the total fluorescence spectra of individual polyphenols, in each spectral region, and of a red wine sample, in the two spectral regions.

Such as we indicated before, in the second wavelength region, two components have been found at the first calibration set. In this case, the first component is associated with resveratrol, based on that the excitation and emission spectra of this analyte are very similar to the emission and excitation profiles corresponding to this first PARAFAC component. Also, a very good correlation was found between the score values of this first component and the concentration of resveratrol ($r = 0.973$). An additional PARAFAC component was necessary for describing the fluorescence behavior at the second calibration set. This third component had an emission maximum at 366 nm being related with vanillic acid and this is supported by the good correlation between its scores and its concentration values ($r = 0.902$).

Prediction results for the validation set of the second calibration (containing catechin), are presented in Fig. 4. The number of analytes that PARAFAC is able to predict, agrees with the number of components found, i.e. 3: vanillic acid, epicatechin plus catechin (or epicatechin when it is alone in the first calibration), and resveratrol. The statistical parameters were evaluated through the relative error of prediction (REP%) and the root mean square error of prediction (RMSEP). These values were satisfactory for vanillic acid and for resveratrol, 16.3% and 0.4, and 13.1% and 0.7%, respectively.

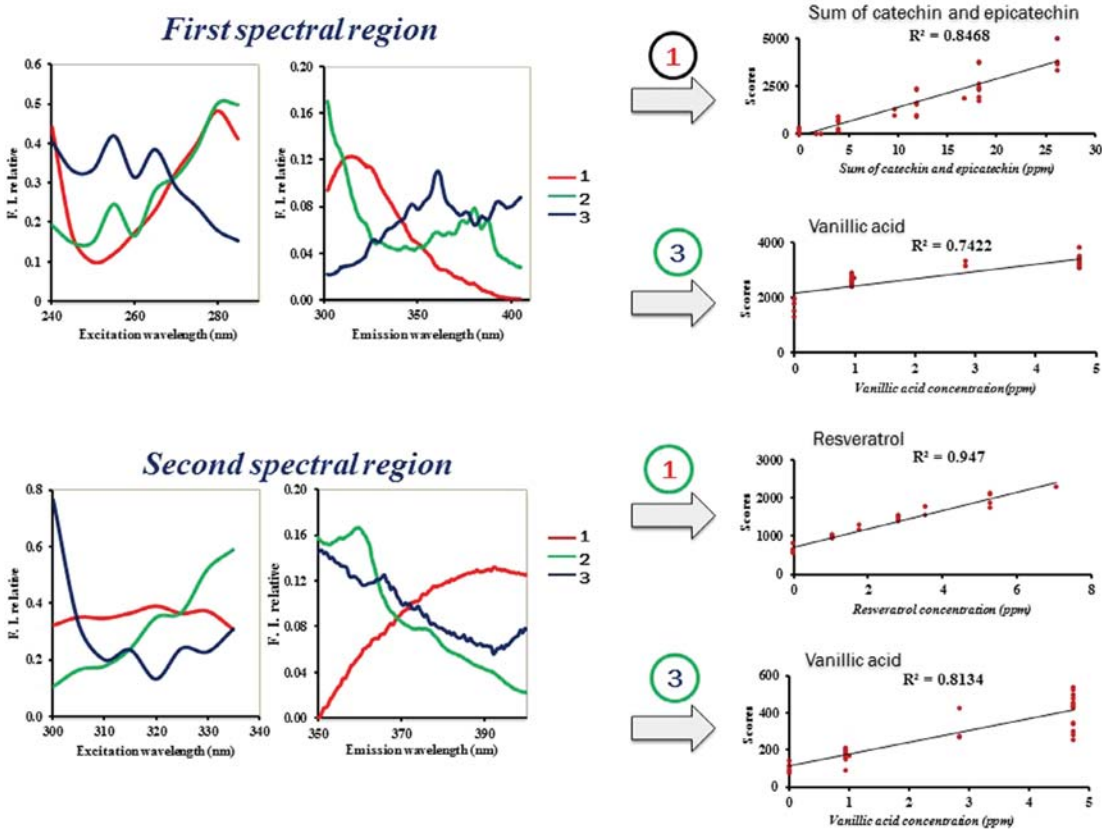


**Fig. 3.** Normalized excitation and emission PARAFAC profiles and normalized excitation and emission spectra of the analytes.

However, for epicatechin plus catechin, higher and not acceptable values were obtained (59% and 9%), (for a more extensive comment see below).

*3.1.2. U-PLS results*

Following the same data analysis procedure than in PARAFAC model, validation samples were studied with U-PLS algorithm in a first phase, and considerably more complex wine samples were subsequently analyzed using RBL to model the regression residues as a sum of bilinear contributions from the unexpected components.

Cross-validation and the Haaland and Thomas criterion (Haaland & Thomas, 1988a, 1988b) were employed to choose the optimum number of factors or latent variables, which are those given a PRESS value statistically no different to the minimum PRESS value (F-ratio probability falling below 0.75), At the first calibration set, the optimum number of latent variables was four for caffeic acid, five for epicatechin and six for vanillic and gallic acids, in the first spectral region, while, in the second spectral region, good results were only found for resveratrol, with three latent variables. At the second calibration set, the optimum number of latent variables was seven for caffeic acid and eight for epicatechin, while the rest of analytes presented the same number of latent variables (six for vanillic and gallic acids).

The U-PLS analyte predictions were very good in the validation samples, and this algorithm allowed the analysis, of two analytes more than PARAFAC, gallic and caffeic acids, as can be seen in Fig. 4. The REP values obtained for caffeic acid, epicatechin plus catechin and gallic acid were higher than 15%. When epicatechin is alone, the REP of epicatechin prediction was 3.7%. Although REP values associated to vanillic acid are similar for both methods, the vanillic acid prediction results obtained by PARAFAC were better than using U-PLS.

A more extensive comment deserves the analysis of epicatechin and catechin with any one of the two chemometric algorithms. In the first calibration set, where catechin is absent, the results obtained for epicatechin by PARAFAC are not good. For all validation samples, the concentrations found for this analyte were lower than the nominal values, Fig. 4C. On the other hand, when both analytes are present, the predictions were very poor. However, U-PLS/RBL predictions were very successful for epicatechin in the validation samples of the first calibration, with recoveries of 99.0%, and for the sum of epicatechin and catechin in the second calibration. Even so, predictions were unsuitable for catechin alone with either of the two methods. The poor PARAFAC results may be ascribed to lack of selectivity due to the identical EEMs of these flavonoids, and the not strictly trilinear behavior of these analytes.

Therefore, the results show that U-PLS/RBL offered the better statistical parameters and results. This fact can be justified by the use of latent variables, which are flexible enough to overcome the problem of the high degree of spectral similarity among certain analytes.

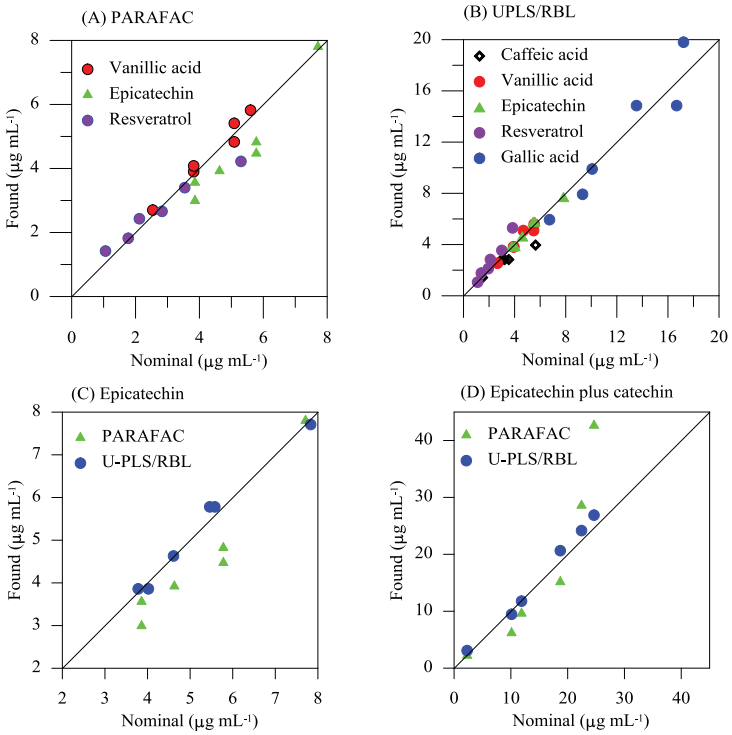


**Fig. 4.** Plots for predicted concentrations in validation samples as a function of the nominal values (the solid lines are the perfect fits), A) by PARAFAC, B) by U-PLS/RBL, C) for epicatechin by PARAFAC (▲) and U-PLS/RBL (●), and D) for epicatechin plus catechin by PARAFAC (▲) and U-PLS/RBL (●).

### *3.2. Quantification of polyphenols in wine samples*

Once chemometric methods were validated with standards, the analysis of red wine samples was conducted. For that, the corresponding excitation-emission matrix of each analyzed wine, not submitted to any prior pretreatment, was recorded in the front-face mode by means of a variable angle front face accessory. EEMs were immediately registered after opening the bottle. Simultaneously, wine samples were analyzed by means of a chromatographic method with a rapid resolution column, for validation of the obtained results.

#### *3.2.1. LC method*

With the object of validating the obtained results by the chemometric methods, a LC procedure, with DAD and fluorescence detection, was developed.

Although the bibliography on LC methods for the quantification of the polyphenols in wine samples is broad, in this case we use a rapid resolution column with small particle size (ZORBAX Eclipse XDB C18 4.6 × 50 mm, 1.8 μm) and it was necessary to optimize the elution of the polyphenols. Solvents for mobile phase were methanol-formic acid-water (10:2:88, *v:v:v*) as solvent A, and methanol-formic acid-water (90:2:8, v:v:v) as solvent *B*.

After assaying different gradients and flow rates, the following gradient was chosen as optimum: elution started at 0% B and it was increased to 15% until 15 min, then between 15 and 25 min was increased to 30%, and between 25 and 34 min to 70%, and finally, the column was regenerated for 5 min. For the chromatographic elution, the flow rate was set at 0.5 mL $min^{-1}$, the injection volume was set at 10 μL, and the column was set at room temperature. Under these conditions, a suitable separation of polyphenolic compounds was obtained in 40 min. The eluate was photometrically monitored at 270, 290, 340 and 370 nm, and fluorometrically, in multiemission mode, exciting at 270 nm and measuring the fluorescence intensity at 313, 360, 433 and 460 nm. These pairs of $\lambda_{ex}/\lambda_{em}$ allow us to obtain the maximum signal for the target compounds: 270/313 nm (epicatechin and catechin), 270/360 nm (gallic and vanillic acids), 270/433 nm (*p*-coumaric and resveratrol), and 270/460 nm (caffeic acid). Calibration curves and analytical figures of merit were performed by means of the ACOC program, in MATLAB code (Espinosa Mansilla, Muñoz de la Peña, & González Gómez, 2005).

Under these optimized conditions, linearity was established in ultrapure water in the range LOQ–6.62 μg $mL^{-1}$, and the calibration curves were estimated by least-squares regression. Three replicates for each calibration level were analyzed, and different linearities were obtained depending on the compound, Table 1. Determination coefficients ($r^2$) were higher than 0.99 for all compounds, and LODs of fluorescence signals ranged between 0.04 and 0.30 μg $mL^{-1}$, while LODs of DAD signals ranged from 0.07 to 0.12 μg $mL^{-1}$, according to Long and Winerfordner criterion (Long & Winerfordner, 1983).

The quantification of the polyphenols in red wines was carried out by standard addition methodology due to the presence of matrix effect. An aliquot of 2 mL of each wine sample, spiked in the concentration range between 0.5 and 4 μg $mL^{-1}$, was diluted to a final volume of 10 mL with solvent A. Eleven wines were analyzed following the methodology described in Section 2.4 and the results obtained for the polyphenols are shown in Table 2.

**Table 1**
Validation parameters of the LC proposed method with UV and FL detection.

| | Gallic acid | Vanillic acid | Caffeic acid | Epicatechin | *p*-Coumaric acid | Resveratrol | Quercetin |
|---|---|---|---|---|---|---|---|
| Retention time (min) | 2.3 | 11.1 | 12 | 16 | 18.4 | 29.5 | 33.5 |
| UV Detection (nm) | 270 | 270 | 290 | 270 | 290 | 290 | 370 |
| Linearity range (μg/mL) | 0.25–5.69 | 0.25–4.07 | 0.22–5.66 | 0.34–5.78 | 0.30–5.38 | 0.30–5.30 | 0.40–6.62 |
| Linear regresion | $y = (129.9 \pm 1.2)x + (1.6 \pm 3.2)$ | $y = (96.7 \pm 1.4)x + (1.6 \pm 2.7)$ | $y = (179.8 \pm 1.6)x + (-2.8 \pm 4.3)$ | $y = (24.50 \pm 0.31)x + (-0.13 \pm 0.91)$ | $y = (252.4 \pm 2.5)x + (-5.3 \pm 6.5)$ | $y = (246.1 \pm 2.6)x + (-4.2 \pm 6.6)$ | $y = (165.7 \pm 2.3)x + (-21.4 \pm 6.9)$ |
| Determination coefficient ($r^2$) | 0.998 | 0.995 | 0.998 | 0.996 | 0.997 | 0.997 | 0.995 |
| LOD (μg/mL) | 0.07 | 0.08 | 0.07 | 0.11 | 0.08 | 0.08 | 0.12 |
| LOQ (μg/mL) | 0.22 | 0.24 | 0.21 | 0.33 | 0.23 | 0.24 | 0.37 |
| Linearity (%) | 99 | 99 | 99 | 99 | 99 | 99 | 99 |

| | Gallic acid | Vanillic acid | Caffeic acid | Epicatechin | *p*-Coumaric acid | Resveratrol |
|---|---|---|---|---|---|---|
| Retention time (min) | 2.3 | 11.1 | 12 | 16 | 18.4 | 29.5 |
| Detection ($\lambda_{exc}/\lambda_{em}$) | 270/360 | 270/360 | 270/460 | 270/313 | 270/433 | 270/433 |
| Linearity range (μg/mL) | 1.0–5.7 | 0.1–3.0 | 0.6–5.6 | 0.3–4.8 | 0.8–5.4 | 0.45–5.4 |
| Linear regresion | $y = (6.57 \pm 0.20)x + (0.92 \pm 0.69)$ | $y = (482.2 \pm 4.6)x + (-7.0 \pm 6.9)$ | $y = (5.59 \pm 0.12)x + (-0.57 \pm 0.33)$ | $y = (187.8 \pm 2.8)x + (9.8 \pm 6.5)$ | $y = (10.01 \pm 0.28)x + (-0.50 \pm 0.79)$ | $y = (51.71 \pm 0.81)x + (-3.5 \pm 2.1)$ |
| Determination coefficient ($r^2$) | 0.9829 | 0.998 | 0.9861 | 0.994 | 0.9819 | 0.9926 |
| LOD (μg/mL) | 0.31 | 0.04 | 0.17 | 0.10 | 0.23 | 0.12 |
| LOQ (μg/mL) | 0.94 | 0.13 | 0.53 | 0.31 | 0.71 | 0.366 |
| Linearity (%) | 97 | 99 | 98 | 98 | 97 | 98 |

**Table 2**
Concentration of polyphenols in red wines expressed as μg $mL^{-1}$. Comparison of the obtained results by U-PLS/RBL and by HPLC.

| | Vanillic acid | | Caffeic acid | | Epicatechin | | Resveratrol | |
|---|---|---|---|---|---|---|---|---|
| | U-PLS/RBL | HPLC-FLD | U-PLS/RBL | HPLC-FLD | U-PLS/RBL | HPLC-FLD | U-PLS/RBL | HPLC-FLD |
| Wine 1 | 1.05 | 0.89 | 7.77 | 8.03 | 4.39 | 9.9 | 0.58 | 0.67 |
| Wine 2 | 1.66 | 1.69 | 11.26 | 10.44 | 0.22 | 0.32 | 0.49 | 0.53 |
| Wine 3 | 1.74 | 2.06 | 12.87 | 9.3 | 3.24 | 3.70 | 1.74 | 1.91 |
| Wine 4 | 1.64 | 1.41 | 11.94 | 13.98 | 5.57 | 5.50 | 0.21 | 0.21 |
| Wine 5 | 1.12 | 1.13 | 9.39 | 9.05 | 3.97 | 4.39 | 0.95 | 0.95 |
| Wine 6 | 1.35 | 1.19 | 12.77 | 12.14 | 4.63 | 8.60 | 2.27 | 1.74 |
| Wine 7 | 1.22 | 2.15 | 4.86 | 4.78 | 3.53 | 3.88 | 1.25 | 1.29 |
| Wine 8 | 0.65 | – | 11.87 | 11.49 | 3.01 | – | 1.59 | 1.48 |
| Wine 9 | 1.57 | 2.02 | 4.79 | 5.66 | 5.09 | 5.34 | 1.57 | 1.57 |
| Wine 10 | 1.97 | 2.81 | 5.23 | 5.75 | 3.49 | 5.23 | 1.13 | 0.94 |
| Wine 11 | 1.61 | 1.45 | 5.21 | 6.30 | 0.12 | 0.22 | 0.69 | 0.34 |

*3.2.2. Chemometric quantification*

In the first spectral region, all excitation-emission matrices of wine samples showed three emission zones, as can be seen in Fig. 2C, where the EMMs, as contour plots of an analyzed wine sample, are shown. The first emission zone appears in the range 300–320 nm when the samples were excited at 280–290 nm. The second emission zone appears at 340–380 nm, when the samples were excited at 200–280 nm, and the last zone at the emission range 400–410 nm, with excitation range between 240–250 nm. In the second spectral region, only one fluorescent zone has been observed over the emission range 380–400 nm, and excitation range 305–320 nm.

Prior to the analysis by U-PLS/RBL is necessary to take into account that U-PLS is a second-order multivariate calibration method, which requires the application of the residual bilinearization (RBL) algorithm to achieve the second-order advantage. When U-PLS/RBL was applied to wine samples, it was necessary to determine the number of unexpected components to be employed in the RBL procedure. This was done by analyzing the residuals, and the necessary number of factors for interferences reaches one. The number of unexpected components was different for each polyphenol. The choice of two RBL components for most of the analytes seems acceptable and the predicted analyte concentrations did not significantly change with respect to the use of higher number of unexpected components. The results obtained for caffeic and vanillic acids, epicatechin, and resveratrol in the wine samples analyzed, are summarized in Table 2.

When PARAFAC was employed, core consistency analysis was applied for each wine sample. The result was that the majority of wine samples required the consideration of one additional factor, but the obtained results for the quantification of polyphenols were not good. As it was previously described, this algorithm only gave good results for the analysis of vanillic acid, and this was the only analyte that could be quantified in wine samples, by PARAFAC calibration.

*3.3. Comparison between chemometric and LC results*

The results obtained in the analysis of red wine samples by the U-PLS/RBL algorithm and by LC, are summarized in Table 2. The results obtained by U-PLS/RBL for epicatechin, caffeic acid, vanillic acid and resveratrol were comparable to those obtained by LC. The representation of the values obtained for both methods gives us a very good correlation for caffeic acid (r = 0.957), epicatechin

($r = 0.960$ only for concentration from 0.08 until 5.50 μg $mL^{-1}$) and for resveratrol, with regression coefficient higher than 0.954.

PARAFAC gives very good results only for vanillic acid with a correlation coefficient of 0.950. This fact can be explained due to the differentiated fluorescent properties of this acid, showing three excitation maxima and an emission wavelength, 354 nm, relatively distant from the wavelengths of the other polyphenols studied in the first spectral region.

The results are encouraging, taking into account that the simultaneous determination of four analytes is easily and rapidly performed in matrices as complex as the wine samples analyzed.

## 4. Conclusions

In this work, a new method based on front-face EEMs fluorescence spectroscopy coupled with PARAFAC and U-PLS/RBL for the analysis of some of the principal phenolic compounds of red wines has been proposed. Fluorescence spectra of wines can be measured without any sample preparation or modification in a fast and potentially nondestructive manner. The EMMs of wine reflect the specificity of intrinsic fluorophores, especially polyphenols. Two spectral regions exhibited the largest difference among fluorescence relative to the different fluorescent behavior of the polyphenols.

Among the two assayed algorithms, the best results was obtained with UPLS/RBL, which provided good results for the quantification of caffeic and vanillic acids, and resveratrol, and acceptable results for epicatechin in red wine samples. The proposed methodology represents a new example of the power of coupling the partial least-squares algorithm with residual bilinearization for the resolution of very complex systems.

The great advantage of the proposed approach is that it allows the determination of the analytes through the intrinsic fluorescence of the wines, using a non-destructive technique and without pretreatment of the samples. The experimental time and the errors associated with multiple experimental steps are substantially diminished. On the basis of the obtained results, one can assert that the proposed method favorably compares with more sophisticated approaches.

## Acknowledgments

The authors are grateful to the Ministerio de Economía y Competitividad, Spain (Project CTQ2014-52309-P) and the Gobierno de Extremadura (GR15090-Research Group FQM003), both co-financed by the European FEDER funds, for financially supporting this work.

## References

Airado-Rodríguez, D., Durán Merás, I., Galeano Díaz, T., & Wold, J. P. (2011). Front-face fluorescence spectroscopy: A new tool for control in the wine industry. *Journal of Food Composition and Analysis, 24*, 257–264.

Airado-Rodríguez, D., Galeano-Díaz, T., Durán-Merás, I., & Wold, J. P. (2009). Usefulness of fluorescence excitation-emission matrices in combination with PARAFAC, as fingerprints of red wines. *Journal of Agricultural and Food Chemistry, 57*, 1711–1720.

Albani, J. R. (2012). Fluorescence Spectroscopy in Food Analysis. *Encyclopedia of Analytical Chemistry, 10*. http://dx.doi.org/10.1002/9780470027318.a1011.

Andersen, C. M., & Bro, R. (2003). Practical aspects of PARAFAC modelling of excitation–emission data. *Journal of Chemometrics, 17*, 200–215.

Azcarate, S. M., Gomes, A. A., Alcaraz, M. R., Araújo, U., Camiña, J. M., & Goicoechea, H. C. (2015). Modeling excitation-emission fluorescence matrices with pattern recognition algorithms for classification of Argentine white wines according grape variety. *Food Chemistry, 184*, 214–219.

Bro, R. (1997). PARAFAC. Tutorial and applications. *Chemometrics and Intelligent Laboratory Systems, 38*, 149–171.

Callejón, R. M., Amigo, J. M., Pairo, E., Garmón, S., Ocaña, J. A., & Morales, M. L. (2012). Classification of Sherry vinegars by combining multidimensional fluorescence, PARAFAC and different classification approaches. *Talanta, 88*, 456–462.

Dufour, É., Letort, A., Laguet, A., Lebecque, A., & Serra, J. N. (2006). Investigation of variety, typicality and vintage of French and German wines using front-face fluorescence spectroscopy. *Analytica Chimica Acta, 563*, 292–299.

Espinosa Mansilla, A., Muñoz de la Peña, A., & González Gómez, D. (2005). Using univariate linear regression calibration software in the MATLAB environment. Application to chemistry laboratory practices. *Chemical Educator, 10*, 337–345.

Fontana, R. A., & Bottini, R. (2014). High-throughput method based on quick, easy, cheap, effective, rugged and safe followed by liquid chromatography-multi-wavelength detection for the quantification of multiclass polyphenols in wines. *Journal of Chromatography A, 1342*, 44–53.

García-Cañas, V., Simó, C., Herrero, M., Ibañez, E., & Cifuentes, A. (2012). Present and future challenges in food analysis: Foodomics. *Analytical Chemistry, 84*, 10150–10159.

Gonçalves, J., Mendes, B., Silva, C. L., & Câmara, J. S. (2012). Development of a novel microextraction by packed sorbent-based approach followed by ultrahigh pressure liquid chromatography as a powerful technique for quantification phenolic constituents of biological interest in wines. *Journal of Chromatography A, 1229*, 13–23.

Granato, D., Katayama, F. C. U., & de Castro, I. A. (2011). Phenolic composition of South American red wines classified according to their antioxidant activity, retail price and sensory quality. *Food Chemistry, 129*, 366–373.

Haaland, D. M., & Thomas, E. V. (1988a). Partial least-squares methods for spectral analyses. 1. Relation to other quantitative calibration methods and the extraction of qualitative information. *Analytical Chemistry, 60*, 1193–1202.

Haaland, D. M., & Thomas, E. V. (1988b). Partial least-squares methods for spectral analyses. 2. Application to simulated and glass spectral data. *Analytical Chemistry, 60*, 1202–1208.

Hougaard, A. B., Lawaetz, A. J., & Ipsen, R. H. (2013). Front face fluorescence spectroscopy and multi-way data analysis for characterization of milk pasteurized using instant infusion. *Food Science and Technology, 53*, 331–337.

Ivanova-Petropulos, V., Hermosín-Gutiérrez, I., Boros, B., Stefova, M., Stafilov, T., Vojnoski, B., & Kilár, F. (2015). Phenolic compounds and antioxidant activity of Macedonian red wines. *Journal Food Composition and Analysis, 41*, 1–14.

Lenhardt, L., Bro, R., Zekovic, I., Dramicanin, T., & Dramicanin, M. D. (2015). Fluorescence spectroscopy coupled with PARAFAC and PLS DA for characterization and classification of honey. *Food Chemistry, 175*, 284–291.

Long, G. L., & Winerfordner, J. D. (1983). Limit of detection: A closer look at the IUPAC definition. *Analytical Chemistry, 55*, 712A–724A.

Monago-Maraña, O., Durán-Merás, I., Galeano-Díaz, T., & Muñoz de la Peña, A. (2016). Fluorescence properties of flavonoid compounds. Quantification in paprika samples using spectrofluorimetry coupled to second order chemometric tools. *Food Chemistry, 196*, 1058–1065.

Mulero, J., Martínez, G., Oliva, J., Cermeño, S., Cayuela, J. M., Zafrilla, P., ... Barba, A. (2015). Phenolic compounds and antioxidant activity of red wine made from grapes treated with different fungicides. *Food Chemistry, 180*, 25–31.

Olivieri, A. C., Wu, H. L., & Yu, R. Q. (2009). MVC2: a MATLAB graphical interface toolbox for second-order multivariate calibration. *Chemometrics and Intelligent Laboratory Systems, 96*, 246–251.

Rubio, L., Sarabia, L. A., & Ortiz, M. C. (2015). Standard addition method based on four-way PARAFAC decomposition to solve the matrix interferences in the determination of carbamate pesticides in lettuce using excitation-emission fluorescence data. *Talanta, 138*, 86–99.

Sádecká, J., & Tóthová, J. (2007). Fluorescence spectroscopy and chemometrics in the food classification – A review. *Czech Journal Food Science, 25*, 159–173.

Vallverdú-Queralt, A., Boix, N., Piqué, E., Gómez-Catalan, J., Medina-Remon, A., Sasot, G., ... Lamuela-Raventos, R. M. (2015). Identification of phenolic compounds in red wine extracts samples and zebrafish embryos by HPLC-ESI-LTQ-Orbitrap-MS. *Food Chemistry, 181*, 146–151.

Wine Annual Report and Statistics (2015). Aproved by C. Sloop; prepared by O. Bettini, pp. 3–11.

Wold, S., Geladi, P., Esbensen, K., & Öhman, J. (1987). Multiway principal components and PLS analysis. *Journal of Chemometrics, 1*, 41–56.

# ARTÍCULO 2

## Front-face fluorescence excitation-emission matrices in combination with three-way chemometrics for the discrimination and prediction of phenolic response to vineyard agronomic practices

Manuel Cabrera-Bañegil, Esperanza Valdés-Sánchez, Daniel Moreno, Diego Airado-Rodríguez, Isabel Durán-Merás

*Food Chemistry,* ***2019****, 270, 162-172*
*DOI: https://doi.org/10.1016/j.foodchem.2018.07.071*

Food Chemistry 270 (2019) 162–172

Contents lists available at ScienceDirect

Food Chemistry

journal homepage: www.elsevier.com/locate/foodchem

Analytical Methods

# Front-face fluorescence excitation-emission matrices in combination with three-way chemometrics for the discrimination and prediction of phenolic response to vineyard agronomic practices

Manuel Cabrera-Bañegil[a,*], Esperanza Valdés-Sánchez[b], Daniel Moreno[b], Diego Airado-Rodríguez[c], Isabel Durán-Merás[b,d]

[a] Department of Analytical Chemistry, Faculty of Sciences, University of Extremadura, 06006 Badajoz, Spain
[b] Technological Institute of Food and Agriculture (CICYTEX-INTAEX), Junta of Extremadura, 06007 Badajoz, Spain
[c] Department of Sciences and Mathematics Education, Education School, University of Extremadura, 06006 Badajoz, Spain
[d] Research Institute on Water, Climate Change and Sustainability (IACYS), University of Extremadura, 06006 Badajoz, Spain

ARTICLE INFO

*Keywords:*
Front-face fluorescence
Catechin
Epicatechin
Resveratrol
PARAFAC
LDA

ABSTRACT

Phenolic extracts from *cv* Tempranillo grapes subjected to water stress and irrigation treatment, both of them with high and low crop load, were analyzed by front-face fluorescence. Excitation-emission matrices (EEMs) were analyzed by means of unsupervised parallel factor analysis (PARAFAC), PARAFAC supervised by linear discriminant analysis, and discriminant unfolded partial least-squares. All algorithms allowed to differentiate between water stress and irrigation grape samples when the fluorescence maxima region of catechin and epicatechin, and resveratrol was considered. A central composite design was employed for the calibration of catechin, epicatechin and resveratrol. Resveratrol was quantified by U-PLS in both, irrigated and water stressed samples, and levels between $3.46 \pm 0.22$ and $4.67 \pm 0.08\,\mu g\,mL^{-1}$ and $2.43 \pm 0.60$ and $3.03 \pm 0.10\,\mu g\,mL^{-1}$, respectively, were found. PARAFAC only allowed the determination of the sum of catechin plus epicatechin ($R^2 = 0.9397$). The determination of total catechin plus epicatechin by means of PARAFAC was successfully validated by liquid chromatography.

## 1. Introduction

The possibility of monitoring the agricultural techniques is essential for achieving the desirable quality and to give response to the consumers' demands. The water regime in grapevine crops is crucial for obtaining grapes with determined physical-chemical and sensory features (Kyraleou et al., 2016). Different researches show that the water status of the vineyard affects to the chemical composition of grapes influencing the color intensity, sugar accumulation and concentration of polyphenols and anthocyanins (Romero et al., 2013) and its control is necessary for reducing the excessive vine vigor, improving the correct compromise between yield and quality (Gil et al., 2013). In other words, a water deficit during berry growth reduces yield and, depending on variety, it is usually considered beneficial for wine quality (Valdés et al., 2009). The effect of irrigation on consumer acceptability of red and white wines has been studied (Mirás-Avalos et al., 2017). In semiarid climates, the main goal when cultivating grapes for wine production should be to obtain the best grape composition with the highest possible yield while maximizing the available water resources. This can be achieved with an appropriate balance between vegetative growth and yield. One purpose of a modern viticulture is establishment practices for being able to limit vineyard yield and improve grape composition. In this sense, the cluster thinning and leaf removal are some interesting practices to balance the source-sink relationship by increasing carbohydrate sources in relation to sinks (Uriarte et al., 2015). In both cases, an increase and better distribution phenolic composition of grape berries has been demonstrated (Gatti, Bernizzoni, Civardi, & Poni, 2012; Moreno et al., 2015).

The consumption of the phenolic compounds has a positive effect on human-health due to their antioxidant activity, preventing illnesses (Saiko, Szakmary, Jaeger, & Szekere, 2008). In addition to this, among the typical kinds of phenolic compounds present in the most of grape varieties, it is important to highlight the presence of stilbenes, non-flavonoids compounds, which present beneficial and interesting biological properties. The synthesis of stilbenes is carried out when grapevine defense response is stimulated with exogenous molecules often

* Corresponding author.
*E-mail address:* manuelcb@unex.es (M. Cabrera-Bañegil).

https://doi.org/10.1016/j.foodchem.2018.07.071
Received 4 January 2018; Received in revised form 8 June 2018; Accepted 11 July 2018
Available online 18 July 2018

originated from microbes or plants (Delaunois et al., 2014). The most well-known bioactive stilbene is resveratrol, which possesses to biological and pharmacological properties (Witte, Kerti, Margulies & Flöel, 2014). On the other hand, another interesting phenolic compounds present in grapes are the flavanols, specifically monomeric flavan-3-ols such as catechin and epicatechin. These contribute to wine sensory perception, such as astringency, bitterness and mouth-feel.

In this sense, the determination of total phenols and their distribution is essential for the quality control of red grapes. In addition, the amount and distribution of polyphenols in the grape determines the harvest time. So, faster and easy to perform methodologies are, therefore, necessary for making decisions in the vineyard. Traditionally, the determination of phenols has supposed long times and reagent consuming reactions. The individual phenolic information of grapes can be obtained by means of a liquid chromatography (LC) (Da Silva Padilha et al., 2017) which is not available for most vine growers and small winemarkers. LC, among other techniques requires qualified personnel, high elution times and high organic solvents consumption. In this context, the development of new, fast, cost effective methodologies with simple sample preparation would be very welcome in winemaking sector (viticulture and enology sectors). Near infra-red spectroscopy (NIRS) coupled with chemometric algorithms has been successfully employed for predicting major sugar and organic acids of homogenized extract of grape berries at various developmental stages (Musingarabwi, Nieuwouldt, Young, Eyéghè-Bickong, & Vivier, 2016). NIRS has also been used for evaluation of phytosanitary status of intact grapes (Beghi, Giovenzana, Brancadoro, & Guidetti, 2017). On the other hand, NIR hyperspectral imaging with chemometrics has been used for the determination of anthocyanins and total phenolic in intact grapes berries (Diago, Fernández-Novales, Fernandes, Melo-Pinto, & Tardaguila, 2016; Martínez-Sandoval et al., 2016; Nogales-Bueno et al., 2015) and UV–visible spectroscopy with chemometrics has allowed to determine the phenolic profiles of grapes (Aleixandre-Tudo, Nieuwoudt, Olivieri, Aleixandre, & du Toit, 2018). However, fluorescence spectroscopy has hardly ever been used for studying the effects of irrigation and water stress conditions in phenol content of red grapes. Several studies show that fluorescence excitation emission (EEMs) can be a useful tool for quality control of red wine (Airado-Rodríguez, Durán-Merás, Galeano Díaz, & Petter Wold, 2011; Airado-Rodríguez, Galeano-Díaz, Durán-Merás, & Petter Wold, 2009; Cabrera-Bañegil, Hurtado-Sánchez, Galeano-Díaz, & Durán-Merás, 2017) and it can be used also for the classification of white wines according to grape variety (Azcarate et al., 2015) and grape ripening stage (Le Moigne et al., 2008). The information provided by fluorescence spectroscopy has been commonly analyzed by second order multivariate algorithms such as parallel factor analysis (PARAFAC) and unfolding partial least squares (U-PLS) (Durán-Merás, Domínguez Manzano, Airado Rodríguez & Muñoz de la Peña, 2018). Furthermore, the application of PARAFAC can be carried out in unsupervised way or supervised by linear discrimination analysis (LDA) to maximize the separation of groups (Muñoz de la Peña et al., 2016).

Considering the potential fluorescence information obtained from excitation emission matrices data, the main goal of this study was the development of a fast and simple front-face fluorescence methods in combination with PARAFAC, alone and combined with LDA, and discriminant unfolding partial least square (DU-PLS).

## 2. Materials and methods

### 2.1. Reagents, solvents and phenolic standards

Catechin, epicatechin and resveratrol were purchased from Sigma-Aldrich Chemie (Steinheim, Germany). Diethyl ether (Panreac, Barcelona, Spain) was used for phenols extraction and for preparing the calibration samples. Oxalic acid was purchased from Scharlau (Barcelona, Spain). Ultrapure water was obtained from a Milli-Q water system (Millipore S.A.S., Molsheim, France).

### 2.2. Samples

#### 2.2.1. Vineyard site, sampling and preliminary selection

The experiment was carried out in an experimental *Vitis vinifera*, L. cv. Tempranillo vineyard located in Badajoz, Extremadura (western Spain) (lat. 38°51′N; long. 6°40′W; elevation 198 m above sea level. Tempranillo cultivar, grafted on rootstock 110R, were planted in 2001 and trained to a vertical trellis on a bilateral cordon system east/west oriented. Vines were spaced 1.20 m within the row and 2.50 m between rows (3333 vines/ha). Vines were trained in a vertical shoot-positioning system oriented north-west to southeast. The vineyard soil was a silt-loam with 37.3% sand, 25.5% clay, 36.1% silt, and 1.1% organic matter. Volumetric water content was 0.30 $m^3/m^3$ at field capacity and 0.16 $m^3/m^3$ at the permanent wilting point.

The irrigation regimes were as follows: Non irrigated (only rain-fed, NI) and full irrigated vines (FI), corresponding to 100% of crop evapotranspiration (ETc). ETc is a parameter related with water requirements and it was calculated by means of a weighing lysimeter installed in the experimental vineyard under study (Picón-Toro, González-Dugo, Uriarte, Mancha & Testi, 2012).

The experimental orchard was divided in 12 randomised experimental plots, six non irrigated, and other six full irrigated. For each irrigation regime, two shoots load levels were established: Control with 12 shoots/vine (high crop level), and shoot-thinned treatment, in which the load was adjusted at 6 shoots/vine (low crop level).

Grapes of each experimental plot were randomly sampled by picking berries from the top, central and bottom parts of the cluster. Four samples were sampled from each experimental plot, and after sampling, grapes were immediately transported to the laboratory. With the aim to improve the physiological homogeneity of the different samples, berries were calibrated according to their density (Carbonell-Bejerano et al., 2016). The berries used for the different analysis were those which floated in 150–170 g/L sodium chloride solution, corresponding to berries with a total soluble solid content about 23–24 °Brix.

### 2.3. Extraction and HPLC analysis of phenolic compounds

Phenolic extraction was carried out according to a modification of the methodology previously described (Kontoudakis, Esteruelas, Fort, Canals & Zamora, 2010). 250 g of berries were crushed and homogenised in a blender (Worwek Model TM-31, Germany, speed 3, 1 min). Three replicates of 50 g of the homogenized sample were then used to extract total phenolic compounds after maceration with 50 mL of oxalic acid 0.3 M (pH 1.00). All samples were macerated during 16 h at 22–24 °C. The extracts, previously filtered (0.25 μm diameter Chromafil filters, Düren, Germany), were analyzed by HPLC (1200 LC; Agilent Technologies, Palo Alto, CA). The HPLC system is equipped with a photodiode array detector. The analytical column employed was a Kromasil® column (100-5-C18 250 × 4.6 mm, Akzonobel, Bohus, Sweden) and during the analysis, the temperature was maintained at 40 °C. The elution was carried out as previously described (Natividade, Corrêa, Souza, Pereira, & Lima, 2013). The injection volume was 10 μL. Detection was performed at 280 for catechin and epicatechin and 320 nm for resveratrol.

### 2.4. Front-face fluorescence

Two dimensional fluorescence spectra, as excitation-emission matrices (EEMs), were recorded using a Fluorescence Spectrophotometer Varian Model Cary Eclipse (Agilent Technologies, Madrid, Spain). Measurements were made with a variable front-face accessory, and in a 10-mm quartz cell at room temperature. The slits of excitation and emission monochromators were set at 5 and 5 nm, respectively, and the scan rate was 300 nm $min^{-1}$. For each sample, EEM was collected as a

set of emission spectra, in the excitation range from 250 to 350 nm, each 5 nm, and emission range from 284 to 399 nm, each 2.5 nm. Measurements were performed, within a short period of time (2 days) in order to avoid instrumental fluctuations.

### 2.5. Chemometric treatment

EEMs were pretreated as previously described (Airado-Rodríguez et al., 2009). Briefly, Rayleigh signals were removed by inserting missing values in bands centered on the identity line ($\lambda_{ex} = \lambda_{em}$) and in the line $2\lambda_{ex} = \lambda_{em}$. The calculations were speeded by inserting zero values rather than missing values in this region. Setting zeros close to the identity line can give bias in the solution (Andersen & BrO, 2003). For solving this problem, the insertion of missing values for a band of emission wavelengths below excitation and zeros to the remainder was carried out. The visual data inspection allowed to estimate the bandwidth of missing values (Rinnan & Andersen, 2005).

Data analysis has been performed using the MVC2 routine (Olivieri, Wu, & Yu, 2009) in Matlab environment (Matlab R2008a, MATLAB Version 7.6, The Marhworks, Natick, Massachusetts, US, 2010). The EEM data were analyzed with the aid of parallel factor analysis (PARAFAC) and discriminant unfolded partial least-squares regression (DA-UPLS). A in house MatLab routine was used for LDA calculations (Kemsley, 1998).

The chemometric algorithms applied in this work have been:

- PARAFAC. This algorithm often achieves the unique decomposition of fluorescence three-way data arrays, such as EEMs, allowing concentrations and spectral profiles to be extracted (Bro, 2003). For this purpose, the EEMs are arranged in a three-way array $X$ of dimensions $I \times J \times K$, where $I$, $J$, and $K$ are the number of samples, number of emission wavelengths, and number of excitation wavelengths, respectively. The whole dataset is decomposed by PARAFAC attempts to decompose it into three matrices, called $A$ (scores), $B$ and $C$ (loadings) with elements $a_{in}$, $b_{jn}$, $c_{kn}$, respectively, where $n$ indicates the component number. An element of $X$ is given by

$$x_{ijk} = \sum_{n=1}^{N} a_{in} b_{jn} c_{kn} + e_{ijk} \quad (1)$$

  where $x_{ijk}$ is the fluorescence intensity for sample $i$ at the emission wavelength $j$ and excitation wavelength $k$ and $e_{ijk}$ refers an element of the array E, which contains the variability not accounted by the model. For a given component $n$, the elements $a_{in}$, $b_{jn}$, and $c_{kn}$ are arranged in the score vector $a_n$ and in the loading vectors $b_n$ and $c_n$ which estimated its emission and excitation profiles, respectively. The elements of $a_n$ are directly proportional to its concentration in each sample. The array of EEMs data is fitted to Eq. (1) by least-squares.
- Linear discriminant analysis (LDA) is a well-known algorithm, which calculates a surface separating the sample groups, by establishing a linear discriminant function that maximizes the ratio of the between class and the within-class variances (Berrueta, Alonso-Salces & Héberger, 2007; Kemsley, 1998). Categories are supposed to follow a multivariate normal distribution and be linearly separated. With the $A$ score matrix of PARAFAC, and *the* $I \times g$ dummy matrix $Y$ of binary digits representing the group assignments (being $I$ the number of samples and $g$ the number of categories), the best representation is obtained when if the ratio of the between-groups variance $B_c$ matrix and the within-groups variance $W_c$ matrix is maximized. Suitable expressions for the matrices $B_c$ and $W_c$ employed for group assignment are:

$$\mathbf{B_c} = (\mathbf{g}-1)^{-1}\mathbf{A^T Y}(\mathbf{Y^T Y})^{-1}\mathbf{Y^T A} \quad (2)$$

$$\mathbf{W_c} = (\mathbf{I}-\mathbf{g})^{-1}[\mathbf{A^T A}-(\mathbf{g}-1)\mathbf{B_c}] \quad (3)$$

- It can be shown that the canonical variate (CV) scores contain the successively maximized between-groups variance/within-groups variance ratios. They are obtained by principal component analysis of the matrix ($W_c^{-1}B_c$) and projection of the data matrix $A$ onto the first loadings. The samples are then represented on a three- dimensional space defined by the first CV scores for each sample.
- DA-UPLS (Discriminant Analysis Unfolding Partial Least Squares Regression). Although the mathematical foundations of U-PLS were originally developed for multivariate purposes, its application to the classification of samples has been reported extensively. For discriminant analysis purposes, the variable y contains a coding integer representing the class label of the samples. As DA-UPLS is a classification method, instead of containing concentrations in the variable $y$, contains a coding integer representing the class label of the samples. PLS regression is conducted between the instrumental response (unfolded second-order matrix data) and the class label using training samples. The optimal number of latent variables is chosen by means of cross-validation. The final model with $n$ latent variables is used to predict the class label in the test set according to:

$$y_{\mathbf{test}} = \mathbf{t}_{\mathbf{test}}^{\mathbf{T}}\mathbf{v} \quad (4)$$

  where $y_{test}$ is the label class predicted, $t_{test}^{T}$ are the scores of test samples obtained by projection of $x_{test}$ onto the training loadings and v is the vector of the regression coefficients. In the ideal case scenario, the calculated values of $y_{test}$ – for two classes of samples – are 1 or 2; in practice, $y_{test}$ values are often close to 1 and 2.

## 3. Results and discussion

### 3.1. Excitation-emission matrices of grape phenolic extracts

With the aim of removing the turbidity of the aqueous phenolic extracts, a second liquid-liquid extraction with diethyl ether from the grape aqueous extracts, in relation 1:1 (v:v), was performed. Two dimensional excitation-emission fluorescence spectra, in front-face mode, were obtained for the organic extracts. Fig. 1 shows the EEMs as contour maps, after removing Rayleigh scattering of different grape samples from rain-fed vines (Fig. 1A and B) and from full irrigated vineyards (Fig. 1C and D). In all EEMs, two main fluorescence emission areas can be distinguished: one of them with emission at about 335–365 nm and excitation between 265 and 285 nm; and the second over an emission range 365–400 nm and excitation between 320 and 340 nm. The fluorescence intensity of these regions seems to be influenced by the water status of the vines, since the samples obtained from irrigated vineyards (Fig. 1C and D) present higher fluorescence than the samples from the rain-fed vines. No differences in the EEMs physiognomy have been observed between control and cluster thinned vines for the same irrigation treatment.

With the aim to obtain information about the fluorophores present in the extracts, emission and excitation spectra have been extracted from the EEMs. The excitation spectra, obtained at emission wavelength of 309 nm, are similar for all samples, showing only a maximum centred at 280 nm (Supplementary material). In the shape of these spectra it can be seen the influence of the water status, so samples from full irrigated vines show emission maxima more defined than the corresponding samples from rain-fed vines. The emission spectra for non-irrigated samples are a broad band with a maximum in a wavelength interval between 310 and 345 nm. For full-irrigated samples, these emission spectra presented a broad band with two maxima, one of them at 309 nm. However, the position of the second maximum is influenced by the water status, in grape samples from rain-fed vines it is centred at 350 nm, and for the irrigated vines it is bathochromically shifted at 375 nm.

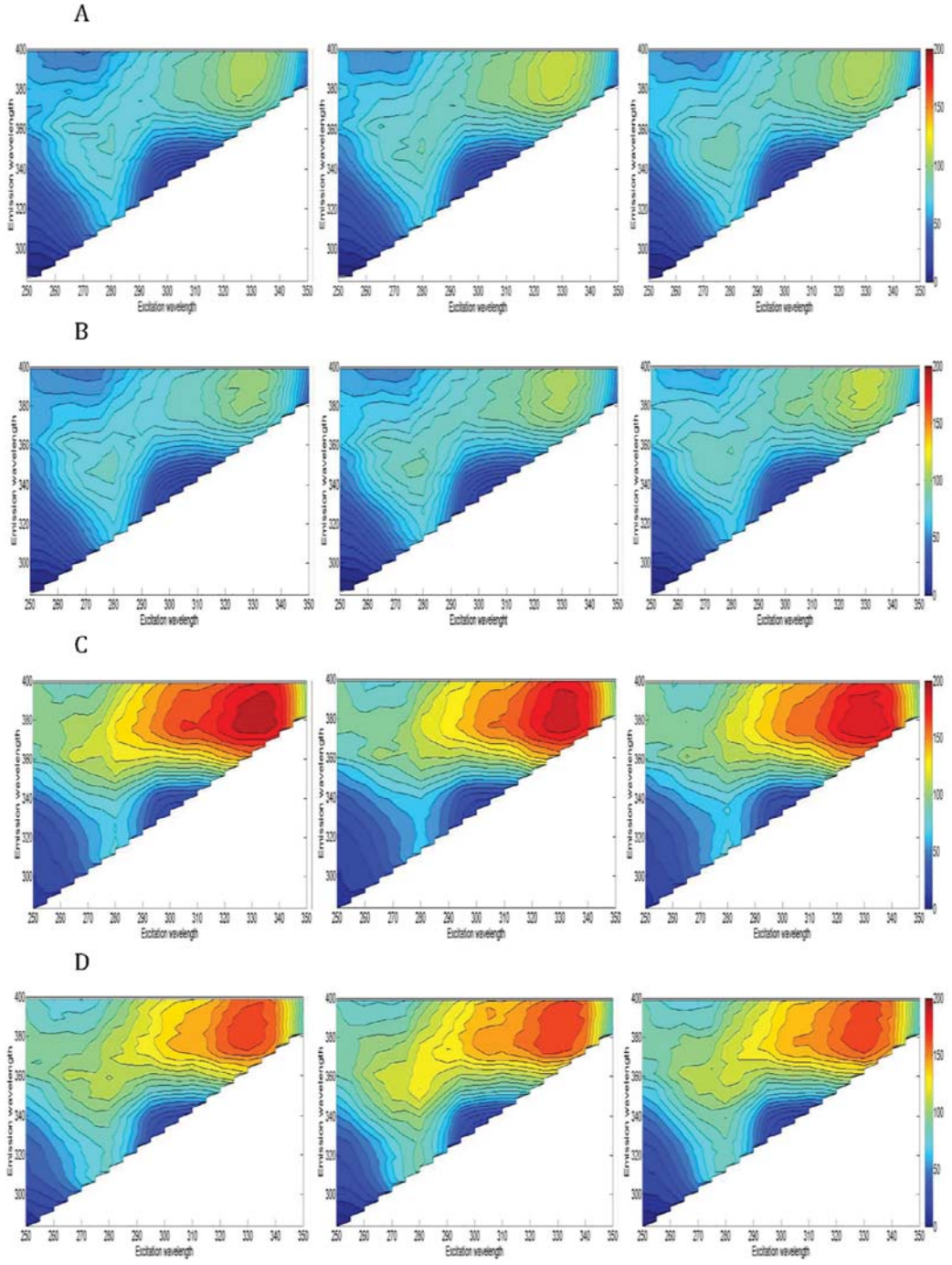


**Fig. 1.** Fluorescence contour plots of samples corresponding to grapes from rain-fed (A, B) and full-irrigation vines (C, D), both of them high crop load (A, C) and low crop load (B, D).

The emission spectra obtained exciting at 320 nm are very similar for all samples, showing a single maximum centred a 374 nm (Supplementary material). The presence of this emission maximum has already been described by Dufour, Letort, Laguet, Lebecque, and Serra (2006). The fluorescence emission spectra of Gamay and Dornfelder cultivars, which were studied (Dufour et al., 2006), had a maximum at 376 nm and a shoulder at 315 nm (exciting at 260 nm). No-irrigated samples had a lower emission fluorescence signal at 374 nm than full-irrigated samples. On the other hand, the excitation spectra of non-irrigated samples were also much lower than those obtained for full-irrigated samples. The excitation maximum of both types of samples was centred at 320 nm.

### 3.2. Chemometric analysis

The usefulness of different algorithms has been tested in order to discriminate between the fluorescence fingerprints of grapes subjected to different irrigation treatments, from vineyards with high and low crop load. With this purpose, PARAFAC, PARAFAC supervised by LDA and DA-UPLS were used. Since UPLS is unable to process data with NaN terms, which are introduced for Rayleigh signals elimination, calculations were carried out within two selected wavelength regions where the spectral information provided is more relevant. For the first spectral region, the excitation wavelength range from 250 to 290 nm and emission from 299 to 399 nm. For the second, the excitation wavelength range of 260–350 nm and the emission wavelength range was from 364 to 399 nm. In order to carry out an adequate comparison and interpretation of the results obtained, the same spectral regions were used in PARAFAC.

#### 3.2.1. Classification according to water status of the vine

*3.2.1.1. PARAFAC and LDA-PARAFAC.* PARAFAC algorithm was applied in 48 samples, 24 of them of grapes from no irrigated vines (12 grape samples from high crop load vineyards and 12 grape samples from low crop load vineyards), and the other 24 samples of grapes from irrigated vines (12 from high crop load and 12 from low crop load vineyards). With these data, the EEMs were arranged in two independent 3D arrays, the first one with the fluorescence data in the excitation range from 250 to 290 nm and emission from 299 to 399 nm, with dimensions 48 × 41 × 9 (samples × emission × excitation). For the second 3D array, the emission wavelength range was from 364 to 399 nm and the excitation range of 260–350 nm. These data were arranged in a cube structure with dimensions of 48 × 15 × 19 (samples × emission × excitation).

These three-way arrays were decomposed using PARAFAC. Different numbers of components were assayed (from 1 to 6), and in all cases the non-negativity constraints were used. For the selection of the optimum number of PARAFAC components, the percentages of core consistency and the physiognomy of the loadings were analyzed. Using the CORCONDIA criterion, and considering that the optimal number of components is selected as the largest tested value for which the core consistency is larger than ≈50%, for the first spectral region the optimal number of components was four, since when the number of components goes from four to five, the core consistency percentage falls from 86.8% to 6.9%.

Fig. 2A shows the emission and excitation loadings of the four components for the first spectral region (emission range of 300–399 and excitation range 250–290). They presented excitation maxima at 265 (component 2) and 275 nm (the same wavelength for components 3 and 4), respectively. In the emission mode, the component 1 had the maximum with the highest wavelength at 386 nm. The component 2 showed two maxima at 346 and 361 nm and a small shoulder at 379 nm. The component 3 was characterized by a maximum at 313 nm and a huge shoulder at 349 nm. The component 4 had an only maximum at 324 nm. Component number one presents maximum excitation/emission wavelengths at 290/386 nm and it is one of the main sources of fluorescence of diethyl ether extracts of grapes, regardless of irrigation treatment or vineyard crop load.

With respect to the loadings profiles of the third component, 275/313 nm, they can be match with flavan-3-ol compounds. These profiles have been compared with those corresponding to catechin and epicatechin standards (Fig. 2B), and as it can be observed, there is a high resemblance, especially for the excitation spectra. In the case of emission spectra, the standard of catechin and epicatechin lacked of a shoulder at 349 nm.

For the second spectral region (emission range of 364–399 and excitation range 260–350) the optimal number of factors was three. Fig. 2C shows the loading profiles of three component of the second spectral region. The component 1 showed an excitation/emission maximum at 330/379 nm while the component 2 and 3 showed excitation maxima at 280 nm. In addition to this, the component 2 had a shoulder at 330 nm. The component 1 can be matched with the presence of t-stilbenes (Airado-Rodríguez et al., 2011). The extracted profiles were compared with the excitation and emission spectra of resveratrol standard, Fig. 2D and the similarity observed allowed to confirm the assignation of this component.

Once assigned the components obtained by PARAFAC with phenolic compounds dependent on water status of the vine, the classification of the FI and NI samples were carried out. In order to explore the discriminating potential of the models, the set of the score values obtained with non-supervised PARAFAC in the two spectral regions were represented in a tridimensional plot, and labeled according to water status of the vine (Fig. 3). Also, and with the object to compare the power of discrimination, LDA was applied on the matrix of scores of PARAFAC, to obtain the canonical vectors (CV) and these were represented in a tridimensional plot. In both cases, and with the object of facilitating the visualization of pairwise comparison, each plot includes the projections of the 95% confidence level ellipses over the three planes defined by the corresponding axes. As it can be appreciated in Fig. 3, it is possible to discriminate between irrigated and non-irrigated samples in both spectral regions. Although with LDA-PARAFAC, and in the first spectral region better pairwise discrimination was obtained.

*3.2.1.2. DA-UPLS.* In order to use a chemometric tool with a different data decomposition, the possibility of discriminating between classes was carried out using DA-UPLS For both spectral regions, cross-validation and the Haaland and Thomas criterion (Haaland & Thomas, 1988a, 1988b) were employed to choose the optimum number of factor or latent variables, which are those given a PRESS value statistically no different to the minimum PRESS value (F-ratio probability falling below 0.75). The optimum number of latent variables was five for both restricted ranges.

The discrimination ability of DA-UPLS was tested previously assigning a code to each irrigation treatment. Thirty-eight calibration samples were used as training set, and at each sample the code for each category (1 for irrigated vineyard and 2 for rain-fed vines) was assigned. The predicted *vs* nominal code values are shown in Fig. 3. The samples submitted to irrigation and water stress were clearly predicted and classified.

The obtained results with the three models were in accordance with what has been observed in the contour maps of the samples, Fig. 1, since the best results were obtained in the spectral zone of lower wavelengths. In this zone, the fluorescence signal of grapes from rain-fed vines is not significant and this could contribute to the good classification. Furthermore, the predicted numbers of non-irrigated samples were lower deviation than those obtained for full-irrigated samples in the two spectral regions. According to the EEMs, it was observed that there were some differences between the two crop loads and this could provoke higher deviation of predicted numbers of full-irrigated samples.

According to the obtained results, it was concluded that water status of the vineyards were adequately predicted by the three used

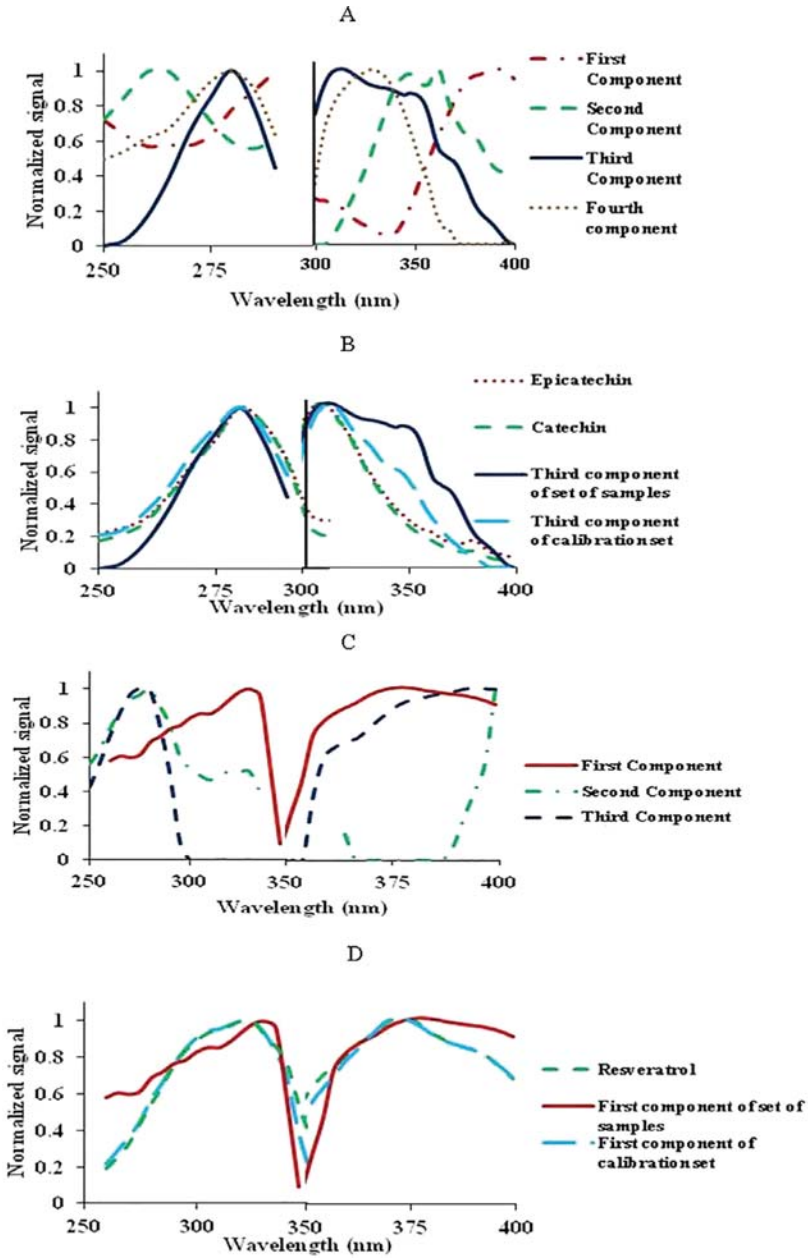


**Fig. 2.** A) Normalized excitation and emission PARAFAC profiles of the samples set (48 samples) for the four components of the first spectral region; B) excitation and emission PARAFAC profiles of the third component of the samples set and of the calibration set, and normalized excitation and emission spectra of catechin and epicatechin; C) Normalized excitation and emission PARAFAC profiles for the three components of the second spectral region; D) Normalized excitation and emission PARAFAC profiles of the first component for the second spectral region and normalized excitation and emission spectra of resveratrol.

algorithms because the full irrigation provoked high changes in the fluorescence composition of grapes.

### 3.2.2. Classification according with the crop load

*3.2.2.1. PARAFAC and LDA-PARAFAC.* A similar study has been carried out using the crop load as categorical variables. This study was carried out with two independents 3D arrays, one with the grape samples of from full irrigated vines and the other with grapes from no irrigated vines. The crop load of irrigated grapes can be used as variable to distinguish between high and low crop load, as it is depicted in Fig. 4. PARAFAC and LDA-PARAFAC were unable to differentiate between crop loads when the first spectral region was used. In the second

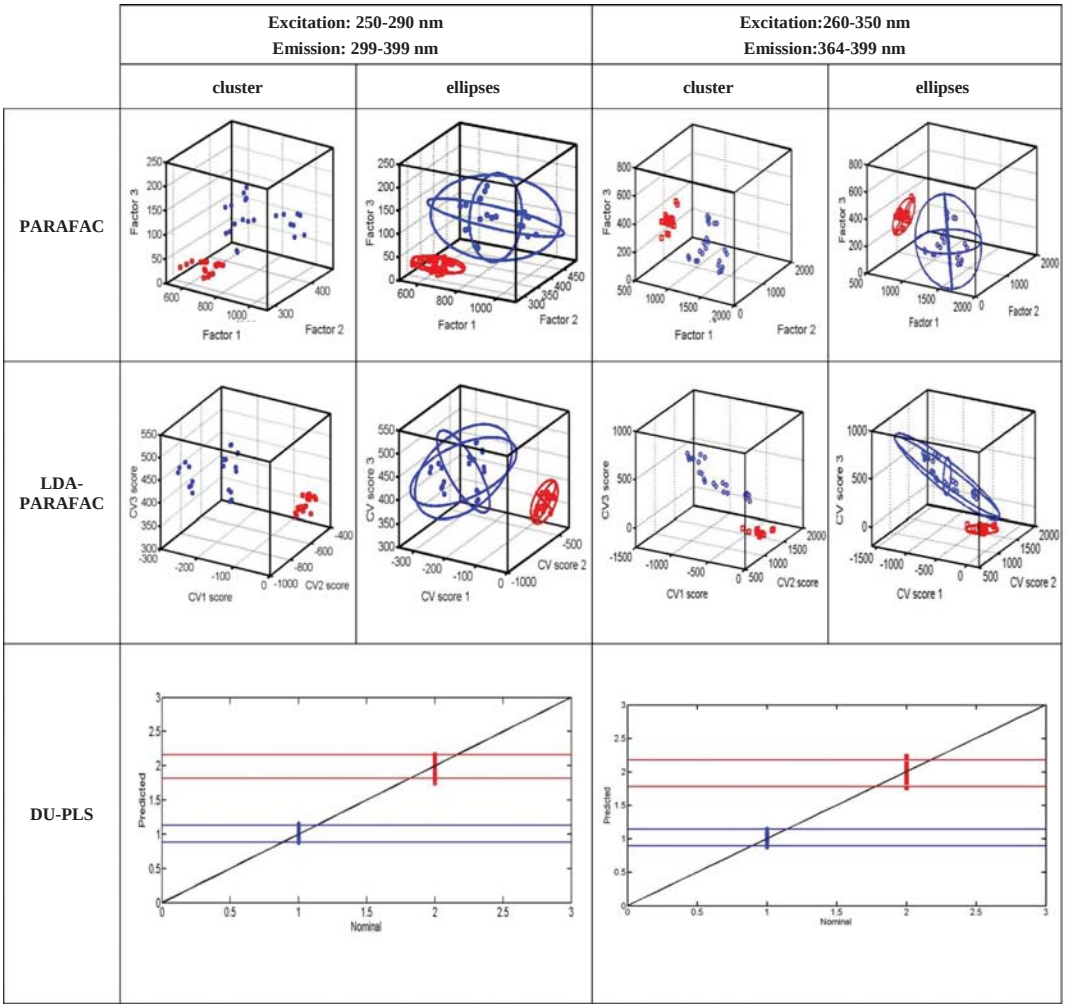


**Fig. 3.** Classification according irrigation treatment. PARAFAC scores and LDA-PARAFAC CV scores of a set of 48 samples, composed by irrigated grapes samples (24 samples) and non-irrigated grapes samples (24 samples). Three dimensional projection of the 95% confidence ellipse for PARAFAC and LDA analysis of the data collected from each type of grape. Plot of the DU-PLS predicted *vs* nominal coded.

spectral region, both algorithms allowed the classification according to crop load. In addition to this, the PARAFAC 95% confident ellipses showed a completely separation of full irrigation grape subjected to high and low crop load in the second spectral region. According to the spectra of high and low crop load, these showed differences in relation to the fluorescence intensity of maxima. Noticeable improvements were achieved when data were analyzed by LDA-PARAFAC. In the case of set of no irrigated vines none of both algorithms was able to distinguish between from high and low crop load (data not shown).

*3.2.2.2. DA-UPLS*. On the other hand, this algorithm was applied to investigate the discriminant possibility based on the crop load. In this case the code of each category was 1 for high crop load and 2 for low crop load. Fig. 4 shows the predicted *vs* nominal code values for the test samples with different crop load. While PARAFAC analysis was not effective enough to separate the classes in the first spectral range, DA-UPLS allowed a completely separation of high and low crop load in both spectral regions.

### 3.3. Phenolic quantification

#### 3.3.1. Second-order calibration methods

Taking into account the similarity between profiles of component 3 of first spectral region and of component 1 of second spectral region with catechin and resveratrol excitation and emission spectra, respectively, it was studied the potential of the proposed models to quantify those components in diethyl ether extracts of grapes. For this reason, in order to assess the ability of the different second-order multivariate tool in the determination of resveratrol, catechin and epicatechin, analytical standards of each one were used for constructing a calibration model only constituted by them. PARAFAC and U-PLS were applied to develop the quantitative models for the phenolic compounds (catechin, epicatechin and resveratrol). A calibration set was built using a central composite design in the concentration ranges between 0.0 and 19.52 μg $mL^{-1}$ for catechin, between 0.0 and 13.33 μg $mL^{-1}$ for epicatechin and between 0.0 and 12.24 μg $mL^{-1}$ for *trans*-resveratrol. Two diethyl ether blanks and five additional samples with only one analyte

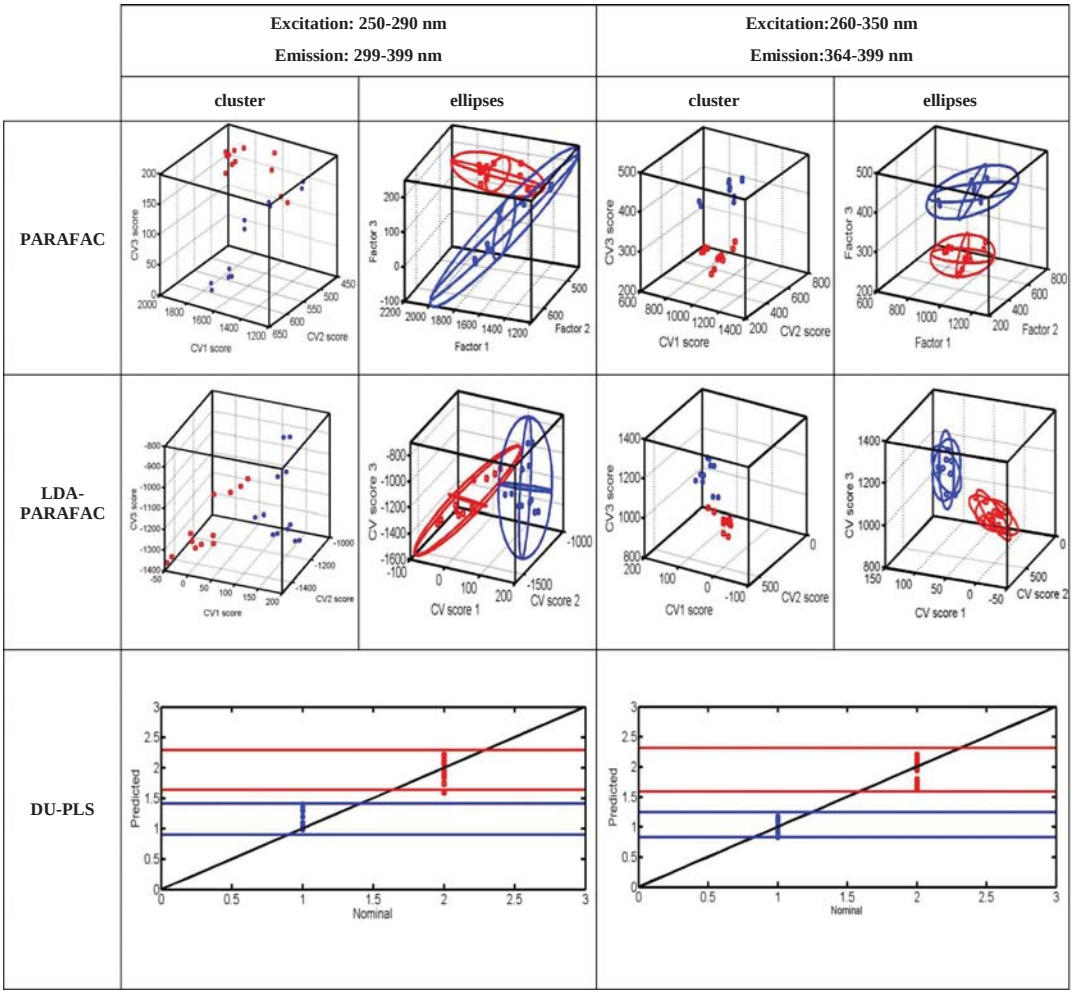


**Fig. 4.** PARAFAC scores and LDA scores for both spectral regions of a set of 24 irrigated samples, composed by high crop load grapes samples (12 samples) and low crop load grapes samples (12 samples). Three dimensional projection of the 95% confidence ellipse for PARAFAC and LDA analysis of the data collected from each type of grape. Plot of the DU-PLS predicted *vs* nominal coded.

were also included. The corresponding volumes of the standards solutions of each analyte, prepared in diethyl ether, were transferred into 10.0 mL calibrated flasks and diethyl ether was added to the mark. Besides, a validation set of nine samples was prepared in the same way as the calibration samples, but employing different concentrations following a random design.

The set of calibration samples were analyzed by PARAFAC and the optimum number of components calculates with the CONCORDIA criterion was 4 for the first spectral region, and 3 for the second spectral region. By U-PLS, cross-validation and the Haaland and Thomas criterion (Haaland & Thomas, 1988a, 1988b) were employed to choose the optimum number of factors and 3 and 4 components respectively were selected for each spectral region.

The fluorescence profiles of the component 3 of the calibration set are very similar to the epicatechin and catechin standards spectra, and also are coincident with the third component of the set of the grape extract samples, Fig. 2B. Also, the scores values of this component present a very good correlation with the concentration of catechin plus epicatechin (($r^2$ = 0.9397) but the scores values were not correlated with the only concentration of catechin or epicatechin. The score values of the first component of the second spectral region are correlated with the resveratrol concentration ($r^2$ = 0.8996). In the second spectral region the first component for the calibration set is very similar to the first component of the set of samples, Fig. 2D. Prediction results and statistical parameters for the validation set obtained with both algorithms and in both spectral regions, are summarized in Table 1. Neither of both algorithms was able to determine the individual concentrations of epicatechin or catechin in the validation samples. In accordance with previous researches (Cabrera-Bañegil et al., 2017), good results were only obtained when they were determined together and the sum of both analytes were considered. The statistical parameters were evaluated through the relative error prediction (REP%) and the root mean square error of prediction (RMSEP). Similar recovery values were obtained in the validation samples for sum of catechin and epicatechin. In the case of resveratrol, the prediction were better for UPLS. Not only the recovery values of resveratrol by UPLS in validation samples were better

**Table 1**
Recoveries and statistical parameters applying PARAFAC and U-PLS in the analysis of the validation set.

| | | PARAFAC | | UPLS | |
|---|---|---|---|---|---|
| | Actual (μg mL$^{-1}$)[a] | Predicted (μg mL$^{-1}$) | Rec (%) | Predicted (μg mL$^{-1}$) | Rec (%) |
| Sum of catechin and epicatechin | 6.7 | 7.1 | 106.0 | 7.1 | 106.0 |
| | 9.8 | 9.6 | 98.0 | 10.9 | 111.2 |
| | 16.5 | 19.0 | 115.1 | 16.0 | 97.0 |
| | 15.5 | 17.9 | 115.5 | 17.1 | 110.3 |
| | 19.3 | 17.2 | 89.1 | 18.1 | 93.8 |
| | 11.8 | 11.7 | 99.1 | 11.8 | 100.0 |
| | 8.2 | 9.1 | 110.9 | 8.3 | 101.2 |
| | 8.1 | 7.1 | 87.7 | 8.2 | 101.2 |
| | 14.9 | 14.7 | 98.7 | 15.1 | 101.3 |
| | Rec[b] ± SD | 102.2 ± 10.4 | | 102.5 ± 5.8 | |
| | RMSEP[c] | 1.44 | | 0.79 | |
| | REP[d] (%) | 11.63 | | 6.45 | |
| | $R^2$ | 0.900 | | 0.967 | |
| Resveratrol | | PARAFAC | | UPLS | |
| | Actual (μg mL$^{-1}$) | Predicted (μg mL$^{-1}$) | Rec (%) | Predicted (μg mL$^{-1}$) | Rec (%) |
| | 8.2 | 9.8 | 119.5 | 8.7 | 106.1 |
| | 8.2 | 10.5 | 128.0 | 10.0 | 121.0 |
| | 0.0 | 0.0 | – | 0.2 | – |
| | 5.7 | 7.8 | 136.8 | 6.1 | 107.0 |
| | 9.8 | 11.1 | 113.3 | 9.8 | 100.0 |
| | 8.2 | 8.6 | 104.9 | 8.0 | 97.6 |
| | 4.1 | 5.0 | 121.9 | 4.3 | 104.9 |
| | 12.0 | 11.7 | 97.5 | 11.9 | 99.1 |
| | 12.2 | 9.3 | 76.2 | 12.0 | 98.4 |
| | Rec ± SD | 112.3 ± 19.2 | | 104.4 ± 7.7 | |
| | RMSEP | 1.71 | | 0.68 | |
| | REP (%) | 20.01 | | 8.04 | |
| | $R^2$ | 0.833 | | 0.974 | |

[a] Actual: solutions prepared for the calibration.
[b] Rec: average recovery.
[c] RMSEP: root mean square error prediction = $\sqrt{\frac{\sum_{i=1}^{I}(y_i-\hat{y}_i)^2}{N}}$, $y_i$ = actual concentration, $\hat{y}_i$ = predicted concentration, N = number of samples in the test set.
[d] REP: relative error of prediction = $\frac{100}{\bar{y}}\sqrt{\frac{\sum_{i=1}^{I}(y_i-\hat{y}_i)^2}{N}}$, $\bar{y}$ = is the mean of the added concentration in the prediction set.

than PARAFAC but also the REP and RMSEP were lower when UPLS algorithm was used.

### 3.3.2. Chemometric quantification and validation by HPLC

Once chemometric methods were validated with analytical standards, the analysis of catechin, epicatechin and resveratrol in grape samples has been carried out with PARAFAC and U-PLS and the results were validated by HPLC. For each water status four samples of three different plots were analyzed and the obtained results are summarized in Table 2. With regard to sum of catechin and epicatechin, while U-PLS was unable to predict the concentration of both analytes, the results obtained applying PARAFAC are very similar to those obtained by HPLC. For resveratrol, the better results were obtained applying UPLS and considerable improvements were achieved when the concentrations were higher, especially in most of irrigated samples. Elliptical join confidence region (EJCR, 95% confidence level) for the slope and intercept of the regression for: catechin and epicatechin by PARAFAC and resveratrol by UPLS are shown in Supplementary material. For all samples, it can be observed that there were correlation between the levels of the phenolic compounds quantified and the irrigation treatment. The sum of catechin and epicatechin from samples from no irrigated vines ranged from 19.98 to 24.84 μg mL$^{-1}$, while in the irrigated vines ranged from 31.22 to 42.05 μg mL$^{-1}$ (by HPLC 20.65–24.44 and 32.04–44.13 μg mL$^{-1}$, respectively). Kyraleou et al. (2016) also found that full-irrigated samples contained higher amounts of catechin and epicatechin than non-irrigated samples. The behavior of resveratrol is similar and in extracts from grapes from no irrigated vines, the concentration ranged between 2.43 and 3.03 μg mL$^{-1}$, and in irrigated samples from 3.46 to 4.67 μg mL$^{-1}$. This could be explained due to resveratrol is generated as plant response of environmental moisture and the irrigation contributes to resveratrol formation. In this work, grapes from fully irrigated vines were richer in phenolic compounds than those from non-irrigated ones, suggesting that selecting the appropriate irrigation treatment is particularly important for winemakers to obtain the desired amount and structure of phenolic compounds for optimum final product properties. On the other hand not significant conclusions can be obtained about the influence of the crop load in the concentration of these phenolic compounds. Wang et al. (2018) found both early and late cluster thinning had no significant effects on total flavan-3-ol concentrations in Cabernet Sauvignon grapes in 2013.

Therefore, this method based in a diethyl ether extraction constitutes a good approach for the resveratrol quantification in grape samples against aqueous extract where resveratrol fluorescent signal is weaker (Galeano Díaz, Durán Merás, & Airado Rodríguez, 2006).

**Table 2**
PARAFAC and U-PLS prediction of resveratrol and sum of catechin and epicatechin in μg mL$^{-1}$. Quantification of resveratrol and sum of catechin obtained by LC.

| | | | Catechin plus epicatechin, μg mL$^{-1}$ | | Resveratrol, μg mL$^{-1}$ | | |
|---|---|---|---|---|---|---|---|
| | | | PARAFAC | HPLC | PARAFAC | UPLS | HPLC |
| Non-irrigated samples | High crop load | Plot 1 | 20.62 ± 1.23 | 22.22 ± 0.80 | 1.12 ± 0.57 | 2.64 ± 0.71 | 2.21 ± 0.60 |
| | | Plot 2 | 23.90 ± 0.98 | 23.97 ± 0.60 | 1.08 ± 0.15 | 2.78 ± 0.15 | 3.00 ± 0.11 |
| | | Plot 3 | 24.00 ± 1.72 | 23.81 ± 0.78 | 1.09 ± 0.10 | 3.03 ± 0.10 | 3.96 ± 0.24 |
| | Low crop load | Plot 4 | 19.98 ± 0.26 | 20.65 ± 0.19 | 0.89 ± 0.09 | 2.61 ± 0.19 | 3.03 ± 0.11 |
| | | Plot 5 | 24.84 ± 1.00 | 24.44 ± 0.43 | 0.99 ± 0.07 | 2.88 ± 0.14 | 3.44 ± 0.13 |
| | | Plot 6 | 20.50 ± 1.37 | 21.55 ± 0.48 | 0.66 ± 0.18 | 2.43 ± 0.60 | 3.37 ± 0.59 |
| Irrigated samples | High crop load | Plot 7 | 32.55 ± 0.78 | 27.64 ± 1.25 | 2.85 ± 0.18 | 4.40 ± 0.21 | 4.81 ± 0.18 |
| | | Plot 8 | 34.05 ± 1.92 | 30.00 ± 0.77 | 2.71 ± 0.06 | 4.45 ± 0.07 | 4.82 ± 0.08 |
| | | Plot 9 | 37.96 ± 3.25 | 33.24 ± 1.89 | 2.19 ± 0.11 | 4.10 ± 0.23 | 4.44 ± 0.17 |
| | Low crop load | Plot 10 | 31.22 ± 3.10 | 32.04 ± 0.91 | 2.42 ± 0.10 | 4.30 ± 0.07 | 4.53 ± 0.64 |
| | | Plot 11 | 42.05 ± 2.10 | 44.13 ± 0.15 | 2.64 ± 0.17 | 4.67 ± 0.08 | 4.68 ± 0.34 |
| | | Plot 12 | 41.63 ± 1.00 | 37.36 ± 2.61 | 1.90 ± 0.05 | 3.46 ± 0.22 | 3.89 ± 0.37 |
| | | | $R^2$ = 0.901 | | $R^2$ = 0.734 | $R^2$ = 0.819 | |
| | | | RMSEP 2.74 | | RMSEP 2.18 | RMSEP 0.51 | |
| | | | REP(%) 9.65 | | REP(%) 56.62 | REP(%) 13.27 | |

For each plot, four samples were analyzed and the results are expressed as $\bar{x}$ ± *RSD*.

## 4. Conclusions

This analytical method of front-face fluorescence in combination with chemometric algorithms supposes a first approach for the determination of fluorescence phenols of the red grapes faster than conventional LC. Qualitatively, the rapid decomposition of EEMs has allowed to differentiate between full-irrigated and non-irrigated grapes. In addition to this, front-face fluorescence in combination with PARAFAC seems to be a good strategy for identifying and quantifying catechin and epicatechin in a short time analysis while U-PLS allows a good quantification for resveratrol.

## Declaration of interest

None.

## Acknowledgements

Manuel Cabrera-Bañegil thanks the sponsorship of Comunidad Autónoma de Extremadura, the Consejería de Economía e Infraestructuras and the co-financing of the Fondo Social Europeo (FSE) for the Grant (PD16015). I. Duran Merás are grateful to Ministerio de Economía y Competitividad of Spain (Project CTQ2017-82496-P) and the Junta de Extremadura (GR18041-Research Group FQM003, and Project IB16058), both co-financed by the European FEDER funds, for financially supporting this work. Thanks to D. Uriarte, L.A. Mancha and M.V. Alarcon for given the grape samples (Project INIA RTA 2012 00029 C02).

## Appendix A. Supplementary data

Supplementary data associated with this article can be found, in the online version, at https://doi.org/10.1016/j.foodchem.2018.07.071.

## References

Airado-Rodríguez, D., Durán-Merás, I., Galeano Díaz, T., & Petter Wold, J. (2011). Front-face fluorescence spectroscopy: A new tool for control in the wine industry. *Journal of Food Composition and Analysis, 24*, 257–264.

Airado-Rodríguez, D., Galeano-Díaz, T., Durán-Merás, I., & Petter Wold, J. (2009). Usefulness of fluorescence excitation-emission matrices in combination with PARAFAC, as fingerprints of red wines. *Journal of Agricultural and Food Chemistry, 57*, 1711–1720.

Aleixandre-Tudo, J. L., Nieuwoudt, H., Olivieri, A., Aleixandre, J. L., & du Toit, W. (2018). Phenolic profiling of grapes, fermenting samples and wines using UV-Visible spectroscopy with chemometrics. *Food Control, 85*, 11–22.

Andersen, C. M., & Bro, R. (2003). Practical aspects of PARAFAC modelling of excitation-emission data. *Journal of Chemometrics, 17*, 200–215.

Azcarate, S. M., de Araújo Gomes, A., Alcaraz, M. R., Ugulino de Araújo, M. C., Camiña, J. M., & Goicoechea, H. C. (2015). Modeling excitation-emission fluorescence matrices with pattern recognition algorithms for classification of Argentine white wines according grape variety. *Food Chemistry, 184*, 214–219.

Beghi, R., Giovenzana, R., Brancadoro, L., & Guidetti, R. (2017). Rapid evaluation of grape phytosanitary status directly at the check point station entering the winery by using visible/near infrared spectroscopy. *Journal of Food Engineering*.

Berrueta, L. A., Alonso-Salces, R. M., & Héberger, K. (2007). Supervised pattern recognition in food analysis. *Journal of Chromatography A, 1158*, 196–214.

Bro, R. (2003). PARAFAC. Tutorial and applications. *Chemometrics and Intelligent Laboratory Systems, 17*, 200–215.

Cabrera-Bañegil, M., Hurtado-Sánchez, M. C., Galeano-Díaz, T., & Durán-Merás, I. (2017). Front-face fluorescence spectroscopy combined with second-order multivariate algorithms for the quantification of polyphenols in red wine samples. *Food Chemistry, 220*, 168–176.

Carbonell-Bejerano, P., Rodríguez, V., Hernáiz, S., Royo, C., Dal Santo, S., Pezzotti, M., & Martínez-Zapater, J. M. (2016). Reducing sampling bias in molecular studies of grapevine fruit ripening: Transcriptomic assessment of the density sorting method. *Theoretical and Experimental Plant Physiology, 28*, 109–129.

Da Silva Padilha, C. V., Miskinis, G. A., Olinda, Alves, de Souza, A. O., Pereira, G. E., De Oliveira, D., ... Dos Santos Lima, M. (2017). Rapid determination of flavonoids and phenolic acids in grape juices and wines by RP-HPLCYDAD: Method validation and characterization of commercial products of the new Brazilian varieties of grape. *Food Chemistry, 228*, 106–115.

Delaunois, B., Farace, G., Jeandet, P., Clément, C., Baillieul, F., Doney, S., & Cordelier, S. (2014). Elicitors as alternative strategy to pesticides in grapewine? Current knowledge on their mode of action from controlled conditions to vineyard. *Environmental Science and Pollution Research, 21*, 4837–4846.

Diago, M. P., Fernández-Novales, J., Fernandes, A. M., Melo-Pinto, P., & Tardaguila, J. (2016). Use of visible and short-wave near-infrared hyperspectral imaging to fingerprint anthocyanins in intact grape berries. *Journal of Agricultural and Food Chemistry, 64*, 7658–7666.

Dufour, E., Letort, A., Laguet, A., Lebecque, A., & Serra, J. N. (2006). Investigation of variety, typically and vintage of French and German wines using front-face fluorescence spectroscopy. *Analitica Chimica Acta, 563*, 292–299.

Durán-Merás, I., Domínguez Manzano, J., Airado Rodríguez, D., & Muñoz de la Peña, A. (2018). Detection and quantification of extra virgin olive oil adulteration by means of autofluorescence excitation-emission profiles combined with multi-way classification. *Talanta, 178*, 751–762.

Galeano Díaz, T., Durán Merás, I., & Airado Rodríguez, D. (2006). Determination of resveratrol in wine by photochemically induced second-derivative fluorescence coupled with liquid-liquid extraction. *Analytical Bioanalytical Chemistry, 387*, 1999–2007.

Gatti, M., Bernizzoni, F., Civardi, S., & Poni, S. (2012). Effects of cluster thinning and preflowering leaf removal on growth and grape composition in cv. Sangiovese. *American Journal of Enology and Viticulture, 63*, 325–332.

Gil, M., Esteruelas, M., González, E., Kontoudakis, N., Jiménez, J., Fort, F., ... Zamora, F. (2013). Effect of two different treatments for reducing grape yield in *Vitis Vinifera* cv Syrah on wine composition and quality: Berry thinning versus cluster thinning. *Journal of Agricultural and Food Chemistry, 61*, 4968–4978.

Haaland, D. M., & Thomas, E. V. (1988). Partial least-squares methods for spectral analyses. 1. Relation to other quantitative calibration methods and the extraction of qualitative information. *Analytical Chemistry, 60*, 1193–1202.

Haaland, D. H., & Thomas, E. V. (1988). Partial least-squares methods for spectral analyses. 2. Application to simulated and glass spectral data. *Analytical Chemistry, 60*, 1202–1208.

Kemsley, E. K. (1998). A genetic algorithm (GA) approach to the calculation of canonical variates (CVs). *Trends in Analytical Chemistry, 17*, 24–34.

Kontoudakis, N., Esteruelas, M., Fort, F., Canals, J. M., & Zamora, F. (2010). Comparison of methods for estimating phenolic maturity in grapes: Correlation between predicted and obtained parameters. *Analitica Chimica Acta, 660*, 127–133.

Kyraleou, M., Kotseridis, Y., Koundouras, S., Chira, K., Teissedre, P. L., & Kallithraka, S. (2016). Effect of irrigation regime on perceived astringency and proanthocyanidin compostion of skins and seeds of *Vitis vinifera* L. cv. Syrah grapes under semiarid conditions. *Food Chemistry, 203*, 292–300.

Le Moigne, M., Dufour, E., Bertrand, D., Maury, C., Seraphin, D., & Jourjon, F. (2008). Front face fluorescence spectroscopy and visible spectroscopy coupled with chemometrics have the potential to characterize ripening of Cabernet Franc grapes. *Analitica Chimica Acta, 621*, 8–18.

Martínez-Sandoval, J. R., Nogales-Bueno, J., Rodríguez-Pulido, F. J., Hernández-Hierro, J. M., Segovia-Quintero, M. A., Martínez-Rosas, M. E., & Heredia, F. J. (2016). Screening of anthocyanins in single red grapes using a non-destructive method based on the near infrared hyperspectral technology and chemometrics. *Journal of Science of Food and Agriculture, 96*, 1643–1647.

Mirás-Avalos, J. M., Fandiño, M., Trigo-Córdoba, E., Rey, B. J., Orriols, I., & Cancela, J. J. (2017). Influence of irrigation on consumer acceptability of Albariño and Godello wines. *LWT-Food Science and Technology, 9*, 1–8.

Moreno, D., Vilanova, M., Gamero, E., Intrigliolo, D. S., Talaverano, I. M., Uriarte, D., & Valdés, M. E. (2015). Effects of preflowering leaf removal on phenolic composition of Tempranillo in the semiarid terroir of western Spain. *American Journal of Enology and Viticulture, 2*, 204–211.

Muñoz de la Peña, A., Mujumdar, N., Heider, E. C., Goicoechea, H. C., Muñoz de la Peña, D., & Campiglia, A. D. (2016). Nondestructive total excitation-emission fluorescence microscopy combined with multi-way chemometrics analysis for visually indistinguishable single fiber discrimination. *Analytical Chemistry, 88*, 2967–2975.

Musingarabwi, D. M., Nieuwouldt, H. H., Young, P. R., Eyéghè-Bickong, H. A., & Vivier, M. A. (2016). A rapid qualitative and quantitative evaluation of grape berries at various stages of development using Fourier-transform infrared spectroscopy and multivariate data analysis. *Food Chemistry,* 253–262.

Natividade, M., Corrêa, L. C., Souza, S., Pereira, G., & Lima, L. (2013). Simultaneous analysis of 25 phenolic compounds in grape juice for HPLC: Method validation and characterization of Sao Francisco Valley Samples. *Microchemical Journal, 110*, 665–674.

Nogales-Bueno, J., Ayala, F., Hernández-Hierro, J. M., Rodríguez-Pulido, F. J., Echávarri, J. F., & Heredia, F. J. (2015). Simplified method for the screening of technological maturity of red grape and total phenolic compounds of red grape sking: Application of the characteristic vector method to near-infrared spectra. *Journal Agricultural and Food Chemistry, 63*, 4284–4290.

Olivieri, C. A., Wu, H. L., & Yu, R. Q. (2009). MVC2: A MATLAB graphical interface toolbox for second-order multivariate calibration. *Chemometrics and Intelligent Laboratory Systems, 96*, 246–251.

Picón-Toro, J., González-Dugo, V., Uriarte, D., Mancha, L. A., & Testi, L. (2012). Effects of canopy size and water stress over the crop coefficient of a "Tempranillo" vineyard in south-western Spain. *Irrigation Science, 30*(2012), 419–432.

Rinnan, A., & Andersen, C. M. (2005). Handling of first-order Rayleigh scatter in PARAFAC modelling of fluorescence excitation emission data. *Chemometrics and Intelligent Laboratory Systems, 76*, 91–99.

Romero, P., Gil-Muñoz, R., Del Amor, F. M., Valdés, E., Fernández, J. I., & Martínez-Cutillas, A. (2013). Regulated Deficit Irrigation based upon optimum water status improves phenolic composition in Monastrell grapes and wines. *Agricultural Water Management, 121*, 85–101.

Saiko, P., Szakmary, A., Jaeger, W., & Szekere, T. (2008). Review. Resveratrol and its analogs: Defense against cancer, coronary disease and neurodegenerative maladies or just a fad? *Mutation Research, 658*(1–2), 68–94.

Uriarte, D., Intrigliolo, D. S., Mancha, L. A., Picón-Toro, J., Valdés, E., & Prieto, M. H. (2015). Interactive effects of irrigation and crop level on Tempranillo vines in semiarid climate. *American Journal of Enology and Viticulture, 66*, 101–111.

Valdés, M. E., Moreno, D., Gamero, E., Uriarte, D., Prieto, M. H., Manzano, R., & Intrigliolo, D. S. (2009). Effects of cluster thinning and irrigation amount on water relations, growth, yield and fruit and wine composition of Tempranillo grapes in Extremadura (Spain). *Journal International Des Science de La Vinga et Du Vin, 43*, 67–76.

Wang, Y., He, Y. N., Chen, W. K., He, F., Chen, W., Cai, X. D., ... Wang, J. (2018). Effects of cluster thinning on vine photosynthesis, berry ripeness and flavonoid composition of Cabernet Sauvignon. *Food Chemistry, 248*, 101–110.

Witte, A. V., Kerti, L., Margulies, D. S., & Flöel, A. (2014). Effects of resveratrol on memory performance, hippocampal functional connectivity, and glucose metabolism in healthy older adults. *The Journal of Neuroscience: The Official Journal of the Society for Neuroscience, 34*, 7862–7870.

# ARTÍCULO 3

## Combination of fluorescence excitation emission matrices in polar and non-polar solvents to obtain three- and four-way arrays for classification of Tempranillo grapes according to maturation stage and hydirc status

Manuel Cabrera-Bañegil, Esperanza Valdés-Sánchez, Arsenio Muñoz de la Peña, Isabel Durán-Merás

*Talanta,* ***2019****, 199, 652-661*
*DOI: https://doi.org/10.1016/j.talanta.2019.03.002*



Talanta 199 (2019) 652–661

Contents lists available at ScienceDirect

Talanta

journal homepage: www.elsevier.com/locate/talanta

# Combination of fluorescence excitation emission matrices in polar and non-polar solvents to obtain three- and four- way arrays for classification of Tempranillo grapes according to maturation stage and hydric status

Manuel Cabrera-Bañegil[a], Esperanza Valdés-Sánchez[b], Arsenio Muñoz de la Peña[a,c], Isabel Durán-Merás[a,c,*]

[a] Department of Analytical Chemistry, Faculty of Sciences, University of Extremadura, Avda. de Elvas S/N, 06006 Badajoz, Spain
[b] Technological Institute of Food and Agriculture (CICYTEX-INTAEX), Junta of Extremadura, Avda. Adolfo Suárez S/N, 06007 Badajoz, Spain
[c] Research Institute on Water, Climate Change and Sustainability (IACYS), University of Extremadura, 06006 Badajoz, Spain

ARTICLE INFO

*Keywords:*
Three-way
Four-way
PARAFAC
Grapes
Maturation stage
Hydric status

ABSTRACT

The applicability of front-face excitation-emission fluorescence spectroscopy to compare grape water extracts of two consecutive sampling dates, corresponding with two maturation stages, and subjected to full irrigation and non-irrigation, was carried out. The decomposition of the obtained three way grape samples was initially analyzed by means of parallel factor analysis (PARAFAC). A tentative identification of fluorophores was done by matching PARAFAC score values with HPLC measurements. It was found that the first PARAFAC component was highly correlated with the sum of concentrations of catechin and epicatechin. The decomposition of the three way fluorescence data by linear discriminant analysis (LDA)-PARAFAC and LDA-unfolding partial least squares (U-PLS) allowed to discriminate between the first and the second maturation stage. The incorporation of an additional mode to the data, achieved by a diethyl ether extraction, giving rise to a four-way excitation-emission-solvent-samples data set, allowed to differentiate between irrigated and non-irrigated samples with the same assayed algorithms. As far as we know, the use of four-way data arrays for classification issues has been reported for the first time.

## 1. Introduction

In food sciences, the auto fluorescence of intact food systems in combination with multivariate data analysis has huge potential for food traceability in the context of calibration, as three-way fluorescence data have significant advantages with regard to selectivity and sensitivity, as well as for characterization and classification issues. Regarding the use of second-order data for classification studies, recent reports have been focused on the development of analytical methodologies for food authentication and traceability [1–4].

Different enological products have been analyzed using excitation-emission fluorescence three way data sets. This methodology has been applied to quantify phenolic compounds in red grapes [5], and wines [6], and for the classification of wines according to grape variety [7,8] and elaboration [9]. In sparkling wines, the browning was assessed by the use of fluorescence excitation–emission matrix spectroscopy combined with PARAFAC [10], and the authentication of Spanish Protected Designation of Origin wine vinegars has been investigated using three-way data combined with several chemometric techniques [11]. Other recent different approaches combined with chemometric algorithms for grapes monitoring are hyperspectral imaging [12], visible and near infrared spectroscopy [13–15], and electronic eye [16].

Third-order data forming four-way arrays have been scarcely proposed for the resolution of mixtures of components in complex samples. Third-order data may be acquired in several ways and, in most of the reported analytical applications, excitation emission matrices as function of kinetic reaction time, elution time in chromatographic procedures or pH values in gradient experiments have been recorded [17–21]. Four-way data arrays, obtained by stacking three-way fluorescence data as function of various solvents, have been recently reported by Zhang et al. in the context of calibration [22]. They proposed the strategy of introducing an extra solvent mode in the three-way data, to construct the four-way excitation-emission-solvent-samples data set, to exploit more inherent information in samples [22]. This is rather interesting because some analytical procedures with several extraction steps could be used for construction of four-way EEMs-solvent data sets.

* Corresponding author at: Department of Analytical Chemistry, Faculty of Sciences, University of Extremadura, Avda. de Elvas S/N, 06006 Badajoz, Spain.
*E-mail address:* iduran@unex.es (I. Durán-Merás).

https://doi.org/10.1016/j.talanta.2019.03.002
Received 20 December 2018; Received in revised form 28 February 2019; Accepted 1 March 2019
Available online 02 March 2019
0039-9140/ 

On the other hand, there is a continuous need for improving methods for food characterization and identification of the most relevant compounds (food markers) to reach this goal. In this sense, it is very important to arrange scientifically sound criteria that can provide an objective discrimination and characterization of vegetable products cultivated with different agronomic practices.

The main goal of this work is obtaining significant improvements on the classification of grapes according to water status and maturation stages. For this purpose, excitation- emission matrices of the water extracts of grapes, with different irrigation regimens and maturation stages, were recorded. In first place, the full fluorescence information was analyzed by PARAFAC and the spectral profiles provided chemical information about how the agronomic practices affect the fluorescence of the grapes. Then, supervised discriminant analysis LDA-PARAFAC and discriminant unfolded partial least-squares (DU-PLS) were used with the objective of classification. With the second-order data, the obtained results were not totally satisfactory with respect the hydric variable classification. For this, and with the aim to improve the discrimination between grapes with different hydric status, one extra dimension was added introducing an extra solvent mode, and diethyl ether was selected. The combination of the aqueous and diethyl ether extracts, provided a four-way data array. As it will be shown, second-order data combined with LDA-supervised PARAFAC and DU-PLS shows a high discrimination power between different maturation stages and, for the discrimination according to irrigation stage, the combination of four-way data with both chemometric algorithms was necessary. As far as we known, this is the first report on the use of four-way data with classification purposes.

## 2. Material and methods

### 2.1. Reagents, solvents and phenolic standards

Catechin and epicatechin standards were purchased from Sigma-Aldrich Chemie (Steinheim, Germany). Oxalic acid was purchased from Scharlau (Barcelona, Spain), diethyl ether from Panreac (Barcelona, Spain) and ultrapure water was obtained from a Milli-Q water system (Millipore S.A.S., Molsheim, France).

### 2.2. Samples

The irrigation experiments were carried out in an experimental *Vitis vinifera*, L. cv. Tempranillo vineyard located in Badajoz, Extremadura (western Spain) (lat. 38°51′N; long. 6°40′W; elevation 198 m above sea level). From each experimental plot, samples in two maturation stages, 18th and 26th August 2016, forty-eight samples for each stage, were sampled in 2016 season. To study the influence of hydric status, the experimental design was a split plot with forty eight samples, twenty four samples non-irrigated, only rain-fed (NI), and twenty four samples irrigated (FI). Drip irrigation was based on replacing 100% of crop evaporation (ETc) [23].

### 2.3. Sample preparation methods

For this purpose, 250 g of grapes were crushed and homogenised in a blender (Worwek Model TM-31, Germany, speed 3, 1 min) and, in a first place, a solid-liquid extraction with aqueous solvent was carried out, and then a liquid-liquid extraction with diethyl ether was carried out.

#### 2.3.1. Solid-liquid extraction

Extraction of polyphenols was performed in accordance with Kontoudakis et al. protocol [24] as follows: 250 g of the grapes were crushed in a blender until a homogeneous mixture was obtained. Then, five portions of the mixture were stored in a freezer. For the aqueous extract, 50 g of the homogeneous sample were macerated with 50 mL of oxalic acid 0.3 M (pH 1.00) during 16 h at 22–24 °C. Afterwards, the sample was centrifuged at 3000 rpm and the extract was filtered. This procedure was repeated three times.

#### 2.3.2. Liquid-liquid extraction

To introduce the solvent mode, the aqueous extracts were re-extracted with diethyl ether in relation 1:1 (v:v). After this extraction, all the coloured compounds (e.g. all the anthocyanin family) remain in the aqueous phase, being the organic one completely transparent and uncoloured.

### 2.4. Three and four-way data recording

For the three-way data recording, only the aqueous extracts were used. Fluorescence excitation-emission matrices (EEMs), built as two dimensional spectra, were recorded using a Fluorescence Spectrophotometer Varian Model Cary Eclipse in front-face mode. Measurements were made with a variable-angle front-face accessory, to ensure that reflected light, scattered radiation, and depolarization phenomena were minimized. The angle of incidence, defined as the angle between the excitation beam and the perpendicular to the cell surface, was set at 34°. A 10-mm quartz cell at room temperature was used, the slits of excitation and emission monochromators were set at 5 and 5 nm, respectively, and the scan rate was 300 nm $min^{-1}$. For the aqueous extracts of each sample, EEMs were collected as a set of emission spectra, in the excitation range from 250 to 350 nm, each 5 nm, and emission range from 284 to 399 nm, each 2.5 nm. Measurements were performed, within a short period of time (2 days), in order to avoid instrumental fluctuations.

For the four-way data, the EEMs of the diethyl ether extracts were recorded in the same conditions, and the three-way EMMs obtained in both solvents for each sample were joined into a single four-way data array.

### 2.5. HPLC analysis of phenolic compounds

The aqueous extracts were filtered with 0.25 μm diameter Chromafil filters (Düren, Germany), prior to the injection into the HPLC system (1200 LC; Agilent Technologies, Palo Alto, CA). The analytical column was a Kromasil® column (100-5-C18 250 × 4.6 mm, Akzonobel, Bohus, Sweden) with an analysis temperature of 40 °C. The injection volume was 10 μL. The mobile phase consisted of a gradient mixture of a solvent A (0.85% phosphoric acid solution) and solvent B (acetonitrile), with a flow-rate of 0.5 mL $min^{-1}$. The gradient was started with 100% of solvent A and adjusted for 93% of solvent A and 7% of solvent B in 10 min; 90% of solvent A and 10% of solvent B in 20 min; 88% of solvent A and 12% of solvent B in 30 min; 77% of solvent A and 33% of solvent B in 40 min; 65% of solvent A and 35% of solvent B in 45 min; and 100% of solvent B in 55 min [25]. The HPLC system detection was a photodiode array detector (DAD), set at 280 nm for catechin and epicatechin.

### 2.6. Chemometric treatment

EEMs were pretreated as previously described [26]. Briefly, Rayleigh signals were removed in all EEMs by setting these elements to missing values in bands centered on the identity line ($\lambda_{ex} = \lambda_{em}$). In the zone where $\lambda_{em} < \lambda_{ex}$, zeros were inserted. Zeros instead missing values in this zone speed the calculations; however, setting zeros close to the identity line can give bias in the solution [27]. This problem was handled by inserting missing values for a band of emission wavelengths below excitation and zeros for all other emissions below excitation. The bandwidth of missing values is varied from 0 to twice the estimated width of the Rayleigh scatter line, which is found through visual inspection of the data [28].

The three-way (date of sampling) analysis has been performed using the MVC2 routine [29] in Matlab environment (Matlab R2008a,

MATLAB Version 7.6, The Marhworks, Natick, Massachusetts, US, 2010). The four-way data, obtained by the combination of EEMs of aqueous and organic extracts were analyzed by the MVC3 routine [30,31]. In both cases, the EEMs data were analyzed with PARAFAC (parallel factor analysis), LDA-PARAFAC (linear discriminant analysis-parallel factor analysis) and DU-PLS (discriminant analysis-unfolding partial least squares). An in house MatLab routine was used for LDA calculations [32]. A brief resume of each one is presented below:

- PARAFAC: This algorithm often achieves the unique decomposition of fluorescence three-way data arrays, such as EEMs, allowing concentrations and spectral profiles to be extracted [27]. For this purpose, the EEMs are arranged in a three-way array **X** of dimensions *I x J x K,* where *I*, *J*, and *K* are the number of samples, number of emission wavelengths, and number of excitation wavelengths, respectively. The whole dataset is decomposed by PARAFAC into three matrices, called **A** (scores), **B** and **C** (loadings), with elements $a_{in}$, $b_{jn}$, $c_{kn}$, respectively, where *n* indicates the component number. The decomposition is usually accomplished through an alternating least squares (ALS) minimization scheme. An element of **X** is given by

$$x_{ijk} = \sum_{n=1}^{N} a_{in} b_{jn} c_{kn} + e_{ijk} \quad (1)$$

where $x_{ijk}$ is the fluorescence intensity for sample $i$ at the emission wavelength $j$ and excitation wavelength $k$ and $e_{ijk}$ refers an element of the array **E**, which contains the variability not accounted by the model. For a given component $n$, the elements $a_{in}$, $b_{jn}$, and $c_{kn}$ are arranged in the score vector $\mathbf{a}_n$ and in the loading vectors $\mathbf{b}_n$ and $\mathbf{c}_n$ which estimated its emission and excitation profiles, respectively. The elements of $a_n$ are directly proportional to its concentration in each sample. The array of EEMs data is fitted to Eq. (1) by least-squares.

For four-way data, the quadrilinear PARAFAC model with dimension ($I \times J \times K \times L$) where L is the *l-th* combined extract, the tensor **X** is:

$$x_{ijk} = \sum_{n=1}^{N} a_{in} b_{jn} c_{kn} d_{ln} + e_{ijkl} \quad (2)$$

- Linear discriminant analysis (LDA) is a well-known algorithm, which calculates a surface separating the sample groups, by establishing a linear discriminant function that maximizes the ratio of the between class and the within-class variances [32,33]. Categories are supposed to follow a multivariate normal distribution and be linearly separated. With the **A** score matrix of PARAFAC, and the $I \times g$ dummy matrix **Y** of binary digits representing the group assignments (being $I$ the number of samples and $g$ the number of

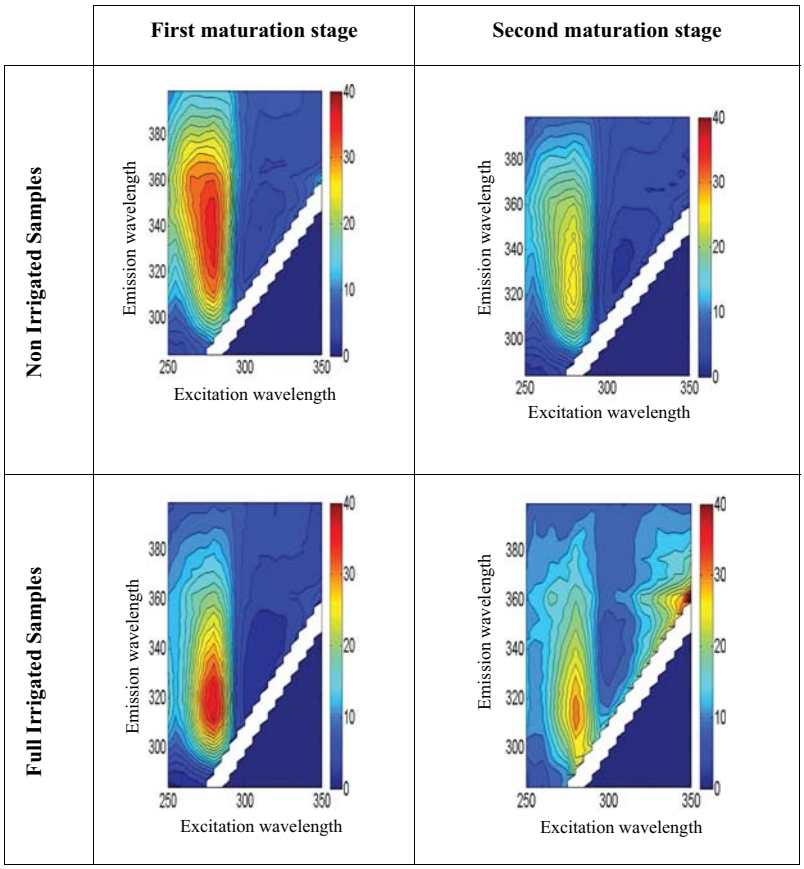


**Fig. 1.** Excitation-emission contour maps of aqueous extracts of grapes sampled in two maturation stages and subjected to full irrigation and no irrigation.

categories), the best representation is obtained when the ratio of the between-groups variance **Bc** matrix and the within-groups variance **Wc** matrix is maximized. Suitable expressions for the matrices **Bc** and **Wc** employed for group assignment are:

$$\mathbf{Bc} = (g - 1)^{-1}\mathbf{A}^T\mathbf{Y}(\mathbf{Y}^T\mathbf{Y})^{-1}\mathbf{Y}^T\mathbf{A} \quad (3)$$

$$\mathbf{Wc} = (1 - g)^{-1}[\mathbf{A}^T\mathbf{A} - (g - 1)\,\mathbf{Bc}] \quad (4)$$

It can be shown that the canonical variate (CV) scores contain the successively maximized between-groups variance/within-groups variance ratios. They are obtained by principal component analysis of the matrix ($\mathbf{W_c}^{-1}\mathbf{B_c}$) and projection of the data matrix **A** onto the first loadings. The samples are then represented on a three- dimensional space defined by the first CV scores for each sample.

- DU-PLS. Although the mathematical foundations of U-PLS were originally developed for multivariate calibration purposes [34], its application to the classification of samples has been reported extensively [35]. PLS is an inverse multivariate calibration which seeks a direct relationship between instrumental response and the property of interest. As DU-PLS is a classification method, instead of containing concentrations in the variable *y*, this is coded 1 or 2, when there are two classes. PLS regression is conducted between the instrumental response (unfolded second-order matrix data) and the class label using training samples. The optimal number of latent variables is chosen by means of cross-validation [36]. The final model with *n* latent variables is used to predict the class label in the test set according to:

$$y_{test} = \mathbf{t}_{test}^T\mathbf{v} \quad (5)$$

where $y_{test}$ is the label class predicted, $\mathbf{t}_{test}^T$ are the scores of test samples obtained by projection of $\mathbf{x}_{test}$ onto the training loadings and **v** is the vector of the regression coefficients. In the ideal case scenario, the calculated values of $y_{test}$, for two classes of samples, are 1 or 2; in practice, $y_{test}$ values are often close to 1 and 2.

## 3. Results and discussion

The EEMs of the aqueous grape extracts, of the two dates of sampling (18th and 26th August 2016), corresponding to two different maturation stages, of full irrigated (FI) and non-irrigated samples (NI), are shown in Fig. 1. In all EEMs the same fluorescence region, with an emission maximum at around 310–340 nm, and excitation at 280 nm, has been observed. Although this fluorescence signal has not been assigned to a single compound, it is likely due to the contribution of several fluorophores, such as some phenolic acids and monomeric catechins [7,37,38]. As it can be seen, the fluorescence decreased in the second date of sampling because of the phenolic content changes during

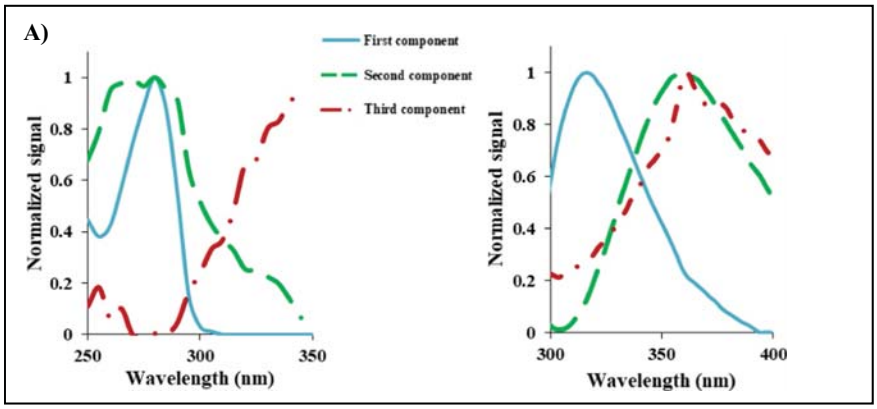


**Fig. 2.** A) Loadings of the second order data PARAFAC model: Left, excitation mode; Rigth, emission mode. B) Regression curves of score values of first component versus sum of catechin and epicatechin chromatographic concentrations for each date of sampling.

grape ripening. Belviso et al. [39] studied the maturation evolution of phenolic compounds, in grape skins of "Italia" table grape, and they found that catechin and epicatechin presented higher contents on the first sampling dates than at the end of ripening. On the other hand, Kennedy et al. [40] characterized the flavonoids changes during fruit ripening in skins from Cabernet Sauvignon grapes, and they found that catechin concentration decreased rapidly from onset of ripening, until reaching rather stable content in early September.

Furthermore, the fluorescence intensity of this region seems to be influenced by the water status of the vineyards. While the water status of the grapes did not seem to influence the excitation spectra, showing all of them high fluorescence intensity at 280 nm, the emission spectra was bathochromically shifted to 340 nm in non-irrigated grapes samples in the first date of grape sampling. In addition to this, emission spectra of non-irrigated samples (NI) showed a wider band than full-irrigated samples. In reference to water, in the second date of sampling the differences between EEMs associated to full irrigated vineyards and rain fed vineyards decreased. On the other hand, in the second maturation stage, and in full irrigated samples, a new fluorescence spectral zone, with emission range between 350 and 365 nm and excitation range between 330 and 350 nm was observed. The presence of this maximum has already been described in wines by Dufour et al. [41]. This fluorescence region could be tentatively assigned to resveratrol content. Under certain conditions, the progressive resveratrol accumulation during berry ripening has been already reported [42,43]. This fact is in accordance with the results obtained by Belviso et al. [39], that found the highest resveratrol content at the end of the ripening period.

### 3.1. Classification according to maturation stage

To investigate if the EEMs of the aqueous extracts allowed to distinguish between classes, a first study with a total of 96 EEMs, comprising 48 samples of each category (first and second sampling date), was carried out. The three-way array excitation-emission-sample data (21 × 47 × 96) were decomposed by PARAFAC, and using in all cases the non-negativity constraints. For the selection of the optimum number of PARAFAC components, the core consistency diagnostic (CORCONDIA) [44], standard deviation residual (SD) test [45] and the physiognomy of the loadings were analyzed. Using the CORCONDIA criterion [44], the optimal number of components was three, since when the number of components goes from three to four, the core consistency percentage falls drastically. As an alternative, the SD residual values were calculated as 3.3, 1.6, 1.0, 0.9 and 0.8, respectively, and the first SD residual value statistically not different to the minimum SD residual value corresponded to three as optimal number of components, in agreement with the CORCONDIA criterion [45]. In addition to this, two data sets composed of 48 EEMs each, corresponding to a single maturation stage, were essayed by separate, and its results, referred to scores and loading profiles, did not differ from the complete set of 96 EEMs.

The excitation and emission PARAFAC loadings of the three components are shown in Fig. 2A. The first component shows its maximum intensity at $\lambda_{ex/em}$ = 280/315 nm, and it was assigned to the sum of catechin and epicatechin concentrations. To verify this, the scores of this component were correlated with the sum of catechin and epicatechin concentrations, obtained by HPLC, finding a good regression coefficient (Fig. 2B). Furthermore, score data of second grape sampling date were better correlated with the content of catechin plus epicatechin than those of the first sampling date. The second component shows a broad band at an excitation wavelength of 280 nm and an emission maximum at 360 nm. When Schueuermann et al. [38] analyzed Pinot Noir grapes juices and wines, by front-face fluorescence in combination with PARAFAC, the decomposition of the set of data gave a second component with a similar physiognomy that the obtained in the present paper, and it was tentatively assigned to the contribution of

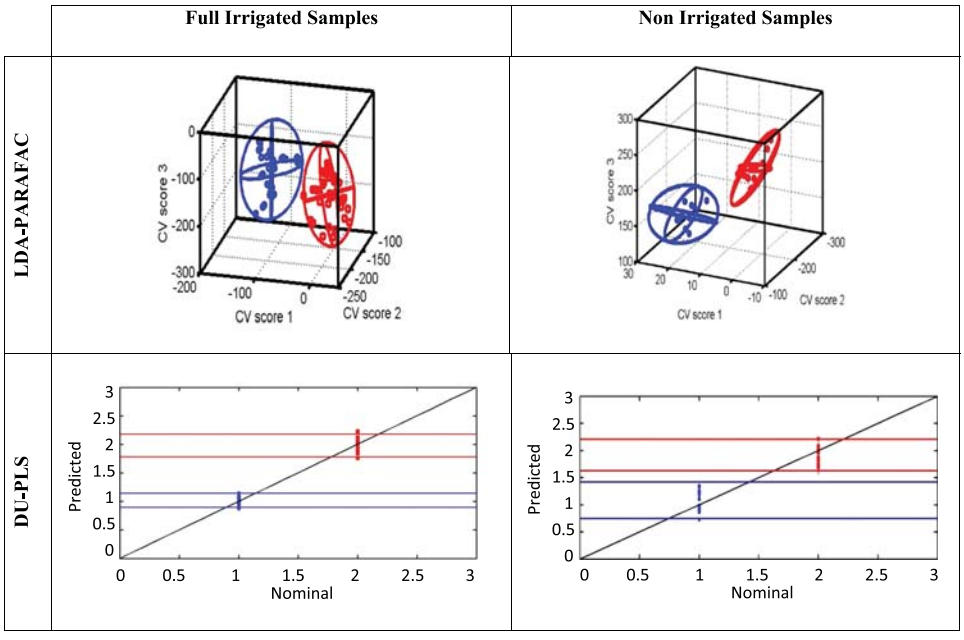


**Fig. 3.** Classification with three-way data according to grape sampling, considering irrigated grape samples and non-irrigated grape samples separately. LDA-PARAFAC-CV scores of a set of 48 samples, composed by first sampling date samples (24 samples) and second sampling date samples (24 samples). Three dimensional projection of the 95% confidence ellipse for LDA-PARAFAC analysis of the data collected from each type of irrigation status. Plot of the DU-PLS predicted *vs* nominal coded.

multiple compounds such as vanillic acid, syringic acid and gallic acid, among others. The third component presented an emission wavelength emission maximum at 360 nm. With the available data, this component could not be assigned to a concrete fluorophore.

LDA was applied to the scores of the three PARAFAC components. Two classification models, according to maturation stage, were built separately, one with non-irrigated samples and other with full irrigated samples. Each training set contains thirty two samples randomly selected, sixteen of each maturation stage, for data modeling and internal validation with the full cross-validation procedure. The test sets, constituted by other sixteen samples (eight of each maturation stage), were used to evaluate the discriminative power of the models. The model built with non-irrigated samples showed an accuracy of 94%; one sample of the first maturation stage was not well assigned, although all samples of second maturation stage were correctly assigned. With full irrigated samples, the classification model shows an accuracy of 100% and all samples were correctly assigned in accordance with their maturation stage.

Also, the canonical vectors (CV) were represented in a tridimensional plot. In order to visualize the classes' separation, each plot includes the projections of the 95% confidence level ellipses over the three planes defined by the corresponding axes. The prediction interval for the multivariate normal distribution yielded a tri-dimensional ellipse consisting of a x vector satisfying the following equation

$$(x-\mu)^{T}\varphi^{-1}(x-\mu) \le \chi^2_k(p) \quad (6)$$

where $\mu$ is the mean, $\varphi$ is the covariance matrix and $\chi^2_k(p)$ is the quartile function for the probability $p$ of the $\chi^2$ distribution with $k$ degrees of freedom, where $k$ is the dimension of the data. The axes are defined by the eigenvectors of the covariance matrix and the radius of each axis is equal to 2.796 times the square root of the corresponding eigenvalue distribution with three degrees of freedom. The value 2.796 is obtained from the square root of the $\chi^2$ distribution with three degrees of freedom and 95% confidence interval [35,46]. As it can be appreciated in Fig. 3, it is possible the correct discrimination between the two dates of grape sampling and, in consequence, between the two maturation stages.

Additionally, the possibility of discriminating between the studied classes using different data decomposition was carried out by DU-PLS. Cross-validation and the Haaland and Thomas criterion [47] were employed to choose the optimum number of factor or latent variables, which are those given a PRESS (predicted residual sum of squares) value statistically not different to the minimum PRESS value (F-ratio probability falling below 0.75). The optimal number of latent variables was five. The discrimination ability of DU-PLS was tested previously assigning a code to the date of grape sampling. From the forty-eight samples of each sampling data, 32 samples were randomly selected as training set, and they formed two different classes, according to grape sampling date (1 for first sampling and 2 for second sampling). The predicted versus nominal code values are shown in Fig. 3. As it can be seen, all the grape samples could be correctly classified according to the predefined classes.

Using other analytical techniques, some authors have achieved to differentiate dates of grapes sampling or, more concretely, grape stages of maturation. In this way, Xiao et al. used the scores PCA plot of NIR data from intact grapes and this allowed to discriminate the green stage

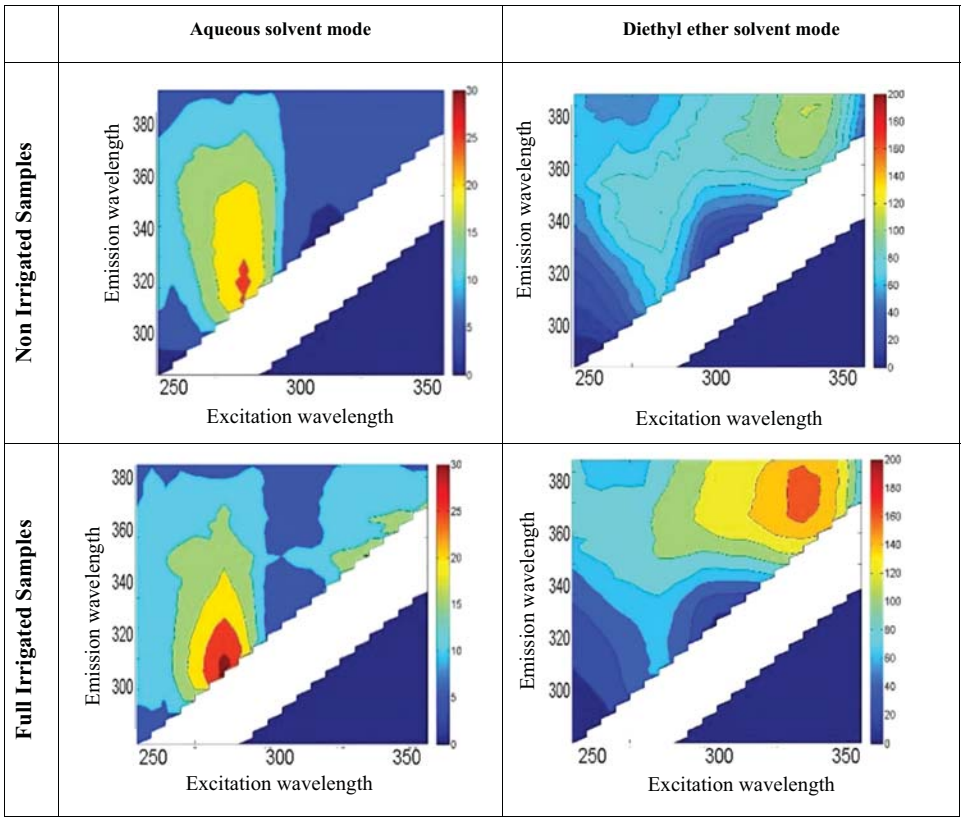


**Fig. 4.** Excitation-emission contour maps of aqueous extracts and diethyl ether extracts of non-irrigated and full irrigated grapes.

(positive scores) from the other four stages, which were comprehensively overlapped [48]. Similar results were obtained by Nogales-Bueno et al. [49], who used the near infrared hyperspectral images of intact grapes during ripening, and found a partial-separation between the early days of ripening and the rest of samples.

### 3.2. Influence of grape hydric status. Four-way data

In basis on a preliminary study, the three way fluorescence information of aqueous extracts, obtained by the assayed algorithms, was unable to discriminate between full irrigated and non-irrigated grape samples. The differences between aqueous EEMs of both water status of the grapes were not enough high to achieve a complete separation.

It is well known that the solvent matrix in which fluorophores are measured may change their fluorescence, and that comparing the same fluorophore in solvent matrices of different polarity may lead to shifts in the emission spectra [50]. The introduction of an extra dimension in the data leads to higher-order-data, and allows for a theoretical increase in the predictive ability of the models. Among the advantages associated to the use of four-way data, which are related to the extraction of more inherent information from data, the following have been reported: a) the enhancement in sensitivity and selectivity; b) the improved resolution of serious co-linearity and high-intensity noise, as well as high background interference [51,52]. According to this, the extraction of aqueous extracts with a non-miscible solvent can offer certainness advantages in the classification. Among possible solvents, diethyl ether has allowed to obtain good extraction recoveries for the stilbene compounds. For this reason, the aqueous extracts were re-extracted with diethyl ether and the EEMs of 48 grape samples were registered.

Fig. 4 shows the EEMs of aqueous and diethyl ether grape extracts for samples belonging to the second maturation stage, and for the two hydric regimens. It can be seen that the EEMs of diethyl ether extracts provide fluorescent information that is not observed in aqueous extracts. A new region appears at excitation wavelengths between 320 and 340 nm and emission at 365–400 nm, and its fluorescence intensity is influenced by the water status of the vineyards, since the samples obtained from irrigated vineyards present higher fluorescence than the samples from the rain-fed vineyards. When the diethyl ether EEMs were compared with aqueous EEMs, some differences were observed. The signal associated to catechin and epicatechin in aqueous medium ($\lambda_{ex/em}$ 280/315) increased in the diethyl ether EEMs. The observed fluorescence signal in aqueous medium of irrigated grapes samples ($\lambda_{ex}$ 330 nm and $\lambda_{em}$ 370 nm) increased in diethyl ether and, in this solvent, this intense signal was presented in all samples.

With the aim to investigate if the water status is a variable allowing the grape discrimination, a four-way analysis was carried out. Hence, the three-way EEMs that contained the data of the aqueous extracts and the diethyl ether extracts were arranged to provide a four-way data set with dimension (21 × 47 × 48 × 2, excitation wavelength × emission wavelength × number of samples × solvents), where the fourth mode is an extra solvent. The non-negativity constraint was imposed for the four ways. Using the CORCONDIA criterion [44], the optimal number of PARAFAC components was three, since when the number of components goes from three to four, the core consistency percentage falls near to

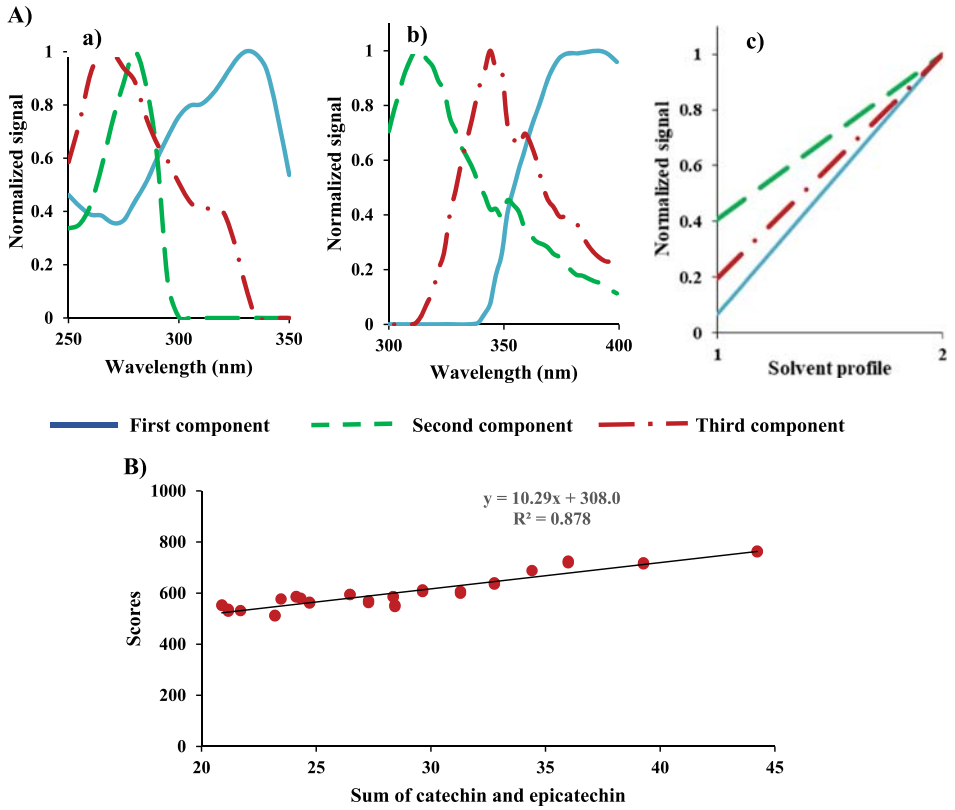


**Fig. 5.** A) Loadings of the four-way PARAFAC model with three factors: a) excitation mode; b) emission mode and c) solvent mode. B) Regression curves of the scores of second component versus sum of catechin and epicatechin chromatographic concentrations.

zero. Taking account that the SD residual of the components two, three, four and five were 3.4, 2.5, 2.3 and 2.0 respectively, the first SD residual value statistically not different than the minimum SD residual value was also three, in agreement with the CORCONDIA criterion.

The PARAFAC loadings obtained using four-way data are shown in Fig. 5A. The first component presents an excitation maximum at 330 and an emission maximum at 380 nm, and it is in agreement with the intense fluorescence signal observed in the diethyl ether EEMs with respect to water. The second component obtained showed its maximum intensities at $\lambda_{ex/em}$ 280/315 nm. Comparing the maxima and the physiognomy of this component with that obtained with the three-way data, both of them corresponded to the same analytes and, as it has been previously indicated, to the sum of catechin and epicatechin contribution. Fig. 5B shows the four-way PARAFAC scores of the second component, and a good correlation with the sum of catechin and epicatechin content was obtained ($R^2 = 0.878$). For last, the excitation and emission loadings of the third component are more defined than the obtained in the three-way analysis, with maxima at 270 and 346 nm, respectively. In view of the obtained results, we can conclude that, the main modification respect to three-way PARAFAC analysis of aqueous grape extracts, was the incorporation of other analyte or others analytes, whose fluorescence intensity in the diethyl ether was the highest and relegated the rest of compounds to second and third components. This contributes to obtain more defined loading profiles and with more differentiated maxima, in agreement with the PARAFAC solvent profiles. The highest increase in solvent profile corresponded to the first component, which practically was null in water. With respect to the solvent extraction mode, the loadings of samples increase from the first to the second solvent, that is, the higher values were obtained for the diethyl ether extracts.

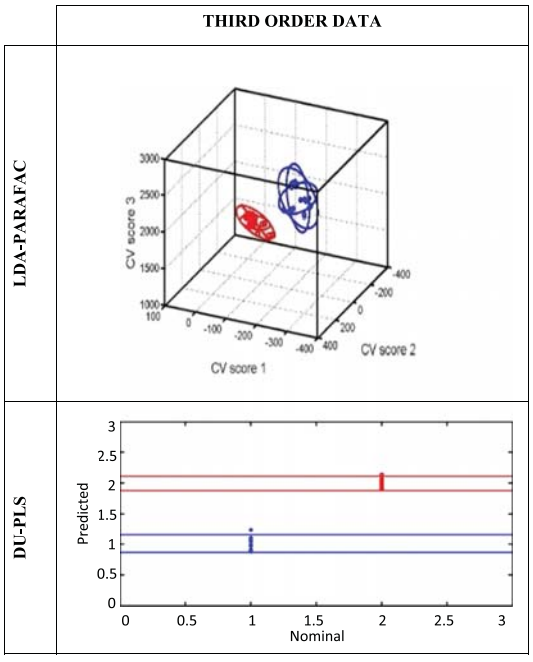


**Fig. 6.** Classification according to the irrigation treatment with third-order samples data. Top) LDA-PARAFAC CV scores (three components model) of a set of 48 samples, (non-irrigated, red circles, irrigated; blue circles). The three dimensional projection of the 95% confidence ellipse is included to facilitate visualization. Bottom) Plot of the DU-PLS (four components model) predicted *vs* nominal coded.

For the discrimination between full irrigated and non-irrigated grape samples, LDA was applied to the PARAFAC scores obtained for the four-way array. The training set was built using 42 samples (21 from each water status). The prediction set consisted of a 16 samples set (8 from each water status) and it constituted an independent set to predict the ability of the model. In this case, an excellent classification of 100% was obtained both in the training and prediction sets.

Finally, the canonical vectors obtained when LDA was applied on the matrix of scores of PARAFAC were represented in a tridimensional plot, Fig. 6, and it can be observed that a correct classification was obtained using the different hydric status as variable for the classification.

When DU-PLS was applied, the number of optimum latent variables, calculated in accordance with Haaland and Thomas criterion [47] was four. Fig. 6 shows the predicted versus nominal code values and, according to this figure, we can say that grape hydric status is correctly predicted.

## 4. Conclusions

This study demonstrated the potential application of front-face excitation-emission fluorescence matrix, in combination with multiway methods, for the characterization and classification of grapes with different agronomic practices. Data of different order, three and four-way data, were combined with LDA-PARAFAC and DU-PLS algorithms. The score values obtained from three-way data PARAFAC decomposition have been used in LDA, allowing the discrimination between maturation stages. Similar results were obtained with DU-PLS.

However, the EEMs obtained from grapes with different hydric status are very similar and, for the classification of these samples, it was necessary to add an extra mode. It was demonstrated that the addition of an extra mode, such as a second solvent, to the three-way EEMs data and, in consequence, the use of four-way data arrays, allowed to extract more information from complex samples. This becomes clear in the loading profiles obtained, which present better definition and less overlapping in their excitation and emission maxima. The solvent profiles yielded the fourth dimension to the data and, in consequence, an increase in sensitivity and selectivity was obtained. The results obtained indicated that the use of three-way and four-way data was a good approach for the discrimination between samples with very similar fluorescence profiles. The results obtained with both supervised algorithms were the same, independently of the data order used. Finally, we want to note that the use of four-way data arrays for classification purposes has been proposed for the first time in this report.

## Acknowledgements

Manuel Cabrera-Bañegil thanks the sponsorship of Comunidad Autónoma de Extremadura, Consejería de Economía e Infraestructuras for the Grant (PD16015). Thanks to D. Uriarte, L.A. Mancha and M.V. Alarcon for supplying the grape samples (Project INIA RTA 2012 00029 C02).

## Funding

This work was funding by Ministerio de Ciencia, Innovación y Universidades of Spain (Project CTQ2017-82496-P) and Junta de Extremadura (GR180541-Research Group FQM003, and Project IB16058), both co-financed by the Fondo Social Europeo funds, for financially supporting this work

## Conflict of interest

The authors declare no competing financial interest.

## References


[1] R. Karoui, C. Blecker, Fluorescence spectroscopy measurement for quality assessment of food systems-a review, Food Bioprocess Technol. 4 (2011) 364–386, https://doi.org/10.1007/s11947-010-0370-0.

[2] E. Salvatore, M. Bevilacqua, R. Bro, F. Marini, M. Cocchi, Chapter 14 - classification methods of multiway arrays as a basic tool for food PDO authentication, in: M. de la Guardia, A. Gonzálvez (Eds.), Food Prot. Des. Orig. Elsevier, 2013, pp. 339–382, , https://doi.org/10.1016/B978-0-444-59562-1.00014-1.

[3] S.M. Azcarate, A. de Araújo Gomes, A. Muñoz de la Peña, H.C. Goicoechea, Modeling second-order data for classification issues: data characteristics, algorithms, processing procedures and applications, TrAC - Trends Anal. Chem. 107 (2018) 151–168, https://doi.org/10.1016/j.trac.2018.07.022.

[4] F. Marini, F. Marini (Ed.), Chemometrics in Food Chemistry, Elsevier, 2013.

[5] M. Cabrera-Bañegil, E. Valdés-Sánchez, D. Moreno, D. Airado-Rodríguez, I. Durán-Merás, Front-face fluorescence excitation-emission matrices in combination with three-way chemometrics for the discrimination and prediction of phenolic response to vineyard agronomic practices, Food Chem. 270 (2019) 162–172, https://doi.org/10.1016/j.foodchem.2018.07.071.

[6] M. Cabrera-Bañegil, M. del, C. Hurtado-Sánchez, T. Galeano-Díaz, I. Durán-Merás, Front-face fluorescence spectroscopy combined with second-order multivariate algorithms for the quantification of polyphenols in red wine samples, Food Chem. 220 (2017) 168–176, https://doi.org/10.1016/j.foodchem.2016.09.152.

[7] S.M. Azcarate, A. de Araújo Gomes, M.R. Alcaraz, M.C. Ugulino de Araújo, J.M. Camiña, H.C. Goicoechea, Modeling excitation-emission fluorescence matrices with pattern recognition algorithms for classification of Argentine white wines according grape variety, Food Chem. 184 (2015) 214–219, https://doi.org/10.1016/j.foodchem.2015.03.081.

[8] R. Saad, D.J.-R. Bouveresse, N. Locquet, D.N. Rutledge, Using pH variations to improve the discrimination of wines by 3D front face fluorescence spectroscopy associated to Independent Components Analysis, Talanta 153 (2016) 278–284, https://doi.org/10.1016/j.talanta.2016.03.023.

[9] Y. Wan, F. Pan, M. Shen, Identification of Jiangxi wines by three-dimensional fluorescence fingerprints, Spectrochim. Acta Part A Mol. Biomol. Spectrosc. 96 (2012) 605–610, https://doi.org/10.1016/j.saa.2012.07.030.

[10] S. Elcoroaristizabal, R.M. Callejón, J.M. Amigo, J.A. Ocaña-González, M.L. Morales, C. Ubeda, Fluorescence excitation–emission matrix spectroscopy as a tool for determining quality of sparkling wines, Food Chem. 206 (2016) 284–290, https://doi.org/10.1016/j.foodchem.2016.03.037.

[11] R. Ríos-Reina, S. Elcoroaristizabal, J.A. Ocaña-González, D.L. García-González, J.M. Amigo, R.M. Callejón, Characterization and authentication of Spanish PDO wine vinegars using multidimensional fluorescence and chemometrics, Food Chem. 230 (2017) 108–116, https://doi.org/10.1016/j.foodchem.2017.02.118.

[12] V.M. Gomes, A.M. Fernandes, A. Faia, P. Melo-Pinto, Comparison of different approaches for the prediction of sugar content in new vintages of whole Port wine grape berries using hyperspectral imaging, Comput. Electron. Agric. 140 (2017) 244–254, https://doi.org/10.1016/j.compag.2017.06.009.

[13] R. Beghi, V. Giovenzana, L. Brancadoro, R. Guidetti, Rapid evaluation of grape phytosanitary status directly at the check point station entering the winery by using visible/near infrared spectroscopy, J. Food Eng. 204 (2017) 46–54, https://doi.org/10.1016/J.JFOODENG.2017.02.012.

[14] J.U. Porep, M.E. Erdmann, A. Körzendörfer, D.R. Kammerer, R. Carle, Rapid determination of ergosterol in grape mashes for grape rot indication and further quality assessment by means of an industrial near infrared/visible (NIR/VIS) spectrometer – a feasibility study, Food Control. 43 (2014) 142–149, https://doi.org/10.1016/j.foodcont.2014.03.008.

[15] D.M. Musingarabwi, H.H. Nieuwoudt, P.R. Young, H.A. Eyéghè-Bickong, M.A. Vivier, A rapid qualitative and quantitative evaluation of grape berries at various stages of development using Fourier-transform infrared spectroscopy and multivariate data analysis, Food Chem. 190 (2016) 253–262, https://doi.org/10.1016/j.foodchem.2015.05.080.

[16] G. Orlandi, R. Calvini, L. Pigani, G. Foca, G. Vasile Simone, A. Antonelli, A. Ulrici, Electronic eye for the prediction of parameters related to grape ripening, Talanta 186 (2018) 381–388, https://doi.org/10.1016/j.talanta.2018.04.076.

[17] M.R. Alcaráz, G.G. Siano, M.J. Culzoni, A. Muñoz de la Peña, H.C. Goicoechea, Modeling four and three-way fast high-performance liquid chromatography with fluorescence detection data for quantitation of fluoroquinolones in water samples, Anal. Chim. Acta 809 (2014) 37–46, https://doi.org/10.1016/j.aca.2013.12.011.

[18] A. Jiménez Girón, I. Durán-Merás, A. Espinosa-Mansilla, A. Muñoz de la Peña, F. Cañada Cañada, A.C. Olivieri, On line photochemically induced excitation-emission-kinetic four-way data. Analytical application for the determination of folic acid and its two main metabolites in serum by U-PLS and N-PLS/residual trilinearization (RTL) calibration, Anal. Chim. Acta 622 (2008) 94–103, https://doi.org/10.1016/j.aca.2008.05.079.

[19] C. Kang, H.-L. Wu, Y.-J. Yu, Y.-J. Liu, S.-R. Zhang, X.-H. Zhang, R.-Q. Yu, An alternative quadrilinear decomposition algorithm for four-way calibration with application to analysis of four-way fluorescence excitation–emission–pH data array, Anal. Chim. Acta 758 (2013) 45–57, https://doi.org/10.1016/j.aca.2012.10.056.

[20] V.A. Lozano, A. Muñoz de la Peña, I. Durán-Merás, A. Espinosa Mansilla, G.M. Escandar, Four-way multivariate calibration using ultra-fast high-performance liquid chromatography with fluorescence excitation-emission detection. Application to the direct analysis of chlorophylls *a* and *b* and pheophytins *a* and *b* in olive oils, Chemom. Intell. Lab. Syst. 125 (2013) 121–131, https://doi.org/10.1016/j.chemolab.2013.04.005.

[21] R.M. Maggio, P.C. Damiani, A.C. Olivieri, Four-way kinetic-excitation-emission fluorescence data processed by multi-way algorithms. Determination of carbaryl and 1-naphthol in water samples in the presence of fluorescent interferents, Anal. Chim. Acta 677 (2010) 97–107, https://doi.org/10.1016/j.aca.2010.07.045.

[22] X.-H. Zhang, H.-L. Wu, X.-L. Yin, Y. Li, X.-D. Qing, H.-W. Gu, C. Kang, R.-Q. Yu, Exploiting third-order advantage using four-way calibration method for direct quantitative analysis of active ingredients of Schisandra chinensis in DMEM by processing four-way excitation–emission-solvent fluorescence data, Chemom. Intell. Lab. Syst. 155 (2016) 46–53, https://doi.org/10.1016/j.chemolab.2016.04.008.

[23] J. Picón-Toro, V. González-Dugo, D. Uriarte, L.A. Mancha, L. Testi, Effects of canopy size and water stress over the crop coefficient of a "Tempranillo" vineyard in south-western Spain, Irrig. Sci. 30 (2012) 419–432, https://doi.org/10.1007/s00271-012-0351-3.

[24] N. Kontoudakis, M. Esteruelas, F. Fort, J.M. Canals, F. Zamora, Comparison of methods for estimating phenolic maturity in grapes: correlation between predicted and obtained parameters, Anal. Chim. Acta 660 (2010) 127–133, https://doi.org/10.1016/j.aca.2009.10.067.

[25] M.M.P. Natividade, L.C. Corrêa, S.V.C. de Souza, G.E. Pereira, L.C. de, O. Lima, Simultaneous analysis of 25 phenolic compounds in grape juice for HPLC: method validation and characterization of São Francisco Valley samples, Microchem. J. 110 (2013) 665–674, https://doi.org/10.1016/j.microc.2013.08.010.

[26] D. Airado-Rodríguez, T. Galeano-Díaz, I. Durán-Merás, J.P. Wold, Usefulness of fluorescence excitation–emission matrices in combination with PARAFAC, as fingerprints of red wines, J. Agric. Food Chem. 57 (2009) 1711–1720, https://doi.org/10.1021/jf8033623.

[27] C.M. Andersen, R. Bro, Practical aspects of PARAFAC modeling of fluorescence excitation-emission data, J. Chemom. 17 (2003) 200–215, https://doi.org/10.1002/cem.790.

[28] Å. Rinnan, C.M. Andersen, Handling of first-order Rayleigh scatter in PARAFAC modelling of fluorescence excitation–emission data, Chemom. Intell. Lab. Syst. 76 (2005) 91–99, https://doi.org/10.1016/j.chemolab.2004.09.009.

[29] A.C. Olivieri, H.-L. Wu, R.-Q. Yu, MVC2: a MATLAB graphical interface toolbox for second-order multivariate calibration, Chemom. Intell. Lab. Syst. 96 (2009) 246–251, https://doi.org/10.1016/j.chemolab.2009.02.005.

[30] A.C. Olivieri, H.-L. Wu, R.-Q. Yu, MVC3: a MATLAB graphical interface toolbox for third-order multivariate calibration, Chemom. Intell. Lab. Syst. 116 (2012) 9–16, https://doi.org/10.1016/j.chemolab.2012.03.018.

[31] S.J. Mazivila, S.A. Bortolato, A.C. Olivieri, MVC3_GUI: a MATLAB graphical user interface for third-order multivariate calibration. An upgrade including new multi-way models, Chemom. Intell. Lab. Syst. 173 (2018) 21–29, https://doi.org/10.1016/j.chemolab.2017.12.012.

[32] E.K. Kemsley, A genetic algorithm (GA) approach to the calculation of canonical variates (CVs), TrAC, Trends Anal. Chem. 17 (1998) 24–34, https://doi.org/10.1016/S0165-9936(97)00085-X.

[33] L.A. Berrueta, R.M. Alonso-Salces, K. Héberger, Supervised pattern recognition in food analysis, J. Chromatogr. A 1158 (2007) 196–214, https://doi.org/10.1016/j.chroma.2007.05.024.

[34] M. Barker, W. Rayens, Partial least squares for discrimination, J. Chemom. 17 (2003) 166–173, https://doi.org/10.1002/cem.785.

[35] A. Muñoz de la Peña, N. Mujumdar, E.C. Heider, H.C. Goicoechea, D. Muñoz de la Peña, A.D. Campiglia, Nondestructive total excitation–emission fluorescence microscopy combined with multi-way chemometric analysis for visually indistinguishable single fiber discrimination, Anal. Chem. 88 (2016) 2967–2975, https://doi.org/10.1021/acs.analchem.6b00264.

[36] M.R. de Almeida, D.N. Correa, W.F.C. Rocha, F.J.O. Scafi, R.J. Poppi, Discrimination between authentic and counterfeit banknotes using Raman spectroscopy and PLS-DA with uncertainty estimation, Microchem. J. 109 (2013) 170–177, https://doi.org/10.1016/j.microc.2012.03.006.

[37] D. Airado-Rodríguez, I. Durán-Merás, T. Galeano-Díaz, J.P. Wold, Front-face fluorescence spectroscopy: a new tool for control in the wine industry, J. Food Compos. Anal. 24 (2011) 257–264, https://doi.org/10.1016/j.jfca.2010.10.005.

[38] C. Schueuermann, P. Silcock, P. Bremer, Front-face fluorescence spectroscopy in combination with parallel factor analysis for profiling of clonal and vineyard site differences in commercially produced Pinot Noir grape juices and wines, J. Food Compos. Anal. 66 (2018) 30–38, https://doi.org/10.1016/j.jfca.2017.11.005.

[39] S. Belviso, F. Torchio, V. Novello, S. Giacosa, L. de Palma, S.R. Segade, V. Gerbi, L. Rolle, Modeling of the evolution of phenolic compounds in berries of "Italia" table grape cultivar using response surface methodology, J. Food Compos. Anal. 62 (2017) 14–22, https://doi.org/10.1016/j.jfca.2017.04.006.

[40] J.A. Kennedy, M.A. Matthews, A.L. Waterhouse, Effect of maturity and vine water status on grape skin and wine flavonoids, Am. J. Enol. Vitic. 53 (2002) 268–274.

[41] É. Dufour, A. Letort, A. Laguet, A. Lebecque, J.N. Serra, Investigation of variety, typicality and vintage of French and German wines using front-face fluorescence spectroscopy, Anal. Chim. Acta 563 (2006) 292–299, https://doi.org/10.1016/j.aca.2005.11.005.

[42] A. Versari, G.P. Parpinello, G.B. Tornielli, R. Ferrarini, C. Giulivo, Stilbene compounds and stilbene synthase expression during ripening, wilting, and UV Treatment in grape cv. Corvina, J. Agric. Food Chem. 49 (2001) 5531–5536, https://doi.org/10.1021/jf010672o.

[43] P. Gatto, U. Vrhovsek, J. Muth, C. Segala, C. Romualdi, P. Fontana, D. Pruefer, M. Stefanini, C. Moser, F. Mattivi, R. Velasco, Ripening and genotype control stilbene accumulation in healthy grapes, J. Agric. Food Chem. 56 (2008) 11773–11785, https://doi.org/10.1021/jf8017707.

[44] R. Bro, H.A.L. Kiers, A new efficient method for determining the number of components in PARAFAC models, J. Chemom. 17 (2003) 274–286, https://doi.org/10.1002/cem.801.

[45] A. Muñoz de la Peña, A. Espinosa Mansilla, D. González Gómez, A.C. Olivieri,

H.C. Goicoechea, Interference-free analysis using three-way fluorescence data and the parallel factor model. determination of fluoroquinolone antibiotics in human serum, Anal. Chem. 75 (2003) 2640–2646, https://doi.org/10.1021/ac026360h.
[46] M. Siotani, Tolerance regions for a multivariate normal population, Ann. Inst. Stat. Math. 16 (1964) 135–153.
[47] D.M. Haaland, E.V. Thomas, Partial least-squares methods for spectral analyses. 1. Relation to other quantitative calibration methods and the extraction of qualitative information, Anal. Chem. 60 (1988) 1193–1202, https://doi.org/10.1021/ac00162a020.
[48] H. Xiao, A. Li, M. Li, Y. Sun, K. Tu, S. Wang, L. Pan, Quality assessment and discrimination of intact white and red grapes from Vitis vinifera L. at five ripening stages by visible and near-infrared spectroscopy, Sci. Hortic. 233 (2018) 99–107, https://doi.org/10.1016/j.scienta.2018.01.041.
[49] J. Nogales-Bueno, J.M. Hernández-Hierro, F.J. Rodríguez-Pulido, F.J. Heredia, Determination of technological maturity of grapes and total phenolic compounds of grape skins in red and white cultivars during ripening by near infrared hyperspectral image: a preliminary approach, Food Chem. 152 (2014) 586–591, https://doi.org/10.1016/j.foodchem.2013.12.030.
[50] J. Christensen, L. Nørgaard, R. Bro, S.B. Engelsen, Jakob Christensen, Lars Nørgaard, A. Rasmus Bro, S.B. Engelsen, Multivariate autofluorescence of intact food systems, Chem. Rev. 106 (2006) 1979–1994, https://doi.org/10.1021/cr050019q.
[51] G.M. Escandar, H.C. Goicoechea, A. Muñoz de la Peña, A.C. Olivieri, Second- and higher-order data generation and calibration: a tutorial, Anal. Chim. Acta 806 (2014) 8–26, https://doi.org/10.1016/j.aca.2013.11.009.
[52] C. Kang, H.L. Wu, L.X. Xie, S.X. Xiang, R.Q. Yu, Direct quantitative analysis of aromatic amino acids in human plasma by four-way calibration using intrinsic fluorescence: exploration of third-order advantages, Talanta 122 (2014) 293–301, https://doi.org/10.1016/j.talanta.2014.01.036.

# ARTÍCULO 4

# Evolution of polyphenols content in plum fruits (Prunus salicina) with harvesting time by second-order excitation-emission fluorescence multivariate calibration

Manuel Cabrera-Bañegil, Nieves Lavado Rodas, María Henar Prieto Losada, Fernando Blanco Cipollone, María José Moñino Espino, Arsenio Muñoz de la Peña, Isabel Durán-Merás

*Microchemical Journal,* ***2020****, 158, 105299*
*DOI: https://doi.org/10.1016/j.microc.2020.105299*

Microchemical Journal 158 (2020) 105299

Contents lists available at ScienceDirect

Microchemical Journal

journal homepage: www.elsevier.com/locate/microc

# Evolution of polyphenols content in plum fruits (*Prunus salicina*) with harvesting time by second-order excitation-emission fluorescence multivariate calibration

Manuel Cabrera-Bañegil[a,*], Nieves Lavado Rodas[b], María Henar Prieto Losada[b], Fernando Blanco Cipollone[b], María José Moñino Espino[b], Arsenio Muñoz de la Peña[a], Isabel Durán-Merás[a]

[a] Department of Analytical Chemistry, Faculty of Sciences, University of Extremadura, Avda de Elvas s/n, 06006 Badajoz, Spain
[b] CICYTEX, Junta of Extremadura, Finca La Orden, Guadajira, Badajoz, Spain

ARTICLE INFO

*Keywords:*
Japanese plum
Chlorogenic acid
Neochlorogenic acid
Polyphenols
Quantification

ABSTRACT

Phenolic extracts from pulp and skin of Japanese plums Angeleno variety, sampled in May and September harvest, were analysed by excitation-emission fluorescence spectroscopy. The exploratory analysis of fluorescence second-order multivariate data was carried out by parallel factor analysis (PARAFAC) and catechin, epicatechin, procyanidin B2, chlorogenic acid and neochlorogenic acid were identified, by comparison of the corresponding PARAFAC loading profiles with their fluorescence spectra. In addition, a central composite design was employed for the determination of catechin, epicatechin, gallic acid, procyanidin B2, caffeic acid, neochlorogenic acid and chlorogenic acid concentrations in plum samples. In the validation set good recoveries were obtained for all analytes except for gallic and caffeic acids. The results obtained in the quantification of these compounds in plum samples were compared with the analysis by HPLC and the results showed that the levels of catechin plus epicatechin and of chlorogenic plus neochlorogenic acids decreased from May to September and these concentrations were higher in the skin than in the pulp. Furthermore, noticeable differences in the number of components were obtained depending on the maturation stage of plums, according to studies in both skin and pulp, separately.

## 1. Introduction

The high degree of appreciation of plums among consumers has promoted it worldwide as one of the most important fruits. Plum fruits are, from a nutritive and dietary point of view, a valuable component of the human diet due to its content in bioactive compounds. A considerable volume of studies indicated that increased fruit consumption, due to high polyphenols content, among other nutrients, is beneficial to human health [1,2]. In Extremadura region, located in the south-west of Spain, plum cultivars have high economic and social importance. Recently, a plum quality mark has been created in this region as a previous step for the creation of Protected Geographical Indication (PGI).

The content of phenolic components contained in fruits is of valuable interest for a number of reasons: 1) There is a correlation between taste (astringency, bitterness) and content of phenolic compounds [3]. 2) Phenolic compounds seem to play an important role in the fruits natural defence mechanisms [4]. 3) Increasing interest in the health benefits of fruits and fruit products is associated with the content of different groups of phenolic compounds with antioxidant effects [5].

On many occasions, it has been reported that plums are a rich source of phenolic compounds, such as chlorogenic acids, proanthocyanidins, flavonoids, and anthocyanins. Phenolic compounds such as chlorogenic and neochlorogenic acids, as well as anthocyanins, are the mayor polyphenols found in plums [6,7]. The concentration and distribution of polyphenols and their antioxidant activity in plums differ based on the cultivar, growing period, soil nutrient content, environmental conditions of horticultural practices, fruit ripening and preharvest and post-harvest practices [6].

In this context, the ever growing concerns of consumers towards the health and safety attributes of foods emphasized the role of agronomic practices as one of the main determinants of food quality. The ripening process in fruit is considered a fundamental factor affecting the biosynthesis of phytochemicals. Both, the total phenolic content and total

* Corresponding author.
*E-mail address:* manuelcb@unex.es (M. Cabrera-Bañegil).

https://doi.org/10.1016/j.microc.2020.105299
Received 13 June 2020; Received in revised form 14 July 2020; Accepted 14 July 2020
Available online 17 July 2020

flavonoid content, have been indicated to decrease during development [8].

Investigations on types of cultivars and their respective effects on different factors, such as fruit weight, firmness, soluble solids, total sugar content, organic acids, phenolics and anthocyanins, are considered to be very important from a quality point of view, as they influence the ripening process [9].

Traditionally, the polyphenolic compounds of plums have been studied using total phenol determination methods for characterization of plum varieties. In this way, the common parameters analysed in a wide range of plum cultivars have been the total phenolic, individual anthocyanin and total sugar content [10]. However, this traditional method offered a partial information about polyphenolics content. Nowadays, individual phenolic concentrations in plum samples have been determined using liquid chromatography (LC) with diode array and mass spectrometry detectors [11]. In this sense, LC-MS has been used to detect and characterize the phenolic compounds in several plum varieties [7].

Powerful methods have been developed using multivariate analysis of the data provided by different analytical methodologies. Visible/near infrared (Vis/NIR) spectroscopy has been used as a non-destructive method to predict quality parameters such as soluble solids content, titratable acidity, pH, firmness, sugar-acid ratio and flesh colour in "Friar" plum [12], and colour, firmness and soluble solids content in "Victoria" and "Majoriés Seedling" plums [13]. Synchronous fluorescence, UV–Vis and near infrared (NIR) spectroscopy, coupled with chemometric methods, have already been used to discriminate samples of high quality plum brandies of different varietal origins [14].

The aim of this study is to show the feasibility of the intrinsic fluorescence of methanolic extracts of skin and pulp of plums, combined with second-order multivariate data analysis, for the simultaneous quantification of the main fluorescence phenolic compounds in plums. This study allows to follow the evolution of the contents of these compounds in two stages of the production and, particularly, the quantification of the main polyphenols using Parallel Factor Analysis (PARAFAC) and Unfolded-Partial Least Squares (U-PLS) algorithms for calibration. The obtained results were validated by HPLC.

## 2. Materials and methods

### 2.1. Reagents, solvents and phenolic standards

Catechin, epicatechin, gallic acid and neochlorogenic acid were purchased from Sigma Aldrich Chemie (Steinheim, Germany), chlorogenic acid was supplied from Fisher Scientific, and procyanidin B2 was supplied from Extrasynthése (Genay, France). Methanol (Panreac, Barcelona, Spain) was used for phenol extraction and for preparing the calibration samples. Ultrapure water was obtained from a Milli-Q water system (Millipore S.A.S., Molsheim, France).

HPLC grade acetonitrile was supplied by Fisher chemical (Loughboruough, UK) and P.A. grade formic acid was purchased from PANREAC (Barcelona, Spain).

### 2.2. Plant material

The study was carried out on an experimental plot located in the "Vegas Bajas del Guadiana" region (Badajoz, Spain) at an altitude of 184 m. The orchard was planted in 2005 with late-maturing Japanese Angeleno plum trees. The arrangement of the trees was in rows in a 6 × 4 m plantation frame, east-west oriented. Eight plum samples from two trees were taken in May and in September.

### 2.3. Extraction of phenolic compounds

Plum samples were transported refrigerated to the laboratory and the different fruit parts were separated by hand to obtain the skin (outer epidermis) and pulp. Each fruit part was frozen by liquid nitrogen and was lyophilized and powdered. Then, 0.05 g of lyophilized sample were weighed and extracted with 10 mL of extracting solution, composed by methanol:water:formic acid (50:49:1), using an ultrasonic bath during 14 min. The extracts were centrifuged during 10 min at 10000 rpm at 4 °C. The supernatant was diluted 1/100 with methanol and was analysed by fluorescence spectroscopy and by HPLC with fluorescence detection, filtering previously through a 0.2 μm nylon syringe filter.

### 2.4. Liquid chromatography analysis

The chromatographic studies were performed on an Agilent 1260 Infinity High Performance Liquid Chromatograph (Agilent Technologies, CA, USA), equipped with an online degasser, quaternary pump (G1311B), column oven compartment (G7116A) and fast scanning fluorescence detector (FSFD) (G1328C). The equipment also has a high speed pump (G7120A) and a binary pump (G7120A) for use in two-dimensional chromatography mode. OpenLAB LC ChemStation software version A.01.04 was used to control the instrument and for data acquisition and data analysis. A Teknokroma Tracer Excel 120 ODS-A column (150 mm × 4.6 mm and 5 μm particle size) was used. The optimal mobile phase was composed of 0.5% (v/v) formic acid in water (A) and pure acetonitrile (B), operating under gradient elution. The gradient program was used as follows: 10% of acetonitrile (eluent B) and 90% of 0.5% (v/v) formic acid in water was held for 20 min. Between 20 and 45 min the percentage of eluent B increases from 10 up to 30% and between 45 min and 46 min the percentage of eluent B increases from 30 up to 100% and the formic acid content decreased in correspondence. These conditions were maintained until 53 min and, finally, the eluent B content was decreased to the initial conditions (10% B), and the column was re-equilibrated for 5 min. A constant flow-rate of 0.5 mL $min^{-1}$ was applied during the whole process. The injection volume was 20 μL using an autosampler. The eluated was fluorimetrically monitored at excitation/emission wavelengths of 270/350 nm, for catechin, epicatechin, procyanidin B2 and gallic acid, and at 320/430 nm for chlorogenic acid, neochlorogenic acid and caffeic acid. The quantification of phenolic compounds was carried out by standard addition calibration.

### 2.5. Fluorescence method and instrumental

Excitation-emission matrices (EEMs) were recorded by using a Fluorescence Spectrophotometer Varian Model Cary Elipse (Agilent Technologies, Madrid, Spain). Measurements were made with a 10-mm quartz cell at room temperature. The slits of excitation and emission monochromators were set at 5 and 5 nm, respectively, and the scan rate was 300 nm $min^{-1}$. EEMs were collected as a set of emission spectra, corresponding to the methanolic extracts of the skin and of the pulp of plums. The EEMs were recorded in the emission range 280–500 nm, each 1 nm, and in the excitation range 240 to 380 nm, each 5 nm.

### 2.6. Chemometric treatment

All calculations were carried out in Matlab (Matlab R2019b). Routines for PARAFAC were available on the internet thanks to Bro (http://www.models.kvl.dk/source/). MVC2, a useful Matlab graphic interface (http://www.iquir-conicet.gov.ar/descargas/mvc2.rar), was used for PARAFAC and U-PLS analysis [15,16].

## 3. Results and discussion

### 3.1. Excitation-emission matrices of plum phenolic extracts

The presence of fluorescence compounds in plums, mainly due to phenolic compounds, allows the use of fluorescence techniques for its characterization. The purpose of this study was using the

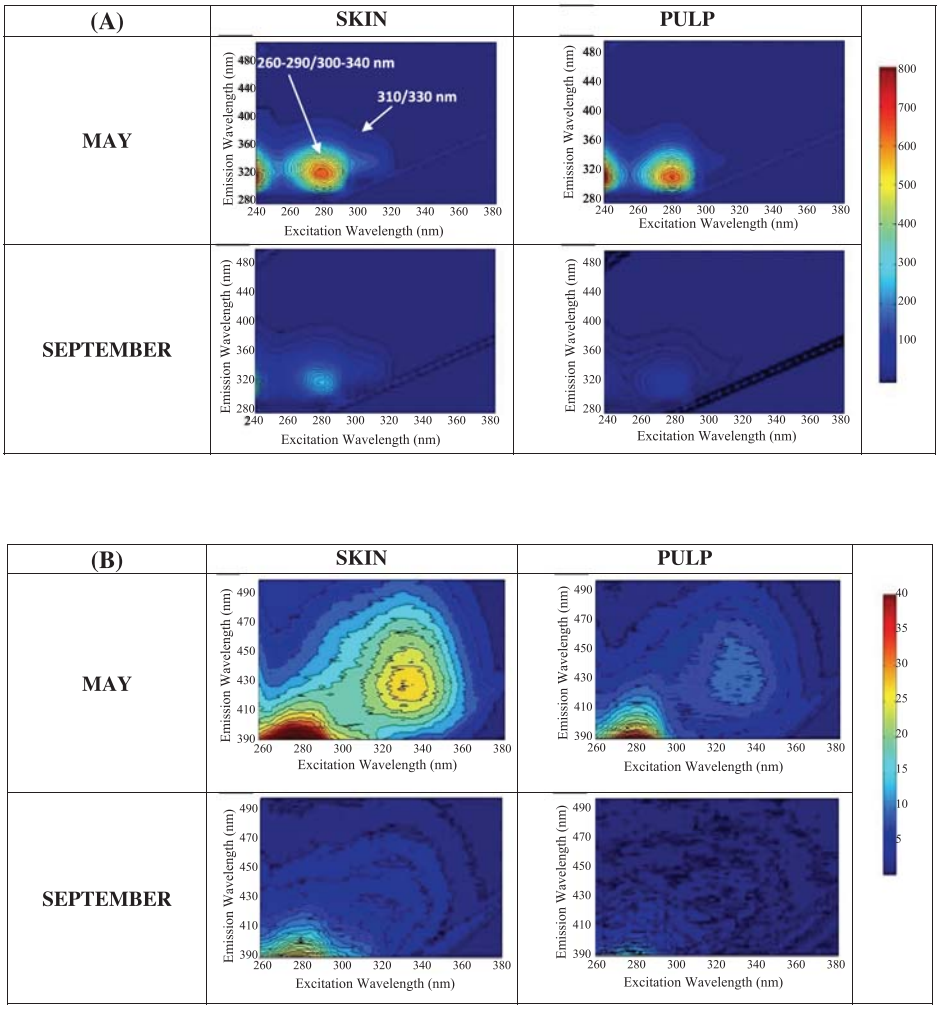


**Fig. 1.** Contour plots of EEMs recorded from methanolic extracts of skin and pulp plums harvested in May and in September. A) EEMs corresponding to excitation and emission wavelength ranges, excitation 240–380 nm and emission 280–500 nm; B) Restricted wavelength range: excitation 260–380 nm and emission 390–500 nm.

autofluorescence of methanolic extracts from the skin and from the pulp of plums to follow the evolution of these compounds in two stages of the production.

With the object of obtaining a complete fluorescence information of the samples, excitation-emission matrices, EEMs, from skin and from the pulp of plums were recorded. Fig. 1 shows the EEMs, as contour maps, of the methanolic extracts of two different plum samples, corresponding to two stages of production. It can be observed that, independently of the part of the plum, two main fluorescence emission regions can be distinguished: one of them highly fluorescent with emission at about 300–340 nm and excitation between 260 and 290 nm. Fig. 1A; and the second one with low fluorescence, over an emission range about 410–450 nm and excitation between 310 and 350 nm in skin plum samples Fig. 1B. The fluorescence intensity of these regions is clearly influenced by the date of sampling, since the plum samples harvested in May present higher fluorescence than the plum samples harvested in September. This is in accordance with other researchers concluding that the phenolic compounds content is higher in unripe fruits and decreased with the ripening [17]. In addition to this, differences in the EEMs physiognomy have been observed between the EEMs of skin and pulp plums. Thus, in the EEMs of the skin it is detectable a fluorescence signal, as a shoulder, at 310/330 nm excitation/emission wavelengths, Fig. 1A, and this signal is not observable in the pulp samples.

Along the maturation process, the fluorescence decreases in both, skin and pulp. Hence, the fluorescence emission between 400 and 500 nm, exciting at 340 nm (Fig. 1B), practically disappears when the plum samples are harvested in September. This region has already been detected in plum spirit, whose excitation/emission fluorescence maxima were at 340 and 425 nm, respectively [18]. According to the literature, chlorogenic acid is one of most abundant chemical compounds in plums [7] and this compound showed a characteristic band at excitation wavelength of 355–365 nm and emission wavelength of 445 nm.

### 3.2. PARAFAC analysis of plum samples. Identification of the compounds

In order to obtain more information about the EEMs of the plums, a set of 32 EEMs samples, corresponding to 8 plum samples harvested in May and 8 plum samples harvested in September, both of them in duplicate, were built, and the decomposition was carried out by PARAFAC. In first place, we tried to analyse the entire spectral region, but due to the low intensity signal of the second region, chlorogenic and neochlorogenic acids cannot be determined in presence of the high fluorescent signal of catechins. For this reason, the spectral region has been divided into two regions during analysis, and independent analysis were carried out with the skin and with the pulp of the plums. Excitation wavelengths from 240 to 290 nm and emission wavelengths from 300 to 460 nm, for the first spectral region, and excitation wavelengths between 250 and 355 nm and emission wavelengths between 360 and 480 nm, for the second spectral region, were selected. These data were arranged in two 3D arrays with dimensions 32 × 161 × 11 (samples × emission × excitation), for the first spectral region, and 32 × 121 × 22 (samples × emission × excitation), for the second spectral region. For both spectral regions, the number of components was estimated using the core consistency criterion (CORCONDIA) [19]. The optimal number of component was four for the first spectral region and five for the second spectral region, both for the analysis of the skin and the pulp of the plum samples. Fig. 2 shows the loading PARAFAC profiles for the first spectral region (Fig. 2A) and for the second spectral region (Fig. 2B). The loading profiles were compared with the fluorescence spectra for standards of the analytes, Fig. 3.

In the first spectral region, the first and second components show an excitation maximum at 280 nm and emission maxima at 315 nm the first component and at 318 nm the second component. According to the excitation and emission wavelengths of the loading profiles for the first component, a comparison of these profiles with the fluorescence spectra for standards of catechin and epicatechin, indicates that the excitation and emission maxima are very similar (Pearson regression coefficients, 95% confidence level, of 0.957 and 1.000, and 0.963 and 0.998 for emission and excitation, and for epicatechin and catechin, respectively). The correlation coefficients for the excitation and emission profiles of the second component, regarding the reference spectra of procyanidin B2, Fig. 3B, were calculated as 0.996 and 0.999 respectively. The third and fourth components showed a fluorescence excitation/emission maxima at 275/336 nm and 250/340 nm, respectively. Neither of them were assigned to the available chemical standards.

In the second spectral region, despite obtaining five components in

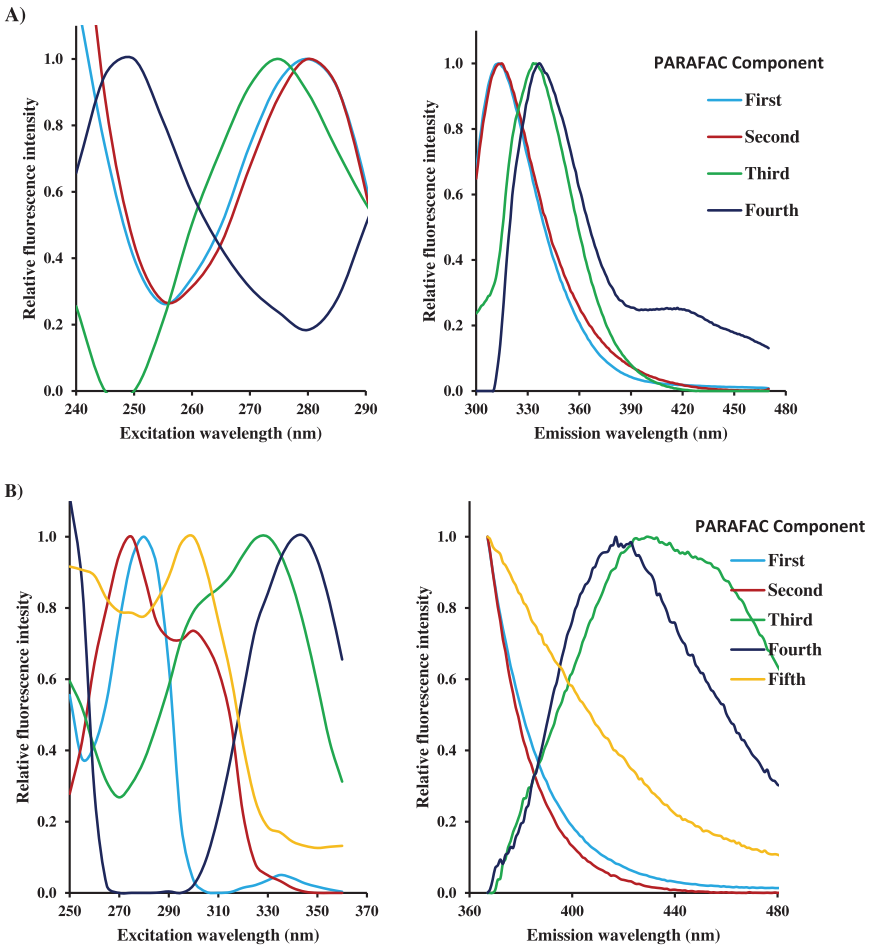


**Fig. 2.** Excitation and emission loading PARAFAC profiles of a set of pulp plum samples for the first spectral region (A) and second spectral region (B).

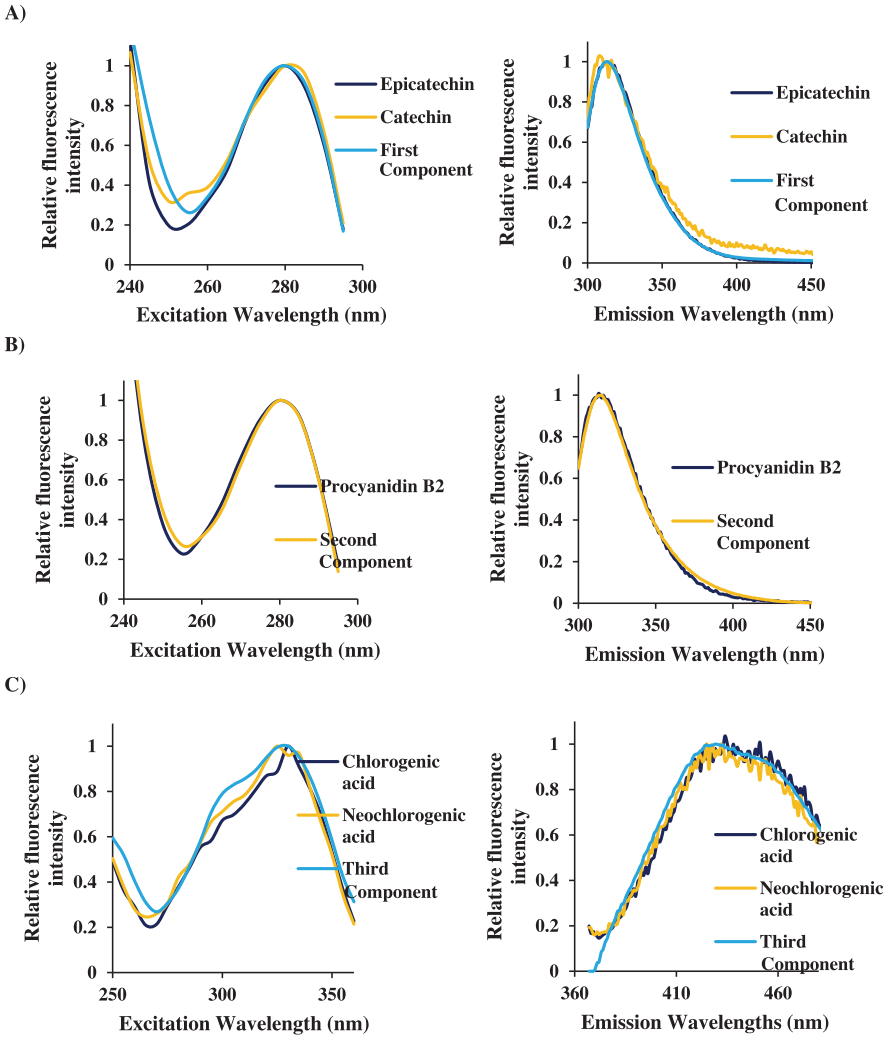


**Fig. 3.** A) Excitation and emission PARAFAC profiles of the first component of the samples set for the first spectral region, and normalized excitation and emission spectra of catechin and epicatechin. B) Excitation and emission PARAFAC profiles of the second component of the samples set for the first region, and normalized excitation and emission spectra of procyanidin B2. C) Excitation and emission PARAFAC profiles of the third component of the samples set for the second spectral region and normalized excitation and emission spectra of chlorogenic acid and neochlorogenic acid.

the emission profiles, only components 3 and 4 were well defined. The third component showed a fluorescent emission maximum at 431 nm, with a shoulder at 457 nm, and an excitation maximum at 325 nm, with a shoulder at 302 nm. Fig. 3C shows the excitation and emission profiles of this component that match with chlorogenic and neochlorogenic acids fluorescence spectra (Pearson regression coefficients, 95% confidence level, of 0.983 and 0.980, and 0.983 and 0.988 for emission and excitation, and for chlorogenic and neochlorogenic acids, respectively). Usually, researchers found these compounds in relatively high concentration in plums [20]. The fourth component had fluorescence excitation/emission wavelengths at 342/417 nm.

Independent spectral sets were decomposed in order to see the differences in loading profiles according to maturation. In the first spectral region, four components were considered when the total set of samples were used. However, when the set of samples of May and September were analysed separately, the decomposition of samples harvested in September needed a lower number of components, and only three were necessary to explain the model.

### 3.3. Quantification of phenolic compounds in plum samples

#### 3.3.1. Calibration set with phenolic standard compounds

With the aim to quantify the main phenolic compounds present in the plums, such as catechin, epicatechin, procyanidin B2, chlorogenic acid and neochlorogenic acid, and other typical phenolic acids, such as caffeic acid and gallic acid, the analysis was first performed with synthetic samples, using pure methanol as solvent.

In first place, a calibration model constituted by all of them was prepared. An experimental central composite design was applied and 24 calibration samples were prepared in methanol. In addition to this,

**Table 1**
Recoveries and statistical parameters applying PARAFAC and U-PLS in the analysis of the validation set.

| | | PARAFAC | | U-PLS | | | | PARAFAC | | U-PLS | |
|---|---|---|---|---|---|---|---|---|---|---|---|
| | Actual | Predicted | Recovery (%) | Predicted | Recovery (%) | | Actual | Predicted | Recovery (%) | Predicted | Recovery (%) |
| Catechin plus epicatechin | 0.34 | 0.34 | 100.0 | 0.41 | 120.6 | Procyanidin B2 | 1.00 | 0.95 | 95.0 | 0.97 | 97.0 |
| | 1.13 | 1.20 | 106.2 | 1.18 | 104.4 | | 1.00 | 0.94 | 94.0 | 1.01 | 101.0 |
| | 2.08 | 2.13 | 102.4 | 2.09 | 100.5 | | 2.01 | 2.04 | 101.5 | 2.14 | 106.5 |
| | 2.25 | 2.22 | 98.7 | 2.25 | 100.0 | | 2.01 | 2.01 | 100.0 | 2.11 | 105.0 |
| | [a]Rec ± SD | 102 ± 3 | | 106 ± 9 | | | Rec ± SD | 98 ± 4 | | 102 ± 4 | |
| | [b]RMSEP | 0.046 | | 0.043 | | | RMSEP | 0.042 | | 0.084 | |
| | [c]REP (%) | 3.1 | | 3.0 | | | REP (%) | 2.8 | | 5.4 | |
| | $R^2$ | 0.997 | | 1.000 | | | $R^2$ | 1.000 | | 0.999 | |
| | | PARAFAC | | U-PLS | | | | PARAFAC | | U-PLS | |
| | Actual | Predicted | Recovery (%) | Predicted | Recovery (%) | | Actual | Predicted | Recovery (%) | Predicted | Recovery (%) |
| Gallic acid | 0.63 | 0.55 | 87.3 | 0.54 | 85.7 | Chlorogenic acid plus neochlorogenic acid | 4.14 | 4.04 | 97.6 | 4.06 | 98.1 |
| | 0.63 | 0.55 | 87.3 | 0.54 | 85.7 | | 2.07 | 1.75 | 84.5 | 2.12 | 102.4 |
| | 0.50 | 0.40 | 80.0 | 0.39 | 78.0 | | 1.52 | 1.33 | 87.5 | 1.56 | 102.6 |
| | 0.32 | 0.30 | 93.8 | 0.32 | 100.0 | | 3.04 | 3.05 | 100.3 | 3.06 | 100.7 |
| | Rec ± SD | 87 ± 6 | | 87 ± 9 | | | Rec ± SD | 92 ± 8 | | 101 ± 2 | |
| | RMSEP | 0.076 | | 0.084 | | | RMSEP | 0.192 | | 0.052 | |
| | REP (%) | 17 | | 19 | | | REP (%) | 7.6 | | 2.0 | |
| | $R^2$ | 0.966 | | 0.932 | | | $R^2$ | 0.992 | | 0.999 | |

[a]Rec: average recovery.

[b]RMSEP: root mean square error prediction= $\sqrt{\frac{\sum_{i=1}(y_i-\hat{y}_i)^2}{N}}$, $\bar{y}$ = actual concentration, $\hat{y}_i$ = predicted concentration, N = number of samples in the test set.

cREP: relative error of prediction = $\frac{100}{\bar{y}}\sqrt{\frac{\sum_{i=1}(y_i-\hat{y}_i)^2}{N}}$, $\bar{y}$ = is the mean of the added concentration in the prediction set.

**Table 2**
Predictions of catechin plus epicatechin, procyanidin B2, chlorogenic and neochlorogenic acid, gallic acid and caffeic acid concentration by PARAFAC and U-PLS. Validation of the results by LC.

| Compounds | Methods | Skin (μg $mL^{-1}$) | | Pulp (μg $mL^{-1}$) | |
|---|---|---|---|---|---|
| | | May | September | May | September |
| Catechin plus epicatechin | PARAFAC | 2.87 | 0.82 | 1.70 | 0.13 |
| | U-PLS/RBL* | 1.91 | 0.75 | 1.48 | 0.17 |
| | LC | 2.20 | 0.71 | 2.04 | 0.25 |
| Procyanidin B2 | PARAFAC | 0.42 | 0.66 | 1.03 | 0.41 |
| | LC | 0.79 | 0.18 | 0.76 | 0.04 |
| Chlorogenic acid plus neochlorogenic acid | PARAFAC | 0.52 | 0.10 | 0.43 | 0.09 |
| | U-PLS/RBL** | 1.09 | 0.08 | 0.75 | 0.42 |
| | LC | 1.01 | 0.10 | 0.79 | 0.41 |
| Gallic acid | PARAFAC | n.d. | n.d. | n.d. | n.d. |
| | U-PLS/RBL | n.d. | n.d. | n.d. | n.d. |
| | LC | n.d. | n.d. | n.d. | n.d. |
| Caffeic acid | PARAFAC | n.d. | n.d. | n.d. | n.d. |
| | U-PLS/RBL | n.d. | n.d. | n.d. | n.d. |
| | LC | n.d. | n.d. | n.d. | n.d. |

*RBL 1.
**RBL 2.

seven additional samples with each one of the analytes were included in the design (complementary material). The concentration ranges were: 0.28 to 2.76 mg/L for caffeic acid; 0.17 to 0.34 mg/L for catechin; 0.96 to 5.73 mg/L for epicatechin; 1.10 to 2.75 mg/L for chlorogenic acid; 0.97 to 1.94 mg/L for neochlorogenic acid; 1.00 to 4.02 mg/L for procyanidin B2, and 0.31 to 0.63 mg/L for gallic acid. Also, a validation set of four randomized samples was prepared in the same way as calibration samples. In all cases, EEMs were recorded and independently analysed in the two spectral regions. With both algorithms, in first place, the calibration samples were processed and the optimum number of components for each one was obtained.

Applying the PARAFAC algorithm, with non-negative constraint for the three ways, the optimum number of components was calculated with the CORCONDIA criterion and 4 factors for the first spectral region, and 5 factors for the second spectral region were obtained. By U-PLS, cross-validation and the Haaland and Thomas criterion [21,22] were employed to choose the optimum number of factors, and 3 and 4 components respectively were selected for each spectral region.

The sum of catechin and epicatechin concentrations was correlated with the score values of the first PARAFAC component in the first spectral region ($R^2$ = 0.861). The fact that both compounds may be considered as a unique component is due to the high similarity of fluorescent spectra. The concentration of procyanidin B2 was correlated with the scores of the second component in the first spectral region ($R^2$ = 0.737). Although the fluorescent spectrum of procyanidin B2 was pretty similar to the catechin and epicatechin spectra, PARAFAC achieved an independent component for this compound. Gallic acid concentrations were correlated with the score values of the fourth PARAFAC component in the first spectral region ($R^2$ = 0.966). Note that correlation coefficient analysed by PARAFAC and U-PLS were 0.966 and 0.932, respectively. With these correlation coefficients, this model cannot accurately predict the concentration of gallic acid.

In the second spectral region, the sum of chlorogenic and neochlorogenic acids was correlated with the first PARAFAC component ($R^2$ = 0.845). In the same way that in the case of catechin and epicatechin, the spectra of chlorogenic and neochlorogenic acids showed high similarity and PARAFAC considered them as a single component. The caffeic acid concentrations were correlated with the scores of the fourth component ($R^2$ = 0.743). The highly noisy fluorescent signal in the second spectral region could explain the low regression coefficients found.

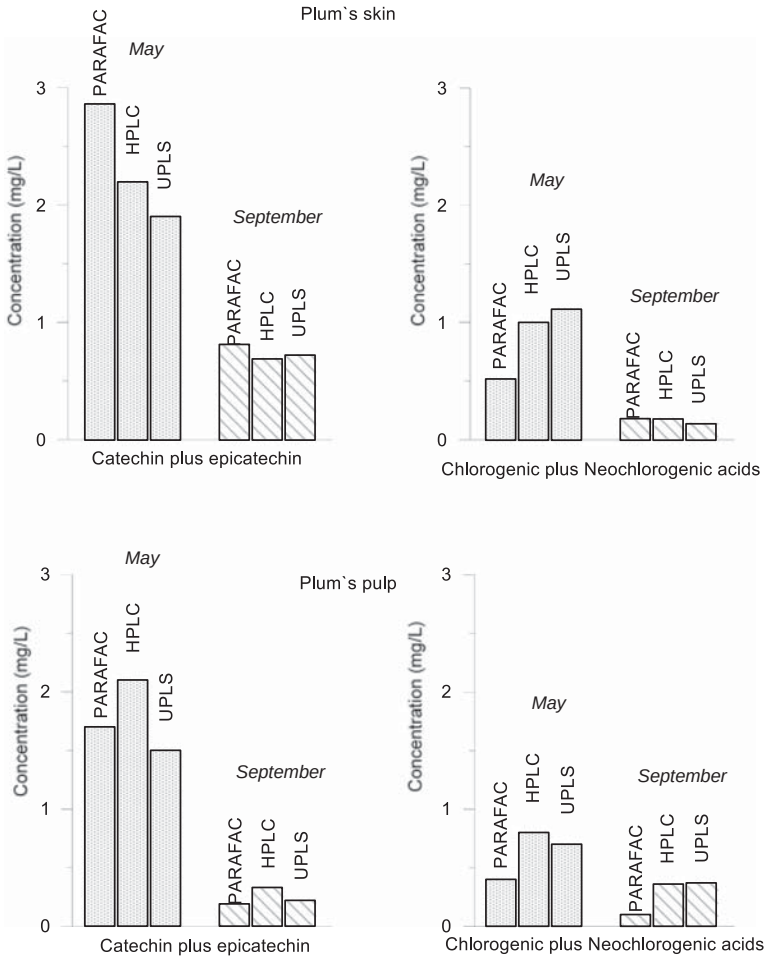


**Fig. 4.** Concentrations of catechin and epicatechin and chlorogenic and nechlorogenic acids in the pulp and in the skin of plums harvested in May and September.

*3.3.2. Validation of phenolic standard compounds*

Four validation samples were analysed by PARAFAC and U-PLS and the results are shown in the Table 1. Catechin plus epicatechin concentrations were correctly predicted by PARAFAC, with a mean recovery value of 101.8%. However, higher recoveries were found in the case of U-PLS (mean recovery value of 106.4%), particularly for the less concentrated sample (mean recovery value of 120.6%). Procyanidin B2 concentration was well predicted by PARAFAC and U-PLS. Similar media recoveries for procyanidin B2 were obtained by PARAFAC and U-PLS with values of 97.6 and of 102.4% respectively, but the REP values were lower by PARAFAC than U-PLS, with values of 2.8 and of 5.4, respectively. Gallic acid recoveries were very similar by PARAFAC and U-PLS, with values of 87.1 and of 87.4% respectively, and similar REP values were obtained, 17 and 19, respectively, as well. Chlorogenic acid plus neochlorogenic acid prediction was better by U-PLS than PARAFAC. Their media recovery values by PARAFAC and U-PLS were 92.5 and 100.9%, respectively. REP values of PARAFAC predictions were higher than U-PLS predictions with values of 7.6 and of 2.0, respectively.

*3.3.3. Phenolic quantification on plum samples*

Once validated the system, each of the analytes were analysed by PARAFAC and U-PLS in plum samples harvested in May or September. Furthermore, different parts of plum, such as skin and pulp plums, were considered in order to see the evolution of the phenolic compounds. All result predictions were compared with the phenolic concentrations obtained by HPLC.

The obtained results for all analytes are summarized in Table 2. As observed, gallic acid and caffeic acid were not detected in any part of the plums neither with HPLC and with any of the algorithms used.

The recoveries obtained with both algorithms and by HPLC for catechins and for chlorogenic acids are represented in Fig. 4. The concentrations of catechin plus epicatechin were concordant with both algorithms and with the values obtained by HPLC. Higher concentrations were found in the skin samples. Due to the maturation process, the catechin plus epicatechin concentration decreased from May to September in both, skin and pulp, plum samples. This tendency is in accordance with catechin and epicatechin quantification along maturation obtained in Natal plums. Both analyte concentrations decreased along maturation in Natal plums harvested in 2017 campaign [23]. Catechin concentration also decreased along maturation in President, Mirabolano and Shiro dry weight plum samples [24].

With respect to chlorogenic and neochlorogenic acids, better results were obtained with U-PLS and again, higher concentrations were found

in skin samples of May. Furthermore, residual bilinearization (RBL) was applied for improving the prediction [25]. In this way, a RBL value of two was applied for all plum samples harvested in May, and a RBL value of 1 for the skin plum samples harvested in September. The decreased of chlorogenic acid during maturation is in accordance with a previous research in Natal plums [23]. Also, neochlorogenic acid and chlorogenic acid concentrations decreased along maturation in President, Mirabolano and Shiro plum dry weight samples [24].

## 4. Conclusions

Based on excitation emission fluorescence matrices in combination with PARAFAC and U-PLS, the sum of catechin and epicatechin, sum of chlorogenic acid and neochlorogenic acid and procyanidin B2 were quantified in Angeleno plums, whose concentrations were comparable with those obtained by HPLC. In the case of catechin and epicatechin, the algorithms were not able to differentiate between both compounds, as concluded in previous studies. As a novelty, similar results were obtained in the present study with chlorogenic and neochlorogenic acids, due the similarities in the fluorescence spectra. In future work, the prediction model will be extended by incorporating more plum varieties as well as more maturation stages, with the purpose of obtaining enough data to help in making decisions about the proper date of harvesting.

## CRediT authorship contribution statement

**Manuel Cabrera-Bañegil:** Investigation, Data curation. **Nieves Lavado Rodas:** Resources, Data curation. **María Henar Prieto Losada:** Resources, Data curation. **Fernando Blanco Cipollone:** Data curation. **María José Moñino Espino:** Resources. **Arsenio Muñoz de la Peña:** Writing - review & editing. **Isabel Durán-Merás:** Formal analysis, Visualization, Writing - original draft.

## Declaration of Competing Interest

The authors declare that they have no known competing financial interests or personal relationships that could have appeared to influence the work reported in this paper.

## Acknowledgements

Manuel Cabrera-Bañegil thanks to Consejería de Economía e Infraestructuras of the Comunidad Autónoma de Extremadura funds for a FPI grant (PD16015), co-financed with the Fondo Social Europeo (FSE). Isabel Durán-Merás and Arsenio Muñoz de la Peña are grateful to Ministerio de Economía y Competitividad of Spain (Project CTQ2017-82496-P) and Gobierno de Extremadura (GR15090-Research Group FQM003), both cofinanced by the Fondo Social Europeo (FSE). Nieves Lavado Rodas, María Henar Prieto Losada, Fernando Blanco Cipollone and María José Moñino Espino are grateful to CCESAGROS financed by European Regional Development Fund (FEDER).

## Funding

This research did not receive any specific grant from funding agencies in the public, commercial, or not-for-profit sectors.

## References

[1] C.G. Fraga, K.D. Croft, D.O. Kennedy, F.A. Tomás-Barberán, The effects of polyphenols and other bioactives on human health, Food Funct. 10 (2019) 514–528, https://doi.org/10.1039/C8FO01997E.
[2] M.S. Swallah, H. Sun, R. Affoh, H. Fu, H. Yu, Antioxidant potential overviews of secondary metabolites (polyphenols) in fruits, Int. J. Food Sci. 2020 (2020) 9081686, https://doi.org/10.1155/2020/9081686.
[3] S. Soares, S. Kohl, S. Thalmann, N. Mateus, W. Meyerhof, V. De Freitas, Different phenolic compounds activate distinct human bitter taste receptors, J. Agric. Food Chem. 61 (2013) 1525–1533, https://doi.org/10.1021/jf304198k.
[4] S.E. Arici, E. Kafkas, S. Kaymak, N.K. Koc, Phenolic compounds of apple cultivars resistant or susceptible to Venturia inaequalis, Pharm. Biol. 52 (2014) 904–908, https://doi.org/10.3109/13880209.2013.872674.
[5] Q. Vuong, Utilisation of Bioactive Compounds from Agricultural and Food Waste, CRC Press, Boca Raton, FL, 2017.
[6] D.O. Kim, O. Kyoung Chun, Y. Jun Kim, H.-Y. Moon, C.Y. Lee, Quantification of polyphenolics and their antioxidant capacity in fresh plums, J. Agric. Food Chem. 51 (2003) 6509–6515, https://doi.org/10.1021/jf0343074.
[7] R. Jaiswal, H. Karaköse, S. Rühmann, K. Goldner, M. Neumüller, D. Treutter, N. Kuhnert, Identification of phenolic compounds in plum fruits (Prunus salicina L. and Prunus domestica L.) by high-performance liquid chromatography/tandem mass spectrometry and characterization of varieties by quantitative phenolic fingerprints, J. Agric. Food Chem. 61 (2013) 12020–12031, https://doi.org/10.1021/jf402288j.
[8] Q. Li, X.-X. Chang, H. Wang, C. Stephen Brennan, X.-B. Guo, Phytochemicals accumulation in sanhua plum (Prunus salicina L.) during fruit development and their potential use as antioxidants, J. Agric. Food Chem. 67 (2019) 2459–2466, https://doi.org/10.1021/acs.jafc.8b05087.
[9] V. Usenik, D. Kastelec, R. Veberič, F. Štampar, Quality changes during ripening of plums (Prunus domestica L.), Food Chem. 111 (2008) 830–836, https://doi.org/10.1016/j.foodchem.2008.04.057.
[10] S. Sahamishirazi, J. Moehring, W. Claupein, S. Graeff-Hoenninger, Quality assessment of 178 cultivars of plum regarding phenolic, anthocyanin and sugar content, Food Chem. 214 (2017) 694–701, https://doi.org/10.1016/j.foodchem.2016.07.070.
[11] R. Manzano Durán, J.E.F. Sánchez, B. Velardo-Micharet, M.J.R. Gómez, Multivariate optimization of ultrasound-assisted extraction for the determination of phenolic compounds in plums (Prunus salicina Lindl.) by high-performance liquid chromatography (HPLC), Instrum. Sci. Technol. 48 (2020) 113–127, https://doi.org/10.1080/10739149.2019.1662438.
[12] M. Li, W. Lv, R. Zhao, H. Guo, J. Liu, D. Han, Non-destructive assessment of quality parameters in 'Friar' plums during low temperature storage using visible/near infrared spectroscopy, Food Control. 73 (2017) 1334–1341, https://doi.org/10.1016/j.foodcont.2016.10.054.
[13] B. Li, M. Cobo-Medina, J. Lecourt, N.B. Harrison, R.J. Harrison, J.V. Cross, Application of hyperspectral imaging for nondestructive measurement of plum quality attributes, Postharvest Biol. Technol. 141 (2018) 8–15, https://doi.org/10.1016/j.postharvbio.2018.03.008.
[14] M. Jakubíková, J. Sádecká, A. Kleinová, On the use of the fluorescence, ultraviolet–visible and near infrared spectroscopy with chemometrics for the discrimination between plum brandies of different varietal origins, Food Chem. 239 (2018) 889–897, https://doi.org/10.1016/j.foodchem.2017.07.008.
[15] A.C. Olivieri, H.L. Wu, R.Q. Yu, MVC2: a MATLAB graphical interface toolbox for second-order multivariate calibration, Chemom. Intell. Lab. Syst. 96 (2009) 246–251, https://doi.org/10.1016/j.chemolab.2009.02.005.
[16] A.C. Olivieri, G.M. Escandar, Chapter 3 – Experimental Three-way/Second-order Data, in: A.C. Olivieri, G.M. Escandar (Eds.), Practical Three-Way Calibration, Elsevier, Boston, 2014, pp. 27–45. doi:10.1016/B978-0-12-410408-2.00003-x.
[17] H. Liu, W. Jiang, J. Cao, Y. Li, Changes in extractable and non-extractable polyphenols and their antioxidant properties during fruit on-tree ripening in five peach cultivars, Hortic. Plant J. 5 (2019) 137–144, https://doi.org/10.1016/j.hpj.2019.04.005.
[18] M. Tomková, J. Sádecká, K. Hrobovnová, Synchronous fluorescence spectroscopy for rapid classification of fruit spirits, Food Anal. Methods 8 (2015) 1258–1267, https://doi.org/10.1007/s12161-014-0010-9.
[19] R. Bro, H.A.L. Kiers, A new efficient method for determining the number of components in PARAFAC models, J. Chemom. 17 (2003) 274–286, https://doi.org/10.1002/cem.801.
[20] J. Tomić, F. Štampar, I. Glišić, J. Jakopič, Phytochemical assessment of plum (Prunus domestica L.) cultivars selected in Serbia, Food Chem. 299 (2019) 125113, , https://doi.org/10.1016/j.foodchem.2019.125113.
[21] D.M. Haaland, E.V. Thomas, Partial least-squares methods for spectral analyses. 1. Relation to other quantitative calibration methods and the extraction of qualitative information, Anal. Chem. 60 (1988) 1193–1202, https://doi.org/10.1021/ac00162a020.
[22] D.M. Haaland, E.V. Thomas, Partial least-squares methods for spectral analyses. 2. Application to simulated and glass spectral data, Anal. Chem. 60 (1988) 1202–1208, https://doi.org/10.1021/ac00162a021.
[23] A. Ndou, P.P. Tinyani, R.M. Slabbert, Y. Sultanbawa, D. Sivakumar, An integrated approach for harvesting Natal plum (Carissa macrocarpa) for quality and functional compounds related to maturity stages, Food Chem. 293 (2019) 499–510, https://doi.org/10.1016/j.foodchem.2019.04.102.
[24] S. Moscatello, T. Frioni, F. Blasi, S. Proietti, L. Pollini, G. Verducci, A. Rosati, R.P. Walker, A. Battistelli, L. Cossignani, F. Famiani, Changes in absolute contents of compounds affecting the taste and nutritional properties of the flesh of three plum species throughout development, Foods (Basel, Switzerland). 8 (2019) 486, https://doi.org/10.3390/foods8100486.
[25] D. Bohoyo Gil, A. Muñoz de la Peña, J.A. Arancibia, G.M. Escandar, A.C. Olivieri, Second-order advantage achieved by unfolded-partial least-squares/residual bilinearization modeling of excitation−emission fluorescence data presenting inner filter effects, Anal. Chem. 78 (2006) 8051–8058, https://doi.org/10.1021/ac061369v.

# ARTÍCULO 5

## First-order discrimination of methanolic extracts from plums according to harvesting date using fluorescence spectra. Quantification of polyphenols

Olga Monago Maraña, Manuel Cabrera-Bañegil, Nieves Lavado-Rodas, Arsenio Muñoz de la Peña, Isabel Durán-Merás

*Enviado a Microchemical Journal*

Microchemical Journal

# FIRST-ORDER DISCRIMINATION OF METHANOLIC EXTRACTS FROM PLUMS ACCORDING TO HARVESTING DATE USING FLUORESCENCE SPECTRA. QUANTIFICATION OF POLYPHENOLS

--Manuscript Draft--

| | |
|---|---|
| **Manuscript Number:** | |
| **Article Type:** | Research Paper |
| **Section/Category:** | Chemometrics |
| **Keywords:** | Fluorescence; PCA; PLS-DA; PLS; plums; polyphenols |
| **Corresponding Author:** | Olga Monago Maraña, Ph.D<br>Universidad Nacional de Educación a Distancia: Universidad Nacional de Educacion a Distancia<br>Madrid, SPAIN |
| **First Author:** | Olga Monago Maraña, Ph.D |
| **Order of Authors:** | Olga Monago Maraña, Ph.D |
| | Manuel Cabrera-Bañegil |
| | Nieves Lavado-Rodas |
| | Arsenio Muñoz De la Peña |
| | Isabel Durán-Merás |
| **Abstract:** | Fluorescence spectroscopy in combination with chemometric analysis was applied to discriminate between Japonese Angeleno variety of plums, according to the date of harvesting. Emission spectra of methanolic extracts of plums at two excitation wavelengths were obtained. The fluorescence spectral data were firstly processed by Principal Component Analysis (PCA), as an exploratory study, to extract relevant information from the spectral data, and revealed differentiation between plum samples based in the harvested time. In addition, Partial Least-Squares-Discriminant-Analysis (PLS-DA) was used for the development of the classification models, allowing 100% accuracy to differentiate between the date of harvesting, independently that pulp or skin plum extracts were analyzed. Spectral patterns of plums showed significant differences during maturation period, with a special emphasis between the months of May and September. In addition, calibration models were obtained for different individual polyphenols with partial least-squares (PLS) regression, obtaining the best results for epicatechin and neochlorogenic acid determination. |

# FIRST-ORDER DISCRIMINATION OF METHANOLIC EXTRACTS FROM PLUMS ACCORDING TO HARVESTING DATE USING FLUORESCENCE SPECTRA. QUANTIFICATION OF POLYPHENOLS

Olga Monago-Maraña[a*], Manuel Cabrera-Bañegil[b], Nieves Lavado Rodas[c], Arsenio Muñoz de la Peña[b,d], Isabel Durán-Merás[b,d]

[a]Department of Analytical Sciences, Faculty of Science, Avda. Esparta s/n, Crta. de Las Rozas-Madrid, 28232, Las Rozas, Madrid, National Distance Education University (UNED), Spain

[b]Department of Analytical Chemistry, Faculty of Sciences, University of Extremadura, Avda de Elvas S/N 06071 Badajoz, Spain.

[c]CIYTEX, Junta de Extremadura, Finca La Orden, Guadajira 06187, Badajoz, Spain

[d]Research Institute on Water, Climate Change and Sustainability (IACYS), University of Extremadura, Badajoz 06006, Spain

*corresponding author: olgamonago@ccia.uned.es

**Abstract**

Fluorescence spectroscopy in combination with chemometric analysis was applied to discriminate between Japonese Angeleno variety of plums, according to the date of harvesting. Emission spectra of methanolic extracts of plums at two excitation wavelengths were obtained. The fluorescence spectral data were firstly processed by Principal Component Analysis (PCA), as an exploratory study, to extract relevant information from the spectral data, and revealed differentiation between plum samples based in the harvested time. In addition, Partial Least-Squares-Discriminant-Analysis (PLS-DA) was used for the development of the classification models, allowing 100% accuracy to differentiate between the date of harvesting, independently that pulp or skin plum extracts were analyzed. Spectral patterns of plums showed significant differences during maturation period, with a special emphasis between the months of May and September. In addition, calibration models were obtained for different individual polyphenols with partial least-squares (PLS) regression, obtaining the best results for epicatechin and neochlorogenic acid determination.

**Keywords:** Fluorescence; Discriminant analysis; PCA; PLS-DA; PLS; plums; polyphenols

## 1. Introduction

Fruit consumption is essential for a healthy diet thanks to the great contribution of benefits thereof [1]. Therefore, the consumption of fruits, increasingly demand strict quality parameters, as well as the objective of preserving for longer time the fresh products in the market. To have a good acceptation of fruits in the market requires appropriate physico-chemical properties related to fruit maturity stages. Typically, the fruit gatherers use morphological changes such as fruit colour, changes in shape, taste and softness, as indicators for determining the optimal maturity stage for harvesting [2]. One of the objectives of the collection of the fruit before its full maturity is to keep the fresh product on the market for a longer time. In consequence, it is important to dispose the sufficient knowledge to ensure that their products have the highest possible quality and to predict early harvest characteristics and post-harvest behaviour, as well as determining the optimum date of harvest. However, the traditional methods for determining the optimal maturity stage for harvesting are destructive, time consuming, laborious, and costly, and require specific sample preparation steps [3].

A common technique widely employed for quality assessment of foods and agricultural products solid samples is Near-Infrared Spectroscopy (NIRs). The benefits of this technique are related to the rapid, non-destructive and low-cost analysis [4]. The first-order data obtained with NIRs are mostly processed with partial least-squares (PLS), being widely applied in food and in agriculture analysis [5,6]. NIR absorption spectra approximately describe the aggregate effect of absorption and scattering in food samples; they do not offer separate information on the absorption and emission properties. Hence, NIRs, in essence, is an empirical technique that relies on statistical methods to relate spectral features to the chemical or physical attributes of food samples. Other important trouble in NIRs analysis of solid samples is the broad and non-homogeneous bands that difficult the extraction of the chemical information [7]. In this context, this spectroscopic technique has been previously used for the prediction of relevant quality parameters in Japanese plum samples [8].

On the other hand, the use of classification techniques has made remarkable progress during the last decades in all fields, for example, food, pharmaceuticals, environmental, biomedical matrices, and so forth. In the agronomic-food field, it is becoming a common tool both for controlling production and for studying the influence of storage on the qualities of the final product [5,9]. Actually, the fact of having instruments not excessively sophisticated that are capable of obtaining abundant information on the characteristics of the samples has facilitated the implementation of these techniques.

The application of classification methods, as chemometric strategies for predicting a qualitative response, implies building a model that can assign an individual to a category based on the data that have been collected to describe it. In this context, a category (or class) is a group of objects sharing similar characteristics. In discriminant analysis, spectral data are assigned to definite classes, so that qualitative information complements quantitative spectral data. The purpose of the classification methods is to obtain weighted combinations of data that minimize variances within classes and maximize variances between classes. Then, the classification rules are used to assign new or unknown samples to the most probable subclasses. Prior to discriminant analysis, principal component analysis is often applied to spectral data sets to reduce data set size and minimizing possible co-linearity effects. The validity of a classification method can be verified by a comparison of distances or testing [10].

Until now, NIR is the most used technique for discrimination, but this technique is not selective and it is necessary a high number of samples to obtain adequate results. The use of fluorescence signal as descriptive variable with classification purposes, in the food field, has the advantage that a relatively small number of the compounds present in food samples contributes to native fluorescence, thus increasing the selectivity of the information. In recent years, the fluorescent properties of compounds naturally present in fruits have been widely exploited for analytical purposes.

With respect to the classifications of plum samples, UV–Vis, near infrared (NIR) and synchronous fluorescence, in combination with chemometric methods, have been used to discriminate samples of high-quality plum brandies of different varietal origins [11], and front-face fluorescence has been used to discriminate samples from different maturation stages [12]. In other food matrices, right angle or front-face fluorescence has been used for the discrimination of apple juices [13], between apple juices belonging to two categories: those produced directly, not from concentrate, and those reconstituted from concentrate apple juices [14], and between commercial berry fruit beverages [15].

In this work, we explore the use of fluorescence from methanolic extracts of plums, in combination with chemometrics (classification and quantification techniques), for the discrimination of plums according to their date of harvesting, and the quantification of the content of the main polyphenol compounds in plums.

## 2. Materials and methods

### 2.1. Samples and standards

A total of fifty-six samples were used in this study. Samples were collected on an experimental plot located in the "Vegas Bajas del Guadiana" (Badajoz, Spain) in an altitude of 184 m. Variety of plums was a late-maturation Japanese Angeleno plum variety planted in 2005. Samples were divided in four groups when they were analyzed: extracts from skin of plums collected in May (group 1), extracts from skin of plums collected in September (group 2), extracts from pulp of plums collected in May (group 3) and extracts from pulp of plums collected in September (group 4).

Standard solutions of catechin, epicatechin, chlorogenic acid, neochlorogenic acid and procyanidin B2 were used to register reference spectra. Catechin, epicatechin and neochlorogenic

acid were purchased from Sigma Aldrich Chemie (Steinheim, Germany), chlorogenic acid was obtained from Fisher Scientific, and procyanidin B2 was supplied by Extrasynthése (Genaym, France).

### 2.2. Preparation of methanolic extracts

Samples were peeled and skin was separated from pulp before lyophilization and extraction to perform the different analysis. Then, 0.5 g of lyophilized samples were used for extraction with 10 mL of methanol:water:formic acid (50:49:1, v/v), using an ultrasonic extraction for 14 minutes. After that, extracts were centrifuged for 10 min, at 10000 rpm, at 4ºC. Supernatants were diluted 1/100 (v/v) with methanol for further analysis.

### 2.3. Reference polyphenols analysis

Polyphenols analysis of samples was performed by HPLC following the method described by Cabrera-Bañegil et al. [16]. An Agilent 1260 Infinity High Performance Liquid Chromatograph (Agilent Technologies, CA, USA) and a Teknokroma Tracer Excel 120 ODS-A column (150 mm × 4.6 mm and 5 μm particle size) were used. Mobile phase was composed of 0.5% (v/v) formic acid and water (A), and acetonitrile (B). Analytes were eluted in gradient mode: 90% of 0.5% (v/v) formic acid in water (eluent A) and 10% of acetonitrile (eluent B) was held for 20 min. Between 20 and 45 min the percentage of eluent B increases from 10 up to 30% and, between 45 min and 46 min, the percentage of eluent B increases from 30 up to 100% and the formic acid content decreased in correspondence. These conditions were maintained until 53 min and, finally, the eluent B content was decreased to the initial conditions (10% B), and the column was re-equilibrated for 5 min. A flow of 0.5 mL/min was used and a volume of 20 μL was employed as injection volume. A fast-scanning fluorescence detector was used and excitation/emission wavelengths were set at 270/ 350 nm, for catechin, epicatechin and procyanidin B2, and at 320/430 nm for chlorogenic and neochlorogenic acids. The quantification of polyphenolic compounds was carried out by standard addition calibration.

### 2.4. Fluorescence measurement

Fluorescence data were obtained by means of a fluorescence spectrophotometer Varian Model Cary Elipse (Agilent Technologies, Madrid, Spain). A quartz cell of 10 mm was used. Emission spectra (280 – 500 nm, each 1 nm) were recorded at an excitation wavelength of 280 nm; and emission spectra (345 – 500 nm, each 1 nm) were also collected at an excitation wavelength of 330 nm. Slits of excitation and emission monochromators were set at 5 nm, respectively, with a scan rate of 300 nm/min. To obtain the excitation – emission matrix the excitation range was from 240 to 380 nm, each 5 nm, and the emission range was from 280 to 500, each 1 nm.

### 2.5. Data processing and multivariate analysis

Firstly, all spectra were smoothed using the Savitzky Golay method to eliminate some noise signals [17]. In order to explore the main variation among the four groups of samples, Principal Component Analysis (PCA) [18] was applied with the whole of all samples. As two excitation wavelengths, 280 and 330 nm, were used, two data sets were considered for analysis.

After that, to evaluate the possibility of discrimination of samples according to the date of harvesting. Partial least-squares-discriminant analysis (PLS-DA) was used as classification algorithm [19]. PLS-DA involves performing a multivariate regression model to establish class limits and placing a numeric value to each object/sample first, and then classifying new samples into a specific class. Data analysis was done using a graphical interface [20] in Matlab (R2016b, The MathWorks, Inc. Natick, MA, USA).

To obtain calibration models for polyphenols quantification, PLS regression was applied [21]. Cross-validation was used to determine the number of components to use in the calibration and to evaluate the performance of the models. Number of components were selected according to the explained variance. The Unscrambler version 6.11 (CAMO Software AS, Oslo, Norway) was used for data analysis.

## 3. Results and discussion

### 3.1. Spectral information

For this study, methanolic extracts from the pulp and from the skin of the plums with different maturation stages, were obtained. In first place, and with the object to visualize the emission spectral zones, excitation-emission fluorescence landscapes of methanolic extracts of skin and pulp of plums were obtained and two characteristics spectral regions were observed (Figure 1A). The first region presented a maximum excitation wavelength at 280 nm, and the second region presented an excitation maximum at 330 nm. Figures 1B and 1C show the emission spectra for the methanolic extracts from the pulp and from the skin, obtained at the two different excitation wavelengths, the most characteristic ones. In Figure 1B (excitation at 280 nm), the main differences correspond with intensity of signals when samples harvested in different months were compared. This is, extracts from May exhibited higher fluorescence, about three times more, than extracts from September in both cases: pulp and skin. These high intensity maxima have been also obtained, by synchronous fluorescence, in plum brandies samples with little differences in function of the presence or absence of color in the sample [22]. In addition, when the emission spectra of the skin and pulp samples were compared some differences could also be highlighted. Although intensities in May were similar for both skin (blue) and pulp (violet) groups, a shift was shown in their spectra. In the case of extracts from skin, an emission maximum is located at 321 nm. However, in the case of extracts from pulp, the emission maximum shows a small hypochromic effect and it is located at 315 nm. This might be related with different polyphenol compounds present in both extracts. This region is characteristic for catechin, epicatechin and procyanidin, main polyphenols presented in plums [16].

In the case of the second excitation wavelength, 330 nm (Figure 1C), similar trends were observed. In this case, an emission maximum appeared at 424 nm for the skin extracts and at 435 nm for the pulp extracts. For both extracts, the emission band presents a wide shape. In this spectral region, and with the samples harvested in May, it is noted that the fluorescence intensity

of the skin extracts is significantly higher than the pulp extracts. With respect to the samples harvested in September, the fluorescence of the skin extracts decreases, and the fluorescence of the pulp extracts disappears. In accordance with previous studies, this region is characteristic for chlorogenic and neochlorogenic acids, that are the predominant phenolic acids in plums [16,23,24]. Also, this fluorescence region maximum has been observed by synchronous fluorescence in colored and colorless plum brandies samples [22].

### 3.2. Exploratory analysis: Principal Component Analysis

In order to evaluate the main differences between the four groups, an exploratory analysis was performed with PCA. This is an unsupervised method, and it was used to evaluate whether clustering exists without using class membership information. Samples were divided in two data sets according to the excitation wavelength. For each data set, all groups of samples (skin September, pulp September, skin May and pulp May) were analyzed.

In the set of emission spectra with excitation at 280 nm, best discrimination was obtained for scores for PC1 and PC2, explaining 98 and 2% of the variance, respectively. Figures 2A and 2B show the scores and loadings obtained, respectively. Score values for PC1 are higher for samples harvested in May, which means that positive loadings are positively related to these samples. The main variable affecting the separation of groups is observed in the loading for PC1, Figure 2B, and was located at an emission wavelength of 318 nm. This variable might be related with procyanidin and epicatechin that exhibit maxima signal around 314 nm (Figures 3A and 3B). This result is in accordance with the general decrease of total phenolic and total flavonoids in plums of Sanshua variety during fruit maturation [25]. Another group was observed, according to the PC2, which explained only 2% of variance but it was enough for differentiation. In this case, the main variable affecting the separation was at 308 nm (positive) and 340 nm (negative). Score values for PC2 were higher for samples from pulp than from skin. In this case, differentiation might be due to the presence of catechin that presents a maximum signal around 308 nm (Figure 3C).

In the set of spectra with excitation at 330 nm, best discrimination was obtained for scores of PC1 explaining 99% of the variance. Figures 2C and 2D show the scores and loadings obtained, respectively. Along the first component, samples were divided by harvesting date, being the contribution of first component higher for May than for September. In this case, no differentiation was observed according to skin and pulp. In this set, the loadings of the PC1 can be related with the presence of chlorogenic and neoclorogenic acids in plums, showing the main variables affecting the separation of groups at 424 nm for emission wavelength.

### 3.3. Classificatory analysis: Partial Least-Squares – Discriminant Analysis

After PCA, classificatory analysis was performed with different strategies. In a first step, all samples were considered as training samples and PLS-DA was assayed in both sets of data. With two components, the total variance was explained (100%) in both cases. Results are shown in Table 1. As seen, results confirmed the good classification of the four groups. In this case, a test set was not used as all samples were used as training set. It was observed that better discrimination was obtained for spectra at 280 nm of excitation wavelength (error rate (ER) = 0) than for spectra at 330 nm (ER = 3.5%).

A second strategy consisted on dividing the entire sample data set into the training set, comprising the 50% of the samples, and use the rest of samples as test samples. In this case, also two components were enough to explain 100% of the variance. For the training set, acceptable predictions were obtained (Table 2), with ERs of 3.5 and 7% respectively, for the two different excitation wavelengths. However, when the test set (50% of samples) was predicted using these models, all samples were well-attributed to their group, Table 2.

Finally, a third strategy, using 30% of samples as training set and 70% of samples as test set was carried out. Total variance was explained by two components in both cases. For training set, 100% of accuracy was obtained in both data sets. In this case, acceptable predictions were obtained for test set, with ERs of 3 and 8%, respectively. These classification studies demonstrated the huge

variability between four groups, being possible to create models with only four samples per class and obtain good results for predicted samples. In short, all models could be considered acceptable taking into account the criteria that ER were lower than 10% in all cases [26].

### 3.4. Quantification of polyphenols

In addition, quantification studies were performed. For that, random samples of plums (twenty-three samples) were analyzed by HPLC to obtain the reference values of polyphenols.

Correlation coefficients (Pearson's r) between the different polyphenolic compounds were obtained. The results revealed a high correlation between catechin and epicatechin (r = 0.86), which means, those samples with high content of catechin also present high content of epicatechin. In addition, a high correlation was found between procyanidin and catechin (r = 0.85) and epicatechin (r = 0.90). In the case of chlorogenic and neochlorogenic acids, weak correlation were found with the previous ones, but the correlation between them was 0.58. The high correlations between some polyphenols might influence in the calibration models when individual polyphenols try to be quantified.

Using the spectra as X and individual polyphenol content obtained by HPLC as Y, calibration models were obtained by means of cross-validation procedure. Table 3 provides the results obtained for the different models based on the spectra at the two excitation wavelengths. Components were selected according to the explained variance, obtained few components (2 or 1) in all cases, which means that overfitting did not occurred.

As observed, the best model was obtained for epicatechin, with a low prediction error and a high determination coefficient ($R^2$). The regression coefficients for this model are shown in Figure 4B, corresponding the main variables affecting the models with the maxima obtained in the spectrum for the pure standard (Figure 3B). Also, acceptable models were obtained for catechin and procyanidin. Regression coefficients for procyanidin model (Figure 4C) offered same information than in the case of epicatechin (Figure 4B), which may be expected due to the similarity of

standard spectra for both compounds (Figure 3C). However, in the case of catechin (Figure 4A), the regression coefficients did not show the main variables from catechin (Figure 3A), so this model might be a bit uncertain due to the low concentration of this compound in samples.

In the case of chlorogenic and neochlorogenic acids, the best model was obtained for the last one. Both compounds presented a similar spectrum (Figure 3D and 3E), as a result, similar regression coefficients (Figure 4D and 4E) were obtained for their corresponding models, although a shift in the main variables was observed. The better results obtained for neochlorogenic acid might be related with the fact that the concentration interval found for this compound is wider than for chlorogenic acid. Similar determination coefficient was obtained and a high root-mean-square-error for cross validation. (RMSECV) resulted.

Calibration models offered promising results which need to be expanded including more samples with high variability. It would be possible to quantify polyphenols in methanolic extracts using simple fluorescence spectra and avoiding large procedures by HPLC, which requires more time, solvents and higher cost.

## 4. Conclusions

Emission spectra of methanolic extracts of plums were used as fingerprints for their differentiation. Combining these spectra with PCA and PLS-DA samples were able to be discriminated by date of harvesting (May or September) and by part of plum (skin or pulp), obtaining better results for PLS-DA than PCA. Also, models composed by reduced number of samples offered acceptable prediction results. Classification results were due to polyphenol content. In addition, calibrations models obtained by PLS provided good results about individual quantification of polyphenols, which could be interesting to investigate in the future to expand the calibration models with more samples.

**Acknowledgements**

Financial support was provided by the Ministerio de Ciencia, Innovación y Universidades of Spain (Project CTQ2017-82496-P) and Junta of Extremadura (Project GR18041-Research Group FQM003), both co-financed by the Fondo Europeo de Desarrollo Regional. Manuel Cabrera-Bañegil thanks to Consejería de Economía e Infraestructuras of the Comunidad Autónoma de Extremadura for a FPI grant (PD16015), co-financed with the Fondo Europeo de Desarrollo Regional.

**References**


[1] O.O. Oguntibeju, E.J. Truter, A.J. Esterhuyse, The Role of Fruit and Vegetable Consumption in Human Health and Disease Prevention, in: O. Oguntibeju (Ed.), Diabetes Mellit. - Insights Perspect., InTech, 2013: pp. 117–130.

[2] A. Ndou, P.P. Tinyani, R.M. Slabbert, Y. Sultanbawa, D. Sivakumar, An integrated approach for harvesting Natal plum (Carissa macrocarpa) for quality and functional compounds related to maturity stages, Food Chem. 293 (2019) 499–510.

[3] G. M. El-Masry, S. Nakauchi, Image analysis operations applied to hyperspectral images for non-invasive sensing of food quality – A comprehensive review, Biosyst. Eng. 142 (2016) 53–82.

[4] F. Zhu, H. Yao, Z. Hruska, R. Kincaid, R. Brown, D. Bhatnagar, T. Cleveland, Integration of Fluorescence and Reflectance Visible Near-Infrared (VNIR) Hyperspectral Images for Detection of Aflatoxins in Corn Kernels, Trans. ASABE. 59 (2016) 785–794.

[5] V. Cortés, J. Blasco, N. Aleixos, S. Cubero, P. Talens, Monitoring strategies for quality control of agricultural products using visible and near-infrared spectroscopy: A review, Trends Food Sci. Technol. 85 (2019) 138–148.

[6] J.G. Kim, Y. Park, M.H. Shin, S. Muneer, R. Lerud, C. Michelson, D. Il Kang, J.H. Min, H.M.P.C. Kumarihami, Application of NIR-Spectroscopy to predict the harvesting maturity , fruit ripening and storage ability of Ca-chitosan treated baby kiwifruit, J. Stored Prod. Postharvest Res. 9 (2018) 44–53.

[7] K.B. Beć, C.W. Huck, Breakthrough Potential in Near-Infrared Spectroscopy: Spectra Simulation. A Review of Recent Developments, Front. Chem. 7 (2019) 1–22.

[8] E.D. Louw, K.I. Theron, Robust prediction models for quality parameters in Japanese plums (Prunus salicina L.) using NIR spectroscopy, Postharvest Biol. Technol. 58 (2010) 176–184.

[9] H. El-Mesery, H. Mao, A. Abomohra, Applications of Non-destructive Technologies for Agricultural and Food Products Quality Inspection, Sensors. 19 (2019) 846–869.

[10] A. Dankowska, W. Kowalewski, Comparison of different classification methods for

analyzing fluorescence spectra to characterize type and freshness of olive oils, Eur. Food Res. Technol. 245 (2019) 745–752.

[11] M. Jakubíková, J. Sádecká, A. Kleinová, On the use of the fluorescence, ultraviolet–visible and near infrared spectroscopy with chemometrics for the discrimination between plum brandies of different varietal origins, Food Chem. 239 (2018) 889–897.

[12] O. Monago-Maraña, J. Domínguez-Manzano, A. Muñoz de la Peña, I. Durán-Merás, Second-order calibration in combination with fluorescence fibre-optic data modelling as a novel approach for monitoring the maturation stage of plums, Chemom. Intell. Lab. Syst. 199 (2020) 103980.

[13] K. Włodarska, K. Pawlak-Lemańska, I. Khmelinskii, E. Sikorska, Explorative study of apple juice fluorescence in relation to antioxidant properties, Food Chem. 210 (2016) 593–599.

[14] K. Włodarska, I. Khmelinskii, E. Sikorska, Authentication of apple juice categories based on multivariate analysis of the synchronous fluorescence spectra, Food Control. 86 (2018) 42–49.

[15] E. Sikorska, K. Wlodarska, I. Khmelinskii, Application of multidimensional and conventional fluorescence techniques for classification of beverages originating from various berry fruit, Methods Appl. Fluoresc. 8 (2020) 015006.

[16] M. Cabrera-Bañegil, N. Lavado Rodas, M.H. Prieto Losada, F. Blanco Cipollone, M.J. Moñino Espino, A. Muñoz de la Peña, I. Durán-Merás, Evolution of polyphenols content in plum fruits (Prunus salicina) with harvesting time by second-order excitation-emission fluorescence multivariate calibration, Microchem. J. 158 (2020) 105299.

[17] A. Savitzky, M.J.E. Golay, Smoothing and differentiation of data by simplified least squares procedures, Anal. Chem. 36 (1964) 1627–1639.

[18] S. Wold, K.I.M. Esbensen, P. Geladi, Principal Component Analysis, Chemom. Intell. Lab. Syst. 2 (1987) 37–52.

[19] M. Barker, W. Rayens, Partial least squares for discrimination, J. Chemom. 17 (2003) 166–173.

[20] D. Ballabio, V. Consonni, Classification tools in chemistry. Part 1: linear models. PLS-DA, Anal. Methods. 5 (2013) 3790–3978.

[21] H. Martens, T. Naes, Multivariate Calibration, Wiley, New York, 1989.

[22] M. Tomková, J. Sádecká, K. Hrobovnová, Synchronous Fluorescence Spectroscopy for Rapid Classification of Fruit Spirits, Food Anal. Methods. 8 (2015) 1258–1267.

[23] M. Liaudanskas, R. Okulevičiūtė, J. Lanauskas, D. Kviklys, K. Zymonė, T. Rendyuk, V. Žvikas, N. Uselis, V. Janulis, Variability in the Content of Phenolic Compounds in Plum Fruit, Plants. 9 (2020) 1611.

[24] N. Nakatani, S. Kayano, H. Kikuzaki, K. Sumino, K. Katagiri, T. Mitani, Identification, Quantitative Determination, and Antioxidative Activities of Chlorogenic Acid Isomers in Prune (Prunus domestica L.), J. Agric. Food Chem. 48 (2000) 5512–5516.

[25] Q. Li, X.-X. Chang, H. Wang, C.S. Brennan, X.-B. Guo, Phytochemicals Accumulation in Sanhua Plum (Prunus salicina L.) during Fruit Development and Their Potential Use as Antioxidants, J. Agric. Food Chem. 67 (2019) 2459–2466.

[26] L. Cuadros-Rodríguez, L. Valverde-Som, A.M. Jiménez-Carvelo, M. Delgado-Aguilar, Validation requirements of screening analytical methods based on scenario-specified applicability indicators, TrAC - Trends Anal. Chem. 122 (2020) 115705.

**Figure captions**

**Figure 1.** A) Excitation-emission matrix and contour plot of a methanolic extract from pulp plum sample. B) Samples emission spectra obtained exciting at 280 nm. C) Samples emission spectra obtained exciting at 330 nm.

**Figure 2.** Score values (A) and loadings (B) obtained from PCA of emission spectra at 280 nm for excitation. Score values (C) and loadings (D) obtained from PCA of emission spectra at 330 nm for excitation.

**Figure 3.** Emission spectra for different standards: epicatechin (A), procyanidin (B), catechin (C), chlorogenic acid (D) and neochlorogenic acid (E). A, B and C were obtained at 280 nm excitation wavelength and D and E were obtained at 330 nm excitation wavelength.

**Figure 4.** Regression coefficients obtained for the different models: catechin (A), epicatechin (B), procyanidin (C), chlorogenic acid (D), neochlorogenic acid (E) and chlorogenic + neochlorogenic acids (F).

**Table 1.** Confusion matrices for the different training sets studied.

| **All samples (Training set)** | | | | |
|---|---|---|---|---|
| **Excitation 280 nm** | | | | |
| **Real/ Predicted** | **May (skin)** | **September (skin)** | **May (pulp)** | **September (pulp)** |
| **May (skin)** | 14 | - | - | - |
| **September (skin)** | - | 16 | - | - |
| **May (pulp)** | - | - | 12 | - |
| **September (pulp)** | - | - | - | 14 |
| **Excitation 330 nm** | | | | |
| | **May (skin)** | **September (skin)** | **May (pulp)** | **September (pulp)** |
| **May (skin)** | 12 | - | 2 | - |
| **September (skin)** | - | 16 | - | - |
| **May (pulp)** | - | - | 12 | - |
| **September (pulp)** | - | - | - | 14 |
| **50% samples (Training set)** | | | | |
| **Excitation 280 nm** | | | | |
| **Real/ Predicted** | **May (skin)** | **September (skin)** | **May (pulp)** | **September (pulp)** |
| **May (skin)** | 7 | - | - | - |
| **September (skin)** | - | 7 | 1 | - |
| **May (pulp)** | - | - | 6 | - |
| **September (pulp)** | - | - | - | 7 |
| **Excitation 330 nm** | | | | |
| **Real/ Predicted** | **May (skin)** | **September (skin)** | **May (pulp)** | **September (pulp)** |
| **May (skin)** | 5 | - | 2 | - |
| **September (skin)** | - | 8 | - | - |
| **May (pulp)** | - | - | 6 | - |
| **September (pulp)** | - | - | - | 7 |
| **30% samples (Training set)** | | | | |
| **Excitation 280 nm** | | | | |
| **Real/ Predicted** | **May (skin)** | **September (skin)** | **May (pulp)** | **September (pulp)** |
| **May (skin)** | 4 | - | - | - |
| **September (skin)** | - | 5 | - | - |
| **May (pulp)** | - | - | 4 | - |
| **September (pulp)** | - | - | - | 4 |
| **Excitation 330 nm** | | | | |
| **Real/ Predicted** | **May (skin)** | **September (skin)** | **May (pulp)** | **September (pulp)** |
| **May (skin)** | 4 | - | - | - |
| **September (skin)** | - | 5 | - | - |
| **May (pulp)** | - | - | 4 | - |
| **September (pulp)** | - | - | - | 4 |

**Table 2.** Confusion matrices for the different tests set studied.

| **50% samples (test set)** | | | | |
|---|---|---|---|---|
| **Excitation 280 nm** | | | | |
| **Real/ Predicted** | **May (skin)** | **September (skin)** | **May (pulp)** | **September (pulp)** |
| **May (skin)** | 7 | - | - | - |
| **September (skin)** | - | 8 | - | - |
| **May (pulp)** | - | - | 6 | - |
| **September (pulp)** | - | - | - | 7 |
| **Excitation 330 nm** | | | | |
| **Real/ Predicted** | **May (skin)** | **September (skin)** | **May (pulp)** | **September (pulp)** |
| **May (skin)** | 7 | - | - | - |
| **September (skin)** | - | 8 | - | - |
| **May (pulp)** | - | - | 6 | - |
| **September (pulp)** | - | - | - | 7 |
| **70% samples (test set)** | | | | |
| **Excitation 280 nm** | | | | |
| **Real/ Predicted** | **May (skin)** | **September (skin)** | **May (pulp)** | **September (pulp)** |
| **May (skin)** | 9 | 1 | - | - |
| **September (skin)** | - | 11 | - | - |
| **May (pulp)** | - | - | 8 | - |
| **September (pulp)** | - | - | - | 10 |
| **Excitation 330 nm** | | | | |
| **Real/ Predicted** | **May (skin)** | **September (skin)** | **May (pulp)** | **September (pulp)** |
| **May (skin)** | 8 | - | 2 | - |
| **September (skin)** | - | 11 | - | - |
| **May (pulp)** | - | - | 9 | - |
| **September (pulp)** | - | - | - | 9 |

**Table 3.** Summary of PLS regression models obtained for predicting different polyphenols.

| **Excitation 280 nm** | | | | |
|---|---|---|---|---|
| | **Range (μg/mL)** | **Nº components** | **$R^2$ (CV)** | **RMSECV (μg/mL)** |
| Catechin | 0 – 0.32 | 2 | 0.73 | 0.05 |
| Epicatechin | 0.1 – 2.6 | 1 | 0.89 | 0.23 |
| Procyanidin B | 0 – 1.7 | 1 | 0.67 | 0.29 |
| **Excitation 330 nm** | | | | |
| | **Range (μg/mL)** | **Nº components** | **$R^2$ (CV)** | **RMSECV (μg/mL)** |
| Chlorogenic acid | 0 – 0.52 | 1 | 0.54 | 0.09 |
| Neochlorogenic acid | 0 – 1.8 | 1 | 0.74 | 0.18 |
| Chlorogenic acid + Neochlorogenic acid | 0 – 1.8 | 1 | 0.73 | 0.24 |

RMSECV: root-mean-square-error for cross validation

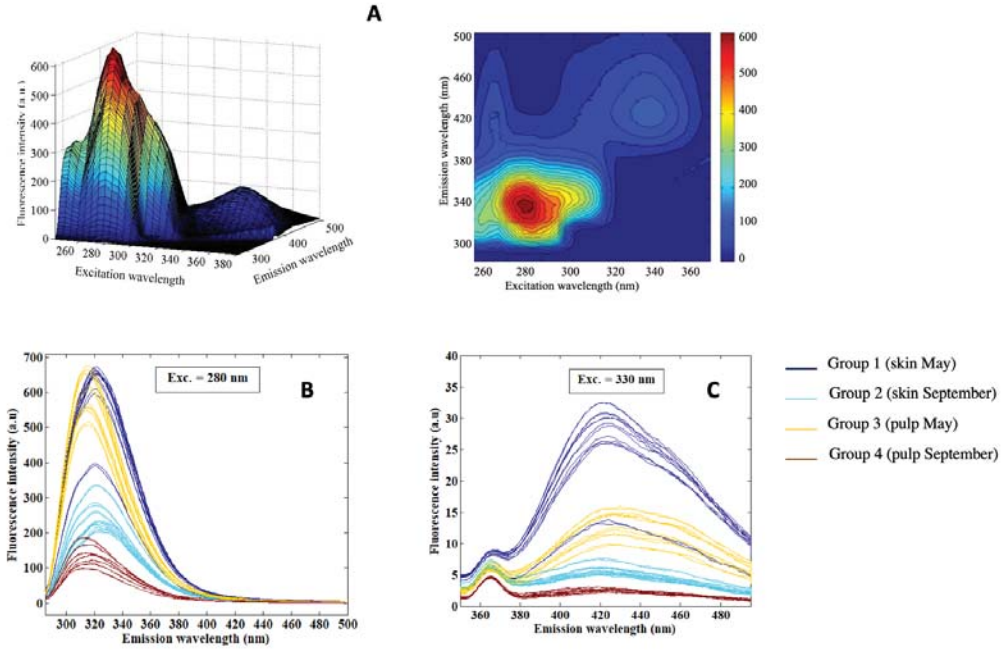
A
Fluorescence intensity (a.u)
Excitation wavelength
Emission wavelength
Emission wavelength (nm)
Excitation wavelength (nm)
Exc. = 280 nm
B
Fluorescence intensity (a.u)
Emission wavelength (nm)
Exc. = 330 nm
C
Fluorescence intensity (a.u)
Emission wavelength (nm)
Group 1 (skin May)
Group 2 (skin September)
Group 3 (pulp May)
Group 4 (pulp September)

**Figure 1**

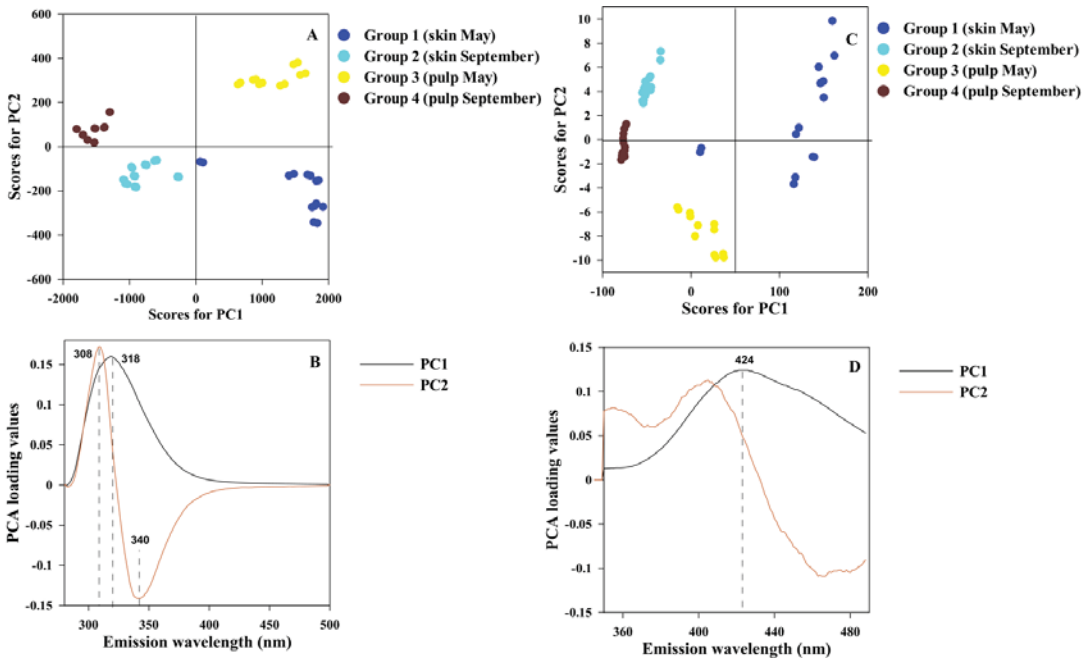
A
Group 1 (skin May)
Group 2 (skin September)
Group 3 (pulp May)
Group 4 (pulp September)
Scores for PC2
Scores for PC1
C
B
PC1
PC2
PCA loading values
308
318
340
Emission wavelength (nm)
D
424

**Figure 2**

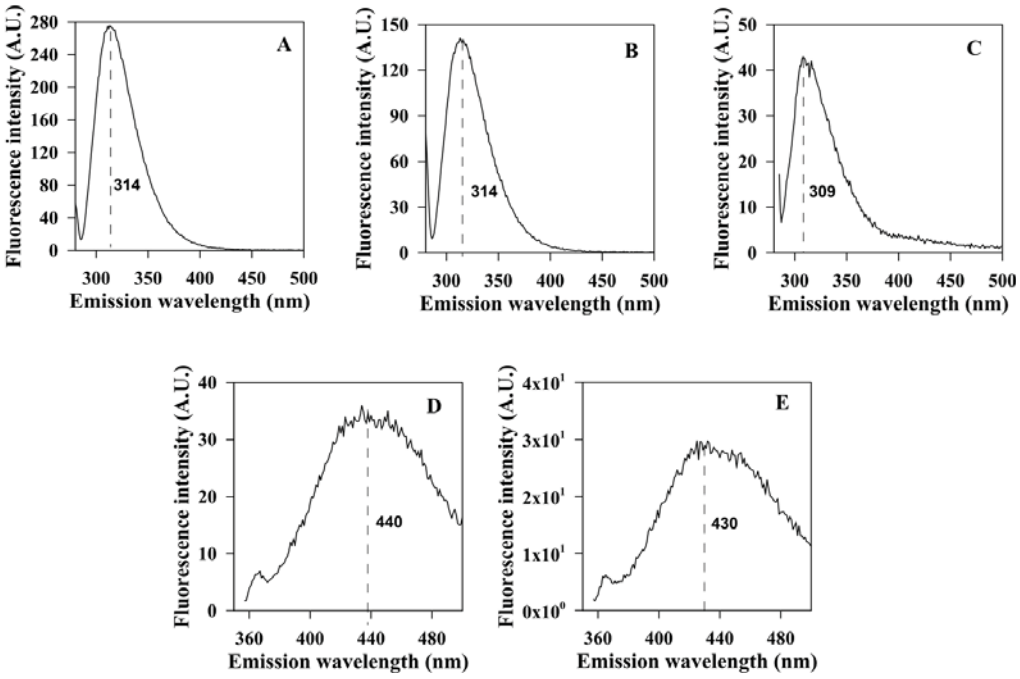
A
Fluorescence intensity (A.U.)
Emission wavelength (nm)
314
B
314
C
309
D
440
E
430

**Figure 3**

**Conflict of interest**

Authors declare no conflict of interest.

# ARTÍCULO 6

## Control of olive cultivar irrigation by front-face fluorescence excitation-emission matrices in combination with PARAFAC

Manuel Cabrera-Bañegil, Daniel Martín-Vertedor, Emanuele Boselli, Isabel Durán-Merás

*Journal of Food Composition and Analysis,*
***2018**, 69, 189-196*
*DOI: https://doi.org/10.1016/j.jfca.2018.01.021*

Journal of Food Composition and Analysis 69 (2018) 189–196

Contents lists available at ScienceDirect

Journal of Food Composition and Analysis

journal homepage: www.elsevier.com/locate/jfca

Original research article

# Control of olive cultivar irrigation by front-face fluorescence excitation-emission matrices in combination with PARAFAC

Manuel Cabrera-Bañegil[a,*], Daniel Martín-Vertedor[b], Emanuele Boselli[c], Isabel Durán-Merás[a,d]

[a] Department of Analytical Chemistry, Faculty of Sciences, University of Extremadura, Avda. de Elvas S/N, 06006 Badajoz, Spain
[b] Technological Institute of Food and Agriculture (CICYTEX-INTAEX), Junta de Extremadura, Avda. Adolfo Suárez S/N, 06007 Badajoz, Spain
[c] Free University of Bozen-Bolzano, Faculty of Science and Technology, Piazza Università 1, 39100 Bozen-Bolzano, Italy
[d] Research Institute on Water, Climate Change and Sustainability (IACYS), University of Extremadura, 06006 Badajoz, Spain

ARTICLE INFO

*Chemical compounds studied in this article:*
(+)-Catechin (PubChem CID 9064)
Epicatechin (PubChem CID 72276)
Oleuropein (PubChem CID 5281544)
Vanillic acid (PubChem CID 8468)

*Keywords:*
Food analysis
Food composition
Olive fruit pulp
Biophenolic compounds
Irrigation treatments
Front-face fluorescence
PARAFAC
Vanillic acid
Catechins
Oleuropein

ABSTRACT

Due to their antioxidant properties, biophenolic compounds from vegetables and derived products are very demanded by the consumers. The olive fruit pulp is rich in these compounds, and, in this paper, the influence of irrigation on the levels of these compounds has been investigated. Methanolic extracts from olive paste samples submitted to different irrigation treatments were analyzed by front-face fluorescence. Excitation-emission matrices, recorded as a set of emission spectra in the range 290–450 nm, and in the excitation range of 240–290 nm, were analyzed by means of Parallel Factor Analysis (PARAFAC). The loadings and scores corresponding to three components were obtained. In the same samples, polyphenols were also analyzed by chromatography. High correlations were found between the first component PARAFAC scores and epicatechin (R = 0.856) and catechin plus epicatechin concentrations (R = 0.873), second component scores and oleuropein (R = 0.892, only when epicatechin concentration is lower than 0.55 mg/L) and the third component scores and vanillic acid concentrations (R = 0.877). The representation of the two first PARAFAC component scores allowed discriminate between the different irrigation treatments. Polyphenol concentrations obtained by both methods were analyzed statistically by ANOVA and Duncańs multiple test. The obtained results showed significant differences between the irrigation treatments.

## 1. Introduction

In our days, and due to their antioxidant properties, consumers are interested in biophenolic compounds from vegetables and derivate products (Difonzo et al., 2017; Talhauoi et al., 2015). Various studies suggest that these compounds are associated with beneficial effects, and they are related with a reduction in cancer colon (Bassani et al., 2016; Terzuoli et al., 2016). Olive fruits fresh pulp (*Olea europaea*) contains approximately a 3% (w/w) of hydrophilic (phenolic acids, phenolic alcohols, flavonoids and secoiridoids) and lipophilic (cresols and tocopherols) phenolic compounds.

In the last years, consumers consider the contents of biophenolic compounds as important quality markers (Servili et al., 2004). The concentration of biophenolic compounds and phenolic profile in olive fruits depend on the cultivar, agroclimatic conditions (rainfall and/or water stress), ripening stage, and agronomical techniques (Franco et al., 2014a; Tovar et al., 2002). Among the possible agronomical strategies to achieve a better quality, a cultivar-based tailor made irrigation treatment can improve the final olive oil quality (Machado et al., 2013). Furthermore, in super intensive olive orchard, and with the object to control the excessive vigor of olive trees, a regulated deficit irrigation should be controlled. In addition, the irrigation has influence in the productivity and quality of olive fruits (Alegre et al., 2000; Lavee et al., 2007).

The quality control of the fruit is the first step for the classification of the olives at the start of the production process, avoiding mixing of olives of different qualities (Guzmán et al., 2012). In most cases, quality control at factory reception is based on visual observation of the olives or information provided by the farmer. The implementation of online analytical control systems in the olive industries, at an initial stage of the production process, would provide for identification, quickly and accurately, the quality parameters of the raw material (intact olives) and, consequently, the final product (Salguero-Chaparro et al., 2013).

The quality control from harvesting and transformation to storage and the traceability and authentication of olive products are, nowadays, the main challenges for olives industry and control laboratories. In

* Corresponding author.
*E-mail address:* manuelcb@unex.es (M. Cabrera-Bañegil).

https://doi.org/10.1016/j.jfca.2018.01.021
Received 31 July 2016; Received in revised form 30 December 2017; Accepted 26 January 2018
Available online 31 January 2018
0889-1575/ 

order to protect customers and producers against adulteration and false declarations, international organizations, such as European Union and International Olive Oil Council, have established rules and guidelines for the olive oil certification, including various physicochemical parameters and reference limits (Binetti et al., 2017). The improvement of product's quality continuously stimulates the search for new technologies. In addition, the olives industry has great interest on checking the quality using fast and reliable techniques. The inclusion of these data on the labels holds a potential added value, either in economic terms or in trade competitiveness (Cayuela and García, 2017). The reason is that from a consumer's perspective, there is a noticeable interest in information about food bioactive compounds content, among other substances.

Chromatography is the most popular analytical technique for olive oil individual phenolic compounds determination. However, in olive fruits this methodology is less common (Dagdelen et al., 2013; Machado et al., 2013; Pistarino et al., 2013). On the other hand, it is important to develop a rapid, cost-effective and simple sample treatment method. Among the possible alternative analytical methods, front-face fluorescence is a very useful technique because it allows handling samples practically without a pretreatment. Although front-face fluorescence has not yet been applied for the determination of biophenolic compounds in olive paste, numerous studies on the application of intrinsic fluorescence of olive oil, in combination with second order multivariate calibration techniques, such as PARAFAC and Unfolded Principal Component Analysis (UPCA), have been reported. In fact, the olive oil autofluorescence is associated to minor components, chemical species such as tocopherols, phenols and chlorophylls.

Two spectral ranges have been used for improving the explorative analysis of the excitation-emission fluorescence matrices (EEMs) of virgin and pure olive oils, by unfolded PCA and PARAFAC (Guimet et al., 2004). The first range was composed by chlorophylls, while the oxidation products and vitamin E were the predominant compounds in the second range. The application of unfolded PCA and PARAFAC to the EEMs allows distinguishing between virgin and (non-virgin) olive oils, mainly due to the contribution of the oxidation products. In fact, the differentiation between two types of oils was more efficient when the chlorophyll fluorescence region was excluded from the model. The potential of EEM fluorescence and three-way methods of analysis, to detect adulterations of pure olive oils from protected denomination of origin "Siurana", has been studied (Guimet et al., 2005). Unfolded-PCA and PARAFAC were applied for exploratory analysis. Linear discriminant analysis (LDA) and discriminant N-PLS regression, applied in training and validation sets, gave a classification rate close to 100%.

On the other hand, the quantification of chemical compounds of olive oil by means of fluorescence measures in combination with chemometric techniques has been also possible. In this content, the levels of chlorophylls *a* and *b* and pheophytins *a* and *b* of oils diluted in acetone have been determined, using a partial least square (PLS) calibration (Galeano Díaz et al., 2003). The tocopherols previously separated from olive oils were studied by means of a calibration of standards diluted in hexane using EEMs combined with PLS regression (Galeano Díaz et al., 2006).

The aim of this study was to develop a simple and fast fluorescence front-face method, in combination with PARAFAC, for the determination of different biophenolic compounds, in the paste of olives obtained from cultivars, with different irrigation treatments. The calculated concentration data were statistically compared with the results obtained by HPLC. For this statistical analysis, a 2-way factorial design was accomplished, in order to considerer the different factor effects between the methods (chemometric and chromatographic) and irrigation treatments.

## 2. Materials and methods

### 2.1. Samples

The study was carried out in a super-high-density olive orchard located in the area "Vegas Bajas del Guadiana", in a Junta de Extremadura property land, Solana de los Barros, Badajoz, Spain, (38°44′N, 6°38′W and an altitude of 263 m above sea level) and planted exclusively with Arbequina variety (*Olea europaea* L.).

The applied irrigation treatments consisted of watering with 75 (T1), 50 (T2) and 25% (T3) of the dose applied to the Control (C), respectively. Samples of olives were collected in November, with a ripeness index between 2 and 3 (spotted), using the subjective evaluation of color of the skin and flesh (Uceda and Frías, 1975). The olive sampling was carried out in the morning, and olives were randomly ripened in different sides of the olive tree, assuming a total of 10 kg per treatment in triplicate. After harvesting, the olives were immediately transported to the laboratory within 1 h, in ventilated storage at 4 °C trays, to avoid compositional changes.

### 2.2. Front-face fluorescence method

Fluorescence was determined using a Fluorescence Spectrophotometer (Varian Model Cary Eclipse Fluorescence Spectrophotometer, Agilent Technologies, Madrid, Spain), equipped with two Czerny-Turner monochromators (excitation and emission), a xenon lamp and two photomultiplier tubes as detector. The equipment was connected to a PC microcomputer via an IEEE 488 (GPIB) serial interface. The Cary Eclipse 1.0 software was used for data acquisitions. Measurements were carried out with a variable-angle front-face accessory, to ensure that reflected light, scattered radiation, and depolarization phenomena were minimized. The angle of incidence, defined as the angle between the excitation beam and the perpendicular to the cell surface, was set at 34°. Fluorescence measurements were recorded in a 10-mm quartz cell at 15 °C (room temperature). The slits of excitation and emission monochromators were set at 2.5 and 5 nm, respectively. EEMs were registered as a set of emission spectra with 0.5 nm of resolution. The photomultiplier tube sensitivity was 700 V and the scan rate was set at 300 nm $min^{-1}$. EEMs were recorded with an excitation range from 240 to 290 nm (each 5 nm), and emission from 290 to 450 nm (each 0.5 nm), according to Cabrera-Bañegil et al. (2017a). The total scanning time per sample was approximately 5 min. Measurements were performed by triplicate within a short period of time (2 days), to minimize the effects of instrumental fluctuation, mainly lamp intensity.

An EEM of a standard solution of each of the phenolic compounds present in olive paste was registered in the same front-face conditions.

### 2.3. Chemometric treatment

A PARAFAC model was built using the EEMs of a set of 5 olive samples grown with the highest water stress treatment (25%) (T3), 8 and 7 olive samples of 50% (T2) and 75% (T1) irrigation doses referred to control, respectively, and 10 olive samples of the Control group (the most irrigated group). The emission ranges of the data set were fixed at 302–450 nm, in order to reduce the Rayleigh signals, before the application of PARAFAC. In this way, the EEMs of 30 samples were arranged in a three-dimensional structure with a size of 30 × 296 × 11 (samples x number of emission wavelengths x number of excitation wavelengths). This array was decomposed by PARAFAC (Bro, 1997), applying the core consistency diagnostic tool for optimization of the number of components (Bro and Kiers, 2003). In all cases, non-negative constraints for the resolved profiles for all modes were applied with the purpose to obtain a realistic solution, because concentrations and spectral values are positive.

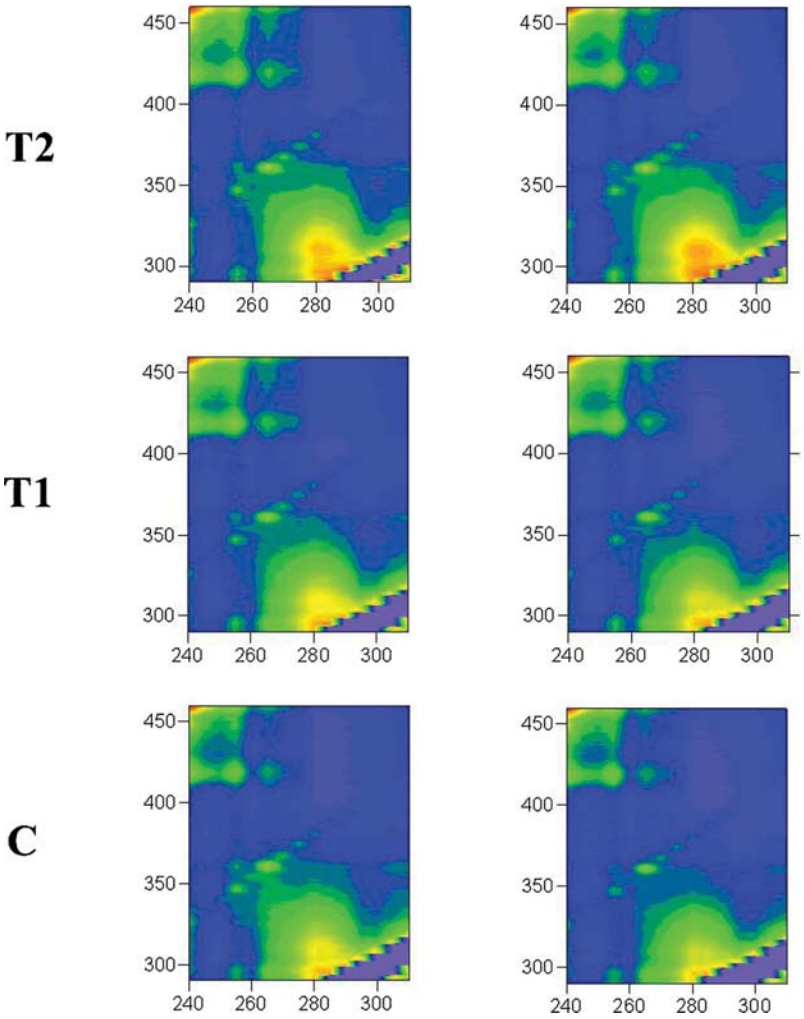


**Fig. 1.** Fluorescence contour plots corresponding to different irrigations treatment samples: C (control), T1 (irrigation treatment 1) and T2 (irrigation treatment 2).

*2.3.1. PARAFAC analysis*

The data analysis was performed using Matlab R2008a (MATLAB Version 7.6, The Mathworks, Natick, MA, USA, 2010) and the MVC2 routine (Olivieri et al., 2009).

*2.4. HPLC analysis of phenolic compounds*

*2.4.1. Reagents, solvents and phenolic standards*

Catechin, epicatechin, tyrosol and vanillic acid were purchased from Sigma-Aldrich (Steinheim, Germany). Standards of phenolic compounds such as hydroxytyrosol, oleuropein, procyanidin B1 and procyanidin B2 were supplied by Extrasynthése (Genay, France). Standard solutions of individual analytes were prepared in methanol.

HPLC grade acetonitrile and HPLC grade methanol, which were supplied by Fisher chemical (Loughborough, UK), and P.A. grade formic acid, which was purchased from PANREAC (Barcelona, Spain), were used for preparing mobile phases. Sodium fluoride was obtained from Sigma-Aldrich (Steinheim, Germany).

*2.4.2. Instrumentation*

The separation and quantification of phenolics was performed with an Agilent 1100 model HPLC system (Hewlett-Packard, Waldbronn, Germany), consisting of a quaternary pump with a vacuum degasser, an autosampler, a thermostatted column compartment, a diode array detector (DAD) and a fluorescence detector (FLD). The system was controlled by ChemStation for LC 3D Rev. B.03.02 software.

*2.4.3. Extraction of polyphenols*

Phenolic compounds were extracted from Arbequina olive samples using a previously optimized procedure (Cabrera-Bañegil et al., 2017b). Approximately, 1 g of olive paste was accurately weighed into a 30 mL polypropylene tube. Then, 10 mL of a mixture of methanol and 2 mM sodium NaF (9:1 v/v) was added. The solid-liquid dispersions were sonicated for 40 min at 4 °C, in a P-Selecta ultrasonic bath (model 3000513, Ultrasons 6 L, P-Selecta, Abrera, Barcelona, Spain) as extraction assistance. Afterwards, the sample was centrifuged for 10 min at 4 °C at 10,000 rpm. All supernatant extracts were isolated and filtered, through a 0.22 µm nylon syringe filter (FILTER-LAB, Barcelona, Spain), before injecting into the HPLC system.

*2.4.4. Reversed-phase-HPLC analysis*

Chromatographic separation was performed on a Gemini-NX C18 column (150 × 4.6 mm i.d., 3 µm thickness, Phenomenex, Torrance, CA, USA), following the method of determination of polyphenolic compounds in olive paste described by Cabrera-Bañegil et al. (2017b). The mobile phases A and B were composed of (A) 0.1% formic acid in aqueous phase and (B) 0.1% formic acid in acetonitrile, respectively. The acetonitrile percentage was increased as follows by means of a gradient system: 0–1 min, 3% B; 1–30 min, linear gradient from 3% to 35% B; 30–33 min, from 35% to 50% B; 33–34 min, from 50% to 100%; 34–50 min, 100% B. The column was re-equilibrated for 3 min with 3% B between injections. The injection volume was 10 µL. The flow rate was 1 mL $min^{-1}$ and the column temperature was held constant at 40 °C. Fluorescence detection (FLD) at $\lambda_{ex}/\lambda_{em}$ 275/315 nm allowed the quantification of catechin, epicatechin, hydroxytyrosol, oleuropein, procyanidin B1, procyanidin B2, tyrosol and vanillic acid. An external standard calibration, using peak area as analytical signal, was carried out. The linearity values ranged from 99.30 for hydroxytyrosol to 99.78 for tyrosol. All phenolic detection limits, according to Clayton criterion, were lower than 0.4 mg/L, except for hydroxytyrosol and oleuropein, which were approximately 1.0 mg/L. The chromatographic concentrations of the polyphenolic compounds were above their chromatographic limit of quantification. All of them were lower than 4.0 mg/L, being the lowest for catechin, epicatechin and vanillic acid with values close to 0.5 mg/L.

*2.5. Statistical analysis*

A statistical analysis of data, obtained by both method and with samples subjected to different irrigation treatments, was carried out. The factors involved in the model were: method (chemometric and chromatographic) and irrigation treatments. The model included interactions between each factor for each of the dependent variables. The data were statistically analyzed, by ANOVA and Duncańs multiple range tests, to determine which levels of the factors influenced the dependent variables. Statistical significance was accepted at a confidence level of $p < .05$. The results of two methods with no significant differences were reported as mean values followed by the standard deviation (SD). Data were analyzed using SPSS 18.0 statistical software (SPSS Inc., Chicago, IL, USA).

## 3. Results and discussion

*3.1. Excitation-emission matrices of methanol extracts*

The EEMs of the methanol extracts, obtained from olive paste samples subjected to different irrigation treatments, is shown in Fig. 1. The plots show a visual qualitative display of the presence of different fluorophores in a large emission range. All samples emitted the highest fluorescent radiation, at emission wavelengths at 310 and 340 nm, when the samples are excited at wavelengths between 270 and 285 nm. In this sense, the emission range from the front-face EEMs of methanol extracts was similar to that found in the bibliography (Hernández-Sánchez et al., 2017). Dupuy et al. (2005) mathematically demonstrated that selected phenolic and tocopherol compounds contributed to the fluorescence emission spectra of virgin olive oil, in the emission range between 275 and 400 nm. Furthermore, most of the fluorescence spectra of typical standard phenolic components of olive oils presented their fluorescence emission maxima in the range 362–420 nm, when excited at 270 nm (Tena et al., 2009).

Regarding the different irrigation treatments applied, the fluorescence radiation was more intense in the paste extract of olives obtained in conditions of water stress, thus in the least irrigated samples (T3). On the other hand, the EEMs of the samples from the higher irrigation treatments (C and T1) presented the lowest intensity of fluorescence in this region. These results could indirectly reveal that deficit irrigation applied to the olive trees provoked more synthesis of phenolic compounds in the olive paste, or that the phenolic concentration is high just because of a low moisture content of the water stressed olives. At our best knowledge, there are no data in the literature concerning the application of this innovative instrumental technique, for the quantification of polyphenolic compounds of samples of paste, extracted from olives subjected to different water stress treatments.

Moreover, some EEMs seemed to present two excitation-emission maxima in the registered spectral region. This is the case of flavan-3-ols, such as catechin and epicatechin, which belong to a minor phenolic fraction of the olive fruit, but contributed to a high fluorescence radiation. These compounds do not usually appear in the reports about the presence of phenolic compounds of table olives. However, catechin has been quantified in table olivés varieties after 71 days of fermentation (Kiai and Hafidi, 2014). The intense emission of these compounds was identified at 315–330 nm, as previous researchers have found in native olive oil (Zandomeneghi et al., 2005).

Furthermore, other phenolic compounds, such as tocopherols, which are slightly present in the olive paste, show their fluorescence maxima in the same region as catechin and epicatechin, at excitation wavelength around 296 nm and emission wavelength around 330 nm (Lara-Ortega et al., 2017). They could contribute to a slight interference and overlap of the analytical signal.

A high methanol concentration (91% v/v) was needed to extract phenols and to avoid the extraction of tocopherols, which are potential fluorescence interferents. However, the Arbequina variety exhibits a lower concentration of tocopherols (mainly α, β and γ tocopherols), in the spotted stage of maturation, than other typical varieties (Franco et al., 2014b). In addition, this variety shows the lowest concentration of secoiridoid derivatives of hydroxytyrosol and tyrosol (Franco et al., 2014a).

As it can be observed in Fig. 1, another less intense fluorescence zone was located at 360 nm. In this zone, samples were excited at 260 nm. In red wines, this fluorescence was attributed to vanillic acid (Airado-Rodríguez et al., 2009). The concentration of vanillic acid was found in other table olives varieties (Peres et al., 2016), and also in Arbequina olive oil (Morelló et al., 2004a). This fact could justify the observed fluorescence radiation.

*3.2. PARAFAC*

For the interpretation of PARAFAC, the emission range was restricted from 303 to 450 nm, in order to avoid interferences of Rayleigh signals.

The first step consisted of the choice of the appropriate number of components for building the PARAFAC model. Thus, the basis of core consistency diagnostic was taken to make a decision. The model showed that the core consistency percentages were the following: 100.0, 100.0, 79.3 and 9.5% for one, two, three and four studied components, respectively. Therefore, the three first components were chosen due to their high percentage; this algorithm was used for the following studies to obtain the profile of the main fluorescence components (Fig. 2).

Before registering the fluorescence EEMs of different irrigation samples, the resulting model was validated to verify its reliability and robustness. For that reason, the individual phenolic standard substances were prepared in triplicate, in the same solvent used for the extraction, to verify the wavelength of emission and excitation and to evaluate the accuracy of the results. The information extracted from these individual phenolic standards EEMs served for the subsequent fluorophoreś identification.

The PARAFAC model revealed that the first component excitation profile presented a maximum of excitation at 280 nm, and an emission maximum at 309 nm. The profiles and their maxima were coincident with the fluorescent spectra of catechin and epicatechin. In this case, both phenolic compounds presented the excitation and emission

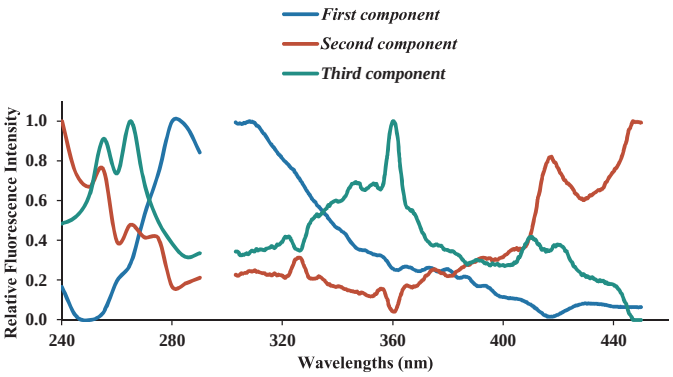


**Fig. 2.** Normalized excitation and emission PARAFAC fluorescence loadings.

maxima pairs at 280/313 nm. Using only the spectral characteristics, it is not possible to associate the second component to any phenolic compound. Not only one but several compounds are presumably contributing to this analytical signal. The third component has an excitation profile with a maximum situated at 265 nm with a shoulder at 255 nm and an emission maximum centered at 360 nm. These spectral characteristics are rather similar to the vanillic acid fluorescence spectrum, with an emission maximum at 360 nm and two excitation peaks at 255 and 265 nm (Fig. 2).

The model obtained with PARAFAC showed the score for each analyte, which represents the contribution of each individual component in the different EEMs data set. In this sense, each EEM can be reconstructed by means of adding the score value of each individual componenťs profile.

### 3.2.1. Identification of fluorophores

Once a previous identification of PARAFAC components on the basis of the fluorescence spectrum was done, it was interesting to evaluate the relationship between the PARAFAC component scores and the concentration of each individual phenolic compound. The concentration was obtained by HPLC-FLD in the methanol extracts of olive paste subjected to different irrigation treatments. For this reason, Fig. 3 examines the correlation between the two reported parameters, in order to find out an equation relating the two variables.

High correlations between the first component scores and epicatechin (R = 0.855) and the sum of catechin and epicatechin concentrations (R = 0.874) were found (Fig. 3). Both plots are important because the epicatechin concentration obtained with chromatography presented similar values, in practically all the samples subjected to different irrigation treatments. The epicatechin concentration was a little higher in the more irrigated samples, while the PARAFAC score differences observed are due to the different catechin chromatographic concentrations. In fact, the score of the samples with severe water stress presented higher catechin concentration.

The samples obtained with more water stress had a high value of oleuropein concentration and a low epicatechin concentration (lower than 0.55 mg/L). A good correlation was found between the second component scores and the oleuropein concentrations (R = 0.892).

In relation with the third component, the PARAFAC score correlated well with vanillic acid obtained by chromatography (R = 0.877). These results are in agreement with those found by Airado-Rodríguez et al. (2009).

These results confirm that the PARAFAC method seems to be useful to identify phenolic compounds in methanol extracts, and it could be a potentially rapid method to determine some of the phenolic compounds present in the olive paste. Furthermore, the biophenolic concentrations in mg/L can be obtained, by converting the scores with the corresponding polyphenol regression equation.

### 3.2.2. Explorative study of the score values

The score values corresponding to each PARAFAC component were plotted against each other, in order to obtain further information from fluorescence data, in order to distinguishing among the different irrigation treatments. The score values of the second PARAFAC component versus the first PARAFAC component allowed to differentiate all irrigation treatments (Fig. 4). The first component scores corresponding to T3 samples were higher than the other irrigation treatments (Control, T1, and T2). In the same way, the second component scores of T2 were smaller than Control, T1 and T3. The Control and T1 scores of the second component were influenced by the low ratio of oleuropein/epicatechin (chromatographic concentrations). The fluorescence of epicatechin could interfere with the second PARAFAC component. T2 and T3 samples showed a higher oleuropein/epicatechin ratio; thus, the contribution of epicatechin to the second component was much lower for these two samples.

Preliminarly, to perform the statistical analysis, polyphenol chemometric concentrations were calculated, introducing the scores in the corresponding phenolic equation obtained in each correlation, according to results obtained in Fig. 3.

Then, the phenolic concentrations of samples submitted to different irrigation treatments, obtained with the two methods, PARAFAC and chromatographic methods, and with the same measurement units (mg/L) were statistically analyzed. For this purpose, a 2-way factorial design was used: the two methods and the different irrigation treatments applied.

The oleuropein concentration of control and T1 samples, and epicatechin concentration of T3 samples, were not considered in this statistical analysis. This decision was made on basis of the oleuropein scores (second component) of control and T1, which were influenced by the noticeable concentrations of epicatechin in these samples. On the other hand, epicatechin concentrations of T3 were low, but the scores of the first component were high due to the influence of the high concentration of catechin in T3 samples. The model included interactions between each factor for each of the dependent variables. The results are presented in Table 1. The phenolic concentrations in the experiment irrigation treatments did not depend on the method used, in fact no significant interaction was found.

Oleuropein is the most important secoiridoid and the precursor of important antioxidant compounds. In general terms, its presence in the olive paste samples was detected in high concentration, in contrast to the data reported for Arbequina variety in previous studies (Morelló et al., 2004b; Artajo et al., 2006). In terms of oleuropein content, a concentration range from 46.8 to 68.1 mg/L was registered. The levels of vanillic acid ranged from 10.7 to 15.3 mg/L in T2 and Control, respectively. Epicatechin plus catechin and epicatechin alone were present as secondary phenolic compounds.

Furthermore, independently of the method used, significant

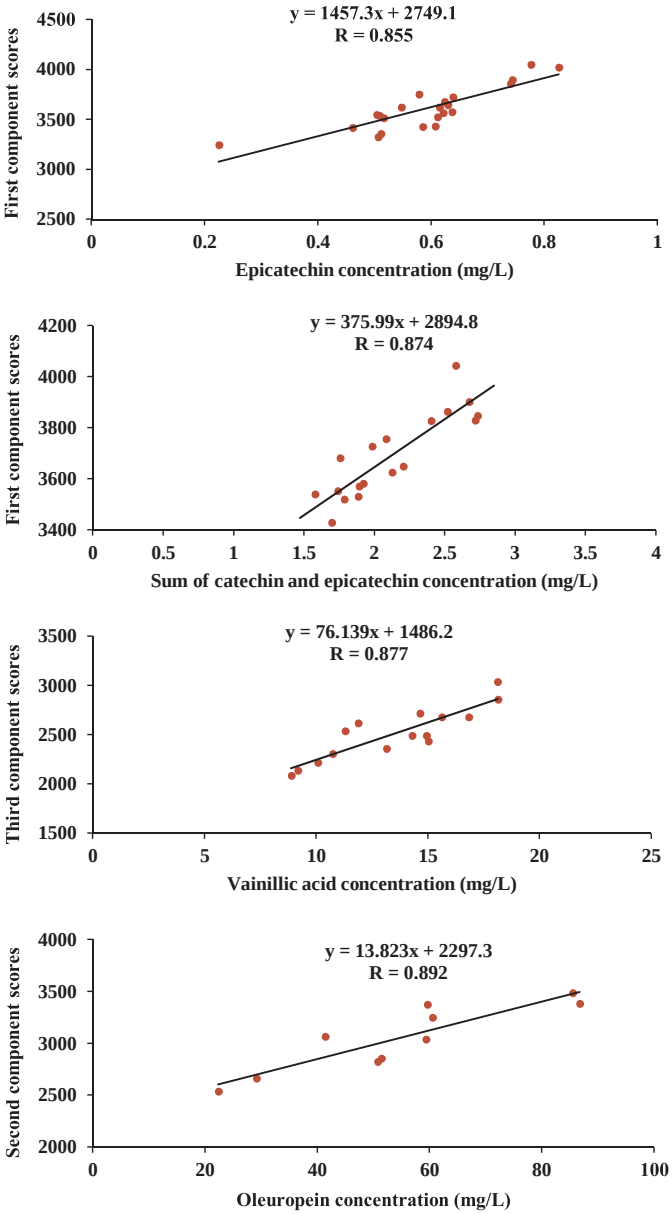


**Fig. 3.** Regression curves between score values and concentration of phenolic compounds obtained by chromatography.

differences in the sum of epicatechin and catechin and epicatechin concentrations were observed, among the irrigation treatments. The epicatechin concentration of T2 was significantly higher than Control and T1; the sum of epicatechin and catechin concentration of T3 and T2 were also significantly higher than Control and T1. The oleuropein concentration of T3 was significantly higher than T2 and the vanillic acid concentration of T2 was significantly lower than the Control, T1 and T3. For this reason, the content of the major phenols was noticeably higher in the olive paste samples from severe water stress (T2 and T3 treatments). This showed that PARAFAC was a good technique to give more information about the quality of the olive paste, and was able to differentiate among different irrigation treatments (T1 and the Control were significantly differentiated from T2 and T3).

This innovative, fast and simple front-face fluorescence method combined with PARAFAC, with a wide range of phenolic concentrations, can serve as a basis for the quantitation of phenolic compounds such as epicatechin, sum of catechin and epicatechin, oleuropein and vanillic acid in olive pastes.

As a practical application, the farmer can be quickly advised, with a tailor-made approach, on the correct irrigation treatments to apply to a specific olive tree variety, in order to gain a better quality of the olives.

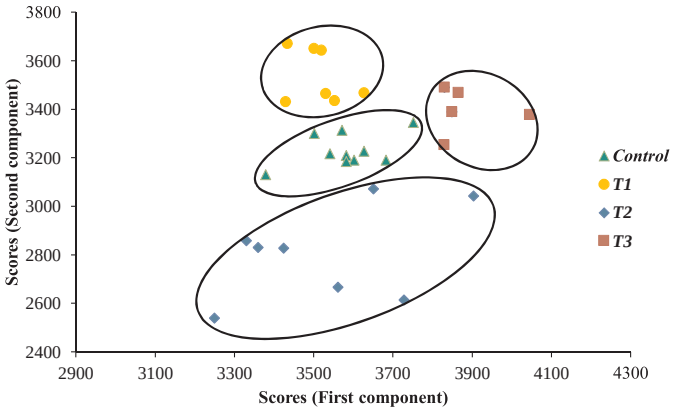


**Fig. 4.** 2D representations of PARAFAC scores corresponding to second component against scores corresponding to the first component. N = 5 olive samples of T3, 8 olive samples of T2, 7 olive samples of T1 and 10 olive samples of the Control.

**Table 1**
Results for the mean and standard deviation (SD) of the biophenolic concentrations (mg/L) in the methanolic extract of olive pastes, by HPLC and by front-face fluorescence, obtained by the two-way ANOVA test. Different small letters in the same column indicate significant statistical differences (Duncańs Test, $p < .05$) between different irrigation treatments. N = 5 olive samples of T3, 8 olive samples of T2, 7 olive samples of T1 and 10 olive samples of the Control.

| Irrigation treatment | Epicatechin + Catechin | Vanillic acid | Oleuropein | Epicatechin |
|---|---|---|---|---|
| Control | 2.05 ± 0.09$^a$ | 15.3 ± 0.6$^b$ | — | 0.61 ± 0.03$^a$ |
| T1 | 1.83 ± 0.09$^a$ | 13.9 ± 0.6$^b$ | — | 0.56 ± 0.02$^a$ |
| T2 | 2.64 ± 0.13$^b$ | 10.7 ± 0.9$^a$ | 46.8 ± 3.3$^a$ | 0.68 ± 0.03$^b$ |
| T3 | 2.60 ± 0.13$^b$ | 14.8 ± 0.9$^b$ | 68.1 ± 4.1$^b$ | — |
| Method x Irrigation treatment interaction | ns | ns | ns | ns |

ns: no significant interactions.

## Acknowledgements

Manuel Cabrera-Bañegil thanks the sponsorship of Comunidad Autónoma de Extremadura, the Consejería de Economía e Infraestructuras and the co-financing of the Fondo Social Europeo (FSE) for the Grant (PD16015). Daniel Martín-Vertedor thanks the sponsorship of Comunidad Autónoma de Extremadura (Consejería de Educación y Empleo) for the grant mobility to the educational personnel and researcher of the University of Extremadura and technological centres of the Comunidad Autónoma de Extremadura in foreign center of higher education and/or research for 2015 (Resolución de 12 de noviembre de 2015, DOE de 26 de noviembre de 2015, n° 228) (MOV15B011). Isabel Durán-Merás is grateful to the Ministerio de Economía y Competitividad of Spain (Project CTQ2017-82496-P) and the Gobierno de Extremadura (GR15090-Research Group FQM003, and IB16058), both cofinanced by the Fondo Social Europeo (FSE).

## References

Airado-Rodríguez, D., Galeano-Díaz, T., Durán-Merás, I., Petter Wold, J., 2009. Usefulness of fluorescence excitation-emission matrices in combination with PARAFAC, as fingerprints of red wines. J. Agric. Food Chem. 57, 1711–1720.

Alegre, S., Marsal, J., Mata, M., Arbones, A., Girona, J., Tovar, M.J., 2000. Regulated deficit irrigation in olive trees (Olea europaea L. cv. Arbequina) for oil production. IV International Symposium on Olive Growing, vol. 586, 259–262.

Artajo, L.S., Romero, M.P., Tovar, M.J., Motilva, M.J., 2006. Effect of irrigation applied to olive trees (*Olea europaea* L.) on phenolic compound transfer during olive oil extraction. Eur. J. Lipid Sci. Technol. 108 (1), 19–27.

Bassani, B., Rossi, T., De Stefano, D., Pizzichini, D., Corradino, P., Macrì, N., Noonan, D.M., Albini, A., Bruno, A., 2016. Potential chemopreventive activities of a polyphenol rich purified extract from olive mill wastewater on colon cancer cells. J. Funct. Foods 27, 236–248.

Binetti, G., Del Coco, L., Ragone, R., Zelasco, S., Perri, E., Montemurro, C., Valentini, R., Naso, D., Fanizzi, F.P., Schena, F.P., 2017. Cultivar classification of Apulian olive oils: use of artificial neural networks for comparing NMR, NIR and merceological data. Food Chem. 219, 131–138.

Bro, R., Kiers, H.A.L., 2003. A new efficient method for determining the number of components in PARAFAC models. J. Chemom. 17, 274.

Bro, R., 1997. Tutorial and applications. Chemom. Intell. Lab. Syst. 38, 149.

Cabrera-Bañegil, M., Hurtado-Sánchez, M.C., Galeano-Díaz, T., Durán-Merás, I., 2017a. Front-face fluorescence spectroscopy combined with second-order multivariate algorithms for the quantification of polyphenols in red wine samples. Food Chem. 220, 168–176.

Cabrera-Bañegil, M., Schaide, T., Manzano, R., Delgado-Adámez, J., Durán-Merás, I., Martín-Vertedor, D., 2017b. Optimization and validation of a rapid liquid chromatography method for determination of the main polyphenolic compounds in table olives and in olive paste. Food Chem. 233, 164–173.

Cayuela, J.A., García, J.F., 2017. Sorting olive oil based on alpha-tocopherol and total tocopherol content using near-infra-red spectroscopy (NIRS) analysis. J. Food Eng. 202, 79–88.

Dagdelen, A., Tümen, G., Musa Özcan, M., Dündar, E., 2013. Phenolics profiles of olive fruits (Olea europea L.) and oils from Ayvalik, Domat and Gemlik varieties at different ripening stages. Food Chem. 136, 41–45.

Difonzo, G., Russo, A., Trani, A., Paradiso, V.M., Ranieri, M., Pasqualone, A., Summo, C., Tamma, G., Silletti, R., Caponio, F., 2017. Green extracts from Coratina olive cultivar leaves: antioxidant characterization and biological activity. J. Funct. Foods 31, 63–70.

Dupuy, N., Le Dreau, Y., Ollivier, D., Artaud, J., Pinatel, C., Kister, J., 2005. Origin of French virgin olive oil registered designation of origin predicted by chemometric analysis of synchronous excitation-emission fluorescence spectra. J. Agric. Food Chem. 24, 9361–9368.

Franco, M.N., Galeano-Díaz, T., López, Ó., Fernández-Bolaños, J.G., Sánchez, J., De Miguel, C., Gil, M.V., Martín-Vertedor, D., 2014a. Phenolic compounds and antioxidant capacity of virgin olive oil. Food Chem. 163, 289–298.

Franco, M.N., Galeano-Díaz, T., Sánchez, J., De Miguel, C., Martín-Vertedor, D., 2014b. Total phenolic compounds and tocopherols profiles of seven olive oil varieties grown in the south-west of Spain. J. Oleo. Sci. 63, 115–125.

Galeano Díaz, T., Durán-Merás, I., Correa, C.A., Roldan, B., Rodríguez Cáceres, M.I., 2003. Simultaneous fluorometric determination of chlorophylls *a* and *b*: and pheophytins *a* and *b* in olive oil by partial least-squares calibration. J. Agric. Food Chem. 51, 6934–6940.

Galeano Díaz, T., Durán-Merás, I., Rodríguez Cáceres, M.I., Roldan Murillo, B., 2006. Comparative of different fluorimetric signals for the simultaneous multivariate determination of tocopherols in vegetables oils. Appl. Spectrosc. 60, 194–202.

Guimet, F., Ferré, J., Boqué, R., Rius, F.X., 2004. Application of unfold principal component analysis and parallel factor analysis to the exploratory analysis of olive oils by means of excitation-emission matrix fluorescence spectroscopy. Anal. Chim. Acta 515, 75–85.

Guimet, F., Ferré, J., Boqué, R., 2005. Rapid detection of olive-pomace oil adulteration in extra virgin olive oils from the protected denomination of origin Siurana using excitation-emission fluorescence spectroscopy and three-way methods of analysis. Anal. Chim. Acta 544, 143–152.

Guzmán, E., Baeten, V., Fernández Pierna, J.A., García-Mesa, J.A., 2012. A portable Raman sensor for the rapid discrimination of olives according to fruit quality. Talanta 93, 94–98.
Hernández-Sánchez, N., Lleó, L., Ammari, F., Cuadrado, T.R., Roger, J.M., 2017. Fast fluorescence spectroscopy methodology to monitor the evolution of extra virgin olive oils under illumination. Food Bioprocess Technol. 10, 949–961.
Kiai, H., Hafidi, A., 2014. Chemical composition changes in four green olive cultivars during spontaneous fermentation. LWT-Food Sci. Technol. 57, 663–670.
Lara-Ortega, F.J., Gilbert-López, B., García-Reyes, J.F., Molina-Díaz, A., 2017. Fast automated determination of total tocopherol content in virgin olive oil using a single multicommuted luminescent flow method. Food Anal. Methods 10, 2125–2131.
Lavee, S., Hanoch, E., Wodner, M., Abramowitch, H., 2007. The effect of predetermined deficit irrigation on the performance of cv: muhasan olives (Olea europaea L.) in the eastern coastal plain of Israel. Sci. Hort. 112, 156–163.
Machado, M., Felizardo, C., Fernandes-Silva, A.A., Nunes, F.M., Barros, A., 2013. Polyphenolic compounds: antioxidant activity and L-phenylalanine ammonia-lyase activity during ripening of olive cv. Cobrançosa under different irrigation regimes. Food Res. Int. 51, 412–421.
Morelló, J.R., Motilva, M.J., Tovar, M.J., Romero, M.P., 2004a. Changes in commercial virgin olive oil (cv *Arbequina*) during storage: with special emphasis on the phenolic fraction. Food Chem. 85, 357–364.
Morelló, J.R., Romero, M.P., Motilva, M.J., 2004b. Effect of the maturation process of the olive fruit on the phenolic fraction of drupes and oils from Arbequina, Farga, and Morrut cultivars. J. Agric. Food Chem. 52 (19), 6002–6009.
Olivieri, A.C., Wu, H.L., Yu, R.Q., 2009. MVC2: a MATLAB graphical interface toolbox for second-order multivariate calibration. Chemom. Intell. Lab. Syst. 96, 246–251.
Peres, F., Martins, L.L., Mourato, M., Vitorino, C., Antunes, P., Ferreira-Dias, S., 2016. Phenolic compounds of Galega Vulgar and Cobrançosa olive oils along early ripening stages. Food Chem. 211, 51–58.
Pistarino, E., Aliakbarian, B., Casazza, A.A., Paini, M., Cosulich, M.E., 2013. Combined effect of starter cultura and temperatura on phenolic compounds during fermentation of Taggiasca black olives. Food Chem. 138, 2043–2049.
Salguero-Chaparro, L., Palagos, B., Peña-Rodríguez, F., Roger, J.M., 2013. Calibration transfer of intact olive NIR spectra between a pre-dispersive instrument and a portable spectrometer. Comput. Electron. Agric. 96, 202–208.
Servili, M., Selvaggini, R., Esposto, S., Taticchi, A., Montedoro, G., Morozzi, G., 2004. Health and sensory properties of virgin olive oil hydrophilic phenols: agronomic and technological aspects of production that affect their occurrence in the oil. J. Chromatogr. A 1054, 113–127.
Talhauoi, N., Taamalli, A., Gómez-Caravaca, A.M., Fernández-Gutiérrez, A., Segura-Carretero, A., 2015. Phenolic compounds in olive leaves: analytical determination, biotic and abiotic influence, and health benefits. Food Res. Int. 77, 92–108.
Tena, N., García-González, D.L., Aparicio, R., 2009. Evaluation of virgin olive oil thermal deterioration by fluorescence spectroscopy. J. Agric. Food Chem. 57, 10505–10511.
Terzuoli, E., Giachetti, A., Ziche, M., Donnini, S., 2016. Hydroxytyrosol, a product from olive oil: reduces colon cancer growth by enhancing epidermal growth factor receptor degradation. Mol. Nutr. Food Res. 60, 519–529.
Tovar, M.J., Romero, M.P., Alegre, S., Girona, J., Motilva, M.J., 2002. Composition and organoleptic characteristics of oil from Arbequina olive (*Olea europaea* L) trees under deficit irrigation. J. Sci. Food Agric. 82, 1755–1763.
Uceda, M., Frías, L., 1975. Harvest dates: evolution of the fruit oil content, oil composition and oil quality. In: Proceedings del Segundo Seminario Oleicola Internacional. COI Córdoba. Córdoba, Spain. pp. 125–128.
Zandomeneghi, M., Carbonaro, L., Caffarata, C., 2005. Fluorescence of vegetable oils: olive oils. J. Agric. Food Chem. 53, 759–766.

# ARTÍCULO 7

## Fluorescence study of four olive varieties paste according to sampling dates and the control in the elaboration of table olives of "Ascolana tenera"

Manuel Cabrera-Bañegil, Daniel Martín-Vertedor, Enrico Maria Lodolini, Isabel Durán-Merás

*Food Analytical Methods,* ***2021****, 14, 307-318*
*DOI: https://doi.org/10.1007/s12161-020-01882-5*

Food Analytical Methods (2021) 14:307–318
https://doi.org/10.1007/s12161-020-01882-5

# Fluorescence Study of Four Olive Varieties Paste According to Sampling Dates and the Control in the Elaboration of Table Olives of "Ascolana tenera"

Manuel Cabrera-Bañegil[1,2] · Daniel Martín-Vertedor[2] · Enrico Maria Lodolini[3] · Isabel Durán-Merás[1]

Received: 28 November 2019 / Accepted: 12 October 2020 / Published online: 17 October 2020


**Abstract**
A fluorescence method combined with chemometric algorithms has been developed for the fruit characterization of four olive varieties ("Arbequina," "Piantone di Falerone," "Piantone di Mogliano," and "Maurino") cultivated in Marche (Italy) according to sampling dates. The score values obtained by parallel factor analysis (PARAFAC) were correlated with the hydroxytyrosol and oleuropein concentrations quantified by liquid chromatographic. The analysis of excitation-emission matrices by PARAFAC and unfolding partial least squares, using the three component score values, allowed to differentiate between varieties. The use of the scores of oleuropein and hydroxytyrosol, which were represented each other, allowed to highlight differences between the three sampling dates. Furthermore, a good discrimination of fresh olive, lye table olives, and natural table olives was also achieved in "Ascolana tenera," another typical olive variety of Marche. Results can be explained by the changes of concentration of tyrosol and oleuropein due to the elaboration method characteristics.

**Keywords** Olive varieties · Phenolic compounds · Maturation stage · Oleuropein · Hydroxytyrosol

## Introduction

The olive tree (*Olea europaea* L.) is one of the most important fruit tree species in the Mediterranean basin. The main commercial products obtained from the olive tree are table olives and virgin olive oils. Although, the traditional tendency is to produce virgin olive oil from ripe fruits due to the high fat content, several studies have been performed to determine the effect of fruit ripening stage on the quality and chemical composition of the olives (Vergara-Domínguez et al. 2016; Sousa et al. 2015) and of the produced oils (Gouvinhas et al. 2015, Köseoglu et al. 2016; Peres et al. 2016; Brahim et al. 2017). The ripening stage has a strong impact on the yield and quality of the oil and of the table olives. Accordingly, it is necessary to develop a methodology for determining the best harvest time for each variety in order to optimize the productivity of the groves and obtain high-quality final product.

On the other hand, since monocultivar olive is given rising in a high-quality table olives, this market is increasing rapidly. In this context, cultivar identification is pivotal for growers, producers, and exporters, and robust and fast analytical tools are required to fulfill these goals.

With regard to non-destructive and rapid method for analyzing chemical composition of olive paste, information about size and mass estimation of olive fruits has been obtained by computer vision techniques (Ponce et al. 2019). Information about cultivar classifications and characterizations of olive oils has been obtained by nuclear magnetic resonance (Binetti et al. 2017; Ruiz-Aracama et al. 2017; Camin et al. 2016), image processing techniques (Beyaz et al. 2017), and electrical conductivity (Justicia et al. 2017). It is also interesting to determine the optimal harvesting time according to quality parameters in non-destructive fruit samples by near infrared spectroscopy (Fernández-Espinosa 2016; Salguero-Chaparro et al. 2013). Another analytical non-destructive technique is the fluorescence spectroscopy. This technique has been extensively used in the analysis of virgin olive oils for the commercial classification (Durán-Merás et al. 2018,

✉ Manuel Cabrera-Bañegil
manuelcb@unex.es

[1] Department of Analytical Chemistry, Faculty of Sciences, University of Extremadura, Avda. de Elvas S/N, 06006 Badajoz, Spain

[2] Technological Institute of Food and Agriculture (CICYTEX-INTAEX), Junta of Extremadura, Avda. Adolfo Suárez S/N, 06007 Badajoz, Spain

[3] Research Centre for Olive, Fruit and Citrus Crops, Council for Agricultural Research and Economics, Via di Fioranello, 52, 00134 Rome, Italy

Domínguez-Manzano et al. 2019; Guimet et al. 2006) or for the detection and quantification of specific chemical compounds (Galeano-Díaz et al. Galeano Díaz et al. 2003, Galeano Díaz et al. 2006). Nevertheless, this technique has not yet been used for direct analysis of olive fruit (Cabrera-Bañegil et al. 2018).

Italy is exceptionally rich in traditional foods and dishes, and their production has been transferred from generation to generation. The composition analysis can constitute interesting additional information about these traditional products (Durazzo et al. 2017). In this context, in the Marche region (central Italy), a high caliber olive variety, named "Ascolana tenera," plays an important role in the elaboration of Ascolana-style olives, which is highly appreciated by gourmets for the crisp, juicy flesh, and delicate flavor, and for local traditional preparations. In particular, the stuffed Ascolana-style olives are prepared from treated green olives in brine from "Ascolana tenera" variety which constitutes a Protected Denomination Origin "Oliva Ascolana del Piceno" since 2005. Ascolana-style olives are filled with triturated meat stuff (beef 40–70%, pork 30–50,; chicken/turkey max 10%) browned with onion, carrot, and celery in olive oil and cooked on low heat with the addition of dry white wine and salt (Lanza 2012).

The Ascolana-style table olive elaboration required a huge investment in terms of time, energy, and costs, because the fruits are very susceptible to damage. While the optimal varieties of olive fruit for Greek and Spanish style are sturdy and can be managed without damages appearance, the "Ascolana tenera" variety shows a very sensible skin and a fleshy pulp, so that it requires more care during picking operations and transport. The higher management costs lead this variety to be less competitive in comparison to other varieties in the international markets but can be valorized in niche markets. For this reason, the set-up of quality monitoring methodology is convenient for assessing the final product standardization.

The objective of this study was to characterize the excitation-emission fluorescence matrices of the olive fruit extracts from four olive varieties cultivated in central Italy according to different sampling dates in order to identify the best harvest time per each studied cultivar. The aim of the research was to study the physic-chemical changes of the fruits during ripening, and to compare the obtained results between cultivars. Moreover, the "Ascolana tenera" fresh fruit and the natural and lye table elaborations were compared according to their fluorescence profiles in each elaboration stage to assess high quality product standardization.

## Material and Methods

### Experimental Fields and Olive Varieties

The study was performed in 2016 in three high-density (4 m × 2 m; 1250 tree $ha^{-1}$) drip-irrigated olive orchards in Marche region (central Italy), i.e., Agugliano (latitude 43° 32′ 53″ N; longitude 13° 21′ 58″ E; altitude 85 m a.s.l.), Fermo (latitude 43° 06′ 05.62″ N; longitude 13° 39′ 29.52″ E; altitude 200 m a.s.l.), and Maiolati Spontini (latitude 43° 28′ 37″ N; longitude 13° 07′ 09″ E; altitude 405 m a.s.l.), respectively.

Four olive varieties ("Piantone di Mogliano," "Piantone di Falerone," "Arbequina," and "Maurino") were selected for the study in each experimental orchard with the exception of "Maurino" that was not present in Maiolati Spontini.

### Fruit Measurements and Sampling

Destructive measurements on the fruits were performed in each of the experimental fields every 12 days during ripening, starting from 22 September until 28 October 2016. Ten healthy fruits were collected from ten homogeneous trees (total 100 fruits per varieties in each field) and the maturation index for each variety was calculated according to Beltran et al. (2004) in the three sampling dates. Data are shown in Table 1.

One hundred additional fruits were collected from 10 trees (10 fruits per tree) in each sampling dates, and immediately transported to the laboratory in ventilated and refrigerated storage trays to avoid compositional changes. Some samples of fruit were crushed with a hammer mill. Then, the obtained paste was stored away from the light in amber-colored glass bottles at − 80 °C until analysis (within 1 month).

### "Ascolana tenera" Table Olives Treatment

"Ascolana tenera" fresh olives with maturation index around 1.0 were collected in the olive orchard located in Fermo and

**Table 1** Maturation index of the fruit in the field for "Arbequina," "Piantone di Falerone," "Maurino," and "Piantone di Mogliano" calculated according to Beltran et al. (2004) in the three considered date of sampling. Different letters indicate significant differences between date of sampling within each olive variety (Tukey's test, $p < 0.05$)

| Date of sampling | "Piantone di Mogliano" | "Piantone di Falerone" | "Arbequina" | "Maurino" |
|---|---|---|---|---|
| First date of sampling | 1.0 ± 0.1a | 1.5 ± 0.7a | 0.6 ± 0.5a | 1.6 ± 0.4a |
| Second date of sampling | 1.6 ± 0.8a | 2.9 ± 0.7b | 1.6 ± 0.8a | 3.2 ± 0.2b |
| Third date of sampling | 3.0 ± 0.4b | 4.2 ± 0.1c | 3.5 ± 0.4b | 4.3 ± 0.1c |

processed according to the Spanish style and natural fermentation (Lodolini et al. 2019). With regard to Spanish style, olive fruits were immersed in 2.5% (w/v) NaOH solution at room temperature (25 °C) until the alkali reached 2/3 of the flesh measured moving from the epidermis to the pit. The NaOH solution was removed by flushing with tap water. Finally, the table olives were placed into a freshly prepared 10% (w/v) NaCl brine. Table olives were sampled immediately after the lye treatment followed by a wash (lye and wash olives).

Table olives of raw material from the same variety were also sampled and they started to be fermented in a natural way, with a spontaneous fermentation (natural table olives). All the fermentation tanks had a capacity of 225 L for about 154 kg of table olives.

## Reagents, Solvents, and Phenolic Standards

Polyphenol analytical standards hydroxytyrosol, oleuropein, procyanidin B1, procyanidin B2 were supplied from the Extrasynthése (Genay, France); and gallic acid monohydrate, tyrosol, and vanillic acid from the Sigma-Aldrich Chemie (Steinheim, Germany). P.A. grade formic acid was obtained from the PANREAC (Barcelona, Spain), and sodium fluoride was supplied by the Sigma-Aldrich Chemie (Steinheim, Germany). HPLC grade acetonitrile and HPLC grade methanol were supplied from the Fisher chemical (Loughborough, UK).

## Instrumentation

Excitation emission matrices (EEMs) were registered using a fluorescence spectrophotometer Varian Model Cary Eclipse, equipped with two Czerny-Turner monochromators (excitation and emission), a xenon light source. The Cary Elipse 1.0 software was used for data acquisitions.

The chromatographic phenolic quantification was performed on Agilent 1100 model HPLC system (Hewlett-Packard, Waldbronn, Germany) controlled by ChemStation for LC 3D system Rev. B.03.02 software.

## Analytical Procedures

### Extraction of Polyphenols

Two grams of homogenized olive paste sample were placed into a polypropylene tube and 10 mL of solvent, composed by methanol and NaF 2 mM, was added. The tubes were subjected to ultrasonic extraction during 30 min and centrifuged at 10,000 rpm during 10 min at 4 °C. The supernatant extracts were filtered through 0.22 μm nylon syringe filter (FILTER-LAB, Barcelona, Spain). The filtered extracts were also analyzed by liquid chromatography following the method proposed by Cabrera-Bañegil et al. (2017).

### Fluorescence Method

The EEMs of olive paste varieties were obtained in the excitation range from 380 and 470 nm (5 nm steps), and emission range from 480 and 600 nm (5 nm steps).

With regard to "Ascolana tenera" table olives, the excitation range of EEMs was from 260 and 295, with resolution of 5 nm, and the emission range from 305 to 350 with resolution of 1 nm. Another range consisted of excitation range comprised between 315 and 365 nm, with resolution of 5 nm, and emission range between 390 and 550 nm with resolution of 1 nm.

For all measurements, both of the slits of excitation and emission monochromators were set at 5 nm. The photomultiplier tube sensitivity was 600 V, and scan rate was of 600 nm $min^{-1}$.

**Chromatographic Conditions** Chromatographic analyses were performed using an Agilent 1100 model LC system (Hewlett-Packard, Waldbronn, Germany) equipped with an UV−Vis diode-array detector and a rapid scan fluorescence spectrophotometer detector (FLD). Separation was executed using a Phenomenex Gemini-NX C18 column (150 × 4.6 mm i.d., 3 μm particle size; Phenomenex, Torrance, CA, USA). The mobile phases are composed of (A) 0.1% formic acid in aqueous phase and (B) 0.1% formic acid in acetonitrile. The gradient system was applied as follows: 0–1 min, 3% B; 1–30 min, linear gradient from 3 to 35% B; 30–33 min, from 3% to 50% B; 33–34 min, from 50 to 100%; 34–50 min, 100% B isocratic. The injection volume of 10 μL and the flow rate of 1 mL $min^{-1}$ at 40 °C were used. The FLD at 275/315 nm was applied for determination of hydroxytyrosol, tyrosol, epicatechin, and oleuropein (Cabrera-Bañegil et al. 2017).

## Chemometric Treatment

For varieties and sampling dates analysis, a PARAFAC model was built using the EEMs of a set of 90 EEMs corresponding to 24 EEMs for "Arbequina," " and 'Piantone di Mogliano," respectively, and 18 EEMs for "Maurino." The EEMs of all samples were arranged in a three-dimensional structure with a size of 90 × 25 × 19 (samples × number of emission wavelengths × number of excitation wavelengths). For "Ascolana tenera" analysis, a PARAFAC model was built using the EEMs of a set of 27 EEMs corresponding to 9 EEMs for fresh olive fruit, lye-wash olives, and natural table olives. The EEMs of all samples were arranged in a three-dimensional structure with a size of 27 × 10 × 8 (samples × number of emission wavelengths × number of excitation wavelengths).

Both arrays were decomposed by PARAFAC applying the core consistency diagnostic tool for optimization of the

number of components (Bro 2003). In all cases, non-negative constraints for resolved profiles for all modes were applied.

Furthermore, for identification of corresponding fluorophores, in both cases, a simple regression analysis was completed to evaluate the linear approach to modeling the relationship between chromatographic phenol contents and the component scores obtained by PARAFAC. The coefficient of determination (*R*-squared values) was calculated to find out the fluorophores in the fluorescent-dependent response variable.

According to Cabrera-Bañegil et al. (2019), linear discriminant analysis was applied for the score matrix of PARAFAC in order to separate sample groups, by establishing a linear discriminant function that maximizes the ratio of the between class and within-class variances (Berrueta et al. 2007; Kemsley 1998). Discriminant analysis unfolding partial least squares regression using codes representing the class label instead of concentrations has been applied for classification purposes.

For the studied sampling dates, an initial explorative analysis of the score values of each component has been carried out plotting each other. This was carried out by means of a calibration considering six samples for each sampling date, and the validation was carried out with three samples for each sampling date. For distinguishing the cultivars in pairs, three components were required; the scores were represented in a tridimensional plot using 95% confidence level ellipses over the three planes defined by the corresponding axes.

### Statistical Analysis

SPSS 18.0 software was used (SPSS, Inc., Chicago, IL, USA) to compare the differences between the three considered sampling date in each variety studied ("Arbequina," "Piantone di Falerone," "Maurino," and "Piantone di Mogliano") for the maturation index and phenolic concentration using a one-way analysis of variance (ANOVA), followed by Tukey's multiple range test. Statistical significance was accepted at a level of $p < 0.05$. Data were expressed as mean ± standard deviation.

## Results and Discussion

The fluorescence method was performed on olive pastes (destructive technique) to characterize the fruit chemical components on four olive varieties ("Arbequina," "Piantone di Falerone," "Piantone di Mogliano," and "Maurino") according to sampling date and on a sensitive variety ("Ascolana tenera") during the manipulation process.

### Fluorescence Excitation-Emission Matrices

The excitation-emission matrices of the olive extracts in different sampling dates were registered, Fig. 1. In all EEMs, two fluorescent regions were observed. The highest intensity signal in the first sampling date of all studied varieties had an excitation/emission wavelength pair located at 470/530 nm.

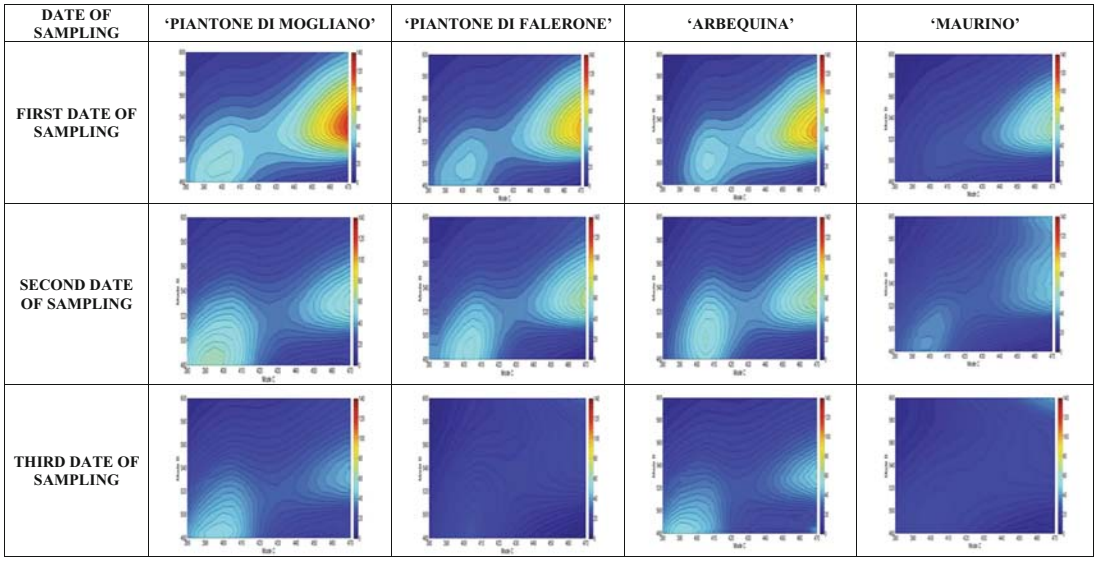


**Fig. 1** Fluorescence contour plots of olive paste samples (destructive technique) for "Piantone di Moglano," "Piantone di Falerone," "Arbequina," and "Maurino" cultivars in three maturation stages

Kyriakidis and Skarkalis (2000) found an intense emission peak at 525 nm in the fluorescence spectrum of virgin olive oils. Their study suggested that the peak at 525 nm could be at least partly originated from vitamin E. Guzmán et al. (2015) attributed the very low intensity of the peaks at 445 and 475 nm to the high content of monounsaturated fatty acids and phenolic antioxidants in virgin olive oils. Hernández-Sánchez et al. (2017) registered fluorescent emission peaks at 444, 466, and 511 nm, among others, in virgin olive oils whose fluorescence evolution was monitored along indirect light exposition for 2 months.

With regard to fluorescence study of different varieties, EEMs of "Piantone di Falerone," "Piantone di Mogliano," and "Arbequina" varieties present similar contour maps in the two first sampling date. Although "Piantone di Mogliano" showed the highest fluorescent intensity region in the first sampling date. The fluorescence intensity of "Piantone di Mogliano," " and 'Arbequina" was rather similar in the second sampling date. In the third sampling date, "Piantone di Falerone" olive paste samples showed weaker fluorescent EEMs than those obtained from "Piantone di Mogliano" and "Arbequina." This trend is in accordance with the fruit maturation index recorded in the field: "Piantone di Falerone," in the sampling date, showed higher values than "Piantone di Mogliano" and "Arbequina." On the other hand, "Maurino" EEMs showed clearly different contour maps in comparison to the other studied varieties in all sampling dates. The EEMs of "Maurino" and "Piantone di Falerone" in the third sampling date are quite similar. In this sampling date, both of them presented the same value of maturation index.

It can be observed that the fluorescence signal of EEMs generally decreased along maturation in all the studied varieties. The relationship between the fluorescence signal and the maturation index recorded in the file showed an inverse relationship. The maturation index increased according to fruit ripening while the fluorescence signal of "Piantone di Falerone" and "Maurino" practically disappeared at the third maturation stage (the highest maturation index). This is in accordance with the general loss of total phenolic compounds registered with the proceeding of the ripening of the fruits (Brahim et al. 2017; Navajas-Porras et al. 2020).

In order to know the evolution of the concentrations of the main fluorescent polyphenolic compounds, the olive paste samples were analyzed by chromatography (Table 2). Oleuropein concentration of the first sampling date was significantly higher in "Arbequina," "Piantone di Falerone," and "Piantone di Mogliano" than on the rest of sampling dates. Also, in other studies, the highest oleuropein concentration was registered at first sampling date, i.e., in "Ayvalik," "Domat" (Dagdelen et al. 2013), and "Manzanilla" varieties (Crawford et al. 2018). No significant differences of oleuropein concentrations were found in "Maurino" in the three sampling dates. In "Sariulak," the highest oleuropein concentration was always recorded in an intermediate harvest date (Arslan and Özcan 2011), whereas in "Galega Vulgar" and "Cobrançosa" varieties, the highest oleuropein concentrations was found in an intermediate and late sampling date, respectively (Ferro et al. 2020). Hydroxytyrosol was higher in the third sampling date in "Arbequina" variety than on the rest of sampling dates. Same result was found in "Manzanilla"

**Table 2** Fluorescent phenolic profile in mg $kg^{-1}$ of the fruit in the field for "Arbequina," "Piantone di Falerone," "Maurino," and "Piantone di Mogliano" in the three considered date of sampling. Different letters indicate significant differences between date of sampling within each olive variety (Tukey's test, $p < 0.05$)

| Olive variety | Phenolic compound | First date of sampling (mg $kg^{-1}$) | Second date of sampling (mg $kg^{-1}$) | Third date of sampling (mg $kg^{-1}$) |
|---|---|---|---|---|
| Arbequina | Oleuropein | 153 ± 12b | 113 ± 10a | 102 ± 10a |
| | Hydroxytyrosol | 414 ± 22a | 428 ± 15a | 468 ± 18b |
| | Tyrosol | 11 ± 1b | 21 ± 1c | 5 ± 1a |
| | Epicatechin | 35 ± 3c | 25 ± 4b | 11 ± 1a |
| Piantone di Falerone | Oleuropein | 525 ± 27b | 293 ± 24a | 219 ± 27a |
| | Hydroxytyrosol | 1180 ± 34 ns | 1191 ± 43 | 1112 ± 34 |
| | Tyrosol | 31 ± 1 ns | 33 ± 1 | 27 ± 2 |
| | Epicatechin | 38 ± 3c | 32 ± 2b | 24 ± 6a |
| Piantone di Mogliano | Oleuropein | 326 ± 10b | 214 ± 5a | 226 ± 8a |
| | Hydroxytyrosol | 753 ± 15 ns | 790 ± 37 | 766 ± 18 |
| | Tyrosol | 37 ± 3a | 42 ± 6a | 48 ± 5b |
| | Epicatechin | 22 ± 2b | 21 ± 3b | 11 ± 2a |
| Maurino | Oleuropein | 111 ± 10 ns | 127 ± 11 | 102 ± 14 |
| | Hydroxytyrosol | 1606 ± 73b | 1127 ± 68a | 947 ± 80a |
| | Tyrosol | 21 ± 2a | 26 ± 2b | 19 ± 1a |
| | Epicatechin | 18 ± 1c | 15 ± 1b | 6 ± 1a |

whose concentration of hydroxytyrosol was the highest in the last sampling date (Crawford et al. 2018). In "Maurino," this phenol was higher in the first sampling date than the other ones. Similar tendency was found in "Frantoio" where hydroxytyrosol concentration showed the lowest values during the last sampling date (Alowaiesh et al. 2018). In "Piantone di Falerone" and in "Piantone di Mogliano," no significant differences in hydroxytyrosol according to sampling date were observed. In the varieties "Domat" and "Gemlik," the hydroxytirosol concentration was similar and low in almost sampling dates from August to December (Dagdelen et al. 2013). The concentration of tyrosol was higher in the second sampling date in "Arbequina," "Piantone di Fallerone," and "Maurino." In "Sariulak" variety, in Silifke location, it was found that tyrosol concentration was the highest in the intermediate sampling dates (Arslan and Özcan 2011). On the other hand, in "Ayvalık," "Domat," "Frantoio," and "Manzanilla" varieties, the tyrosol concentration decreased during maturation (Dagdelen et al. 2013; Alowaiesh et al. 2018). In the four-essayed cultivars, epicatechin decreased according to the later sampling date.

## Fluorophores Identification

In this work, core consistency diagnostic (CORCONDIA) (Bro 2003) was used to estimate the adequate number of components and three factors were selected.

With regard to the three most relevant loadings, Fig. 2, the PARAFAC model revealed that the first component excitation profile showed an emission maximum at 525 nm wavelength (Fig. 2a). The third component had an excitation profile with a peak at 400 nm (Fig. 2b) and an emission maximum centered at 490 nm (Fig. 2a).

Once a previous identification of PARAFAC components on the basis of the fluorescence spectrum was done, it was interesting to evaluate the relationship between the PARAFAC component scores and the concentration of each individual phenolic compound obtained by HPLC-FLD in the different olive varieties. A complete phenolic profile was obtained according to those obtained by Cabrera-Bañegil et al. (2017). For this reason, Fig. 2 examines the correlation between the two reported parameters. A correlation ($R^2 = 0.783$) between the first

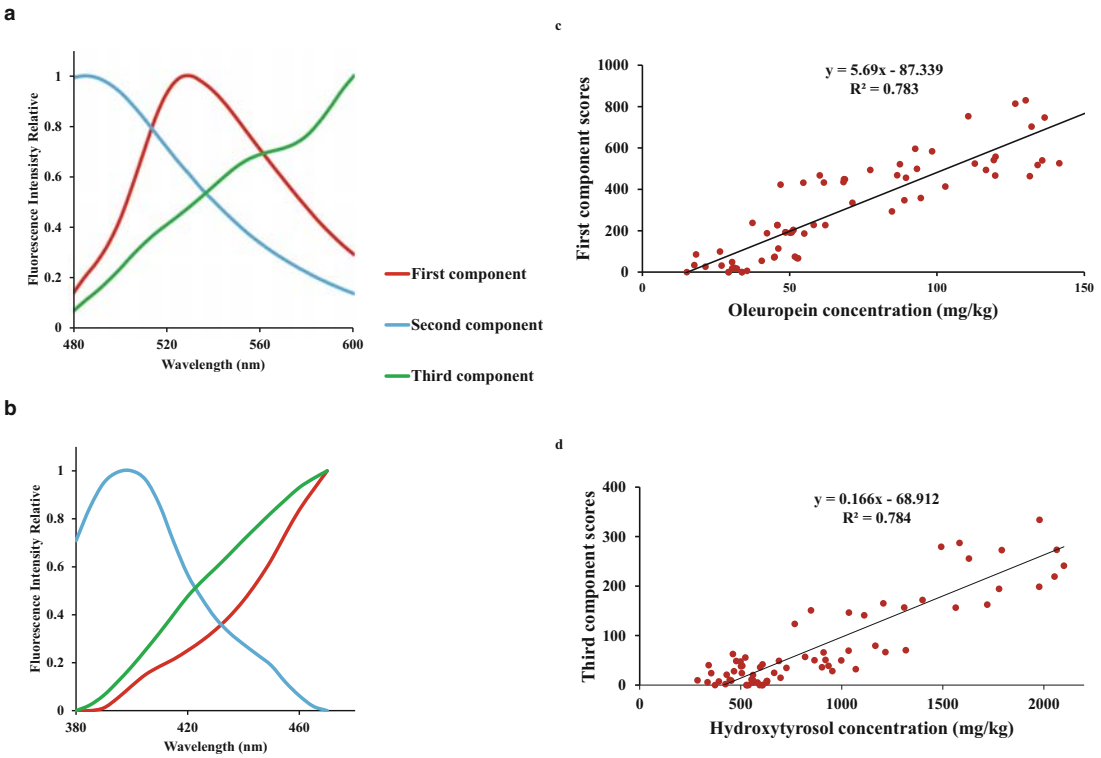


**Fig. 2** **a** Emission loadings. **b** Excitation loadings. **c** Regression curves between score values and oleuropein concentration obtained by chromatography in mg/kg. **d** Regression curves between score values and hydroxytyrosol concentration obtained by chromatography in mg/kg

component scores and oleuropein was found (Fig. 2c). This compound has already been predicted in olive leaves by means of mid-infrared spectroscopy following a similar chemometric methodology (Aouidi et al. 2012). On the other hand, a similar correlation ($R^2 = 0.784$) between the third component scores and hydroxytyrosol was found (Fig. 2d). Both studied compounds have exerted a powerful antioxidant activity in olive leaves (Lee and Lee 2010) and have been fluorescently characterized by a similar methodology by Cabrera-Bañegil et al. (2018) in "Arbequina" olive samples subjected to water stress.

## Classification of EEMs According to Varieties and Sampling Dates

PARAFAC and LDA-PARAFAC classification models were built. LDA was used to improve discrimination between groups that were difficult to separate using PARAFAC. Figure 3 shows the tridimensional plots of the canonical vector score values. The use of the scores of three components represented in tridimensional way was necessary for the suitable separation between classes. As a result, "Piantone di Mogliano" was separated from "Piantone di Falerone" and "Arbequina" but they could not significantly be separated at 95% of confidence. "Maurino" was clearly differentiated from "Piantone di Mogliano" and "Arbequina" by means of two essayed algorithms. In addition to this, the PARAFAC 95% confident ellipses showed complete separation of "Maurino" samples from "Piantone di Mogliano" and "Arbequina." A good discrimination of "Piantone di Falerone" and "Arbequina" olive samples could be achieved by PARAFAC and LDA, both of them at 90% of confidence.

DU-PLS cross-validation and the Haaland and Thomas criterion (Haaland et al. 1988a, b) were employed to choose the optimum number of factor or latent variables, which are those given a PRESS value statistically no difference to the minimum PRESS value (*F*-ratio probability falling below 0.75). Thirty-eight calibration samples were used as training set, and at each sample the code for each category (1 for one olive variety and 2 for another variety) was assigned. The predicted versus nominal code values are shown in Fig. 2. DU-PLS results showed a highly discriminant model using three PLS factors, capable to obtain 100% of correct classification for all studied varieties. Furthermore, the deviation of "Piantone di Falerone" and "Arbequina" was the lowest when they were analyzed each other.

Considering the potential of fluorescence, this paper reports a fast methodology for assessing the traceability of single variety and the quality of the final product. Consumers are demanding for the variety label of the olives because it can be a way to guarantee the origin of the product.

## Sampling Dates Classifications

A similar study has been carried out using the maturation stage as categorical variables with the use PARAFAC. The only use of scores of first represented against scores of third component allowed the best separation between the tree maturation stages. In this way, Fig. 4 reports the scores of first component versus those of the third one for the three studied maturation stages. Loadings of "Piantone di Mogliano," "Arbequina," and "Piantone di Falerone" set of olive paste samples showed the same component order with the first component, whose emission maximum was at 525 nm, the third component with the excitation and emission peak at 400 and 490 nm wavelength, respectively. Loadings of "Maurino" set of samples were inverted: the first and the third components presented an emission peak at 490525 nm, respectively.

The first maturation stage could be separated from the other maturation stages because it exhibits the highest first component scores in the varieties "Piantone di Mogliano," "Piantone di Falerone," and "Arbequina." In this maturation stage, both of them presented low and similar maturation index. This was similar in the variety "Maurino," where the scores of the third component were the highest. The third maturation stage had the lowest third component scores in "Maurino." The scores of "Piantone di Falerone" and "Maurino" decreased in accordance with ripening, proceeding in the first and third component, respectively. For this reason, the similarity between the maturation evolutions of these two varieties was the reason why they could not be correctly separated with a 95% of confidence. Besides, the location where the olive trees were cultivated influenced the third maturation stage of the four studied olive varieties.

## Fluorescence Study of "Ascolana tenera" Elaboration

All the "Ascolana tenera" olive paste samples emitted a fluorescent radiation at a wavelength of 310 nm when the samples were excited at wavelengths between 280 and 290 nm. These fluorescence signals of natural table olives were the highest. Fluorescence differences between fruit paste of "Ascolana tenera" before and after lye-wash processing were not found.

For the classifications, a set of two kinds of samples was built. In the case of PARAFAC, the first step consisted of the choice of the suitable number of components necessary for explaining the obtained fluorescence. In the three classifications, three PARAFAC components were chosen because they showed no overlapping and independent loadings. The PARAFAC model revealed that the first component excitation profile presented a peak of excitation at 280 nm and the emission maximum was at 315 nm. The observed high fluorescence of the paste samples corresponded to the first

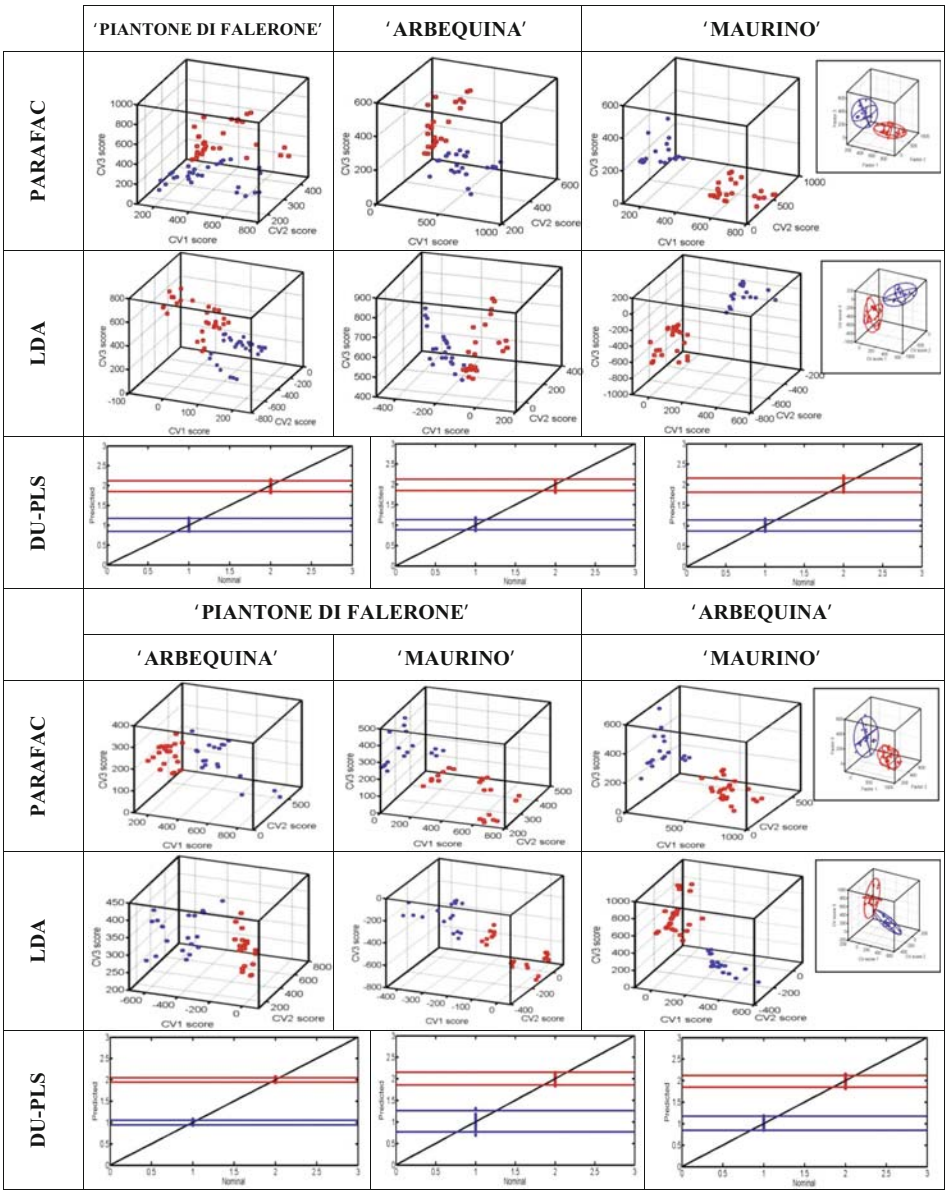


17

**Fig. 3** PARAFAC, LDA, and DU-PLS classification of "Piantone di Mogliano" vs "Piantone di Falerone," "Piantone di Mogliano" vs "Arbequina," "Piantone di Mogliano" vs "Maurino," "Piantone di Falerone" vs "Arbequina," "Piantone di Falerone" vs "Maurino," "Arbequina" vs "Maurino." PARAFAC scores and LDA-PARAFAC CV scores of a set of 48 olive paste samples (destructive technique), composed by one olive variety (24 samples) and another olive variety (24 samples). A total of 18 "Maurino" olive samples were analyzed with a total set of 36 olive paste samples (destructive technique). Three-dimensional projection of the 95% confidence ellipse for PARAFAC and LDA analysis of the data collected from each type of olive variety. Plot of the DU-PLS predicted vs nominal coded

component in all cases. The other fluorescent components were not representative in the registered EEMs and their information was only used for classifications.

For possible fluorophores identifications, the relationship between the PARAFAC component scores and the concentration of the olive samples obtained by HPLC-FLD was

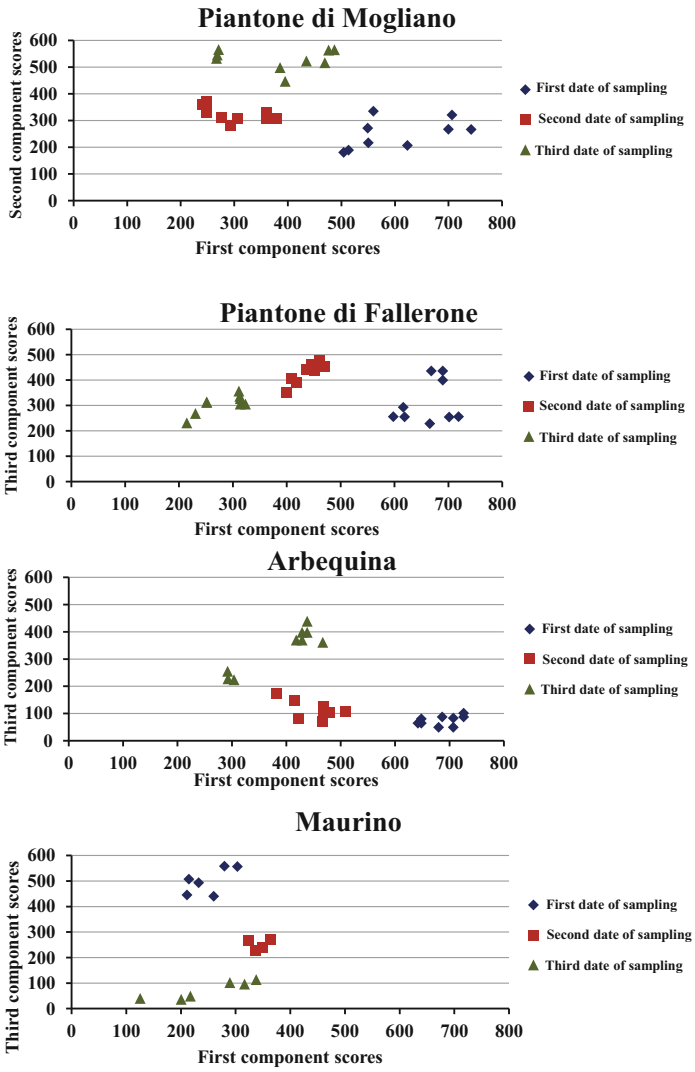


**Fig. 4** Bidimensional PARAFAC classification of three analyzed date of sampling of olive paste samples (destructive technique). PARAFAC scores of a set of 24 samples. A total of 8 olive paste samples constituted each date of sampling, except "Maurino" samples with 6 olive paste samples

evaluated. A high correlation ($R^2 = 0.981$) between the first component scores and tyrosol concentrations was found. The tyrosol concentration was higher in the natural table olive samples. Pistarino et al. (2013) found that tyrosol concentration increased in the brines during the fermentation because of the hydrolysis derivate from salidroside (Ben Othman et al. 2009). While the tyrosol concentrations of fresh and lye olive samples were lower than natural table olives, tyrosol concentrations of lye and wash samples were slightly higher in the lye olive samples.

In order to explore the discriminating power of the models, the set of the score values obtained with the non-supervised PARAFAC model for the first three components were represented in a tridimensional plot, according to elaboration, Fig. 5. On the other hand, and with the objective to compare the results with LDA-PARAFAC, in the same Fig. 5, the cultivar scores of the samples were included. In both cases and to make the visualization of pairwise comparison easier, each plot includes the projections of the 95% confidence level ellipses over the three planes defined by the corresponding axes. With these approaches, it was possible to discriminate by pairs between fresh, lye olives, and natural samples. In all cases, with LDA-PARAFAC, better discrimination was obtained.

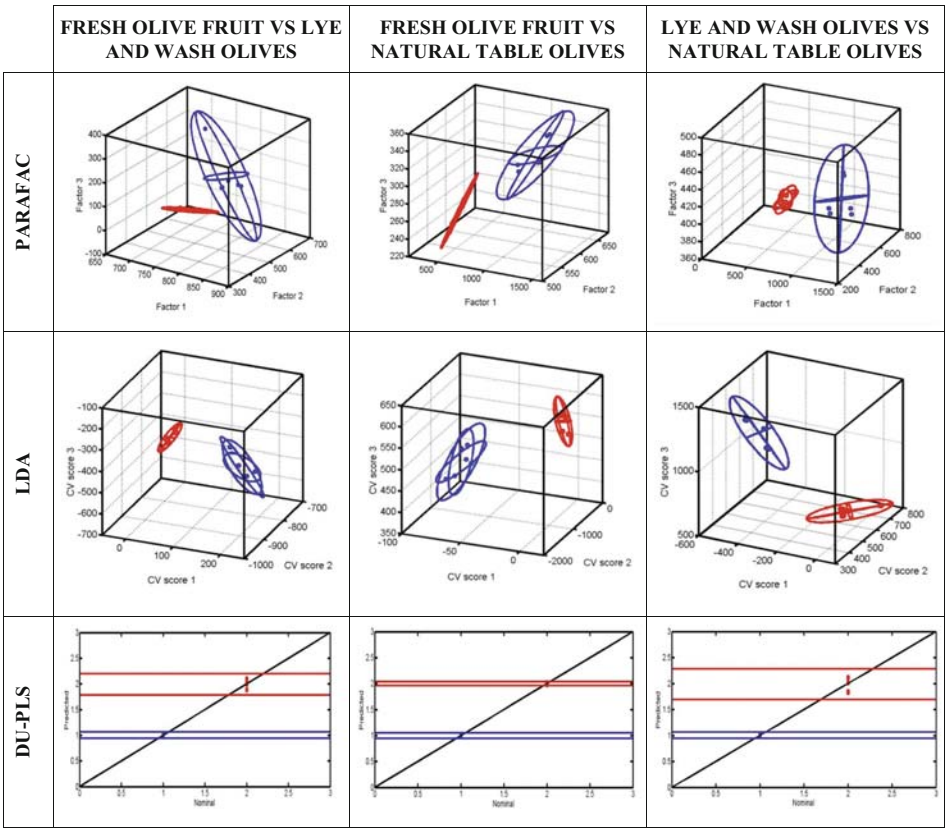


**Fig. 5** Three-dimensional projection of the 95% confidence ellipse for PARAFAC and LDA analysis of the data collected from each olive elaboration status (Fresh olive fruit, lye-wash olives and natural table olives in "Ascolana tenera"). Analyses were performed on olive paste samples (destructive technique). Plot of the DU-PLS 3 factors predicted vs nominal coded

The discrimination ability of DU-PLS was previously tested assigning a code to each elaboration. Ten calibration samples were used as training set, and at each sample, the code for each category was assigned. The predicted versus nominal code values are shown in Fig. 5. The samples of each category were successfully separated from the rest of classes.

According to the obtained results, we can conclude that each elaboration step was appropriately predicted by the three used algorithms.

## Conclusion

Fluorescence spectroscopy analysis combined with chemometrics has been used for the first time for successfully differentiate olive varieties directly from the olive paste independently from maturation stage. In the present study, the proposed method is more simple and faster than traditional physic-chemical analysis and PARAFAC allows obtaining wide information from the EEMs not only about the olive variety but also about the maturation stage. PARAFAC, PARAFAC-LDA, and U-PLS allowed classifying the samples in pairs according to the olive variety. The use of PARAFAC also allowed a good discrimination of the samples according to the maturation stage.

In addition to olive fruit characterization, the proposed method represents a good first approach in the monitoring of table olives during the elaboration process by taking into account the chemical changes of fluorescence compounds during fermentation, especially for very sensitive varieties like "Ascolana tenera."

**Funding** Manuel Cabrera-Bañegil thanks the sponsorship of Comunidad Autónoma de Extremadura, the Consejería de Economía e Infraestructuras and the co-financing of the Fondo Social Europeo (FSE) for the Grant (PD16015). Isabel Durán-Merás is grateful to the Ministerio de Economía y Competitividad of Spain (Project CTQ2017-82496-P) and the Gobierno de Extremadura (GR15090-Research Group FQM003, and IB18041), both co-financed by the Fondo Social Europeo (FSE).

## Compliance with Ethical Standards

**Conflict of Interest** Manuel Cabrera-Bañegil declares that he has no conflict of interest. Daniel Martín-Vertedor declares that he has no conflict of interest. Enrico Maria Lodolini declares that he has no conflict of interest. Isabel Durán-Merás declares that she has no conflict of interest.

**Ethical Approval** This research does not include any experiment with animal and/or human subjects.

**Informed Consent** Informed consent not applicable.

## References


Alowaiesh B, Singh Z, Fang Z, Kailis SG (2018) Harvest time impacts the fatty acid compositions, phenolic compounds and sensory attributes of Frantoio and Manzanilla olive oil. Sci Hortic 234:74–80

Aouidi F, Dupuy N, Artaud J, Roussos S, Msallem M, Perraud Gaime I, Hamdi M (2012) Rapid quantitative determination of oleuropein in olive leaves (*Olea europaea*) using mid-infrared spectroscopy combined with chemometric analysis. Ind Crop Prod 37:292–297

Arslan D, Özcan MM (2011) Phenolic profile and antioxidant activity of olive fruits of the Turkish variety Sariulak from different locations. Grasas Aceites 62:453–461

Beltrán G, del Río C, Sánchez S, Martínez L (2004) Seasonal changes in olive fruit characteristics and oil accumulation during ripening process, J Sci Food Agric 84:1783–1790

Ben Othman N, Roblain D, Chammem N, Thonart P, Hamdi M (2009) Antioxiant phenolic compounds loss during the fermentation of Chétoui olives. Food Chem 116:662–669

Berrueta LA, Alonso-Salces RM, Héberger K (2007) Supervised pattern recognition in food analysis. J Chromatogr A 1158:196–214

Beyaz A, Özkaya MT, Içen D (2017) Identification of some Spanish olive cultivars using image processing techniques. Sci Hortic 225:286–292

Binetti G, Del Coco L, Ragone R, Zelasco S, Perri E, Montemurro C, Valentini R, Naso D, Fanizzi FP, Schena FP (2017) Cultivar classification of Apulian olive oils: use of artificial neural networks for comparing NMR, NIR and merceological data. Food Chem 219: 131–138

Brahim SB, Kelebek H, Ammar S, Abichou M, Bouaziz (2017) LC-MS phenolic profiling combined with multivariate analysis as an approach for the characterization of extra virgin olive oils of four rare Tunisian cultivars during ripening. Food Chem 229:9–19

Bro R (2003) PARAFAC. Tutorial and applications. Chemom Intell Lab Syst 17:200–215

Cabrera-Bañegil M, Schaide T, Manzano R, Delgado-Adámez J, Durán-Merás I, Martín-Vertedor D (2017) Optimization and validation of a rapid liquid chromatography method for determination of the main polyphenolic compounds in table olives and in olive paste. Food Chem 233:164–173

Cabrera-Bañegil M, Martín-Vertedor D, Boselli E, Durán-Merás I (2018) Control of olive cultivar irrigation by front-face fluorescence excitation-emission matrices in combination with PARAFAC. J Food Compos Anal 69:189–196

Cabrera-Bañegil M, Valdés-Sánchez E, Moreno D, Airado-Rodríguez D, Durán-Merás I (2019) Front-face fluorescence excitation-emission matrices in combination with three-way chemometrics for the discrimination and prediction of phenolic response to vineyard agronomic practices. Food Chem 270:162–172

Camin F, Pavone A, Bontempo L, Wehrens R, Paolini M, Faberi A, Marianella RM, Capitani D, Vista S, Mannina L (2016) The use of IRMS, 1H NMR and chemical analysis to characterise Italian and imported Tunisian olive oils. Food Chem 196:98–105

Crawford LM, Holstege DM, Wang SC (2018) High-throughput extraction method for phenolic compounds in olive fruit (*Olea europaea*). J Food Compos Anal 66:136–144

Dagdelen A, Tümen G, Özcan MM, Dündar E (2013) Phenolics profiles of olive fruits (*Olea europaea* L.) and oils from Ayvalik, Domat and Gemlik varieties at different ripening stages. Food Chem 136:41–45

Domínguez-Manzano J, Muñoz de la Peña A, Durán Merás I (2019) Front-face fluorescence combined with second-order multiway classification, base on polyphenol and chlorophyll compounds, for virgin olive oil monitoring under different photo- and thermal-oxidation procedures. Food Anal Methods 12:1399–1411

Durazzo A, Lisciani S, Camilli E, Gabrielli P, Marconi S, Gambelli L, Aguzzi A, Lucarini M, Maiani G, Casale G, Marletta L (2017) Nutritional composition and antioxidant properties of traditional Italian dishes. Food Chem 218:70–77

Durán Merás I, Domínguez Manzano J, Airado Rodríguez D, Muñoz de la Peña A (2018) Detection and quantification of extra virgin olive oil adulteration by means of autofluorescence excitation-emission profiles combined with multi-way classification. Talanta 178: 751–762.

Fernández-Espinosa AJ (2016) Combining PLS regression with portable NIR spectroscopy to on-line monitor quality parameters in intact olives for determining optimal harvesting time. Talanta 148:216–228

Ferro MD, Lopes E, Afonso M, Peixe A, Rodrigues FM, Duarte MF (2020) Phenolic profile characterization of "Galega vulgar" and "Cobrançosa" Portuguese olive cultivars along the ripening stages. Appl Sci 10:3930

Galeano Díaz T, Durán Merás ID, Correa CA, Roldan B, Rodríguez Cáceres MI (2003) Simultaneous fluorometric determination of chlorophylls A and B and pheophytins A and B in olive oil by partial least-squares calibration. J Agric Food Chem 51:6934–6940

Galeano Díaz T, Durán-Merás I, Rodríguez Cáceres MI, Roldan Murillo B (2006) Comparative of different fluorimetric signals for the simultaneous multivariate determination of tocopherols in vegetables oils. Appl Spectrosc 60:194–202

Gouvinhas I, de Almeida JMMM, Carvalho T, Machado N, Barros AIRNA (2015) Discrimination and characterization of extra virgin olive oils from three cultivars in different maturation stages using Fourier transform infrared spectroscopy in tandem with chemometrics. Food Chem 174:226–232

Guimet F, Boqué R, Ferré J (2006) Application of non-negative matrix factorization combined with Fisher's linear discriminant analysis for classification of olive oil excitation-emission fluorescence spectra. Chemom Intell Lab Syst 81:94–106

Guzmán E, Baeten V, Fernández Pierna JA, García-Mesa JA (2015) Evaluation of the overall quality of olive oil using fluorescence spectroscopy. Food Chem 173:927–934

Hernández-Sánchez N, Lleó L, Ammari F, Cuadrado TR, Roger JM (2017) Fast fluorescence spectroscopy methodology to monitor the evolution of extra virgin olive oils under illumination. Food Bioprocess Technol 10:949–961

Haaland DM, Thomas EV (1988a) Partial least-squares methods for spectral analyses. 1. Relation to other quantitative calibration methods and the extraction of qualitative information. Anal Chem 60 (11): 1193–1202

Haaland DM, Thomas EV (1988b) Partial least-squares methods for spectral analyses. 2. Application to simulated and glass spectral data. Anal Chem 60 (11):1202–1208

Justicia M, Madueño A, Ruiz-Canales A, Molina JM, López M, Madueño JM, Granados JA (2017) Low-frecuency characterisation of mesocarp electrical conductivity in different varieties of olives (*Olea europea* L). Comput Electron Agric 142:338–347

Kemsley EK (1998) A genetic algorithm (GA) approach to the calculation of canonical variates (CVs). Trends Anal Chem 17:24–34

Köseoglu O, Sevim D, Kadiroglu P (2016) Quality characteristics and antioxidant properties of Turkish monovarietal olive oils regarding stages of olive ripening. Food Chem 212:628–634

Kyriakidis NB, Skarkalis P (2000) Fluorescence spectra measurement of olive oil and other vegetable oils. J AOAC Int 83(6):1435–1439

Lanza B (2012) Chapter 16 Nutritional and sensory quality of table olives. The olive cultivation, table olive and olive oil industry in Italy 343–372

Lee O, Lee B (2010) Antioxidant and antimicrobial activities of individual and combined phenolics in *Olea europaea* leaf extract. Bioresour Technol 101:3751–3754

Lodolini EM, Cabrera-Bañegil M, Fernández A, Delgado-Adámez J, Ramírez R, Martín-Vertedor D (2019) Monitoring of acrylamide and phenolic compounds in table olive after high hydrostatic pressure and cooking treatments. Food Chem 286:250–259

Navajas-Porras B, Pérez-Burillo S, Morales-Pérez J, Rufián-Henares JA, Pastoriza S (2020) Relationship of quality parameters, antioxidant capacity and total phenolic content of EVOO with ripening state and olive variety. Food Chem 325:126926

Peres F, Martins LL, Mourato M, Vitorino C, Antunes P (2016) Phenolic compounds of "Galega Vulgar" and "Cobrançosa" olive oils along early ripening stages. Food Chem 211:51–58

Pistarino E, Aliakbarian B, Casazza AA, Paini M, Cosulich ME, Perego P (2013) Combined effect of starter culture and temperature on phenolic compounds during fermentation of Taggiasca black olives. Food Chem 138:2043–2049

Ponce JM, Aquino A, Millan B, Andújar JM (2019) Automatic counting and individual size and mass estimation of olive-fruits through computer vision techniques. IEEE Access 7:59451–59465

Ruiz-Aracama A, Goicoechea E, Guillén MD (2017) Direct study of minor extra-virgin olive oil components without any simple modification 1H NMR multisupression experiment: a powerful tool. Food Chem 228:301–314

Salguero-Chaparro L, Baeten V, Fernández-Pierna JA, Peña-Rodríguez F (2013) Near infrared spectrocopy (NIRS) for on-line determination of quality parameters in intact olives. Food Chem 139:1121–1126

Sousa A, Malheiro R, Casal S, Bento A, Pereira JA (2015) Optimal harvesting period for cvs Madural and Verdeal Transmontana based on antioxidant potential and phenolic composition of olives. LWT Food Sci Technol 62:1120–1126

Vergara-Domínguez H, Ríos JJ, Gandul-Rojas B, Roca M (2016) Chlorophyll catabolism in olive fruits (var Arbequina and Hojiblanca) during maturation. Food Chem 212:604–611

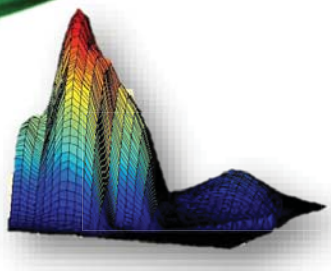

# ARTÍCULO 8

# Avances en la utilización de datos de cuatro y cinco vías, basados en matrices de excitación-emisión de fluorescencia, para aplicaciones analíticas

Arsenio Muñoz de la Peña, Anunciación Espinosa-Mansilla, Isabel Durán-Merás, Olga Monago-Maraña, Manuel Cabrera-Bañegil

*Actualidad Analítica,* ***2020****, 70, 9-12*
*ISSN 2444-8818*

# AVANCES EN LA UTILIZACIÓN DE DATOS DE CUATRO Y CINCO VÍAS, BASADOS EN MATRICES DE EXCITACIÓN-EMISIÓN DE FLUORESCENCIA, PARA APLICACIONES ANALÍTICAS

**A. Muñoz de la Peña, A. Espinosa-Mansilla, I. Durán Martín-Merás, O. Monago-Maraña, M. Cabrera-Bañegil**
**Departamento de Química Analítica, Universidad de Extremadura, Badajoz, España**

## Introducción

El campo de la calibración multivariante se ha expandido en los últimos años con el desarrollo de múltiples aplicaciones analíticas en muestras complejas. En muchas de ellas se han utilizado datos luminiscentes de excitación-emisión de tres vías y, en unos pocos casos, se trabaja con datos de cuatro vías e incluso de cinco vías [1-5]. Las calibraciones que emplean estos datos de cuatro o cinco vías se denominan de tercer o cuarto orden, respectivamente. Aumentar el número de vías para obtener estos datos, a pesar de la complejidad de los mismos, lleva asociada una serie de ventajas.

Booksh y Kowalski, en 1994, definieron un concepto en la calibración de segundo orden (datos de tres vías) que se conoce como la *ventaja de segundo orden*. Dicha ventaja establece que, bajo ciertas circunstancias, las concentraciones de los componentes de interés, en una muestra a analizar, pueden ser obtenidas mediante la separación de las señales de los analitos de interés de las señales no calibradas procedentes de la matriz o de la presencia de interferencias [6]. Los autores se refieren también a una hipotética *ventaja de tercer orden* correspondiente a la calibración de tercer orden (datos de cuatro vías). En la actualidad, 25 años después, diferentes autores han discutido sobre la existencia de dicha ventaja, así como sobre las limitaciones del uso de la calibración de tercer orden o de orden superior [7-9]. Entre las ventajas descritas por diferentes autores, y soportadas por evidencias experimentales, se encuentran: 1) la posibilidad de descomponer una matriz de datos única de una muestra dada independiente de otras muestras, 2) la mejora de la sensibilidad y la selectividad, así como de otras figuras analíticas de mérito, 3) un mayor poder de resolución que los métodos de tres vías y 4) la posibilidad de resolver problemas de co-linealidad al incluir una vía instrumental adicional. Las aplicaciones analíticas descritas hasta el momento se reúnen en un reciente artículo de revisión [9].

La inclusión de esta cuarta vía adicional se ha propuesto utilizando diferentes estrategias que se describen a continuación (Figura 1), unidas a la obtención de matrices de excitación-emisión (excitation-emission matrices, EEMs).

## EEMs-tiempo de reacción (cinética)

Uno de los procedimientos más utilizados para obtener experimentalmente datos de cuatro vías es la inclusión del comportamiento cinético como información adicional, basado en que los compuestos de interés pueden degradarse, oxidarse, reducirse etc.

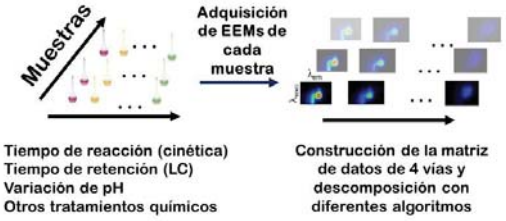


*Fig. 1. Diferentes estrategias experimentales de obtención de datos de cuatro vías.*

Una de las reacciones más utilizada está basada en la oxidación con permanganato potásico. Así, nuestro grupo ha propuesto métodos de determinación de metotrexato y leucovorín en orina humana utilizando análisis paralelo de factores (PARAFAC) y dos nuevos algoritmos propuestos para tratar este tipo de datos, mínimos cuadrados trilineales (TLLS) y mínimos cuadrados parciales desdoblados (U-PLS) combinados con trilinealización residual (RTL) [10, 11]. Similarmente, se determinaron metotrexato y ácido fólico en muestras de orina y suero [12, 13].

En este contexto, con el objeto de obtener una mejora en el método analítico, desarrollamos un nuevo algoritmo de calibración multivariante de tercer orden, basado en la combinación de mínimos cuadrados parciales multidimensional (N-PLS) con RTL, empleándose dicho algoritmo en la determinación de procaína y su metabolito, ácido p-aminobenzoico, en muestras de suero humano, por medio del seguimiento de la hidrólisis de la procaína [14].

Dicho algoritmo fue posteriormente empleado en la determinación de ácido fólico (FA) y sus dos principales metabolitos, ácido tetrahidrofólico (THF) y ácido 5-metil tetrahidrofólico (5-MTF), en muestras de suero que fueron sometidas a degradación fotoquímica por medio de irradiación con una lámpara UV (Figura 2) [15].

Similarmente, la reacción de Hantzsch entre malonaldehido y metilamina, que da lugar a un compuesto altamente fluorescente, se utilizó para el desarrollo de un método de determinación de malonaldehido en aceite de oliva. En esta aplicación, y dada la naturaleza no lineal de la cinética, los datos se analizaron mediante una variante de PARAFAC para datos de tercer orden y un modelo de redes neuronales [16].

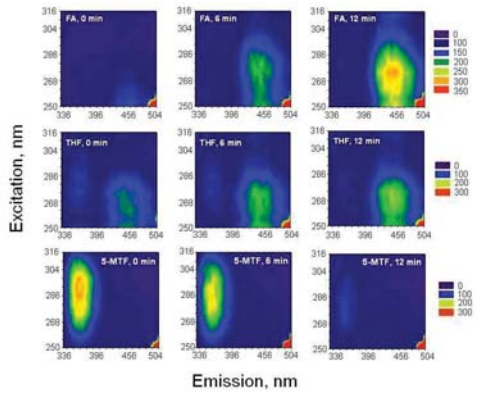


*Fig. 2. Evolución de los gráficos de contornos de las matrices de excitación–emisión con el tiempo de irradiación UV, de disoluciones de FA, THF y 5-MTF. Reimpresa con permiso de la Referencia [15]. Copyright 2008 Elsevier.*

**EEMs- tiempo de retención (cromatografía de líquidos, LC)**

En el campo de la calibración multivariante, la cromatografía de líquidos acoplada a detección fluorimétrica ha ido ganando un creciente interés, dado el alto potencial que se consigue al combinar una elevada resolución con una alta sensibilidad, permitiendo resolver sistemas extremadamente complejos. Sin embargo, el procedimiento analítico de obtención de datos de cuatro vías, desde el punto de visto quimiométrico, no es trivial. Hoy día, la instrumentación disponible nos permite obtener datos multivariantes a partir de experimentos de adquisición de matrices de excitación-emisión durante los registros cromatográficos, aunque el procedimiento tiene sus dificultades técnicas y se han propuesto diferentes estrategias experimentales para conseguirlo.

Nuestro grupo propuso un procedimiento de adquisición de datos de tercer orden, EEMs-LC, utilizando un cromatógrafo de líquidos convencional y un detector de fluorescencia de barrido rápido [17]. Para la adquisición de los datos de tercer orden se registraron distintos espectros de emisión a cada tiempo de elución, de manera que se generaron matrices de tiempo de elución-espectros de emisión (TEMs) en cada barrido cromatográfico. El tercer modo instrumental se obtuvo registrando varios TEMs a diferentes longitudes de onda de excitación. El procedimiento permitió la determinación de clorofilas a y b (Ch a, Ch b) y feofitinas a y b (Phe a, Phe b), en muestras de aceite de oliva, utilizando PARAFAC y U-PLS/RTL para el análisis de los datos obtenidos (Figura 3). Con objeto de mejorar los resultados, se propuso un nuevo procedimiento de análisis de los datos, mediante el algoritmo denominado PARAFAC aumentado (APARAFAC) [18]. El algoritmo se desarrolló para resolver datos de cuatro vías utilizando una estructura de datos de tres vías aumentada, que permite superar el problema de la falta de trilinealidad por medio de la estructura aumentada de los datos, y presentando la ventaja adicional de obtener resultados físicamente interpretables.

La misma estrategia experimental fue utilizada para la determinación de pesticidas en muestras de frutas [19].

Posteriormente, siguiendo el pionero procedimiento descrito por Bro [20], propusimos un procedimiento alternativo de generación de datos de EEMs-LC, aplicándolo a la determinación de tres fluoroquinolonas en aguas [21]. Para ello, se utilizó un colector automático que permitía recoger fracciones cromatográficas en un lector de 96 placas. A continuación, la placa, con la correspondiente fracción, se introdujo en un espectrofluorímetro equipado con un lector de placas, lo que permitió la adquisición de las EEMs de cada una de las placas. Una vez que se registró la EEM, se construyó una matriz tridimensional que comprendía las EEMs obtenidas para cada fracción. Un punto importante a resaltar es el hecho de que cada EEM fue registrada individualmente en condiciones estáticas; de esta manera, el tiempo de elución, la longitud de onda de excitación y la longitud de onda de emisión, son mutuamente independientes, lo que garantiza la trilinealidad de la matriz de datos.

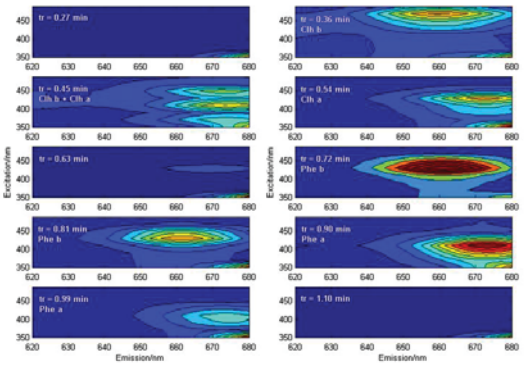


*Fig. 3. Mapas de contorno de EEMs obtenidas para los diferentes tiempos de retención (tr), ilustrando la evolución cromatográfica de Chl a, Chl b, Phe a y Phe b de una muestra. El color rojo corresponde a señales más intensas y el azul a menos intensas. Los contornos corresponden a diez tiempos de retención diferentes, desde 0.27 a 1.1 minutos. Reimpresa con permiso de la Referencia [17]. Copyright 2013 Elsevier.*

**EEMs-otros tratamientos químicos**

La combinación de EEMs con la variación del pH ha sido propuesta por el grupo de Wu y colaboradores, la mayor parte de las veces en conexión con el desarrollo de nuevos algoritmos para el análisis de matrices de datos de cuatro vías. Como ejemplos podemos citar dos recientes trabajos de este grupo, para la determinación de aminoácidos en plasma humano [22] y de tres ácidos fenólicos en muestras de cosméticos [23], en los que

discuten, defienden y demuestran, con datos experimentales, la existencia de la *ventaja de tercer orden.* Otros tratamientos químicos, tales como la adición de un atenuador de la fluorescencia (quencher) [24] o el uso de diferentes disolventes, han sido también descritos en la bibliografía [9].

Un ejemplo, empleando el uso de diferentes disolventes como cuarta vía, ha sido recientemente desarrollado y con un objetivo clasificatorio [25]. El estudio demuestra la capacidad de combinar EEMs, obtenidas en modo front-face, y en diferentes disolventes, con los algoritmos mencionados anteriormente, para realizar procesos de clasificación. Concretamente, en este estudio se establece la capacidad de clasificación de uvas procedentes de viñedos, tratados con diferentes prácticas agronómicas, que involucraban diferentes estados hídricos de las uvas. La descomposición de los datos fluorescentes de tres vías, realizada por análisis discriminante lineal (LDA)-PARAFAC y DA-UPLS, nos permitió la discriminación entre dos estados de maduración diferentes de las uvas. Además, hay que reseñar que, con el objetivo de mejorar la discriminación entre uvas con diferentes estados hídricos, se adicionó una dimensión extra (cuarta vía) que fue la extracción con dos disolventes diferentes. Los datos de la cuarta vía se obtuvieron por combinación de los extractos acuosos y en dietiléter y los resultados para la clasificación de estos datos pueden observarse en la Figura 4.

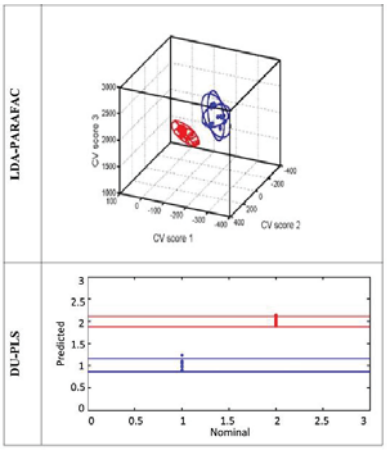


*Fig. 4. Clasificación según el tratamiento de riego con datos de tercer orden. Arriba) Valores de scores obtenidos para LDA-PARAFAC de un conjunto de 48 muestras (no irrigadas, círculos rojos, e irrigadas, círculos azules). Se incluye las proyecciones tridimensionales de las elipses en los tres planos (intervalo de confianza del 95%), Abajo) Gráfico de valores predichos frente a los códigos nominales clasificatorios (1 y 2), obtenidos por DA-UPLS. Reimpresa con permiso de la Referencia [25]. Copyright 2019 Elsevier.*

**Aplicaciones con datos de cinco vías**

Nuestro grupo propuso el primer método de utilización de datos de 5 vías. Para ello, se registraron varias EEMs siguiendo la cinética de la reacción de hidrólisis de carbaril a 1-naftol, a diferentes valores de pH. Los datos obtenidos se procesaron con U-PLS en combinación con un nuevo algoritmo, cuadrilinealización residual (RQL), que es la extensión de U-PLS/RTL a datos cuadrilineales (Figura 5) [26].

**Conclusiones**

A pesar de la complejidad experimental necesaria para obtener datos de cuatro y cinco vías, los avances descritos han permitido el desarrollo de métodos de determinación de compuestos de interés en los campos medioambiental, biológico y de análisis de alimentos, entre otros, en muestras complejas. Asimismo, aun cuando son numerosas las evidencias expuestas por distintos autores sobre las ventajas encontradas al utilizar estos métodos, se necesita profundizar en el desarrollo teórico para comprender las ventajas asociadas a los mismos, siendo recomendable una evaluación comprehensiva de los requerimientos experimentales necesarios, para proveer evidencias más fuertes acerca de las potencialidades de estos métodos.

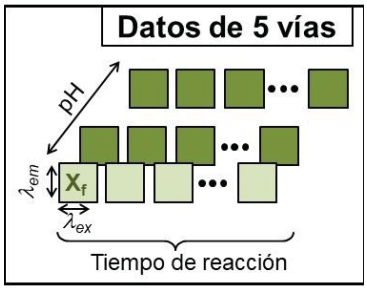


*Fig. 5. Estrategia experimental de obtención de datos de cinco vías EEMs-Tiempo de reacción-pH.*

**Agradecimientos**

Los autores agradecen financiación por parte de la Junta de Extremadura (Ayuda GR18041-Grupo de investigación ANAYCO-FQM003) y del Ministerio de Ciencia, Innovación y Universidades (Proyecto CTQ2017-82496-P).

**Referencias**

[1] G.M. Escandar, N.K.M. Faber, H.C. Goicoechea, A. Muñoz de la Peña, A.C. Olivieri, R.J. Poppi, Second- and third-order multivariate calibration: data, algorithms and applications, Trends Anal. Chem., 2007, 26, 752–765.

[2] A.C. Olivieri, G.M. Escandar, A. Muñoz de la Peña, Second-order and higher-order multivariate calibration methods applied to non-multilinear data using different algorithms, Trends Anal. Chem., 2011, 30, 607–617.

[3] G.M. Escandar, H.C. Goicoechea, A. Muñoz de la Peña, A.C. Olivieri, Second- and higher-order data generation and calibration: A tutorial, Anal. Chim. Acta., 2014, 806, 8–26.
[4] A. Muñoz de la Peña, A.C. Olivieri, G.M. Escandar, H.C. Goicoechea, Fundamentals and analytical applications of multiway calibration, Elsevier, Amsterdam, 2015.
[5] A.C. Olivieri, P.L. Pisano, A. Muñoz de la Peña, H.C. Goicoechea, Data Analysis, in: S. Fanali, P.R. Haddad, C.F. Poole, M.L. Riekkola (Eds.), Liq. Chromatogr. Vol. 1. Fundam. Instrumentation., 2nd ed., Elsevier, Netherlands, 2017: pp. 515–528.
[6] K.S. Booksh, B.R. Kowalski, Theory of Analytical Chemistry, Anal. Chem., 1994, 66, 782A–791A.
[7] A.C. Olivieri, Analytical advantages of multivariate data processing . One Two, Three, Infinity?, Anal. Chem., 2008, 80, 5713–5720.
[8] X.H. Zhang, X.D. Qing, H.L. Wu, Discussion on the superiority of third-order advantage: analytical application for four-way data in complex system, Microchemical Journal, 2019, 145, 1078-1085.
[9] M.R. Alcaraz, O. Monago-Maraña, H.C. Goicoechea, A. Muñoz de la Peña, Four- and five-way excitation-emission luminescence-based data acquisition and modelling for analytical applications. A review, Anal. Chim. Acta, 2019, 1083, 41-57.
[10] A.C. Olivieri, J.A. Arancibia, A. Muñoz de la Peña, I. Durán-Merás, A. Espinosa-Mansilla, Second-order advantage achieved with four-way fluorescence excitation-emission-kinetic data processed by parallel factor analysis and trilinear least-squares. Determination of methotrexate and leucovorin in human urine, Anal. Chem., 2004, 76, 5657–5666.
[11] J.A. Arancibia, A.C. Olivieri, D.B. Gil, A. Espinosa-Mansilla, I. Durán-Merás, A. Muñoz de la Peña, Trilinear least-squares and unfolded-PLS coupled to residual trilinearization: New chemometric tools for the analysis of four-way instrumental data, Chemom. Intell. Lab. Syst., 2006, 80, 77–86.
[12] A. Muñoz de la Peña, I. Durán-Merás, A. Jiménez Girón, Four-way calibration applied to the simultaneous determination of folic acid and methotrexate in urine samples, Anal. Bioanal. Chem., 2006, 385, 1289–1297.
[13] A. Muñoz de la Peña, I. Durán-Merás, A. Jiménez Girón, H.C. Goicoechea, Evaluation of unfolded-partial least-squares coupled to residual trilinearization for four-way calibration of folic acid and methotrexate in human serum samples, Talanta., 2007, 72, 1261–1268.
[14] P.C. Damiani, I. Durán-Merás, A. García-Reiriz, A. Jiménez-Girón, A. Muñoz de la Peña, A.C. Olivieri, Multiway partial least-squares coupled to residual trilinearization: A genuine multidimensional tool for the study of third-order data. Simultaneous analysis of procaine and its metabolite p-aminobenzoic acid in equine serum, Anal. Chem., 2007, 79, 6949–6958.
[15] A. Jiménez Girón, I. Durán-Merás, A. Espinosa-Mansilla, A. Muñoz de la Peña, F. Cañada Cañada, A.C. Olivieri, On line photochemically induced excitation-emission-kinetic four-way data. Analytical application for the determination of folic acid and its two main metabolites in serum by U-PLS and N-PLS/residual trilinearization (RTL) calibration, Anal. Chim. Acta., 2008, 622, 94–103.
[16] A. García-Reiriz, P.C. Damiani, A.C. Olivieri, F. Cañada-Cañada, A. Muñoz de la Peña, Nonlinear four-way kinetic-excitation-emission fluorescence data processed by a variant of parallel factor analysis and by a neural network model achieving the second-order advantage: malonaldehyde determination in olive oil samples, Anal. Chem., 2008, 80, 7248–7256.
[17] V.A. Lozano, A. Muñoz de la Peña, I. Durán-Merás, A. Espinosa-Mansilla, G.M. Escandar, Four-way multivariate calibration using ultra-fast high-performance liquid chromatography with fluorescence excitation – emission detection. Application to the direct analysis of chlorophylls a and b and pheophytins a and b in olive oils, Chemom. Intell. Lab. Syst., 2013, 125, 121–131.
[18] S.A. Bortolato, V.A. Lozano, A. Muñoz de la Peña, A.C. Olivieri, Novel augmented parallel factor model for four-way calibration of high-performance liquid chromatography – fluorescence excitation – emission data, Chemom. Intell. Lab. Syst., 2015, 141, 1–11.
[19] M. Montemurro, L. Pinto, G. Véras, A. de Araújo Gomes, M.J. Culzoni, M.C. Ugulino de Araújo, H.C. Goicoechea, Highly sensitive quantitation of pesticides in fruit juice samples by modeling four-way data gathered with high-performance liquid chromatography with fluorescence excitation-emission detection, Talanta, 2016, 154, 208–218.
[20] R. Bro, Multi-way analysis in the food industry. Models, algorithms and applications., University of Amsterdam, Nethterlands, 1998.
[21] M.R. Alcaraz, G.G. Siano, M.J. Culzoni, A. Muñoz de la Peña, H.C. Goicoechea, Modeling four and three-way fast high-performance liquid chromatography with fluorescence detection data for quantitation of fluoroquinolones in water samples, Anal. Chim. Acta, 2014, 809, 37–46.
[22] C. Kang, H.L. Wu, L.X. Xie, S.X. Xiang, R.Q. Yu, Direct quantitative analysis of aromatic amino acids in human plasma by four-way calibration using intrinsic fluorescence: Exploration of third-order advantages, Talanta, 2014, 122, 293–301.
[23] X. Zhang, X. Qing, H. Wu, Discussion on the superiority of third-order advantage : Analytical application for four-way data in complex system, Microchem. J., 2019, 145, 1078–1085.
[24] L. Rubio, L. A. Sarabia, M. C. Ortiz, standard addition method based on four-way PARAFAC decomposition to solve the matrix interferences in the determination of carbamates pesticides in lettuce using excitation-emission fluorescence data, Talanta, 2015, 138, 86-89.
[25] M. Cabrera-Bañegil, E. Valdés-Sánchez, A. Muñoz de la Peña, I. Durán-Merás, Combination of fluorescence excitation emission matrices in polar and non-polar solvents to obtain three- and four-way arrays for classification of Tempranillo grapes according to maduration stage and hydric status, Talanta, 2019, 199, 652–661.
[26] R.M. Maggio, A. Muñoz de la Peña, A.C. Olivieri, Unfolded partial least-squares with residual quadrilinearization: A new multivariate algorithm for processing five-way data achieving the second-order advantage. Application to fourth-order excitation-emission-kinetic-pH fluorescence analytical data, Chemom. Intell. Lab. Syst., 2011, 109, 178–185.